A STUDY OF SOFTWOOD TORREFACTION

AND DENSIFICATION

FOR THE PRODUCTION OF HIGH QUALITY WOOD

PELLETS

by

Jiang Hong Peng

M. Sc., Tsinghua University, Beijing, 1989
B. Eng., East China University of Science and Technology, Shanghai, 1986

A THESIS SUBMITTED IN PARTIAL FULFILMENT OF

THE REQUIREMENTS FOR THE DEGREE OF

DOCTOR OF PHILOSOPHY

in

THE FACULTY OF GRADUATE STUDIES

(CHEMICAL AND BIOLOGICAL ENGINEERING)

THE UNIVERSITY OF BRITISH COLUMBIA

(VANCOUVER)

July 2012

ABSTRACT

British Columbia (BC) has become a major producer and exporter of wood pellets in the world. But the low energy density, the low water resistivity, the short shelf life, and the transportation cost impede the market development. Torrefaction, a thermal treatment without air or oxygen at 200-300 ^{o}C, may provide a solution.

The present study developed the torrefaction kinetics of BC softwood residues in a thermogravimetric analyzer (TGA), studied the effect of the torrefaction reaction conditions on the properties of torrefied sawdust in a bench-scale fixed bed reactor and a bench-scale fluidized bed reactor, and identified the suitable conditions for making durable torrefied pellets in a press machine using torrefied samples. The weight loss of BC softwood residues significantly depended on the torrefaction temperature, the residence time, the particle size, and the oxygen concentration in the carrier gas. The weight loss could be approximately estimated from the weight loss of the chemical compositions. A two-component and one-step first order reaction kinetic model gave a good agreement with data over short residence time on the weight loss range of 0 to 40% at the temperature of 260-300 ^{o}C.

The heating value of torrefied pellets had a close relationship with the weight loss, increasing with increasing the severity of torrefaction. The torrefied samples were more difficult to be compressed into strong pellets under the same conditions as used for making the control (regular, untreated, conventional) pellets. More energy was needed for compacting torrefied samples into torrefied pellets. Increasing the die temperature and adding moisture into torrefied samples could improve the quality of torrefied pellets. The moisture content and density of torrefied pellets were lower than control pellets.

Considering the quality of torrefied pellets, the optimal torrefaction conditions appeared to correspond to a weight loss of about 30%, which gave a 20% increase in pellet heating value and good hydrophobicity. The suitable densification conditions corresponded to a die temperature of 230 ^{o}C, or over 110 ^{o}C for torrefied samples conditioned to 10% moisture content.

PREFACE

Chapter 1 is based on a literature review conducted at the Biomass and Bioenergy Research Group (BBRG). Part of the literature review, in combination with the torrefaction kinetics in Chapter 3, has been published: Peng, J. H., Bi, X. T., Lim, C. J., Sokhansanj, S., "Development of Torrefaction Kinetics for British Columbia Softwoods," *International Journal of Chemical Reactor Engineering,* Volume 10, Issuer 1, ISSN (Online) 1542-6580, DOI: 10.1515/1542-6580.2878, March **2012**. I was responsible for all the literature review and the paper preparation. The co-authors provided feedback throughout this process and edited the manuscript.

Chapter 3 is based on the experimental work conducted in a TGA. I carried out all the experimental design, data collection and analysis, and paper preparation. Section 3.6 was presented in the 2010 International Symposium on Gasification and Applications: Peng, J. H., Bi, H. T., Sokhansanj, S., Lim, J. C., "Development of Torrefaction Kinetics for BC Softwood," ISGA2010, 5-8 December **2010**, Fukuoka, Japan. A paper has also been published: Peng, J. H., Bi, X. T., Lim, C. J., Sokhansanj, S., "Development of Torrefaction Kinetics for British Columbia Softwoods," *International Journal of Chemical Reactor Engineering,* Volume 10, Issuer 1, ISSN (Online) 1542-6580, DOI: 10.1515/1542-6580.2878, March **2012**. The co-authors provided feedback and insight throughout this process, and edited the manuscript.

Chapter 4 is based on the experimental work conducted in a fixed bed reactor. I was responsible for all the equipment design and set up, experimental design, data collection and analysis, and manuscript preparation. A version of Chapter 4 has been submitted: Peng, J. H., Bi, H.T., Sokhansanj, S., Lim, C. J., "Torrefaction and Densification of

Different Species of Softwood Residues," September 2011. The co-authors provided feedback and insight throughout this process, and edited the manuscript.

Chapter 5 is based on experimental work conducted in both the TGA and the fixed bed reactor at UBC. I was responsible for the experimental design, data collection and analysis, and paper preparation. UBC summer student Pak Chien Hoi provided assistance on the pelletization of some torrefied sawdust samples. A version of Chapter 5 was published: Peng, J. H., Bi, H. T., Sokhansanj, S., Lim, C. J., "A Study of Particle Size Effect on Biomass Torrefaction and Densification," *Energy and Fuels,* DOI: 10.1021/ef3004027, April **2012**. The co-authors provided feedback and insight throughout this process, and edited the manuscript.

Chapter 6 is based on a joint experimental work conducted in a TGA by me and a fluidized bed reactor by Dr. Congwei Wang at UBC. I was responsible for the experimental design, data collection and analysis in the TGA, and the development of the torrefaction oxidation kinetics. Dr. Congwei Wang was responsible for the experimental design, data collection and analysis in the fluidized bed torrefaction unit, pelletization of torrefied sawdust and the manuscript preparation. Dr. Hui Li and Dr. Robert Legros provided advice and assistance in the fluidized bed torrefaction experiment. A manuscript based on Chapter 6 has been submitted: Wang, C. W., Peng, J. H., Li, H., Bi, X. T., Legros, R., Lim, C. J., Sokhansanj, S., "Oxidative Torrefaction of Biomass Residues and Densification of Torrefied Sawdust to Pellets," April **2012**. Other co-authors provided feedback and insight throughout this process, and edited the manuscript.

Chapter 7 is an economical evaluation of torrefied wood pellets based on the present study results conducted at UBC. I was responsible for the data collection the economical

analysis. Part of the result in this chapter has been published: Peng, J. H., Bi, X. T., Sokhansanj, S., Lim, C. J., Melin, S., "An Economical and Market Analysis of Canadian Wood Pellets," *International Journal of Green Energy,* **2010**; 7 (2): 128-142. The co-authors provided feedback and insight throughout this process, and edited the manuscript.

TABLE OF CONTENTS

LIST OF TABLES

xiv

LIST OF FIGURES

NOTATION

A   pore size, *cm*

a_0, a_1, a_2 constants of BC biomass final residual weight fraction

A   pre-exponential factor, s^{-1}

A_1 pre-exponential factor of the fast reaction group torrefaction, s^{-1}

A_2 pre-exponential factor of the medium reaction group torrefaction, s^{-1}

A_j pre-exponential factor of the jth chemical composition, s^{-1}

A_{O1} pre-exponential factor of the fast reaction group oxidation, s^{-1}

A_{O2} pre-exponential factor of the medium reaction group oxidation, s^{-1}

BDt   bone-dry metric tones

Bi   Biot number

$C = C(r, t, R, T_{initial})$ concentration of volatiles inside particles, *mol m^{-3}*

C_1 hemicelluloses fractional content of BC softwood

C_2 cellulose plus lignin fraction content of BC softwood

C_{HC}	hemicelluloses concentration in EFB, *mol m^{-3}*
C_j	fraction of the jth chemical composition
$C_{fast\ group}$	fast reaction group weight fraction
$C_{medium\ group}$	medium reaction group weight fraction
C_O	concentration of volatiles in particle centre, *mol m^{-3}*
C_{O2}	oxygen concentration, *mol m^{-3}*
C_P	heat capacity of particles, *J kg^{-1} K^{1}*
C_{PC}	heat capacity of the nitrogen gas, *kJ kg^{-1} K^{1}*
C_R	concentration of volatiles at particle surface, *mol m^{-3}*
C_∞	concentration of volatiles in bulk gas flow, *mol m^{-3}*
C_{WP}	Weisz-Prater number
D	probe diameter, *m*
D_K	Knudsen diffusion coefficient, *m^2 s^{-1}*
D_m	diffusivity of volatiles, *m^2 s^{-1}*

d_P	particle diameter, m
d_{Pj}	particle diameter for three particle sizes, m
E	apparent activation energy, $kJ\ mol^{-1}$
E_1	apparent activation energy of the fast reaction group torrefaction, $kJ\ mol^{-1}$
E_2	apparent activation energy of the medium reaction group torrefaction, $kJ\ mol^{-1}$
E_j	apparent activation energy of the jth chemical composition, $kJ\ mol^{-1}$
ECN	Energy Research Centre of Netherlands
EFB	oil palm empty fruit bunches
E_{O1}	apparent activation energy of the fast reaction group oxidation, $kJ\ mol^{-1}$
E_{O2}	apparent activation energy of the medium reaction group oxidation, $kJ\ mol^{-1}$
E_{O_2}	activation energy of oxidation, $kJ\ mol^{-1}$
F	maximum force to break a pellet, N
G	superficial mass flux ($u \times \varepsilon \times \rho$, nitrogen gas velocity in $m\ s^{-1} \times$ fraction of void $\times$ nitrogen gas density in $kg\ m^{-3}$), $kg\ m^{-2}\ s^{-1}$
G_1	fractional content of the fast reaction group mostly as hemicelluloses

G_2	fractional content of the medium reaction group as cellulose and lignin
GJ	10^9 joule
h	indentation depth, m
H_A	Heat of decomposition, $J\,g^{-1}$
HHV	high heating value in $MJ\,kg^{-1}$
H_M	Meyer hardness in $N\,mm^{-2}$
i	i^{th} reaction group
ISBL	inside battery limits
j	three different particle sizes
j_H	Chilton-Colburn factor
k	global reaction rate constant, s^{-1}
k_1	global reaction rate constant of the fast reaction group, s^{-1}
k_{1j}	global reaction rate constant of the fast reaction group for three particle sizes, s^{-1}
k_2	global reaction rate constant of the medium reaction group, s^{-1}

k_{2j}	global reaction rate constant of the medium reaction group for three particle sizes, s^{-1}
k_a	heat conductivity of air, $W\,m^{-1}\,K^{-1}$
k_C	chars reaction rate constant, s^{-1}
k_L	tars reaction rate constant, s^{-1}
k_G	gases reaction rate constant, s^{-1}
k_i	global reaction rate constant, s^{-1}
k_m	adsorption rate constant, min^{-1}
k_o	pre-exponential factor, s^{-1}
$k_{O1}\ (= k'_{O1} C_{o2}^{n1})$	lumped oxidation reaction rate constant of the fast reaction group, s^{-1}
k'_{O1}	oxidation reaction rate constant of the fast reaction group, s^{-1}
$k_{O2}\ (= k'_{O2} C_{o2}^{n2})$	lumped oxidation reaction rate constant of the medium reaction group, s^{-1}
k'_{O2}	oxidation reaction rate constant of the medium reaction group, s^{-1}
$k_{0,0_2}$	pre-exponential factor of oxidation, s^{-1}
k_{0_2}	oxidation reaction rate constant, s^{-1}

$k_{oxidation}$	oxidation reaction rate constant, s^{-1}
k_r	real intrinsic reaction constant, s^{-1}
k_s	thermal diffusivity of bulk pine sawdust, $W\ m^{-1}\ K^{1}$
$k_{torrefaction}$	torrefaction reaction rate constant, s^{-1}
k_w	heat conductivity of pine, $W\ m^{-1}\ K^{1}$
l	torrefaction reaction order
L_c	ratio of the particle volume to surface area, m
LHV	Low heating value, $MJ\ kg^{-1}$
m	reaction order with the partial pressure of oxygen
m1	oxidation reaction order for the fast reaction group
m2	oxidation reaction order for the medium reaction group
M	million
M_T	molecular weight, $g\ mol^{-1}$
M_i	initial moisture uptake, %(wt)

M_m	moisture uptake as a function time, %(wt)
MPB	mountain pine beetle
M_s	saturated moisture uptake, %(wt)
Mt	Million metric tones
MWh	Megawatt hour
n	reaction order
n_1	oxygen reaction order for the fast reaction group
n_2	oxygen reaction order for the medium reaction group
n_j	reaction order of the jth chemical composition
OSBL	outside battery limits
P_{O_2}	partial pressure of oxygen level in the atmosphere, Pa
P'_y	Pyrolysis number
r	radii of sphere, m
r(obs)	observed global reaction rate, s^{-1}

$r_1(obs)$	observed global reaction rates of the fast reaction group, s^{-1}
$r_{1j}(obs)$	observed global reaction rates of the fast reaction group for three particle sizes, s^{-1}
$r_2(obs)$	observed global reaction rates of the medium reaction group, s^{-1}
$r_{2j}(obs)$	observed global reaction rates of the medium reaction group for three particle sizes, s^{-1}
R	ideal gas constant, $J\ mol^{-1}\ K^{-1}$
R	radius of sphere, m
Re	Reynolds number
ROI	return on total capital investment
$r_{fast\ group\ oxidation}$	oxidation reaction rate of fast reaction group, s^{-1}
$r_{fast\ group\ torrefactio}$	torrefaction reaction rate of the fast reaction group, s^{-1}
$r_{medium\ group\ oxidation}$	oxidation reaction rate of the medium reaction group, s^{-1}
$r_{medium\ group\ torrefaction}$	torrefaction reaction rate of the medium reaction group, s^{-1}
$r_{overall}$	overall reaction rate, s^{-1}
$r_{oxidation}$	oxidation reaction rate, s^{-1}

$r_{Reaction}$	real global reaction rate, s^{-1}
$r_{torrefaction}$	torrefaction reaction rate, s^{-1}
SCFM	standard cubic feet per minute, $ft^3\ min^{-1}$
STP	standard temperature and pressure
t	reaction time, s
t_d	drying time, s
t_l	low temperature reaction time, s
t_t	reaction time at torrefaction temperature, s
t_c	cooling time , s
T	reaction temperature, K
$T = T(r, t, R, T_{initial})$	temperature inside particles, K
$T_{initial}$	initial temperature, K
TGA	thermogravimetric analyzer
T_O	temperature in particle centre, K

T_R	temperature in particle surface, K
T_∞	temperature in gas flow, K
u	nitrogen gas velocity, $m\ s^{-1}$
v_C	char ratio
w^{calc}	calculation of the overall weight loss fraction
W_{final}	fraction of final residual weight, 1 is the fraction of initial sample weight
W_{TGA}	fraction of residual weight measured as a function time
x	solid conversion (Chapter 1)
y_{O2}	oxygen mole fraction

Greek symbols

α	fractional conversion of biomass (Chapters 1, 3)
α	convection heat transfer coefficient, $W\ m^{-2}\ K^{1}$(Chapter 5)
$α_1$	conversion of hemicelluloses or fast reaction group
$α_2$	conversion of cellulose and lignin or medium reaction group

α_j	conversion of the jth chemical composition
β	particle-shape factor
ε	fraction of free space or void fraction of the packed bed of sawdust
η	effectiveness factor
λ	thermal conductivity of particles, $W\ m^{-1}\ K^{1}$
λ_C	heat conductivity of the nitrogen gas, $W\ m^{-1}\ K^{1}$
ρ_C	nitrogen gas density, $kg\ m^{-3}$
ρ_p	particle density, $kg\ m^{-3}$
ρ_s	pine sawdust bulk density, $kg\ m^{-3}$
ρ_w	pine wood density, $kg\ m^{-3}$
μ	viscosity of nitrogen gas, $kg\ m^{-1}\ s^{-1}$
Γ	unit scale factor
Φ	Thiele module
Φ_1	Thiele module of the fast reaction group

Φ_{1j} Thiele module of the fast reaction group for particle size j

Φ_2 Thiele module of the medium reaction group

Φ_{2j} Thiele module of the medium reaction group for particle size j

ΔH decomposition heat of biomass, *J m^{-3}*

ACKNOWLEDGEMENTS

Finally, I would like to extend my very special appreciation to my family (especially my wife Min Liu, my sons HanChao Peng and BoChao Peng), my parents (my father BenNeng Peng, my mother SuQing Ma), my relatives, and my friends, who supported and encouraged me during the long six years of my PhD study.

CHAPTER 1 INTRODUCTION

1.1 Background

Wood pellets, which are considered as a transportable renewable energy source associated with very low greenhouse gas emissions, are made from densified wood residues. Due to their high volumetric energy density, which is 4-10 times that of wood residues, wood pellets are an efficient form of biomass to store and transport. Also the good flowability of the pellets makes them easier and safer to handle and transport than other forms of biomass. The wood pellet industry gained significant momentum during the last decade in the world due to the effort in European countries to reduce greenhouse gas emissions and the rising oil and natural gas prices. The future pellets market may shift to North America. In 2007, over 10 million tones (Mt) of wood pellets were produced and consumed with an annual increase rate over 40% from 2003 to 2007, and wood pellets hold an extremely promising future [Peng et al. 2010]. Typically, the low heating value (LHV) of as received wood pellets is 15.6-16.2 *MJ kg^{-1}* or 7.8-10.5 *GJ m^{-3}*, with a bulk density ranging from 500 to 650 *kg m^{-3}* and a moisture content of 7-10% by weight [Bergman 2005]. The diameter of the wood pellet is usually 6-12 mm and the length ranges from 6 to 25 mm [Melin 2006]. The production chain of wood pellets starts from feedstock collection and ends with the delivery of pellets to customers. The feedstock is generally a by-product from wood-processing industries, such as sawdust, shavings, chips, and even barks. The quality of wood pellets strongly depends on the quality of the feedstock. A typical pellet plant includes a several unit operations: drying for moisture removal, grinding for size reduction, densification for pelletization, cooling, bagging, and storage. The final product is usually transported by trucks, railcars, and ocean vessels for delivery to domestic and international customers.

In 2005, a combination of torrefaction and pelletization process (TOP) was proposed by Energy Research Centre of Netherlands (ECN) [Bergman 2005]. Torrefaction is a thermal treatment without air or oxygen at 200-300 °C and low particle heating rates (<50 K min^{-1}) with a long residence time (>1 min). During torrefaction, the biomass can increase the energy density on the mass basis and improve the hydrophobicity of the biomass surface. Pelletization, on the other hand, can increase the volumetric energy density, and reduce dust generation. The bulk densities of torrefied wood pellets range from 750 to 850 kg m^{-3}, with a LHV ranging from 20.4 to 22.7 MJ kg^{-1} and the energy density from 14.9 to 18.4 GJ m^{-3} [Bergman 2005]. In comparison with conventional pellets, torrefied pellets can be about 1.4-2.4 times higher in the energy density, which will lower the transportation cost significantly for long distance transportation. Canada holds abundant forest resources for the production of wood pellets. In recent years, Canada has become a major producer and exporter of wood pellets, and can potentially become the largest wood pellet production centre in the future due to its abundant forest resources and its unique location. Therefore, the torrefaction process may be suitable for Canadian wood pellets exported to international market.

1.2 Structure, Composition, Properties of Wood

The physical structures, major chemical compositions, and chemical structures of wood are extremely important for studying thermal chemical behaviours of wood [Orfao 2001]. Wood is composed of microfibrils, bundles of cellulose molecules (C_6 polymers) surrounded by hemicelluloses (predominantly C_5 polymers but including C_6 species). In between the microfibrils, lignin consisting of phenyl-propane molecules is deposited. Extractives are located in the epithelial cells lining the resin canals and flow in the resin canals in the wood.

The cellulose molecules consist of long chains of glucose molecules (normally 8000-10000 glucose molecules), with a general formula of $(C_6H_{10}O_5)_n$ [Sjostrom 1993]. Cotton is almost pure α-cellulose. Cellulose is insoluble in water. The hemicelluloses also consist of glucose molecules and other simple saccharides (normally up to 200 glucose/saccharide molecules), with a general formula of $(C_5H_8O_4)_n$. Unlike cellulose, hemicelluloses are soluble in dilute alkali and consist of branched structures [Salisbury and Ross 1992]. The most abundant hemicelluloses are xylan. Lignin is highly branched, substituted, mononuclear aromatic polymers in the cell walls of certain biomass, especially woody species. Lignin can be broken by treatment with strong sulphuric acid, in which lignin is insoluble.

Normally, a tree consists of 3-8% bark, 3-8% needles (leaves), 7-15% branches, and 65-80% trunk [Delta Research Corporation 2006]. Softwoods are referred to gymnosperm trees (evergreens), which account for about 80% of the timber production source in the world. Hardwoods are referred to the wood from angiosperm (deciduous) trees. Table 1-1 shows the differences of major chemical compositions of softwoods and hardwoods. It is seen that in general softwoods have a much higher lignin content than hardwoods. Conifers such as pine, spruce and fir belong to softwoods. Typically, the pine consists of 40% cellulose, 28% hemi-celluloses, 28% lignin, and 4% extractives, and the outer bark of pine has more lignin, up to 48% (see Table 1-2). A growing tree has approximately 50% water content with variations from 35 to 65% between winter and summer. Normally, the moisture content of the trunk of pine ranges from 45% to 60%, branches 51-56%, and bark 35-65% (see Table 1-3). The wood extractives have the highest heating value in the wood, and lignin has higher heating value than cellulose and hemicelluloses. Typically, the heating value of cellulose is 17-18 GJ/t, hemicelluloses: 16-17 GJ/t, lignin: 25-26 GJ/t, extractives: 33-38 GJ/t (see Table 1-4). There is a slight

difference in heating values of different species and different parts of a tree (see Table 1-5).

Table 1-1 Major chemical compositions of dry softwoods and hardwoods

	Softwoods	Hardwoods
Cellulose	40 – 44%	43 - 47%
Hemicelluloses	25 – 29%	25 -35%
Lignin	25 – 31%	17 – 23%
Extractives	1 – 5%	2 - 8%

Source: Thomas (1977)

Table 1-2 Chemical compositions of woods (bone dry material)

Species	Cellulose, %	Hemicelluloses, %	Lignin, %	Extractives, %	Ash, %
Pine (70 years old)	40	28	28	4	
Trunk	41	27	28	3	1
Bark, inner	36	26	29	5	4
Bark, outer	25	20	48	3	4
Branches	32	32	31	4	1
Needles	29	25	28	13	5
Spruce (110 years old)	42	28	27	2	
Trunk	43	27	28	1	1
Bark	36	20	36	4	4
Branches	29	30	37	2	2
Needles	28	25	35	7	5

Source: Lehtikangas (1999)

Table 1-3 Average moisture content of trees

Species	Trunk	Bark	Branches
Pine	45 – 60%	35 – 65%	51 – 56%
Spruce	40 – 60%	45 – 65%	42 – 46%

Source: Lehtikangas (1999)

Table 1-4 Heating values of the wood chemical components

Chemical Components	Heating Value $MJ\ kg^{-1}$
Cellulose	17 - 18
Hemicelluloses	16 – 17
Lignin	25 – 26
Extractives	33 - 38

Source: Lehtikangas (1999)

Table 1-5 Heating values of different species and different parts of a tree

Items	Unit	Pine	Spruce
Trunk wood with bark	$MJ\ kg^{-1}$	19.3	19.1
Whole tree chips	$MJ\ kg^{-1}$	19.6	19.2
Harvesting residue (excluding needles)	$MJ\ kg^{-1}$	20.4	19.7

Source: Hakkila (1978)

1.3 Thermal Treatment of Wood

During thermal treatment, the decomposition of wood can start at a temperature higher than 130 °C [Chen et al. 2003]. The cellulose, hemicelluloses (xylan, glucuronoxylan, arabinoxylan, glucomannan, and xyloglucan), and lignin behave differently (see Figure 1-1). Hemicelluloses, the most reactive compounds, decompose at the temperature range of 225-325 °C, cellulose at 305-375 °C and lignin gradually over the temperature range of 250-500 °C [Shafizadeh 1985].
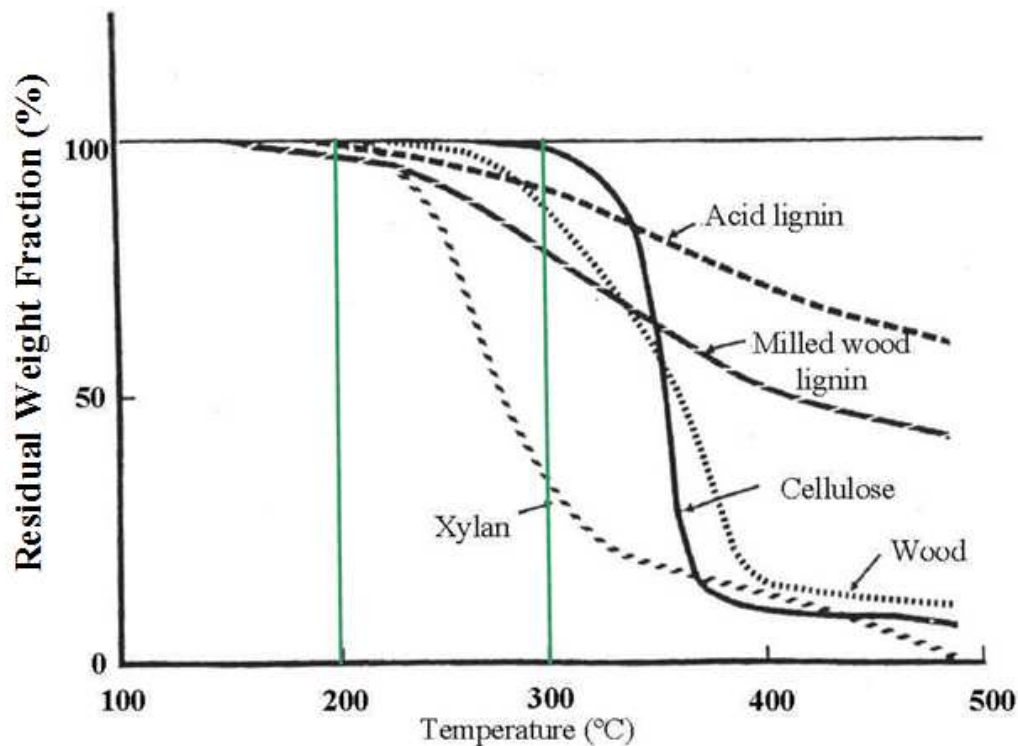
Figure 1-1 Thermal decomposition of wood

(Modified from Shafizadeh 1971with permission from Elsevier)

5

All of these decomposition stages can be grouped into five main reaction regimes at different temperatures (see Figure 1-2) [Shafizadeh 1982, Golova 1975, Halpern and Patal 1969, Koukios 1994]:

Regime A: Conventional drying,

Regime B: Glass transition (also called softening) and infusion of lignin,

Regime C: Depolymerization followed by condensation of the shortened polymers,

Regime D: Devolatilization and carbonization of polymers,

Regime E: Extensive carbonization of all polymers and structures.
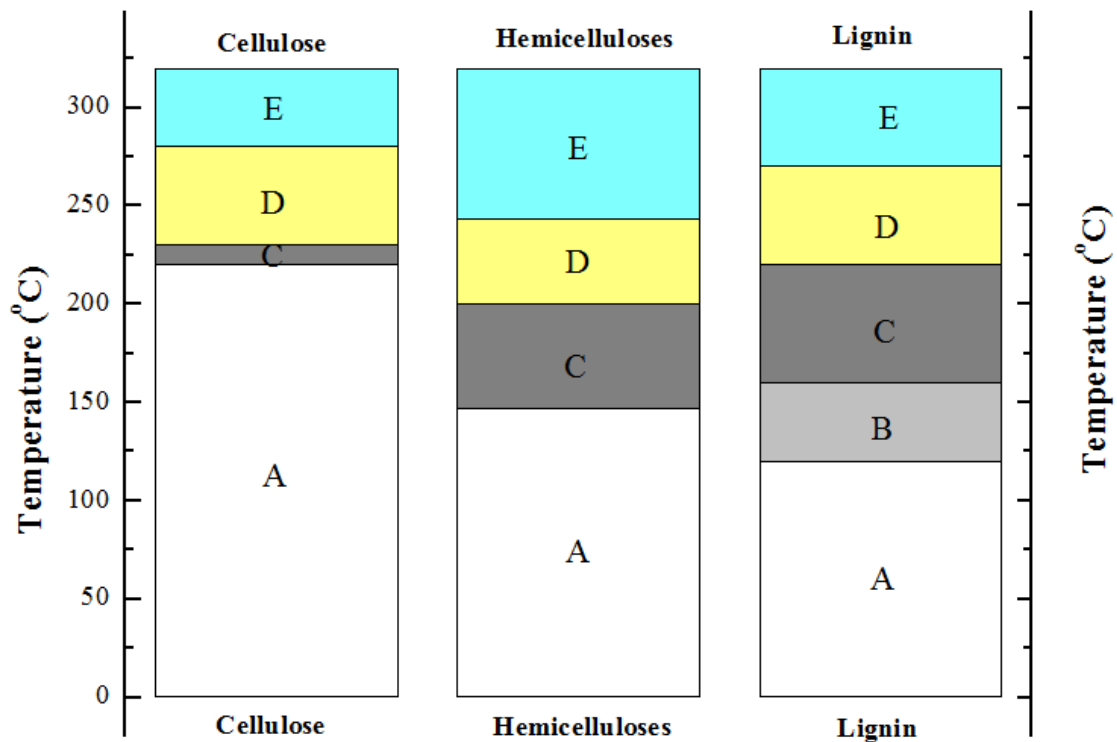
Figure 1-2 Main physic-chemical phenomena of the main components of wood
(A: Drying, B: Glass Transition/Softening, C: Depolymerization and Recondensation, D: Limited Devolatilization and Carbonization, E: Extensive Devolatilization and Carbonization)

Based on the operation temperature, the thermal treatment of wood can be divided into four processes: conventional drying, heat treatment, torrefaction, and pyrolysis. The

conventional drying process occurs at the temperature below 100-130 °C for evaporating most moisture.   Heat treatment of lumber, also called low temperature torrefaction, takes place in kilns with superheated steam at the temperature range of 185-220 °C for increasing the durability, mechanical dimensional stability and water repellent characteristics.   Torrefaction, also called mild pyrolysis, is a thermal treatment without oxygen in the temperature range of 200-300 °C, and usually, the reactions take place at low particle heating rates (<50 $K\ min^{-1}$) with a long residence time, with the final product called torrefied wood [Bergman and Prins 2005].

Pyrolysis is a process without air or oxygen for thermal conversion of wood at temperatures in the range of 400-800 °C. At this temperature range, most of the cellulose, hemicelluloses and part of the lignin will disintegrate to form smaller and lighter molecules, which are mostly gases. As these gases cool, some of the vapors condense to form a liquid, which is called bio-oil (or tar). The remaining wood residue, mainly from parts of the lignin, is a solid called charcoal. The pyrolysis product distribution depends on the heating rate, residence time and maximum reaction temperature. If the purpose is to produce the bio-oil, high heating and heat transfer rates at a carefully controlled temperature range (up to about 650 °C), and a very short residence time (typically less than one second) are preferred. According to the study of Roy et al. (1987), in the fast pyrolysis process, 25% of the pyrolysis product went to charcoal, which contains 40% of the initial energy content, 47% of the mass is converted into the bio-oil, containing 52% of the energy content of wood, 11% of the mass goes to gases, containing only 4% of the energy content, and the other 17% of the mass is water (see Figure 1-3).
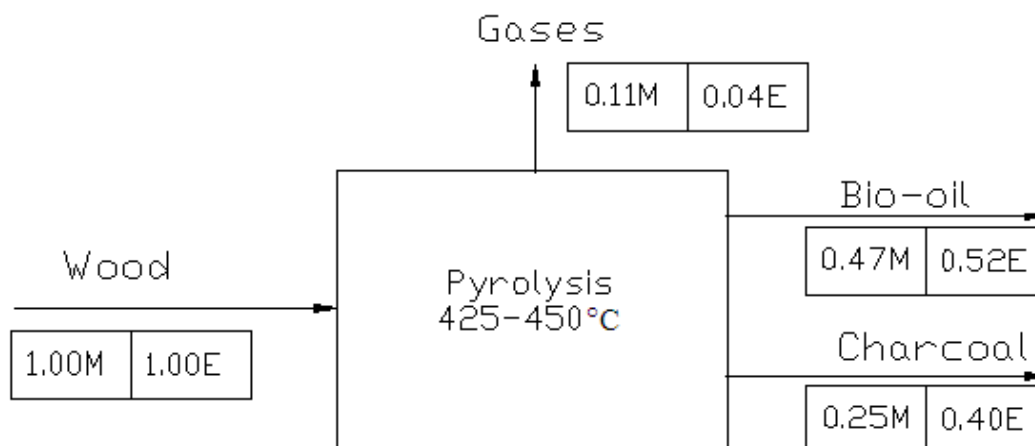
Figure 1-3 Typical mass and energy balance of wood pyrolysis

(Symbols: E=energy, M=mass)

The pyrolysis gases have low $CO + H_2$ content and thus low heating value. Typically, syn-gas ($CO + H_2$) content is under 57 mol% (normally, industrial syn-gas contains more than 70% of CO and H_2), and the heating value is 6.9 $MJ\ kg^{-1}$ (industrial syn-gas >8 $MJ\ kg^{-1}$) [Roy 1987] (see Table 1-6). The properties limit its final use. The solid product of charcoal is used in both industry and household. The liquid product, called bio-oil, is highly acidic (typically pH <2.5), which requires special corrosion resistant materials for transportation, storage and applications. The second problem is that bio-oil has a very low heating value (typically in the range of 17-19 $MJ\ kg^{-1}$), which is not competitive with fossil-based energy (conventional oil 43 $MJ\ kg^{-1}$, coal 29 $MJ\ kg^{-1}$). The third problem is that the production cost for bio-oil is very high. Studies indicated that the cost of bio-oil can be up to 300 $€\ t^{-1}$ [European Biomass Industry Association 2012], which is equivalent to a crude oil price of 127 $US\ barrel^{-1}$ (1€=1.30$US, 2011). Today bio-oil is mainly used for the production of food additives. Table 1-7 shows typical pyrolysis charcoal and bio-oil properties. Slow pyrolysis of biomass for the production of solid charcoal or activated carbon has been successfully used in industries in many countries. For fast

pyrolysis technologies for bio-oil production, only a few small-scale bench units and pilot plants have been built. We believe that the use of pyrolysis to produce bio-oil for transportation purposes still has a very long way to go to penetrate the current liquid fuels market.

Table 1-6 Typical pyrolysis gas properties

Items	Number
Gross Heating Value, *MJ kg⁻¹*	6.9
Gas phase composition, mol %	
CO_2	46.58
CO	36.83
CH_4	4.32
H_2	9.88
C_1-C_4	1.12
Methanol, ethanol, acetone and acetaldehyde	1.26

Source: Roy (1987)

Table 1-7 Typical pyrolysis charcoal and bio-oil properties

Item	Charcoal	Bi-Oil
Water Content, %wt	<1	4.4
Gross Heating Value, *MJ kg⁻¹*	32	22.5
Elemental Analysis, %wt		
C	84.4	55.6
H	3.5	5.8
N	0.2	0.7
S	0.8	0.6
O	11.1	37.3
Proximate Analysis, %wt		
Ash	2.8	0.13
Volatile Matter	18.5	
Fixed Carbon	78.7	
Specific Surface, BET, *m² g⁻¹*	>3	

Source: Roy (1987)

1.4 A Review of Mild Pyrolysis Kinetics

Torrefaction is a mild pyrolysis, with the pyrolysis being widely studied and documented. Several review papers on the reaction mechanisms and the kinetic models of pyrolysis have been published [Rousse 2004; Mohan and Steele 2006; Gronli 1996; Blasi 2008; Turner et al. 2010; van de Stelt et al. 2011; Chew and Doshi 2011]. In this section, the mechanism and kinetics model for pyrolysis of wood and its major chemical compositions at low temperatures of relevance to torrefaction conditions have been reviewed.

Cellulose, hemicelluloses, lignin, and extractives are four major chemical compositions of wood. Extractives of wood include fats, waxes, alkaloids, proteins, phenolics, simple sugars, pectins, mucilages, gums, resins, terpenes, starches, glycosides, saponins, and essential oils and vary from species to species. Typically, the softwood consists of 42% cellulose, 27% hemicelluloses, 28% lignin, and 3% extractives; and the hardwood is 45% cellulose, 30% hemicelluloses, 20% lignin, and 5% extractives [Thomas 1977]. Inorganic matter, also called ash, consists of less than 1% of content in wood (15% in some agricultural residues) [Blasi et al. 1999].

Generally, pyrolysis products are categorized into three groups: permanent gases (CO_2, CO, CH_4 and small amounts of H_2 and C_2 hydrocarbons), tars, and chars, or simply into volatiles (low molecular weight gaseous species, in addition to all condensable, aqueous and high molecular weight organic compounds or tars) and chars [Prins et al. 2006c]. Literatures generally agreed that the reaction temperature plays an important role in pyrolysis at different reaction conditions such as different experimental devices and different characteristics of samples, with different types of pyrolysis kinetics having been proposed.

1.4.1 Cellulose

Cellulose is the most abundant organic substance of wood. The cellulose molecules (C_6 polymers) consist of long linear chains of glucose molecules (normally 8,000-10,000 glucose molecules with a molecular weight range of 300,000-500,000) with a general formula of $(C_6H_{10}O_5)_n$, and form intra and intermolecular hydrogen bonds. Cotton almost is pure α-cellulose. Wood cellulose is mostly generated from the pulp and paper industry. With its fibrous structure and strong hydrogen bonding, cellulose provides wood's strength and is insoluble in most solvents. Cellulose is the most extensively studied material in the field of biomass pyrolysis. Although a significant number of papers have been published, researchers still continue their efforts to improve the mechanisms and models of cellulose pyrolysis.

Shafizadeh (1982) proposed that in the range of 423-573 K cellulose decomposition followed a free radical reaction mechanism. From 423 to 523 K, the cellulose macromolecules rapidly broke into glucose of a molecular weight of about 200, called the "reaction intermediate" ("active cellulose", "anhydrocellulose", or "levoglucosan"), resulting from the rupture of cellulose molecules without the weight loss [Golova 1975]. The weight loss started at 523 K [Gaur and Thomas 1998]. Between 523 and 573 K, the weight loss was caused by dehydration reactions via bond scission with the elimination of H_2O, carbonyl and carboxyl group formation reactions with the elimination of CO and CO_2, and limited devolatilization and carbonization for the production of final tars and chars [Halpern and Patal 1969]. At temperatures above 573 K, the extensive devolatilization involving free radical cleavage of the glucosidic bond (the formation of tars and gases) and the extensive carbonization involving the formation of intermediate carbonium ions (the formation of chars) became dominant. The extensive devolatilization

11

involves free radical cleavage of the glucosidic bond (end-group depolymerization), leading to the formation of tars and gases. The extensive carbonization involves the formation of intermediate carbonium ions (ring scission), leading to chars. The maximum weight loss of cellulose occurs at about 623K.

There are several kinetic models for cellulose pyrolysis. The simplest model for cellulose pyrolysis is a one-step model.

$$Cellulose \xrightarrow{\ k\ } Volatiles + Chars$$
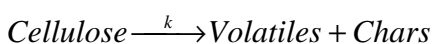
Table 1-8 shows some of the determined one-step first order reaction kinetics model equations for the pyrolysis of cellulose. The activation energy ranged widely from 89 to 260 $kJ\ mol^{-1}$ likely due to the differences in heating programming, TGA devices, types of samples, and even the mathematical procedure for fitting the TG data.

Table 1-8 One-step model reaction kinetic constants for cellulose pyrolysis

Authors	Operating conditions	Reaction rates, s^{-1}
Tang et al., 1964	TGA, 473-733K, 3 K min^{-1}	k=4.3X10^{12}exp(-242400/RT)
Akita et al., 1967	TGA, 0.23-5 K min^{-1}	k=6.6X10^{16}exp(-224000/RT)
Fairbridge et al., 1978	TGA, 7 K min^{-1}	k=2.4X10^{20}exp(-248000/RT)
Bilbao et al., 1989	TGA, 533-563 K, Isothermal	k=1.8X10^{11}exp(-113000/RT)
Williams et al., 1994	TGA, 473-773 K, 5 K min^{-1}	k=3.8X10^{21}exp(-260000/RT)
	80 K min^{-1}	k=9.6X10^{14}exp(-188000/RT)
Orfao et al., 2001	TGA, 450-700 K, 5 K min^{-1}	k=4.0X10^{7}exp(-89000/RT)
Chen and Kuo, 2011b	TGA, 473-573 K Isothermal	k=2.86X10^{9}exp(-124420/RT)

Parks et al. (1955) suggested that cellulose first depolymerized to levoglucosan with a first order reaction. Then the levoglucosan proceeded with two reactions: to form chars with repolymerization and aromatization, and to crack to produce tars and gases.

$$Cellulose \rightarrow Levoglu\cos an \rightarrow Tars + Gases$$

$$\downarrow$$

$$Chars$$
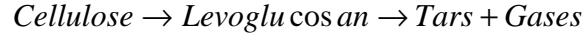
Broido et al. (1965), based on the TG analysis, suggested that the pure cellulose decomposed via two competitive endothermic reaction processes. In the range of 493-553 K, an initial endothermic dehydration reaction of cellulose produced "anhydrocellulose" tars and water. Above 553 K, the endothermic depolymerization of the "anhydrocellulose" led to the formation of chars and gases.

$$Cellulose \rightarrow Anhydrocellulose + H_2O \rightarrow 0.35 Chars + 0.65 Gases$$

$$\downarrow$$

$$Tars$$
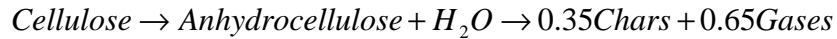
In order to fit the Broido et al. (1965) data to an experimental curve, Broido and Weinstein (1971) modified the original Broido model by adding one more reaction step.

$$Cellulose \rightarrow \Pr ecursor \rightarrow Anhydrocellulose + H_2O \rightarrow Anhydroglu\cos e + H_2O \rightarrow Chars$$

$$\downarrow$$

$$Tars$$
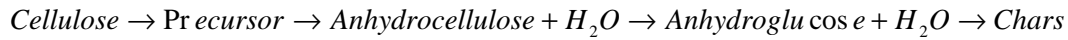
Bradury et al. (1979) proposed a Broido-Shafizadeh model. An initiation reaction led to the formation of "activated cellulose". The "activated cellulose" then decomposed following two competitive first order reactions: one producing volatiles, and the other yielding chars and gases.

$$Cellulose \rightarrow Activated \quad Cellulose \rightarrow Volatiles$$

$$\downarrow$$

$$Chars + Gases$$

13
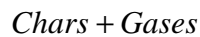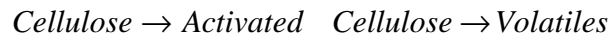
Varhegyi et al. (1994) proposed a modified Broido-Shafizadeh model. In this model, the "activated cellulose" was eliminated, and a fractional ratio between chars and gases was introduced.

$$Cellulose \longrightarrow v_C Chars + (1 - v_C) Gases$$

$$\downarrow$$

$$Tars$$
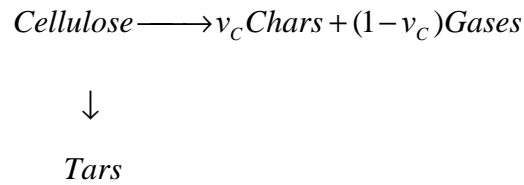
1.4.2 Hemicelluloses

The second chemical composition of wood is hemicelluloses. Hemicelluloses (predominantly C_5 polymers but also including C_6 species) are a mixture of various polymerized monosaccharides such as glucose, mannose, galactose, xylose, arabinose, 4-O-methyl glucuronic acid and galactuonice acid residues, and consist of glucose molecules and other simple saccharides (normally 50-200 glucose/saccharide molecules with the molecular weight up to 32,000) with a general formula of $(C_5H_8O_4)_n$. Unlike cellulose, hemicelluloses have branched structures that vary with wood species. The most abundant hemicelluloses are xylan. Hemicelluloses are easy to hydrolyse, and soluble in dilute alkali. Compared to cellulose, few studies have been done on hemicelluloses pyrolysis because of its unstable nature and different chemical behaviour from species to species.

Blasi and Lanzetta (1997) proposed a two-step mechanism for the thermal decomposition of hemicelluloses. The reactions in the first step at temperatures below 423 K were depolymerization, leading to the formation of altered and rearranged polysugar structures. In the range of 423-573 K, the second step reactions, including the decomposition of oligosaccharides and monosaccharides, formed chars, CO, CO_2 and H_2O. Light volatiles such as carbonyl compounds formed from the fragmentation of the carbon skeleton.

The simplest kinetic model for hemicelluloses pyrolysis is the one-step model.

$$Hemicelluloses \xrightarrow{\quad k \quad} Volatiles + Chars$$
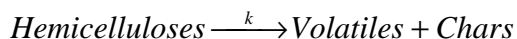
As shown in Table 1-9, the activation energy of hemicelluloses pyrolysis ranges from 43 to 258 $kJ\ mol^{-1}$. Williams et al. (1993) reported that the increase in heating rate causes the decrease of the activation energy.

Table 1-9 One-step model reaction kinetic constants for hemicellulose pyrolysis

Authors	Operating conditions	Reaction rates, s^{-1}
Stamm, 1956	Isothermal glass bulb reactor, 383-493K	$k=1.3\times10^{14}exp(-111000/RT)$
Ramiah, 1970	Isothermal TGA, 488-523K	$k=7.8\times10^{12}exp(-125000/RT)$
Hirata, 1974	TGA, 513-523K, 5 K min^{-1}	$k=1.7\times10^{20}exp(-119000/RT)$
Min. 1977	Ceramic tube, up to 833K, 30 K min^{-1}	$k=5.2\times10^{12}exp(-124000/RT)$
Bilbao et al., 1989	TGA, 473-673K, 1.5 K min^{-1}	$k=3.5\times10^{4}exp(-43000/RT)$
	20 K min^{-1}	$k=7.2\times10^{7}exp(-72000/RT)$
	80 K min^{-1}	$k=2.7\times10^{9}exp(-86000/RT)$
Williams et al.,1993	TGA, up to 993K, 5 K min^{-1}	$k=6.7\times10^{25}exp(-258000/RT)$
	20 K min^{-1}	$k=9.6\times10^{7}exp(-257000/RT)$
	40 K min^{-1}	$k=1.1\times10^{19}exp(-194000/RT)$
	80 K min^{-1}	$k=5.8\times10^{12}exp(-125000/RT)$

More complicated kinetic models have also been proposed in the literature. Chen and Kuo (2011b) proposed a one-step model with 3rd order reaction for the torrefaction of hemicelluloses and a one-step model with 9th order reation for the torrefaction of xylan. Several multi-step pyrolysis models for hemicelluloses were proposed in some studies [Shimiza et al. 1969; Blasi et al., 1997; Koufopanos et al. 1989] based on pyrolysis of xylan and related compounds. Some authors also argued that hemicelluloses pyrolysis could not be modeled by simple kinetic models [Orfao et al. 1999].

$$Hemicelluloses \longrightarrow Volatiles \qquad\qquad \text{[Shimiza et al. 1969]}$$

$$\downarrow$$

$$Chars + Gases$$

$$Hemicelluloses \rightarrow Intermediates \rightarrow Chars \qquad \text{[Blasi et al. 1997]}$$

$$\downarrow \qquad\qquad\qquad \downarrow$$

$$Volatiles \qquad\qquad Volatiles$$

$$Hemicelluloses \rightarrow \text{Intermediate} \rightarrow Volatiles \qquad \text{[Koufopanos et al. 1989]}$$

$$\downarrow$$

$$Chars + Gases$$

1.4.3 Lignin

The third chemical composition of wood is lignin. Lignin is referred to the complex three-dimensional mononuclear aromatic polymers(p-coumaryl, coniferyl, and sinapyl structures) that consists of an irregular array of variously bounded "hydroxy-" and "methoxy-" substituted phenyl propane units, highly branched. The physical and chemical properties of lignin vary significantly from species to species, with lignin extracted from a same biomass depending on the extraction or isolation method used. Lignin is the main binder for the agglomeration of fibrous cellulosic components with an amorphous structure and interlinkages and covalent linkages between individual units, causing the non-selective random reactions. The structure and chemistry are still unclear. Lignin generally cannot be broken down into simple monomeric units and is insoluble in most solvents. The lignocellulosic complex can be broken by treatment with strong sulphuric acid to separate the lignin fraction. Therefore, thermal decomposition studies on lignin extracted from biomass will not necessarily match the pyrolysis behaviour of lignin present in the original biomass. Few studies have been conducted on pyrolysis of the extracted lignin and the pseudo-lignin.

Thermal degradation of lignin occurs over a wide range of temperatures, resulting in 30-50% of chars and a significant amount of gases. At below 473 K, lignin pyrolysis occurs with a small weight loss. In the range of 513-573 K, chars and volatiles can be produced by devolatilization and carbonization. Extensive devolatilization and carbonization of lignin occur at temperatures above 573 K, with the maximum weight loss at 673 K. Since lignin contains various oxygen functionalities that have different thermal stability, the scission of the functional groups takes place at different temperatures. For instance, products from decomposition of hardwood lignin are different from softwood lignin, and different reaction mechanism is thus expected. The presence of cations (Na^+, NH_4^+, Ca_2^+) also has a significant effect on the decomposition result.

Tang (1967) proposed a simple one-step global reaction model for lignin pyrolysis based on TG results under vacuum conditions at two temperature stages for lignin isolated from spruce by sulfuric acid. In this case, activation energies of 87.8 *kJ mol^{-1}* in the range of 553-617 K and 37.6 *kJ mol^{-1}* in the range of 617-708 K were found. Williams et al. (1994) reported the activation energy of the pseudo-lignin as 124 *kJ mol^{-1}* (see Table 1-10).

Table 1-10 One-step model reaction kinetic constants for lignin pyrolysis at low temperatures

Authors	Operating conditions	Reaction rates, s^{-1}
Tang, 1967	TGA, 553-617 K	k=5.9X10^{7}exp(-87800/RT)
	617-708 K	k=3.4X10^{3}exp(-37600/RT)
Williams et al., 1994	TGA, 423-773 K, 5K min^{-1}	k=1.5X10^{11}exp(-124000/RT)
Chen and Kuo, 2011a	TGA, 473-573 K Isothermal	k=6.6exp(-37580/RT)

1.4.4 Wood

Due to the multiple components composition of wood, its associated properties and transport phenomena, and the existence of a large number of complex reactions, it is difficult to derive a widely acceptable biomass thermal chemical conversion kinetic model. Another difficulty in kinetic study of wood lies in the decoupling of the chemistry from transport phenomena. Therefore, for simplification, most studies have used the overall and lumped reaction kinetics.

The simplest kinetic model for wood pyrolysis is a one-step model.

$$Wood \xrightarrow{k} Volatiles + Chars$$

Table 1-11 shows a summary of one-step model reaction kinetic constants for wood pyrolysis. The activation energy varies widely from 88 to 174 $kJ\ mol^{-1}$ under different heating conditions, using different experimental devices (TGA, tube furnaces, entrained and fluid bed reactors, screen heaters, and drop tubes) and samples of different characteristics (size, mass, and wood species), and applying different mathematical treatment methods for the experimental data.

Table 1-11 One-step model reaction kinetic constants for wood pyrolysis

Authors	Materials	n	Operating conditions	Reaction rates, s^{-1}
Rogers et al. 1980	Whatman	0.5	TGA, 473-673 K, 1.5K/min, N_2	$k=2.1 \times 10^{11} \exp(-153000/RT)$
Thurner et al. 1981	Oak, 650 µm	1	Isotherm tube furnace, 573-673 K	$k=2.47 \times 10^{6} \exp(-106500/RT)$
Gorton et al. 1984	Hardwood, 300-350 µm	1	Isotherm entrained flow reactor, 677-822 K	$k=1.483 \times 10^{6} \exp(-89520/RT)$
Ward et al. 1985	Wild cherry	1	Isotherm tube furnace, 538-593 K	$k=1.19 \times 10^{12} \exp(-173700/RT)$
Font et al. 1990	Almond shells,300-500 µm	1	Pyroprobe 100, 733-878 K	$k=1.885 \times 10^{6} \exp(-108000/RT)$
Gronli et al. 1992	Pine	1	TGA,423-773 K,	$k=5.01 \times 10^{8} \exp(-88000/RT)$
	Epicea	1	5 K min^{-1}	$k=1.58 \times 10^{6} \exp(-92000/RT)$
Avat 1993	Hetre	0.01	TG, dynamic, 293-673K, 5 K min^{-1}	$k=7.7 \times 10^{9} \exp(-111000/RT)$
Wagenaar et al. 1993	Pine, 100-125 µm	1	TGA drop tube, 553-673 K	$k=1.4 \times 10^{10} \exp(-150000/RT)$
Reina et al. 1998	Forest waste, <1000 µm,	1	Isotherm TGA, 498-598 K	$k=7.68 \times 10^{7} \exp(-124870/RT)$
	25 mg	1	973-1173 K	$k=6.33 \times 10^{2} \exp(-91530/RT)$
Blasi et al. 2001	Beech, <80 µm, 9 mg	1	Tube furnace, 573-708 K	(a)$k=2.4 \times 10^{5} \exp(-95400/RT)$
				(b)$k=4.4 \times 10^{9} \exp(-141000/RT)$

Shafizadeh and Chin (1977) proposed a one-component three-reaction kinetic model at fast heating rates or high temperatures for the evolution of each main product fraction.

$$Chars$$
$$\uparrow k_C$$
$$Wood \xrightarrow{\;k_L\;} Tars$$
$$\downarrow k_G$$
$$Gases$$

Table 1-12 shows a summary of kinetic constants for the one-component model for wood pyrolysis.

Table 1-12 One-component model reaction kinetic constants for wood pyrolysis

Authors	Materials	n	Operating conditions	Reaction rate, s^{-1}
Thurner et al. 1981	Oak, 650 μm	1	Isotherm tube furnace, 573-673 K	$k_C=7.4\times10^5\exp(-106500/RT)$
				$k_L=4.12\times10^6\exp(-112700/RT)$
				$k_G=1.43\times10^4\exp(-88600/RT)$
Chan et al. 1985				$k_C=1.08\times10^7\exp(-121000/RT)$
				$k_L=2\times10^8\exp(-133000/RT)$
				$k_G=5.13\times10^8\exp(-92100/RT)$
Font et al. 1990	Almond shells, 300-500 μm, 2 mg	1	Pyroprobe 100, 733-878 K	$k_C=2.98\times10^3\exp(-73000/RT)$
				$k_L=5.85\times10^6\exp(-119000/RT)$
				$k_G=1.52\times10^7\exp(-139000/RT)$
Wagenaar et al. 1993	Pine, 100-125 μm	1	TGA Drop tube, 553-673 K, 773-873 K	$k_C=3.05\times10^7\exp(-125000/RT)$
				$k_L=9.28\times10^9\exp(-149000/RT)$
				$k_G=1.11\times10^{11}\exp(-177000/RT)$
Blasi et al. 2001	Beech, <80 μm, 9 mg	1	Tube furnace, 573-708 K	$k_C=3.3\times10^6\exp(-112000/RT)$
				$k_L=1.1\times10^{10}\exp(-148000/RT)$
				$k_G=4.4\times10^9\exp(-153000/RT)$

Some researchers used multi-step models for wood pyrolysis to predict the reaction rates and the product yields.

$$Wood \rightarrow \mathrm{Re}action \quad Intermediates \rightarrow \mathrm{Re}action \quad Intermediates \rightarrow Chars$$

$$\downarrow \qquad\qquad \downarrow \qquad\qquad\qquad \downarrow$$

$$Volatiles \qquad Volatiles \qquad\qquad Volatiles$$
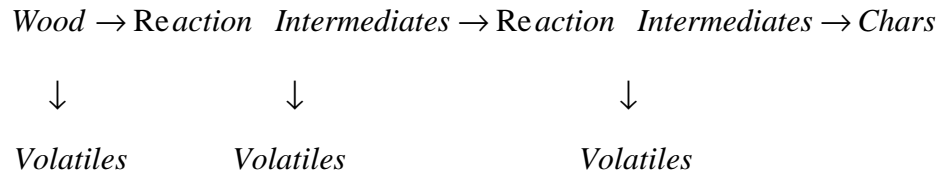
For a three-step model for wood pyrolysis, Branca and Blasi (2003), estimated the kinetic parameters for beech wood for three-step reactions at different temperature ranges: depolymerization (528-593 K), devolatilization (528-708 K), and charring (603-708 K).

The dynamic thermogravimetric analysis of wood materials shows over-lapped peaks for the decomposition of cellulose, hemicelluloses, lignin, and extractives for weight loss over a wide temperature range [Gronli et al. 2002]. A practical way for the mathematical description of the process is the assumption that each pseudo-component is formed by

different fractions of wood's major organic components decomposing in a similar way within temperature ranges. For each pseudo-component, a conversion (reacted fraction) α_j and a reaction rate, $d\alpha_j/dt$, are defined. The overall reaction rates are a linear combination of these partial reactions:

$$\frac{\partial w^{calc}}{\partial t} = -\sum_{j=1}^{M} c_j \frac{\partial \alpha_j}{\partial t} \qquad (1\text{-}1)$$

$$\frac{\partial \alpha_j}{\partial t} = k_j (1-\alpha_j)^{n_j} \qquad (1\text{-}2)$$

$$k_j = A_j e^{-\frac{E_j}{RT}} \qquad (1\text{-}3)$$

Roberts (1971) proposed a two-component model for wood pyrolysis, based on the consideration that the reaction time of hemicelluloses in wood pyrolysis was only a few seconds. Therefore, wood pyrolysis could be modeled for the pyrolysis of cellulose and lignin.

$$Wood_{Cellulose} \rightarrow Volaties + Chars$$

$$Wood_{Lignin} \rightarrow Volatiles + Chars$$
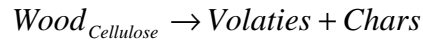
The reaction kinetic parameters were estimated by multi-peak decoupling curve fitting. Normally, the component contribution of hemicelluloses was roughly 20-30% for the total mass fraction, cellulose: 28-38%, and lignin: 10-15%. Table 1-13 shows the reported activation energies of pseudo-hemicelluloses, pseudo-cellulose, and pseudo-lignin with first order reaction by different researchers in the literatures.

Table 1-13 Three pseudo-component model reaction kinetic constants for wood pyrolysis

Authors	Materials	Operating conditions	Reaction rates, s^{-1}
Williams et al., 1994	Cellulose	TGA, 473-773K, 5K min^{-1}, N_2	$k=6.31\times10^{19}\exp(-260000/RT)$
	Cellulose	80 K min^{-1}, N_2	$k=1.587\times10^{13}\exp(-188000/RT)$
	Hemicelluloses	5 K min^{-1}	$k=2.1\times10^{22}\exp(-259000/RT)$
	Hemicelluloses	80 K min^{-1}, N_2	$k=1.58\times10^{9}\exp(-125000/RT)$
	Lignin	5 K min^{-1}	$k=2.51\times10^{9}\exp(-124000/RT)$
Orfao et al., 2001	Cellulose	TG, dynamic,450-700 K,	$k=6.6\times10^{5}\exp(-89000/RT)$
	Hemicelluloses	5 K min^{-1}, N_2	$k=1.1\times10^{5}\exp(-198000/RT)$
	Lignin		$k=5.3\times10^{14}\exp(-18100/RT)$

Miller et al. (1996) proposed a multi-step and multi-component model for wood pyrolysis.

$$Components \rightarrow Intermediates \rightarrow Tars$$

$$\downarrow$$

$$\nu_C Chars + (1-\nu_C)Gases$$

Chen and Kuo (2011b) reported the torrefaction of a blend of cellulose, hemicelluloses, and lignin. The result showed that the weight loss of the blend was very close to the linear superposition of weight losses of the three chemical compositions torrefied individually.

1.4.5 Oxygen Effect

Senneca et al. (2002) suggested that the low-temperature oxidation of solid fuel has two parallel pathways. One is the direct burning of the pure solid fuel and the second is the oxidation of chars and volatiles produced by pyrolysis.

$$Fuel \xrightarrow{\quad Oxidation \quad} H_2O + CO_2 + CO$$

$$Fuel \xrightarrow{\quad Pyrolyssi \quad} Volatiles + Chars$$

$$Volatiles + Chars \xrightarrow{\quad Oxidation \quad} H_2O + CO_2 + CO$$
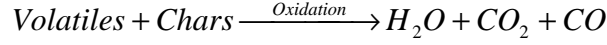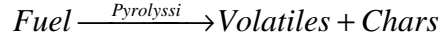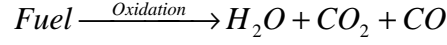
Senneca et al. (2004) further proposed a power law kinetics model for the oxidative pyrolysis of solid fuels based on fitting the weight loss TG curves with the oxygen concentration of 5-21%:

$$\frac{dx}{dt} = -k_{0,O_2} \exp(-\frac{E_{O_2}}{RT}) x^m P_{O_2}^n \tag{1-4}$$

where x is the solid conversion (dry basis), t is the reaction time, k_{0,O_2} is the pre-exponential factor of oxidation, E_{O_2} is the activation energy of oxidation, m is the reaction order with the partial pressure of oxygen, T is the reaction temperature, P_{O_2} is the partial pressure of oxygen level in the atmosphere, n is the oxygen effect reaction order.

Uemura et al. (2011) suggested that the reaction kinetics of oil palm empty fruit bunches (EFB) torrefaction with the oxygen concentration of 0-21% followed two parallel pathways. One is the hemicelluloses decomposition which represents the original trorrefaction reaction, and the other is the biomass oxidation.

$$-r_{overall} = (-r_{torrefaction}) + (-r_{oxidation}) = k_{torrefaction} C_{HC}^l + k_{oxidation} C_{EFB}^m C_{O_2}^n \tag{1-5}$$

where $-r_{overall}$ is the reaction rate of EFB, $-r_{torrefaction}$ is the torrefaction reaction rate of EFB, $-r_{oxidation}$ is the oxidation reaction rate of EFB, $k_{torrefaction}$ is the torrefaction reaction rate constant, $k_{oxidation}$ is the oxidation reaction rate constant, C_{HC} is the hemicelluloses concentration in EFB, C_{EFB} is the EFB concentration, C_{O2} is the oxygen concentration, l is the torrefaction reaction order, m is the reaction order with the partial pressure of oxygen, and n is the oxygen effect order.

1.4.6 Summary of Kinetics

The simple one-step kinetic model with the first order reaction can be used to predict the reaction time and the solid products formation rate for biomass pyrolysis.

$$Biomass \rightarrow Volatiles + Chars$$
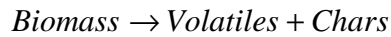
For the modeling of the biomass pyrolysis at temperatures below 573 K (torrefaction temperatures), Prins et al. (2006b) postulated that the weight loss of biomass degradation was primarily from the decomposition of hemicelluloses based on data from willow (hardwood, deciduous wood), and suggested that the Blasi and Lanzetta (1997) model, a two-step kinetic model with parallel reactions to form solids and volatiles, was suitable for biomass torrefaction (mild pyrolysis). They further showed that for wood pyrolysis below 573 K, the reactions were the rate-limiting step for particles smaller than 2 mm where the impact of intraparticle heat and mass transfer becomes insignificant.
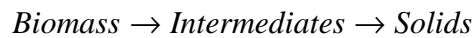
$$Biomass \rightarrow Intermediates \rightarrow Solids$$
$$\downarrow \qquad\qquad \downarrow$$
$$Volatiles \qquad Liquids$$

At the temperatures above 573 K, the Broido-Shafizadeh model for biomass degradation

24

has been widely used [Bradbury et al. 1979], which involved an initiation reaction of biomass leading to the formation of "Intermediates". Then the "Intermediates" decomposed following two competitive first order reactions, with one producing volatiles and the other yielding chars and gases.

$$Biomass \rightarrow Intermediates \rightarrow Volatiles$$
$$\downarrow$$
$$Chars + Gases$$
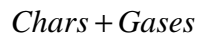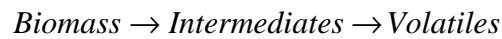
1.5 Wood Torrefaction

In the 1930's the principles of wood torrefaction were first reported and the technology was used to produce a gasified fuel [Bioenergy 2000]. In the 1980's, some attempts were made to use torrefied wood as the reduction agent in metallurgical applications, with a demonstration plant built, but then dismantled in the early 1990's. In the last decade, the torrefaction technology has been studied again for upgrading wood for different final uses, such as co-firing in existing coal-fired power stations [Bergman et al. 2005], gasification [Prins et al. 2006a; Deng et al. 2009], syn-gas production [Couhert et al. 2009], and barbeque fuel production [Winkler 2011].

Different wood behaves differently during torrefaction due to the different contents of components. Figure 1-4 shows that the mass loss of larch is lower than beech and willow. One of the reasons is that coniferous wood (larch) contains slightly more lignin than deciduous wood (beech and willow) (25-35 %wt versus 18-25 %wt), slightly less cellulose (35-50%wt versus 40-50%wt) and, on average, comparable amounts of the hemicelluloses (20-32%wt versus 15-35%wt). For xylan-based hemicelluloses, more than half of mass is lost at 267 °C (see Figure 1-4b).
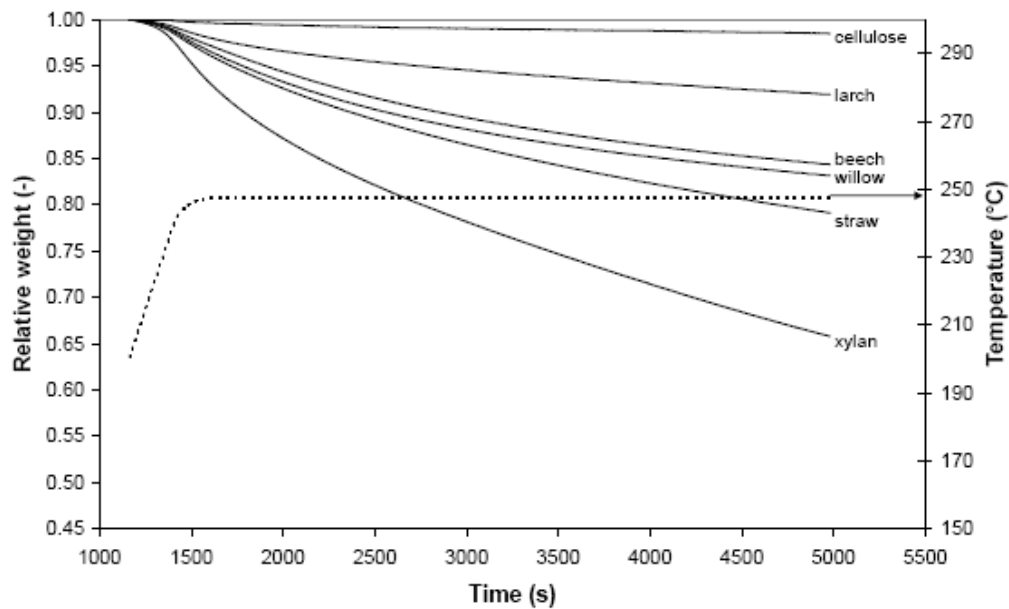
(a)
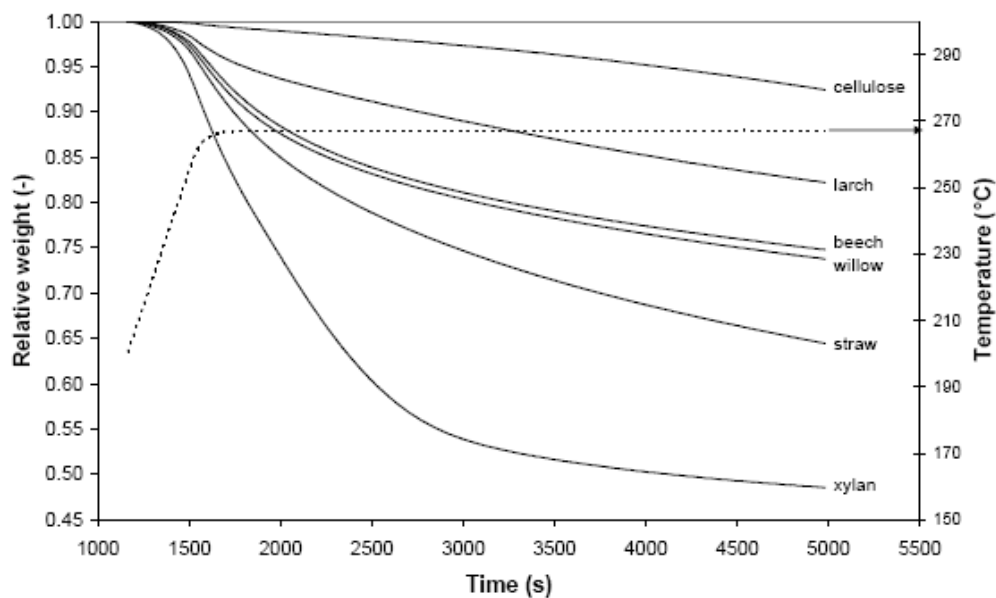
(b)

Figure 1-4 Torrefaction decomposition of the main components of woods
((a) at 248°C and (b) at 267°C, heating rate 10 K min^{-1}, particle size 0.5-2mm)
(Reprinted from Prins et al. 2006b with permission from Elsevier)

Many kinds of reactors have been considered for torrefaction. One typical wood
torrefaction process obtained from a batch fixed bed torrefaction reactor included several

stages (see Figure 1-5):

- **Drying:** The sample is heated by the furnace and flowing hot N_2 gas from room temperature to 200 °C. Free water and physically bound water are released during this stage, as well as some light organic compounds from evaporation.

- **Low Temperature Reaction:** The temperature of samples increases from 200 °C to the target torrefaction temperature. Decomposition starts at 200 °C.

- **Torrefaction:** The sample is maintained at the target torrefaction temperature over the target residence time.

- **Cooling:** Torrefaction stops when the sample is cooled to below 200 °C. The solid product is further cooled from 200 °C to the desired final temperature.
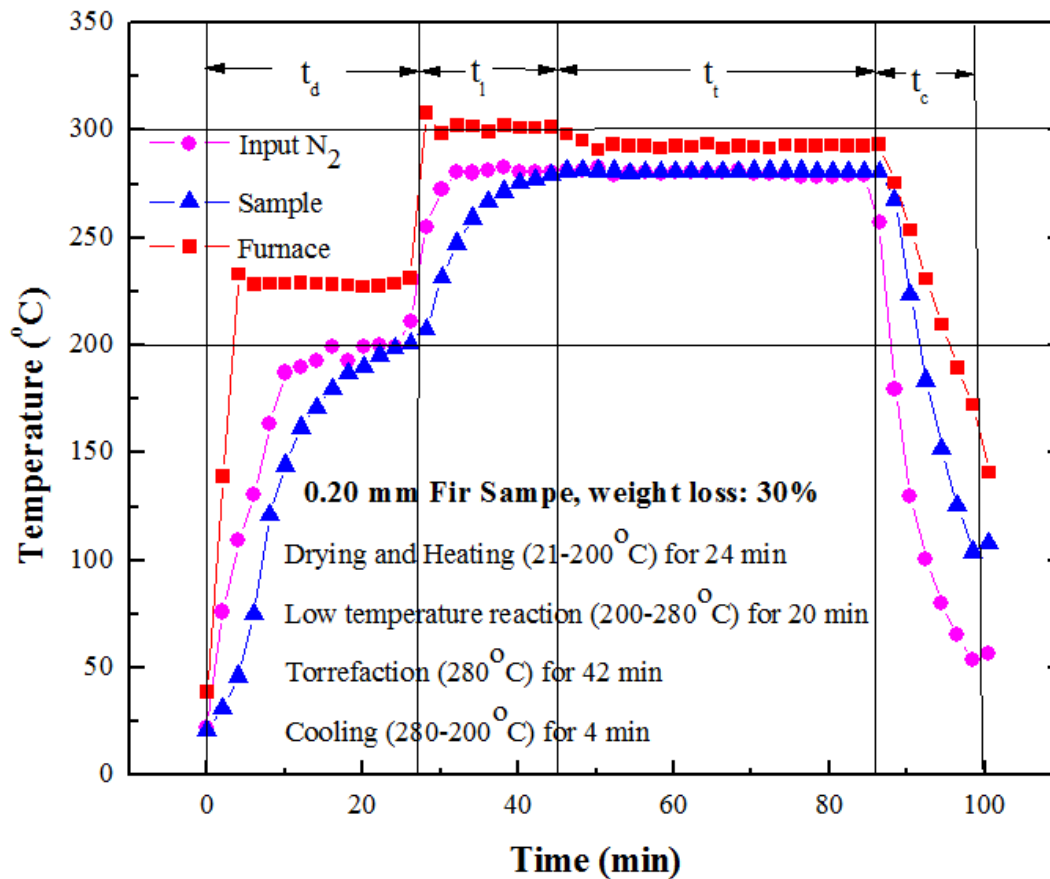
Figure 1-5 Typical torrefaction cycle
(t_d=drying time, t_l=low temperature reaction time,
t_t=reaction time at torrfaction temperature, t_c=cooling time)

The product distribution strongly depends on the torrefaction conditions (temperature, heating rate, and residence time) and the biomass properties. After torrefaction, biomass can be classified into three phases (gas, liquid, and solid) at the room temperature. The gas phase includes carbon dioxide and carbon monoxide with small amounts of hydrogen, methane, benzene and toluene. The liquid phase can be divided into reaction water, organics (sugars, polysugars, acids, alcohols, furans, ketones), and lipids (terpenes, phenols, fatty acids, waxes, tannins). The solid phase consists of original sugar structures, modified sugar structures, large newly formed polymeric structures, typical carbon rich char structures, and the ash fraction.

Prins et al. (2006a) provided an overview of mass and energy balances for torrefaction of dry willow, which includes two experimental runs: at a reaction temperature of 250 °C for a reaction time of 30 min, and 300 °C for 10 min (see Figure 1-6). During torrefaction, more volatiles are removed at higher temperatures so that the solid product for the two cases is 87% and 67%, respectively. The energy balance shows that 95% and 79% of the input energy are retained in the solid product, respectively. So, compared to the original willow, the increases of lower heating valve (LHV) on the mass basis for the torrefied willow for the two cases are 10% and 19%, respectively (see Table 1-14).

Table 1-14 Mass and energy balances for torrefaction of 1 kg dry willow

	Item	Torrefaction (250°C 30 min)		Torrefaction (300°C 10 min)	
		Mass, kg	LHV, kJ	Mass, kg	LHV, kJ
1	Solid				
	Torrefied wood	0.859	16883	0.655	14024
	Ash	0.013	0	0.013	0
	Total	0.872	16883	0.668	14024
2	Liquid (Condensable)				
	Water	0.057	0	0.066	0
	Acetic acid	0.021	300	0.072	1001
	Other organics	0.018	258	0.142	2280
	Total	0.096	558	0.28	3281
3	Gas (Permanent)				
	Carbon dioxide	0.029	0	0.04	0
	Carbon monoxide	0.003	30	0.012	121
	Hydrogen	Trace	1	Trace	1
	Methane	Negl.	0	Trace	2
	Total	0.032	31	0.052	124

Source: Prins et al. (2006a)
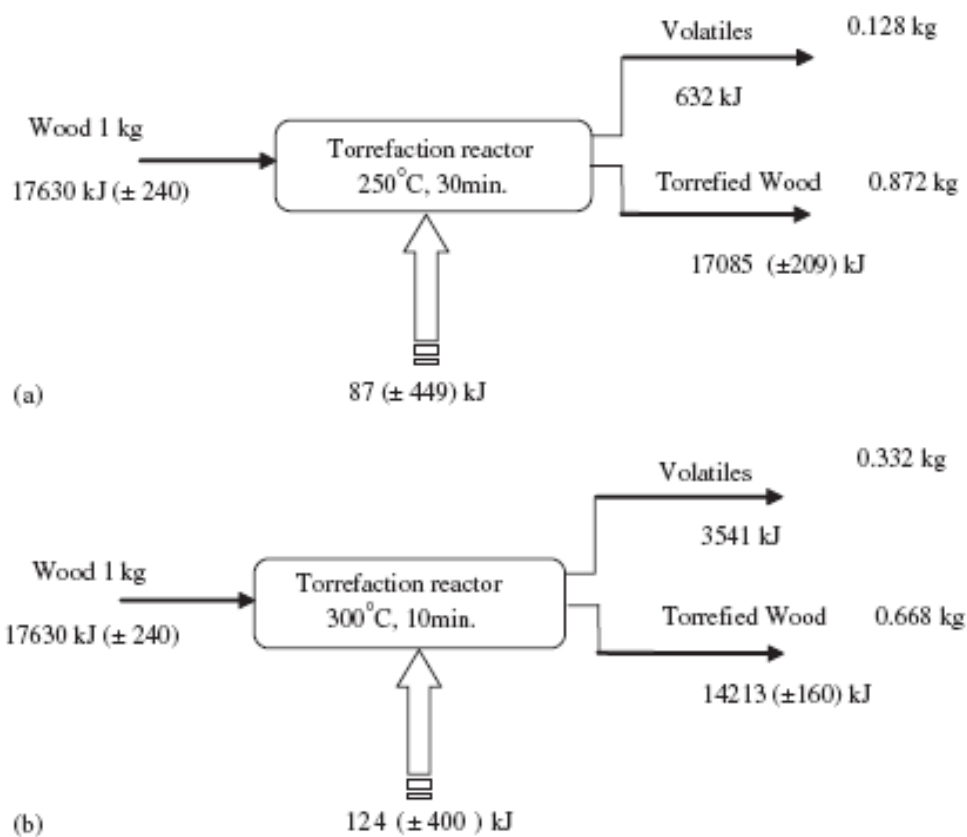
Figure 1-6 Overall mass and energy balances for torrefaction of dry willow
((a) 250°C and 30 min (b) 300°C and 10 min)
(Reprinted from Prins et al. 2006a with permission from Elsevier)

Torrefied wood has a brown colour. The properties of torrefied wood were found to be between wood and coal. After torrefaction, the LHV of willow increases from 17.6 to 19.4 and 21 *MJ kg⁻¹*, respectively, for the two temperatures investigated, because most of the weight loss is from hemicelluloses, which has a low energy content (see Table 1-15).

Some experimental studies with different targets have been conducted on the torrefaction of wood. The wood species, torrefaction temperature, and reaction time were considered to be the most influential parameters. Table 1-16 summarizes the energy yield and the high heating value increase of torrefied wood of different species.   From Table 1-16, the energy yield was in the range of 61-98%. The high heating value increase was in the range of 1 to 40%. Deep torrefaction can increase the heating value, but decrease the energy yield.

Table 1-15 Composition and LHV of willow and torrefied willow

Items	Wood	Torrefied Wood	
		250°C 30 min	300°C 10 min
Carbon	47.2%	51.3%	55.8%
Hydrogen	6.1%	5.9%	5.6%
Oxygen	45.1%	40.9%	36.2%
Nitrogen	0.3%	0.4%	0.5%
Ash	1.3%	1.5%	1.9%
LHV, MJ kg⁻¹	17.6	19.4	21.0

Source: Prins et al. (2006c)

Table 1-16 Energy yield and high heating value increase of torrefied different wood

Author	Wood	HHV MJ kg⁻¹	Operating conditions	Weigh loss %	HHV MJ kg⁻¹	Energy yield %	HHV increase %
Pach et al., 2002	Birch	16.44	250°C 60min	14.50	18.83	97.93	14.54
Felfli et al., 2005	Wood briquette	20.02	220°C 30min	6.00	20.43	95.91	2.05
		20.02	250°C 30min	26.00	21.21	78.39	5.94
		20.02	270°C 30min	44.00	22.77	63.70	13.74
		20.02	220°C 60min	10.00	20.99	94.36	4.85
		20.02	250°C 60min	35.00	22.06	71.63	10.19
		20.02	270°C 60min	46.00	22.98	61.99	14.79
Bridgeman et al., 2008	Willow	19.00	230°C 30min	4.90	20.20	96.05	6.32
		19.00	250°C 30min	10.40	20.60	92.29	8.42
		19.00	270°C 30min	20.20	21.40	85.39	12.63
		19.00	290°C 30min	28.00	21.90	78.84	15.26
Phanphanich and Mani, 2011	Logging residue chip	18.79	225°C 30min	12.00	19.79	92.68	5.32
		18.79	250°C 30min	19.00	21.21	91.43	12.88
		18.79	275°C 30min	30.00	22.03	82.07	17.24
		18.79	300°C 30min	48.00	26.41	73.09	40.55
	Pine	18.46	225°C 30min	11.00	19.48	93.92	5.53
		18.46	250°C 30min	18.00	20.08	89.20	8.78
		18.46	275°C 30min	27.00	21.82	86.29	18.20
		18.46	300°C 30min	48.00	25.38	71.49	37.49
Wannapeera et al., 2011	Leucaena	20.30	200°C 30min	9.00	21.00	94.14	3.45
		20.30	225°C 30min	13.50	21.20	90.33	4.43
		20.30	250°C 30min	27.00	21.20	76.24	4.43
		20.30	275°C 30min	45.50	22.80	61.21	12.32

It should be mentioned that the volume of torrefied wood decreases only slightly although the energy density on a mass basis increases significantly after torrefaction. This means that the volumetric energy density is not improved. In addition, after torrefaction, wood loses its tenacious, water uptake, and biological degradation natures.

1.6 Wood Densification

Densification can enhance the bulk density of biomass particles from the initial 40-200 kg m^{-3} to the final 600-1200 kg m^{-3} [Holley 1983; Mani et al. 2003; Obernberger & Thek 2004; McMullen et al. 2005; Adapa et al. 2007]. Wood densification is a process applying a mechanical force to compact wood residues or wood wastes (sawdust shavings, chips or slabs) into a uniform size shaped like pellets, briquettes and logs. The target of wood densification is to increase the volumetric energy density, easy storage and handling, reduce the transportation cost and the moisture content. Wood pellets are usually 6–12 mm in diameter with the length ranging from 6 to 25 mm [Melin 2006]. Typically, the bulk density of wood pellets is between 500 and 650 kg m^{-3} with a moisture content of 7–10% by weight [Bergman 2005]. Most wood pellets are nowadays used in combustion for the heating of single-family houses, district heating systems, and electricity generation. Briquettes are generally disk shaped with a 50-100 mm in diameter and 20-50 mm in length. The bulk density of briquettes ranges from 320 to 560 kg m^{-3}, and the moisture content is 10-12% by weight [Bissen 2009]. The final use of briquettes is for both residential and industrial applications. Logs produced from the same machines as briquettes are cylindrical in shape with 50-100 mm in diameter and 300-400 mm in length. The logs are mainly for residential uses such as fireplace and wood stove [Sims et al. 1988].

Rumpf (1962) first explained the densification mechanisms of particles into the briquettes and pellets: attraction forces between solid particles, interfacial forces and capillary pressure to move liquid such as water into surfaces, adhesion and cohesion forces, solid bridges, and mechanical interlocking or form-closed bonds.

The pellet quality and the pellet density mainly determine the compaction pressure, the

preheating temperature, and the pressure holding time. Li et al. (2000) and Liu et al. (2000) reported that the compaction pressure for the strong logs made from sawdust at room temperature was at least 100 MPa. The target of the preheating temperature is to reach the glass transition temperature of lignin. The lignin is a natural binder for densification. The lignin cooled and reformed into solid can give the good shape and orientation of pellets, briquettes and logs. Normally, the glass transition temperature of lignin is 100-140 $^{\circ}$C (see Figure 1-2). In the moisture content of 8-10%, the temperature reduces to 60-100 $^{\circ}$C [Kaliyan and Morey 2009]. Therefore, the quality of pellets can improve with preheating temperature. The pressure holding time is for the formation of densification.

Biomass densification has been practiced commercially in large-scale pellet plants. In this section, the technology of wood pellets has been reviewed in order to develop the new method for producing the torrefied pellets. The technology of wood pellets is available for large-scale production of wood pellets. The quality of wood pellets strongly depends on the quality of the feedstock as well as processing conditions, such as fiber sources, particle size, particle moisture content, particle temperature, biomass feed rate, die size and shape, die speed and temperature, [Bissen, 2009]. More specifically:

- **Moisture content:** Acceptable moisture content of wood residues for making wood pellets is 9-12%wt.

- **Particle size:** The screens size for biomass grinding to make sawdust is typically less than 3.20 mm.

- **Chemical composition characteristics:** Lignin in wood is a natural binder for making wood pellets. The high lignin contain of wood residues can improve the strength of wood pellets.

- **Conditioning:** Normally, steam is used for preconditioning the feedstock. The added moisture and heat can help the lignin to soften and improve the feedstock lubrication, saving the energy for making pellets and increasing the die life.

- **Temperature:** The glass transition temperature of chemical compositions of wood residues is 50 to 130 ^{o}C. Normally, the die temperature is controlled at 70 ^{o}C. The higher die temperature can improve the quality of wood pellets, but will increase the die wear. The maximum die temperature used in the industry is 110 ^{o}C. If the die temperature is over 150 ^{o}C, the die wear will be substantially accelerated.

- **Pressure force and force application rate:** The high pressure force of the die can improve the quality of wood pellets, but increase the energy consumption. To make strong wood pellets, the pressure is usually over 125 MPa.

- **Hold time: A** long hold time can improve the quality of wood pellets. In most experimental conditions, the hold time is about 1 minute.

- **Die:** Normally, the die is shaped as a cylinder of 6.3 mm in diameter.

The properties of torrefied wood materials are significantly different with the raw wood such as the chemical composition and the moisture content.   There have been only a few studies reported on this topic, and the operating conditions for making torrefied wood pellets still need to be investigated in order to develop an integrated technology for making torrefied pellets.

1.7 Commercial Development of Wood Torrefaction

The rapid growth of wood pellet industry in recent years has been mainly driven by the effort to reduce greenhouse gas emissions in Europe and the rising oil and natural gas prices. Bergman (2005) developed the TOP process for the production of torrefied wood pellets, which have the higher heating value and hydrophobic properties compared with

regular pellets. Although a number of lab and pilot scale torrefaction units have been in operation, under construction or planning [Boyd et al. 2011; Melin 2011; Kleinschmidt 2011], many technical and business barriers still need to be solved in order to build a commercial scale plant. In Europe and Canada, some major joint programs have been recently initiated to demonstrate the torrefied pellet process, targeting the first commercialization in 2015 and producing 8-12 $t\ h^{-1}$ torrefied pellets (see Table 1-17).

From Table 1-17, it can be seen that torrefaction has been conducted in several types of reactors such as screw conveyor, rotary drum, moving bed, belt conveyor and torbed, but few studies have been conducted on densification. To build a commercial plant for the production of torrefied pellets, both the torrefaction and the densification technologies need to be considered and demonstrated.

Table 1-17 Some commercial development torrefaction projects

Developers	Torrefaction reactors	Locations	Capacity t h^{-1}	Starting operation
Producing or in Commissioning				
Topell Energy	Torbed	Duiven, Netherlands	8	2011
Integro Earth Fuels	Turbo Dryer	Roxboro, USA	6	2010
Stramproy Green	Belt conveyor	Steenwijk, Netherlands	5.5	2010
4Energy Invest	Rotary drum	Amel, Belgium	5.5	2010
Zilkha Biomass Energy	Unknown	Crockett, USA	5	2011
Torrsys	Moving bed	Vanderhoof, Canada	5	2012
AtmosClear	Rotary drum	Latvia	5	2011
Agri-tech	Screw conveyor	Columbia, USA	5	2011
Biolake	Screw conveyor	North-Holland	5	2011
Torr-Coal	Rotary drum	Dilsen Stokkem, Belgium	4.5	2011
Fox Coal	Screw conveyor	Winschoten, Netherlands	4.2	2011
BioEnergy Inc	Rotary drum	O-vik, Sweden	3.0	2011
Thermya	Moving bed	San Sebastian, Spain	2.5	2011
New Earth	Belt conveyor		2	2011
Under Construction or Publically announced				
CanBiocoal	Micro wave reactor	Terrace, Canada	12	2012
Fox Coal	Screw conveyor	Netherlands	12	2012
Diacarbon	Diacarbon		8	2014
ECN	Moving bed	Netherlands	5	2012
WPAC	TBA	British Columbia, Canada	5	2012
ETPC	BioEndev		4.5	2013

Source: Boyd et al. (2011), Melin (2011), Kleinschmidt (2011)

1.7.1 TOP Process

Torrefaction can increase the energy density of wood on the mass basis, and solve the problems of the durability and biological degradation associated with conventional pellets. Pelletization, on the other hand, can increase the volumetric energy density, and solve the drawbacks of torrefied biomass, such as the low volumetric energy density and dust formation. The TOP process was proposed by ECN (see Figure 1-7). During torrefaction, the biomass is directly heated by the recycled hot gases. The combustion of

the liberated torrefaction gases generates the necessary heat for torrefaction and drying. Torrefaction was carried out in a heated screw type reactor with controlled temperature and a minimal pressure drop. Currently, the process is under development at ECN.
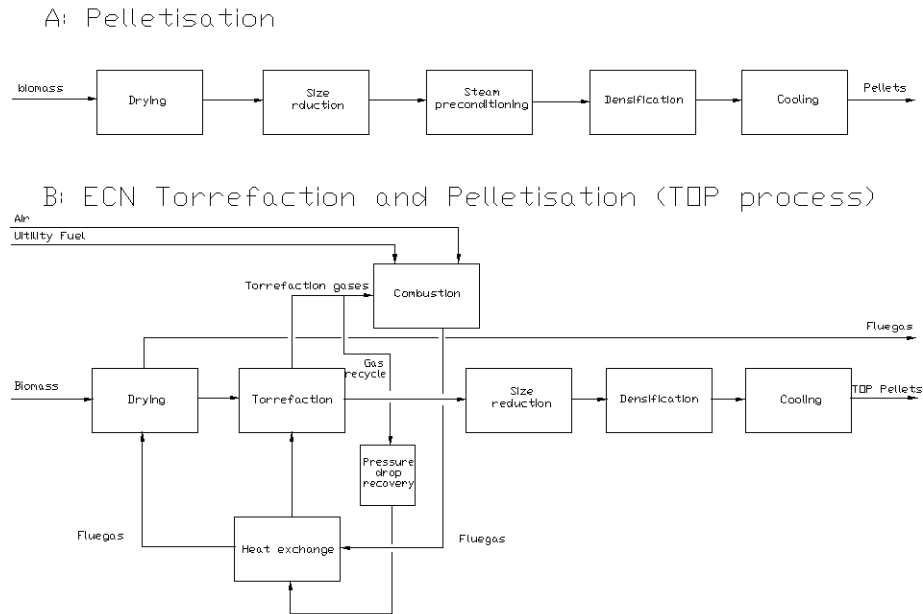
Figure 1-7 Process flowsheet of pelletisation and ECN combined torrefaction and pelletisation

The bulk densities of torrefied pellets range from 750 to 850 $kg\ m^{-3}$, with the dry high heating value of 20.4-22.7 $MJ\ kg^{-1}$ and the bulk energy density from 14.9 to 18.4 $GJ\ m^{-3}$. Conventional wood pellets have a bulk density of 520 to 640 $kg\ m^{-3}$ and the bulk energy density of 7.8-10.5 $GJ\ m^{-3}$ (see Table 1-18). Therefore, torrefied pellets can be about more higher in energy density than conventional pellets.

Torrefied pellets contain less volatile components, and are hydrophilic and hardly biologically degradable. Therefore, the durability is better than conventional pellets. This means that torrefied pellets will have fewer problems associated with off-gassing, spontaneous ignition, and dust generation.

Table 1-18 Properties of wood, torrefied wood, wood pellets and TOP pellets

Properties	Unit	Wood	Torrefied Wood	Wood Pellets		TOP Pellets	
				low	high	Low	High
Moisture content	%wt	35%	3%	10%	7%	5%	1%
LHV							
as received	MJ kg^{-1}	10.5	19.9	15.6	16.2	19.9	21.6
Dry	MJ kg^{-1}	17.7	20.4	17.7	17.7	20.4	22.7
Mass density (bulk)	Kg m^{-3}	550	230	500	650	750	850
Energy density (bulk)	GJ m^{-3}	5.8	4.6	7.8	10.5	14.9	18.4
Pellet strength				Good		very good	
Dust formation		moderate	High	Limited		limited	
Hygroscopic nature		water uptake	Hydrophobic	swelling/water uptake		poor swelling/hydrofobic	
Biological degradation		possible	Impossible	Possible		impossible	
Seasonal influences		high	Poor	High		poor	
Handling properties		normal	Normal	Good		good	

Source: Bergman (2005)

ECN provides an overview of the technical performance characteristics of the conventional pellet process and its torrefied pellets process (see Table 1-19). Both processes were thermally balanced by using natural gas for required heat input for drying. A major advantage of the torrefied pellets process is in the volumetric production rate of pellets. The torrefied pellet process produces 70 *Mm^3 annum^{-1}* of torrified pellets with 40 MW energy content, compared to the conventional pelletization process at 133 *Mm^3 annum^{-1}* of pellets with 44 MW energy content. This enormous volume reduction offers a major advantage for torrefied pellets in the logistic and transportation operations.

Table 1-19 Technical performances of conventional pelletisation and the TOP processes

Item	Unit	Conventional pelletization	TOP process	Conventional pelletization	TOP process
Feedstock		Sawdust	Sawdust	Green wood chips	Green wood chips
Feedstock capacity	kt a^{-1}	170	170	170	170
Moisture content	wt	57%	57%	57%	57%
LHV feed (ar)	MJ kg^{-1}	6.2	6.2	6.2	6.2
Production capacity	kt a^{-1}	80	56	80	56
	Mm^3 a^{-1}	133	70	133	70
	MW fuel	44	40	44	40
Moisture content	%wt	9	3	9	3
LHV product (ar)	MJ kg^{-1}	15.8	20.8	15.8	20.8
Cooling water	m^3 t^{-1} product		16.7		16.7
Steam	t t^{-1} product	0.025		0.025	
Utility fuel	MW	10.4	3.9	11.3	4.7
Power consumption	MW	1.26	0.83	1.84	1.01
Thermal efficiency	LHV(ar)	93.9%	98.5%	92.2%	96.5%
Net efficiency	LHV(ar)	88.0%	93.7%	84.0%	90.8%

Source: Bergman (2005)

The economic analysis of the ECN's torrefied pellet process was based on estimations of the feedstock delivery cost, the production cost, the logistic cost, and the transportation cost. The best comparison between both processes is on the basis of $€\,GJ^{-1}$ and the total production cost of torrefied pellets from sawdust is 2.2 $€\,GJ^{-1}$ (3.3 $\$\,GJ^{-1}$, 1€=1.51\$), compared to 2.6 $€\,GJ^{-1}$ (3.9 $\$\,GJ^{-1}$) for conventional pellets (see Table 1-20).

Table 1-20 Production costs of the conventional process and the TOP process

Item	Unit	Conventional Pelletisation	TOP process	Conventional Pelletisation	TOP process
Feedstock		Sawdust	Sawdust	Green wood	Green wood
Production rate	kt a^{-1}	80	56	80	56
Total Capital Investment*	M€	3.9	5.6	5.9	7.4
Total production costs	€ t^{1}	41	45	54	50
	€ GJ^{1}	2.6	2.2	3.4	2.5
Financing	€ t^{1}	2	4.4	3.2	5.9
Depreciation	€ t^{1}	4	8.8	6.5	11.7

Source: Bergman (2005), *: Including working capital of about 0.5 to 0.7M€

The total costs per tonne of product are similar for both processes, but the total costs on the basis of $€\,GJ^{-1}$ in the whole production chain are significantly less (32%) for the torrefied pellets, due to the lower production volumes and higher bulk density. The most significant savings are found in the ocean transportation for pellets made in South Africa and exported to Europe (see Table 1-21).

Table 1-21 Cost analysis of TOP pellets and conventional pellets for the sawdust case
(Production in South Africa and Consumption in Northwest Europe)

		TOP process		Conventional process	
Production capacity	kt a^{-1}	56		80	
	MW	40		44	
	Density, kg m^{-3}	800		650	
		$€\,t^{-1}$ product	$€\,a^{-1}$	$€\,t^{-1}$ product	$€\,a^{-1}$
South Africa	Feedstock gate delivery	15	840000	11	840000
South Africa	Pellet production & product storage	45	2520000	41	3280000
South Africa	Road Transportation to harbor	4.4	245000	4.4	350000
South Africa	Storage in harbor	1.5	81900	1.8	144000
South Africa	Transfer & handling harbor	3.3	182000	4	320000
	Sea transportation	28	1575000	35	2769231
NW Europe	Transfer & handling harbor	3.3	182000	4	320000
NW Europe	Storage in harbor	1.7	95550	2.1	168000
NW Europe	Water transportation to end-user	1.6	91000	2	160000
	Total costs, $€\,t^{-1}$	104	5812450	104	8351231
	$€\,GJ^{-1}$	4.99		6.61	

Source: Bergman (2005)

ECN provided the market price of torrefied pellets, based on the differences in net heating value. The estimated market price of torrefied pellets is nearly $150\,€\,t^{-1}$ ($226\,\$\,t^{-1}$) (against conventional pellets $120\,€\,t^{-1}$ ($181\,\$\,t^{-1}$)) for the co-firing market and $185\,€\,t^{-1}$ ($279\,\$\,t^{-1}$) (against conventional pellets $150\,€\,t^{-1}$ ($226\,\$\,t^{-1}$)) for the domestic market (see Table 1-22).

Table 1-22 Market prices of TOP pellets
(Values are derived from the market prices of conventional wood pellet)

Item	Unit	Co-firing market		Domestic market	
		Conventional Pellets	TOP Pellets	Conventional Pellets	TOP Pellets
LHV (ar)	GJ t^{-1}	16.5	20.4	16.5	20.4
Gate price	€ t^{1}	120	148	150	185
	€ GJ^{1}	7.3	7.3	9.1	9.1

Source: Bergman (2005)

1.7.2 Other Under Development Processes

Currently, Torftech Ltd., Alterna Energy Inc., NewEarth Renewable Energy Inc., and Agri-Tech Producers, LLC. also developed their torrefaction technologies and processes. Some commercial plants are under construction. The major difference among their technologies is in the design of the torrefaction reactor.

Torften Ltd. Developed a Torbed torrefaction reactor [Hamburg 2009]. There are no moving parts inside the reactor. High temperature process gases pass through the reactor to torrefy raw materials. The advantages are that the heat and mass transfer are very efficient, the pressure drop is low, and a wide range of particle sizes can be used. At the batch mode, a variety of biomass including woodchips, grass, straw, palm oil kernels, etc., has been tested with the torrefaction temperature range of 280-320 ºC. The LHV of torrefied pellets (also called TOPELL pellets) ranges 20-25 GJ t^{-1}. A capacity of 60 kt annum^{-1} commercial plant has been under construction in Duiven, Netherlands. This reactor behaves between the moving bed reactor and the fluidized bed reactor, and has both advantages.

The Alterna Energy torrefaction unit is a fix bed reactor [Kutney 2008]. Raw materials are loaded into a box, and the box is then moved into a kiln. The raw materials are

torrefied in the high temperature kiln. After torrefaction, the box is moved out and torrefied materials are unloaded. The technology is mature, but the heat transfer efficiency is low. Based on the low thermal conductivity of biomass, the torrefaction residence time may be hours. The product is also called biocarbon.

The rotating drum technology is used for torrefaction by NewEarth Renewable Energy Inc., and the torrefaction technology also is called ECO Pyro-Torrefaction (EPT) [NewEarth, 2009]. The company claimed that NewEarth's EPT plant is the world's first operating commercial scale torrefacton production facility with more than one thousand hours of successful operation. The raw materials and hot process gases are in direct contact during torrefaction to achieve high heat and mass transfer efficiency.

Based on the technology originally developed in North Carolina State University, Agri-Tech Producers, LLC developed a ATP torrefaction process [James, 2009]. A screw reactor is used as the torrefaction reactor. The reactor is operated with a temperature range of 300-400 ℃. The high temperature process gases indirectly heat the raw materials.

1.8 Research Objectives

Based on the literature review presented above, we can see that torrefaction is a promising technology to improve the energy density and hydrophobicity of the conventional wood pellets. The main objective of this thesis is to study the torrefaction of BC softwoods in order to develop a torrefaction and densification process for the production of high quality torrefied pellets.

The specific research tasks to be conducted in this research program include:

- To investigate the torrefaction of BC softwoods in a TGA so as to develop the specific torrefaction reaction kinetics for BC softwood as a function of torrefaction temperature, residence time, and particle size. 2 to 20 mg sawdust samples of various particle sizes were used for each TGA test. The sample weight during torrefaction in the TGA was continuously monitored. The temperature was varied from 200 to 300 °C, with the heating rate varied from 1 to 50 K min^{-1}. The TGA curves of the weight loss versus time were used for the determination of reaction kinetics of wood samples.

- To optimize the operating conditions such as torrefaction temperature, residence time, and particle size in a bench-scale fixed bed reactor based on the quality of torrefied pellets. A bench fluidized bed reactor was also built and used to investigate the performance of the torrefaction process under various operating conditions.

- To identify the suitable conditions for making torrefied pellets, including die temperature, pressure or compression force, particle size, and the moisture content. The torrefied sawdust was compressed into pellets in a single die pelleting unit in order to identify the optimal torrefaction conditions.

- To study the torrefied pellet properties such as pellet density, moisture content, water uptake rate, and the hardness.

- To develop a combined torrefaction and pelletization process. The experimental torrefaction data were analyzed to obtain the torrefaction kinetics of BC softwoods, identify the suitable industrial torrefaction and densification conditions, and develop a new torrefied wood pellet manufacturing process.

- To evaluate the economics of torrefied wood pellets based on the torrefaction and densification results.

1.9 Thesis Outlines

Chapter 2 presents the experimental setup and the raw materials used in the tests, as well as the instrument used for sample and product characterization.

TG curves of weight loss for major BC softwood species (pine, fir, spruce, and SPF) and three major chemical compositions (cellulose, hemicelluloses, and lignin) in the TGA have been investigated. Based on fitting TG curves, torrefaction kinetic models have been developed in Chapter 3.

Chapter 4 presents a study of torrefaction in a bench-scale tubular reactor unit and densification with a MTI 50K press machine to indentify the optimal torrefaction and densification conditions for the production of high quality torrefied wood pellets.

Based on TG curves of weight loss, the effect of particle size on torrefaction kinetics has been investigated in Chapter 5. Chapter 5 also discusses the difference in weight loss results between the TGA and the fixed bed unit and the particle size effect on densification in a MTI 50K press machine.

In order to indirect use the flue gases from the combustion of torrefaction volatiles, Chapter 6 examined the effect of oxygen content in the carrier gas on the torrefaction in both the TGA and a fluidized bed reactor unit. Based on the TGA test data, a simple torrefaction kinetics incorporating the oxygen effect has been developed. A fluidized bed reactor unit has been used to prepare the torrefied samples under oxidative environment for the production of torrefied wood pellets.   And the oxygen effect on densification has been studied by the comparison of wood pellets prepared from torrefied sawdust at different oxygen content of carrier gases.

Based on the torrefaction and densification results of this study, Chapter 7 presents an economical evaluation of BC torrefied wood pellets in comparison to regular wood pellets.

The overall conclusions and recommendations for future work will be presented in Chapter 8 for guiding other researchers for further development of the torrefaction process.

CHAPTER 2 EXPERIMENTAL SETUP AND SAMPLES PREPARATION

2.1 Preparation of Softwood Samples

Six types of BC softwood samples, fir, and SPF woodchips from Fiberco, pine and spruce woodchips from FPInnovations, pine bark and SPF shavings from Wood Pellet Association of Canada, have been tested in this study. SPF woodchips samples obtained from the wood industry was a mix of spruce, pine and fir woodchips, with pine as the major constitute. Woodchips and bark samples were prepared by drying in a THELCO laboratory PRECISION oven (Thermo Electron Corporation) (see Figure 2-1) at 378 K for 24 hours and crushing in a hammer mill (Glenmills Inc., USA; Model: 10HMBL) (see Figure 2-2) installed with different size screens. The SPF shavings (see Figure 2-3) and pine samples prepared in a hammer mill installed with three different screen sizes (0.79 mm, 3.18 mm, and 6.35 mm) were used for the study of temperature, residence time and particle size effects.   The 0.79 mm screen was installed in the hammer mill for grinding spruce, fir, SPF, and pine bark residues for the study of different BC softwood species (see Figure 2-4).

Figure 2-1 Photo of the THELCO laboratory PRECISION oven

Figure 2-2 Photo of the hammer mill

Figure 2-3 4.0 mm screen size SPF shavings samples

Spruce

Fir Sawdust

SPF Sawdust

Pine bark

Figure 2-4 0.79 mm screen size spruce, fir, SPF, and pine bark samples

Table 2-1 shows the proximate and ultimate analyses of BC softwoods. The volatile matter, fixed carbon, and ash content were measured by using a TG analyzer

(SHIMADZU TGA-50) (see Figure 2-5). The chemical composition was measured by FPInnovations using a high-performance liquid chromatography. The elemental analysis was conducted in an EA 1108 elemental analyzer (see Figure 2-6) in the Chemistry Department at the University of British Columbia. From Table 2-1, the properties of spruce, pine, fir and SPF particles were seen to be very close, but different from pine bark. The mean particle size of BC softwood samples was 0.09 - 0.23 mm, much less than the screen opening of the hammer mill.

Table 2-1 Proximate and ultimate analyses of BC softwoods (oven dry material)

	Pine	Fir	Spruce	SPF	Pine Bark
Volatile matter, %wt	82.79	82.88	80.49	84.43	75.84
Fixed carbon, %wt	16.81	17.00	19.42	15.33	21.61
Ash, %wt	0.40	0.12	0.24	0.24	2.55
Chemical composition, %wt					
Cellulose	36.74	37.11	42.37	NA	26.17
Hemicelluloses	26.30	24.97	20.02	NA	17.89
Lignin	33.61	35.04	35.08	NA	41.01
Extractives	2.95	2.76	2.43	NA	12.38
Elemental analysis, %wt					
C	51.22	50.01	51.24	50.30	53.21
H	6.02	6.07	5.95	6.09	5.98
O	42.64	43.77	42.68	43.48	40.29
N	0.12	0.15	0.12	0.13	0.52

Note: chemical composition of SPF is not measured because it depends on different fractions of spruce, pine and fir.

Figure 2-5 Photo of the TG analyzer

Figure 2-6 Photo of the EA 1108 elemental analyzer

The PRECISION oven was used to evaluate the moisture content for particle samples. A 25 ml glass cylinder was used to determine the bulk density. A multipycnometer (Quantachrome Instruments, USA) (see Figure 2-7) was used to measure the true density. The high heating value was measured by a calorimeter (Parr 6100, USA) (see Figure

50

2-8). Particle size distributions were determined by a Ro-Tap sieve shaker (Tyler Industrial Products, USA) (see Figure 2-9). For the determination of the particle size distribution of samples prepared by the grinder installed with 6.35 mm, 4.00 mm and 3.18 mm screens, the following sieves were used: 5, 7, 10, 14, 18, 25, 35, 45, 60, 80, 100, and 120 mesh (corresponding to 4.00, 2.80, 2.00, 1.41, 1.00, 0.707, 0.500, 0.354, 0.250, 0.177, 0.149, and 0.125 mm). For samples prepared by the grinder installed with the 0.79 mm screen, following sieves were used: 18, 25, 35, 45, 60, 80, 100, 120, 170 and 230 mesh (corresponding to 1.00, 0.707, 0.500, 0.354, 0.250, 0.177, 0.149, 0.125, 0.088 and 0.063 mm). Sieving time was controlled at 5 minutes for each test. In total, two replicates were measured for each sample. Figures 2-10 and 2-11 show the measured particle size distribution of different BC softwood species with 0.79 mm screen size. Figures 2-12 and 2-13 show the measured particle size distributions of 4.00 mm screen size SPF shavings and pine samples prepared from three screen sizes (0.79, 3.18 and 6.35 mm). From Figures 2-10 and 2-11, it is seen that the particle size distributions of spruce, pine, fir and SPF were very close, but different from pine bark. Table 2-2 shows the properties of BC softwood samples. The true material density of BC softwoods was around 1400 kg m^{-3}. The pine bark had a higher high heating value. From Table 2-2, the Sauter mean particle sizes (diameters) of spruce, pine, fir and SPF particles were very close, but different from pine bark.

Table 2-2 Properties of BC softwood particle samples

	0.79mm Screen Size					Pine		SPF
	Spruce	Pine	Fir	SPF	Bark	3.2mm	6.4mm	4.0mm
Moisture content, %wt	9.54	7.44	3.19	3.46	7.20	9.33	9.09	9.94
Bulk density, kg m^{-3}	199	225	232	176	310	215	158	156
True density, kg m^{-3}	1413	1412	1441	1430	1380	1361	1364	1346
High heating value, MJ kg^{-1}	18.33	18.60	18.38	18.56	19.52	18.79	18.62	18.13
Sauter mean particle size (diameter), mm	0.21	0.23	0.20	0.21	0.09	0.67	0.81	1.10

Figure 2-7 Photo of the multipycnometer

Figure 2-8 Photo of the calorimeter

Figure 2-9 Photo of the Ro-Tap sieve shaker

For the particle size effect study in a TGA, pine woodchips were crushed in a Model GP-140 disc style grinder (Modern Process Equipment Inc., Chicago, IL) (see Figure 2-14) and separated in a Gilson Test-Master sieving device (Gilson Company Inc., Lewis Center, Ohio) (see Figure 2-15). Figure 2-16 shows the three prepared pine sawdust particles of different sizes (<250 µm, 250-500 µm, and 500-1000 µm). Table 2-3 shows the properties of Fiberco pine particle samples.

Table 2-3 Properties of Fiberco pine particle samples

Particle size group, µm	0-250	250-500	500-1000
Average particle size, µm	125	375	750
Moisture content, %wt	8.33	9.09	6.67
Bulk density, kg m^{-3}	158	215	248
True particle density, kg m^{-3}	1470	1420	1444

The sawdust sample, obtained from RONA furniture store in Vancouver, is a mixture of spruce and fir, with spruce as the main component. The sample was separated into six size fractions, and 250-355 μm is chosen for fluidized bed reactor in this study.
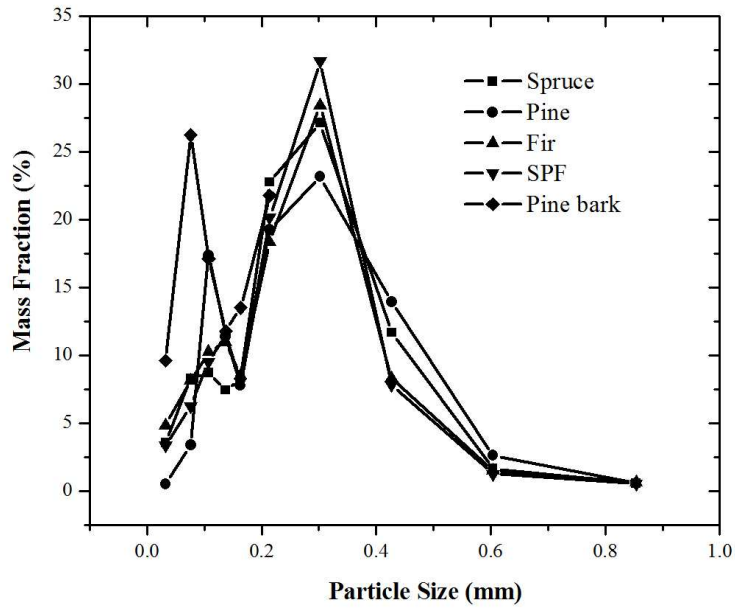
Figure 2-10 Differential particle size distributions of different BC softwood samples prepared using a screen opening of 0.79 mm
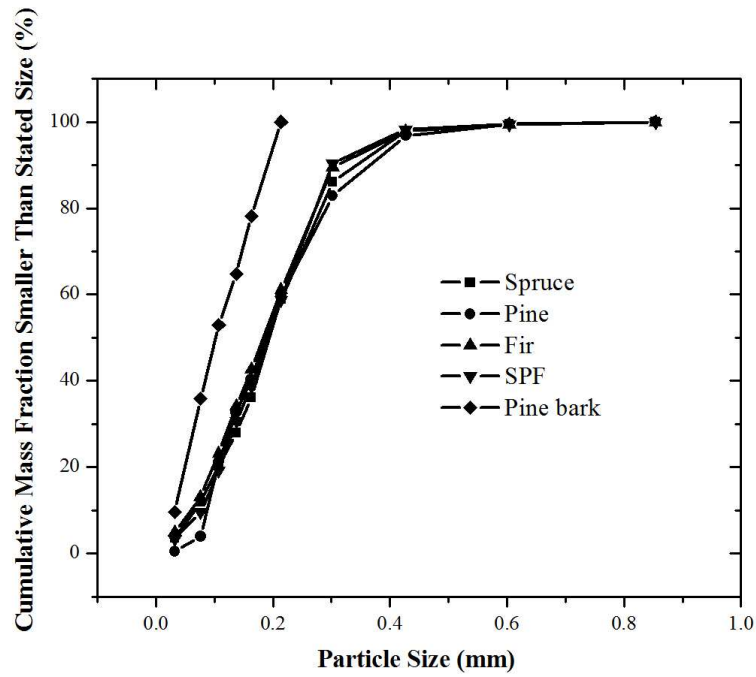
Figure 2-11 Cumulative particle size distributions of different BC softwood samples prepared using a

screen opening of 0.79 mm
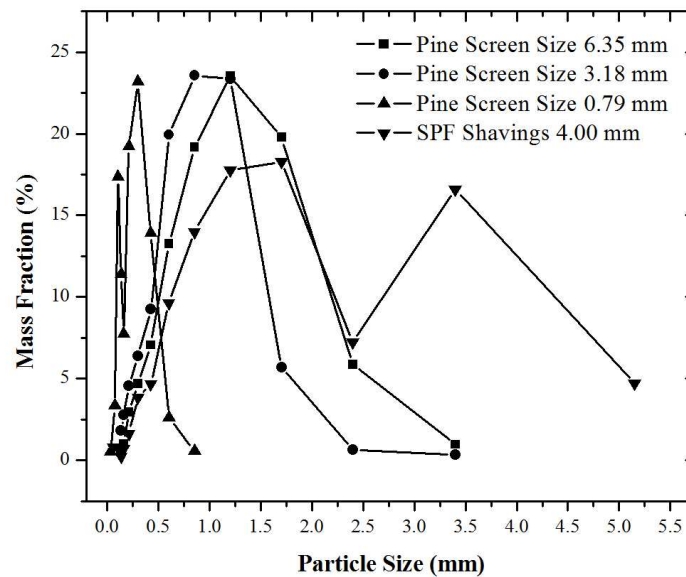
Figure 2-12 Differential particle size distributions of pine samples and SPF shavings
prepared from different screen openings
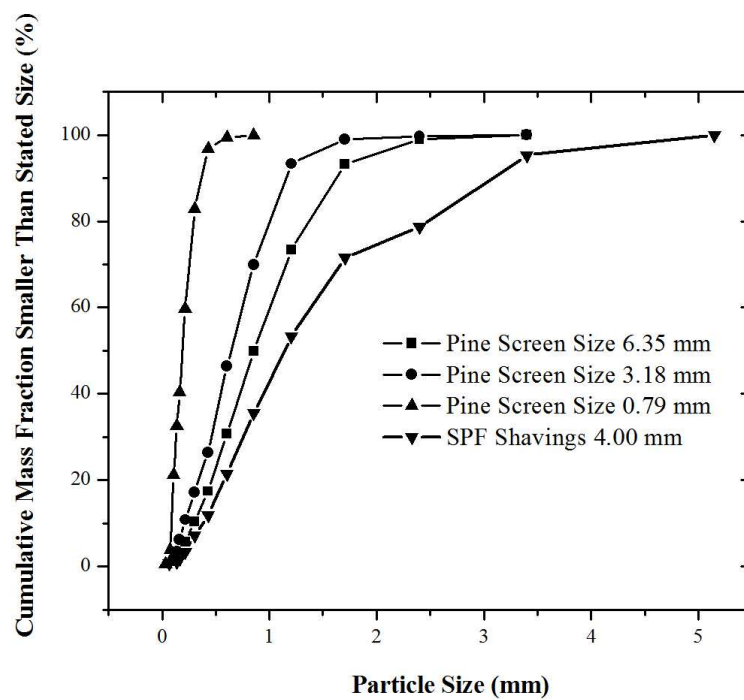
Figure 2-13 Cumulative particle size distributions of pine samples and SPF shavings

prepared from different screen openings

Figure 2-14 Photo of the Model GP-140 disc style grinder

Figure 2-15 Photo of the Gilson Test-Master

Six pure components of biomass in powder form were used in this study. Two cellulose samples (fibrous medium and fibrous long) separated from Israel cotton, two xylan samples separated from birchwood and oat, and two lignin samples (lignin alkali with a molecular number of 5000 and a molecular weight of 28000 separated from Norway spruce, and lignin alkali of low sulfonate content with a molecular number of 10000 and a molecular weight of 60000 produced from synthetic organics), were purchased from Sigma-Aldrich Inc.   Table 2-4 shows the properties of six pure components of biomass.

Table 2-4 Properties of six pure components of biomass

	Cellulose		Xylan		Lignin	
	Medium	Long	Birchwood	Oat	Alkial	Low sulfonate
Moisture content, %wt	4.12	4.27	12.81	11.31	9.90	9.49
Ash, %wt	0.02	0.01	6.02	12.28	13.72	13.09
High heating value, MJ kg^{-1}	17.39	17.06	17.40	17.33	26.20	24.37
Elemental Analysis, %wt						
C	43.05	42.83	36.07	31.66	41.83	45.23
H	6.32	6.33	5.80	5.12	4.37	4.65
O	50.53	50.77	52.03	50.88	39.93	36.91
N	0.07	0.05	0.08	0.07	0.14	0.13

2.2 A TGA for Torrefaction Kinetics Study and Experimental Design

The TG analyzer (SHIMADZU TGA-50) was used to study the weight loss or torrefaction kinetics. For each TG experiment, a sample of several (5-20) milligrams was put into a platinum sample cell, which was then located on a sample pan hanging inside a furnace tube under a nitrogen flow rate of 50 ml (STP) min^{-1}. The instrument continuously monitored the change of sample weight as well as the temperature. The temperature was ramped from room temperature to 1073 K with the heating rate varied from 1 to 50 K min^{-1}.

The temperature program for the dynamic experiments was: (1) heating from room temperature to 383 K at a heating rate of 50 K min^{-1}, (2) holding at 383 K for 20 min to have the sample dried, (3) heating from 383 K to 1073 K at a heating rate of 1 K min^{-1} to complete the thermal degradation of the sample and to clean the sample pan. The low heating rate with small particle size aims to eliminate the internal heat and mass transfer effects.

The temperature program for the isothermal experiments was: (1) heating from the room temperature to 383 K at a rate of 50 K min^{-1}, (2) holding at 383 K for 10 min to have the sample dried (Note that the dynamic TG results showed that the samples were completely dried in less than 5 min. So the holding time for drying in the isothermal experiments was decreased to 10 min.), (3) heating up to the torrefaction temperature at a rate of 50 K min^{-1}, (4) holding at the torrefaction temperature for 10 hours, (5) heating up to 1073 K at a rate of 50 K min^{-1} to complete the thermal degradation of the sample and to clean the sample pan. Several torrefaction temperatures were chosen for the isothermal experiments. To shorten the heating up time in the isothermal tests, a heating rate of 50 K min^{-1} was selected, which gave rise to less than 5% weight loss associated with the

58

heating period for all tests carried out at 563 K.

Pine particles of 0.23 mm in mean size were used in the TG experiment. The torrefaction temperature was 553 K, with a residence time of 10 hours. The N_2-O_2 gas mixture flow rate was 50 ml min^{-1}, with O_2 concentrations of 0%, 3%, 6%, 10% and 21% being selected.

2.3 A Fixed Bed Torrefaction Unit and Experimental Design

A bench-scale fixed bed unit was used for torrefaction performance tests (see Figure 2-16). The unit includes a tubular reactor, an electrical gas preheater with a temperature controller and a power supply (booster), an electrically heated furnace, a cooler, a condensate receiver, and a computer. The reactor has a 27.0 mm inside diameter and 575 mm in length made from stainless steel. The reactor is located inside an electrically heated furnace with a reaction zone of 102 mm in length. In the unit, the sample was heated up by both the preheated hot nitrogen flow and the electrical furnace. The hot nitrogen flows into the reactor from top to bottom. The temperature of the reactor zone was controlled by the electric power via a temperature controller. The raw sample was added into the reactor from the top of the reactor, and the torrefied sample was discharged from either the bottom or the top of the reactor when the reaction was complete. All condensable gases are collected in a condensate receiver cooled by water, and non-condensable gases are collected by a gas sampling bag or discharged to a ventilation system (see Figure 2-17). In this study, the unit was loaded with 20-40 gram samples each time in a batch mode.

Figure 2-16 Photo of the fixed bed reactor unit
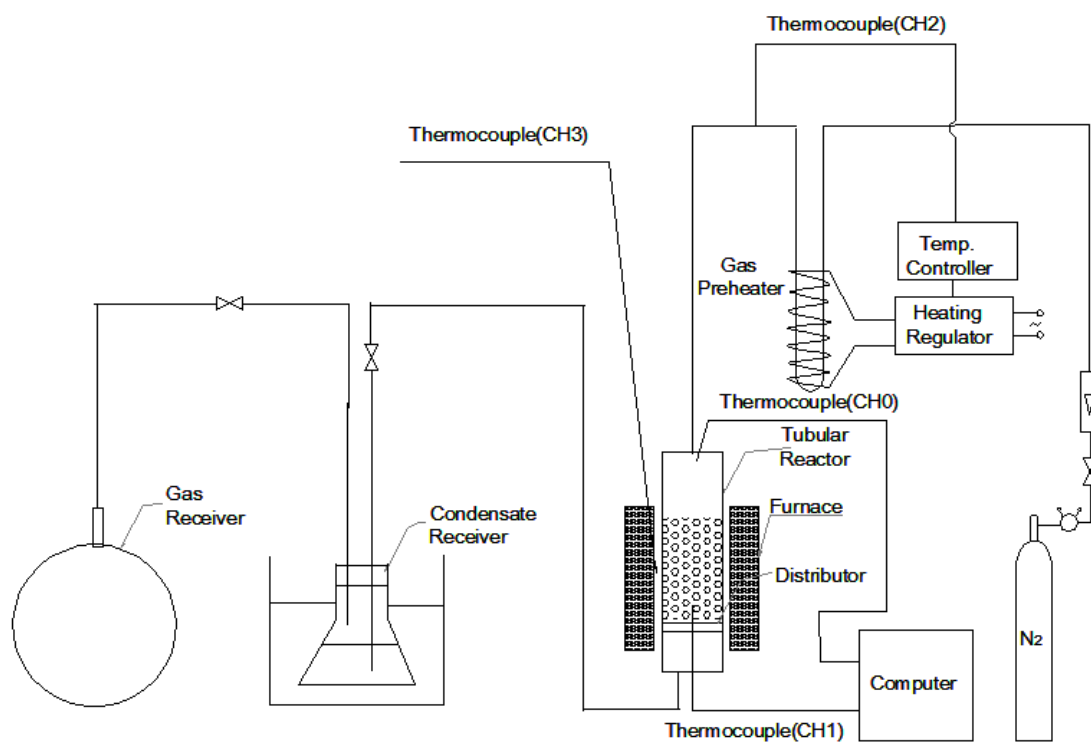
Figure 2-17 Schematic of the fixed bed torrefaction test unit

During the torrefaction test, the nitrogen flow rate was 0.5 standard cubic feet per minute (SCFM). After the torrefaction, the flow rate increased to 1.0 SCFM to cool down the torrefied sample. Four thermocouples are located in the unit to monitor the temperature. Thermocouple CH0 is for monitoring the N_2 flow temperature. CH1 is for the sample bed temperature. CH2 is for the gas heater surface temperature and CH3 is for the furnace temperature. The temperature programming procedures were: (1) increasing the nitrogen flow temperature and the furnace temperature to 210 ℃, which takes about 15 min; (2) setting up the furnace temperature to 5-10 ℃ above the target torrefaction temperature, with the sample reaching the torrefaction temperature over a few minutes; (3) controlling the furnace temperature to maintain the sample temperature at the target torrefaction temperature for the preset residence time; (4) turning off the gas heater and furnace powers to cool the unit by keeping passing the cooling nitrogen, until the sample temperature lowered to below 200 ℃; (5) continuing to cool the unit for a few hours, until the sample temperature dropped to room temperature.

Two sets of tests were conducted. In the first set, SPF shavings were torrefied at different temperatures and different residence times to investigate the effect of torrefaction temperature and residence time on the properties of torrefied sawdust and pellets. In the second set of tests, different species of softwood of similar particle size were torrefied at the same residence time and torrefaction temperature, followed by densification, to examine the performance of different wood species. For each sample, at least two replicates were tested for each reaction condition.

2.4 A Fluidized Bed Unit and Experimental Procedure

The batch fluidized bed reactor is made of stainless steel, 1.5 m tall and 50 mm in diameter, as shown in Figure 2-18. In the torrefaction tests, the sample of 250-355 μm was used to minimize the internal heat and mass transfer. In order to operate the fluidized bed reactor fully fluidized during the hot test, a minimum stable operating gas velocity of 0.26, m s^{-1} corresponding to gas flow rate of 1.83 m^3 h^{-1}, for sawdust load of 10 g was determined from the cold unit experiments, with details provided in an early publication from our group [Li et al. 2012]. First, with the sweeping flow of nitrogen, the preheater, the heating tape and the fluidized bed reactor were heated up to 650, 450 and 200 ℃, respectively, and kept stable. Then the fluidized bed reactor was further heated up to the targeted torrefaction temperature slowly and kept stable for at least 10 min. The raw sample was added into the reactor from the top of the reactor, and the sweeping nitrogen gas was changed to the desired oxygen content. After torrefaction over the targeted residence time, the pre-heater and furnace heater were turned off to allow the unit to cool down, followed by the cut-off of sweeping gas when the sample temperature dropped to below 200 ℃. Finally, after the sample temperature decreased to the room temperature, the torrefied sample was discharged from the bottom of the reactor, completing the test.
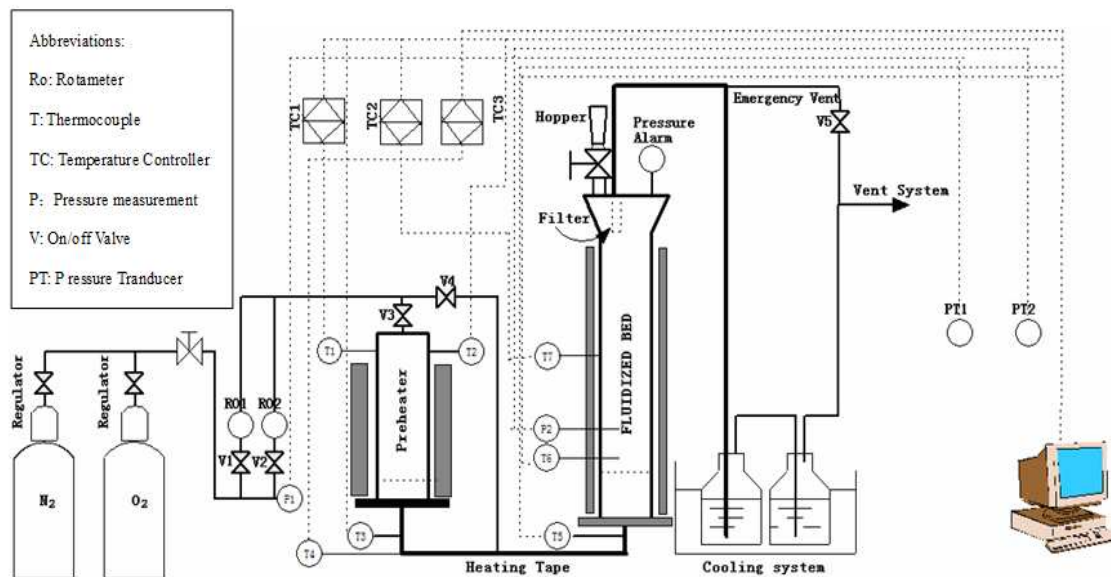
Figure 2-18 Schematic of the fluidized bed torrefaction unit

The simulated flue gas was prepared from mixing nitrogen and oxygen from two separate cylinders. In this study, the concentration of oxygen in the sweeping gas varied from 0 to 6 %, covering the typical range of oxygen concentration in combustion flue gases, with the test with 3% O_2 as the based case.

2.5 Pelletization and Pellet Characterization

A MTI 50K (Measurement Technology Inc.) press machine can be operated at various loading forces monitored by a load cell (see Figure 2-19). A cylinder of 6.35 mm inside diameter and 70 mm in length with a piston 6.30 mm in diameter and 90 mm in length was installed for making a single pellet. The cylinder-piston unit was wrapped by a heating tape with a thermocouple and a temperature controller to preheat the inside cylinder to a certain temperature (also called die temperature) (see Figure 2-20). In this study, the top hole of the cylinder was filled with approximately 0.5 gram samples to make a single pellet of 6.5 mm in diameter and ~12 mm in length. The sample was

pressed by applying a pressure of 125 or 156 MPa and held for a few minutes for the pressure controlled manually. Then the machine was continued to press the sample until a maximum pressure of 156 or 187 MPa was reached. Normally, for making control pellets, the die temperature was maintained at 70 ^{o}C with 125 MPa pressure over 1 minute holding time.

Figure 2-19 Photo of the MTI 50K
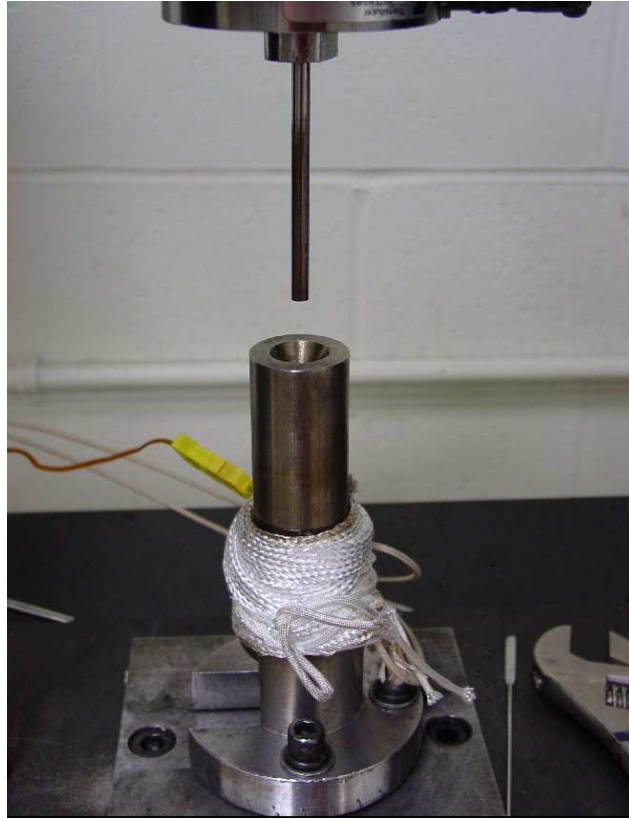
Figure 2-20 Photo of the single pellet machine with a heated die unit

Both increasing the die temperature and preconditioning the sample to higher moisture content have been examined in this study to compress torrefied sawdust into pellets, with the die temperature ranging from 70 to 280 ^{o}C and the different pressure from 125 to 280 MPa. Preconditioning of torrefied sawdust by adding 0, 5, 10 and 15% water and left 24-72 hours before compression was also explored.

The single pellet density was calculated from measured mass and volume of individual pellet. Forces and displacement to form pellets were recorded to calculate the energy consumption. A Humidity Chamber (ESPEC CORP, LHU-113, Japan) at 30 ^{o}C at 90% relative humidity was used for measuring the moisture uptake of torrefied and control pellets (see Figure 2-21) [Lam 2011]. The Meyer hardness (H_M) is measured to represent the durability of pellets [Tabil et al. 2002]. To measure H_M, the pellet was placed between

two anvils under the MTI cross head. The force was diametrical. The maximum force (F) to break a pellet was recorded (see Figure 2-22). The equation of H_M is then obtained as below:

$$H_M = \frac{F}{\pi(Dh - h^2)}$$

(2-1)

where D is the probe diameter and h is the indentation depth.

Figure 2-21 Photo of the Humidity Chamber

Figure 2-22 Photo of the single pellet machine Meyer hardness test

CHAPTER 3 TORREFACTION KINETICS OF BC SOFTWOODS FROM A TGA

In this chapter, wood torrefaction kinetics was investigated in a TGA for major BC softwood species (pine, fir and spruce), their mixtures (SPF, a mixture of spruce, pine, and fir), pine bark, and three major chemical components (cellulose, hemicelluloses, and lignin). The major chemical compositions were used in order to elucidate the reaction mechanism at low decomposition temperature. To obtain intrinsic torrefaction reaction kinetics, particles of less than 1 mm in diameter were selected to eliminate the limitation of internal heat and mass transfer [Prins et al. 2006b, Maa et al. 1973], with the results being potentially applied directly to guide the development of torrefaction reactor systems where fine biomass particles are used. The particle size effect on torrefaction has also been investigated in this study to elucidate the effect of internal heat and mass transfer effects, which will be presented in Chapter 5. Furthermore, the effect of oxygen content in the carrier gas on torrefaction performance and the quality of torrefied pellets was studied and presented in Chapter 6.

3.1 Experimental

3.1.1 Samples

Five BC softwoods, pine, fir, and SPF woodchips from Fiberco, spruce woodchips from FPInnovations, and pine bark from Wood Pellet Association of Canada, have been tested in this chapter. Table 2-1 shows the properties of BC softwoods. From Table 2-1, the properties of spruce, pine, fir and SPF particles were seen to be very close, but different from pine bark. The mean particle size of BC softwood samples was 0.09 - 0.23 mm,

much less than the screen opening of the hammer mill. The pine bark is very brittle because of the low cellulose content that provides the wood's strength, and of the high ash content, which makes the pine bark samples being crushed easier in the hammer mill, leading to smaller particle size and size distribution than spruce, pine, fir and SPF samples. Figures 2-10 and 2-11 show the measured particle size distribution of BC softwoods. From Figures 2-10 and 2-11, it is seen that the particle size distributions of spruce, pine, fir and SPF are very close, but different from pine bark. The small particle size ensures the elimination of inter- and intra-particle heat and mass transfer limitations, so that intrinsic reaction kinetics can be obtained.

Six pure components of biomass in powder form with <200 µm in mean size were used to minimize the particle size effect. Those samples include two cellulose samples, two xylan samples separated from birch wood and oat from Germany, and two lignin samples, with all samples purchased from Sigma-Aldrich Inc.

3.1.2 Equipment and Procedures

The TG analyzer as described in Chapter 3 was used in this Chapter study. Both dynamic thermal degradation and isothermal degradation have been performed. The temperature programs of the dynamic experiments were: (1) heating from the room temperature to 383 K at a heating rate of 50 $K\ min^{-1}$, (2) holding at 383 K for 20 min, (3) heating from 383 K to 1073 K at a heating rate of 1 $K\ min^{-1}$.

The temperature programs for the isothermal experiments were: (1) heating from the room temperature to 383 K at a rate of 50 $K\ min^{-1}$, (2) holding at 383 K for 10 min, (3) heating up to the torrefaction temperature at a rate of 50 K min^{-1}, (4) holding at the torrefaction temperature for 10 hours, (5) heating up to 1073 K at a rate of 50 $K\ min^{-1}$. Several torrefaction temperatures were chosen for the isothermal experiments.

3.2 Experimental TG Curves

Figures from 3-1 to 3-5 show the dynamic TG curves of BC pine, fir, spruce, SPF, and pine bark samples. It is seen that the weight loss of pine, fir, spruce, and SPF started at around 440 K, but the pine bark was at around 396 K. The weight loss rate in the 473-573 K was steady, and reached a peak at around 598 K for pine, fir, spruce and SPF, and nearly around 589 K for pine bark. The weight loss inflection point of pine, fir, spruce, and SPF occurred at almost the same temperature, 613 K, and the Pine bark was around 605 K. Beyond the inflection point, the weight loss rate decreased. The peak may likely correspond to the maximum decomposition rate of cellulose while the inflection point indicates the complete decomposition of cellulose [Chen and Kuo 2010, 2011a]. It can thus be concluded that BC softwoods, including pine, fir, spruce, and SPF, had almost the same dynamic TG weight loss characteristics due to their similar chemical compositions, which was different from pine bark. When the differential TG curves are compared, the spruce (Figure 3-3) and pine bark (Figure 3-5) show different characteristics in the curve after the inflection point, while pine, fir and SPF showed a similar trend.
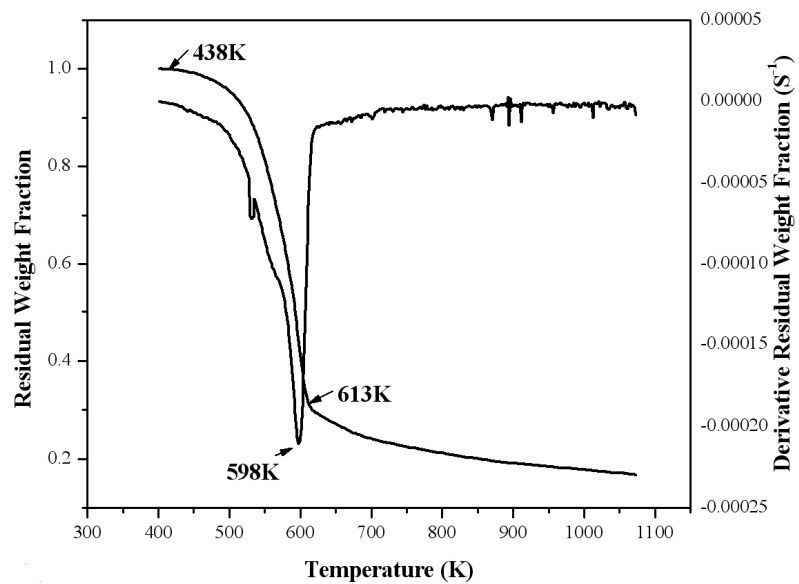
Figure 3-1 Dynamic TG curves of BC pine
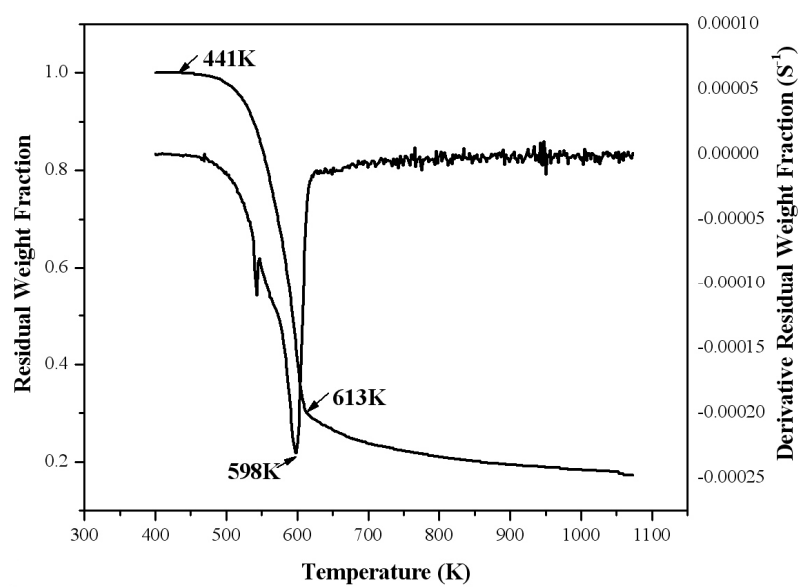
Figure 3-2 Dynamic TG curves of BC fir

71
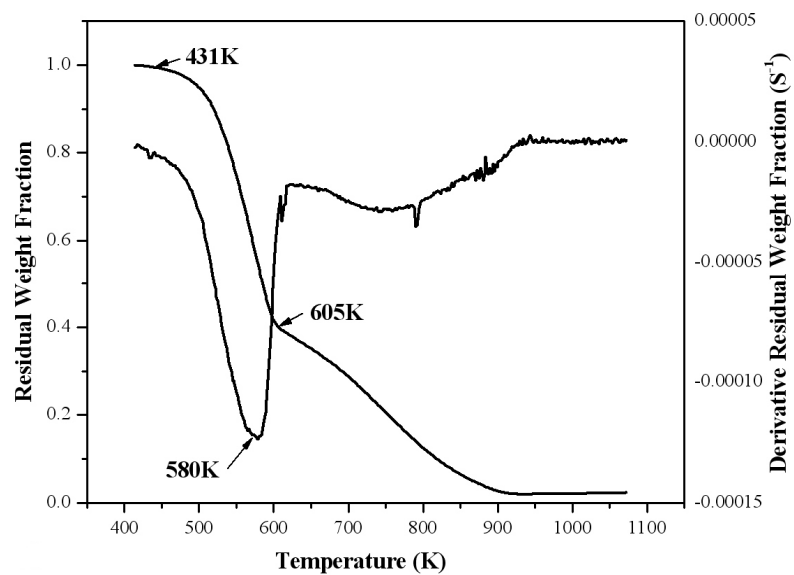
Figure 3-3 Dynamic TG curves of BC spruce
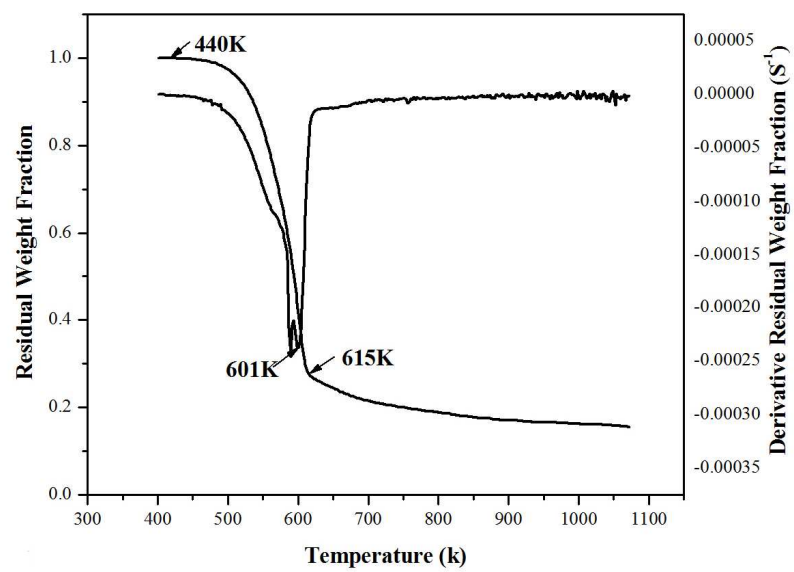
Figure 3-4 Dynamic TG curves of BC SPF

72
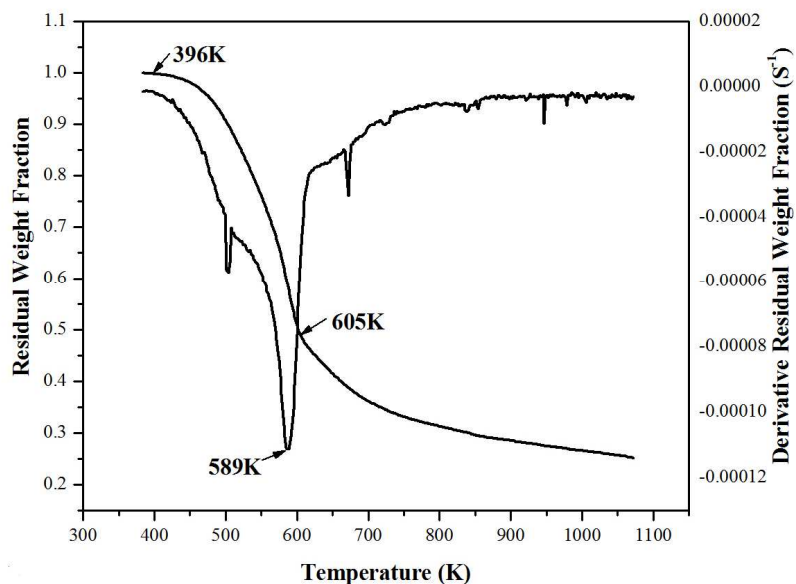
Figure 3-5 Dynamic TG curves of BC pine bark

Figures 3-6 and 3-7 show the isothermal TG curves of BC pine, fir, spruce, SPF, and pine bark at 573 K and 553 K. The TG curves of pine, fir, spruce, and SPF were very close. The weight loss rate of pine was slightly faster than SPF and the SPF rate slightly faster than fir. As the temperature increased, the TG curves of pine, fir, spruce, and SPF became closer. At 553 K the pine bark weight loss rate was faster than pine, fir, spruce, and SPF. At 573 K the pine bark initial weight loss rate was much faster than pine, fir, spruce, and SPF. One can thus conclude that in the typical torrefaction temperature range, BC pine, fir, spruce, and SPF performed very similarly on thermal degradation, but different from pine bark.
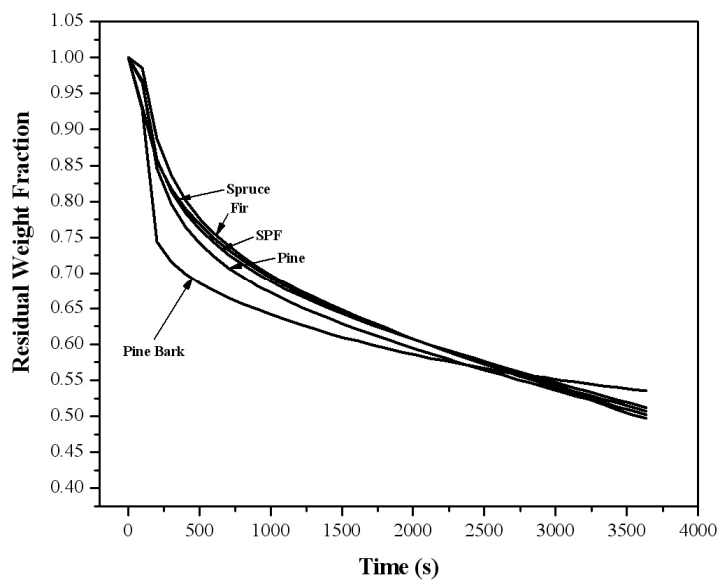
Figure 3-6 Isothermal TG curves of BC softwoods at 573 K
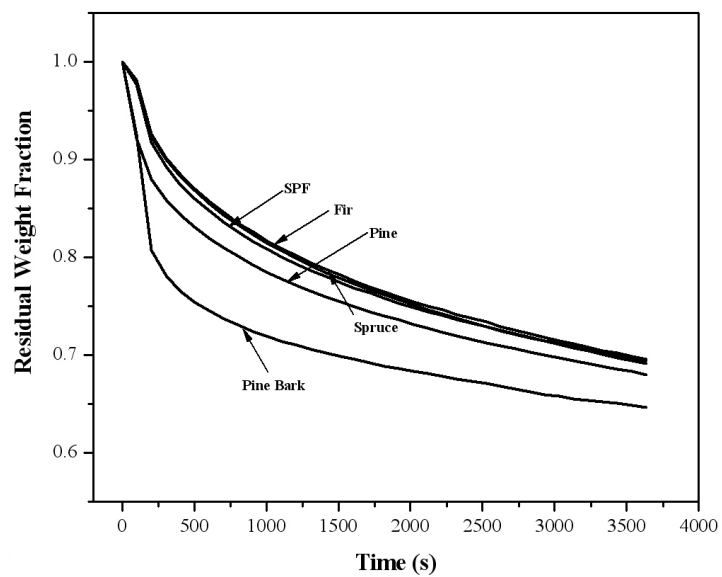
Figure 3-7 Isothermal TG curves of BC softwoods at 553 K

74

Figures from 3-8 to 3-13 show the dynamic TG curves of three major components: cellulose, xylan (hemicelluloses), and lignin extracted from different biomass species. From Figures 3-8 and 3-9, it can be seen that the weight loss of celluloses began at 493 K. Between 493 and 523 K, the weight loss was very small. The major weight loss started at 553 K and the maximum weight loss rate occurred at about 575 K. The decomposition of long fibrous cellulose delayed slightly compared to the medium length fibrous cellulose. Both types of cellulose had an inflection temperature of around 592 K. The thermal decomposition of cellulose ended around 775 K. The weight loss rate was almost the same in the range of 553-592 K. Both the medium and long fibrous cellulose had almost the same TG curves. From Figures 3-10 and 3-11, it can be seen that the weight loss of xylan began at 420 K with the maximum weight loss rate at 516 K. Both xylan samples had two inflections. One inflection at the low temperature range may represent the decomposition of short chain hemicelluloses, while the high temperature inflection point may correspond to the large molecule and hard to decompose component in the hemicelluloses sample. The weight loss of xylan ended in the range of 710-768 K. The result indicates that hemicelluloses were easy to decompose thermally with a complex kinetics. From Figures 3-12 and 3-13, it can be seen that both lignin samples had high weight loss rates and two inflection points. As the molecular weight increased, the weight loss rate decreased, and the thermal decomposition temperature range became wider. The low molecular weight lignin was separated from spruce, and two weight loss peaks were presented above 573 K. The high molecular lignin was produced from synthetic organics. Although part of its thermal properties is close to the natural lignin, the sulfonic acid sodium salt in the lignin may decompose at high temperatures around 950 K (see Figure 3-13) (OECD, 2005).
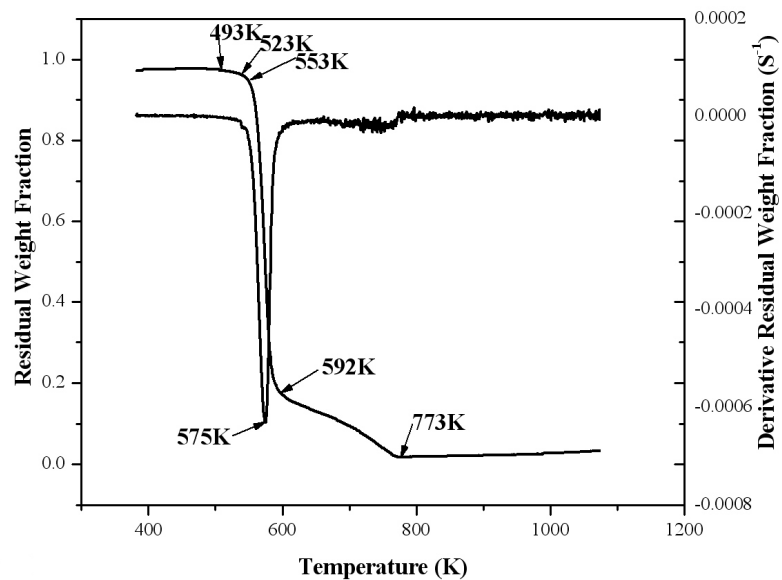
Figure 3-8 Dynamic TG curves of fibrous medium cellulose
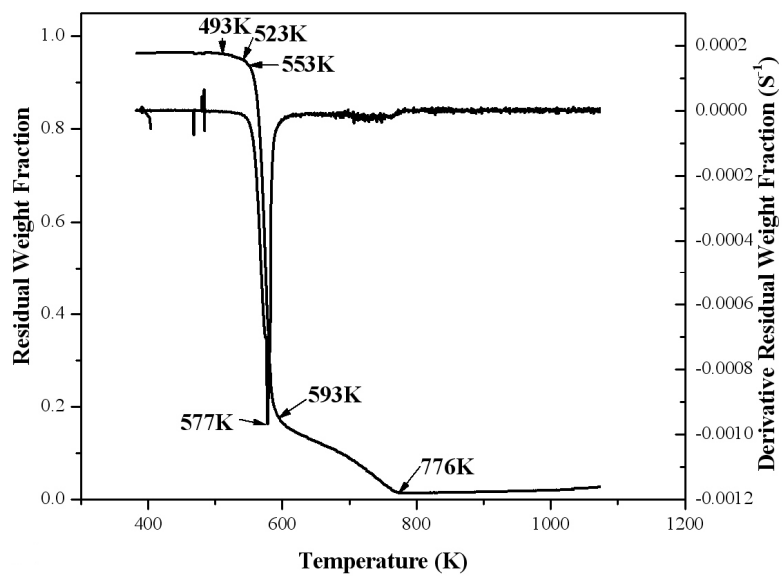
Figure 3-9 Dynamic TG curves of fibrous long cellulose
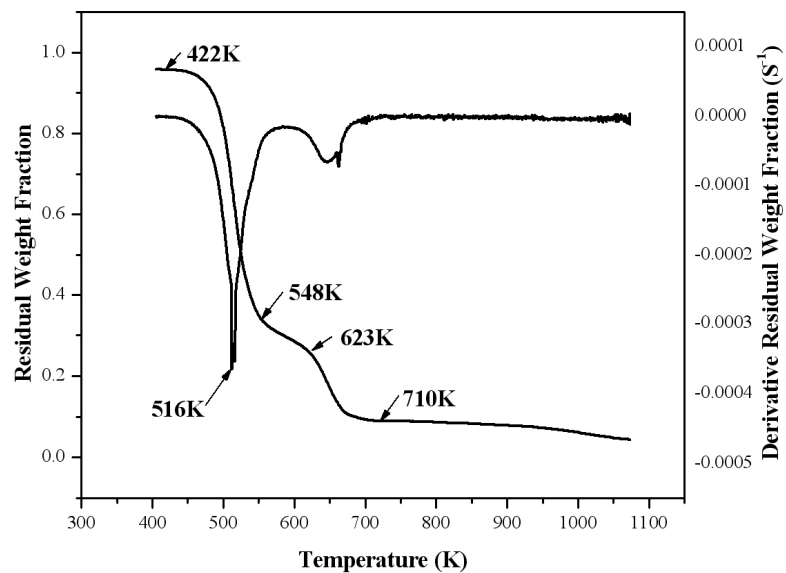
Figure 3-10 Dynamic TG curves of birchwood xylan
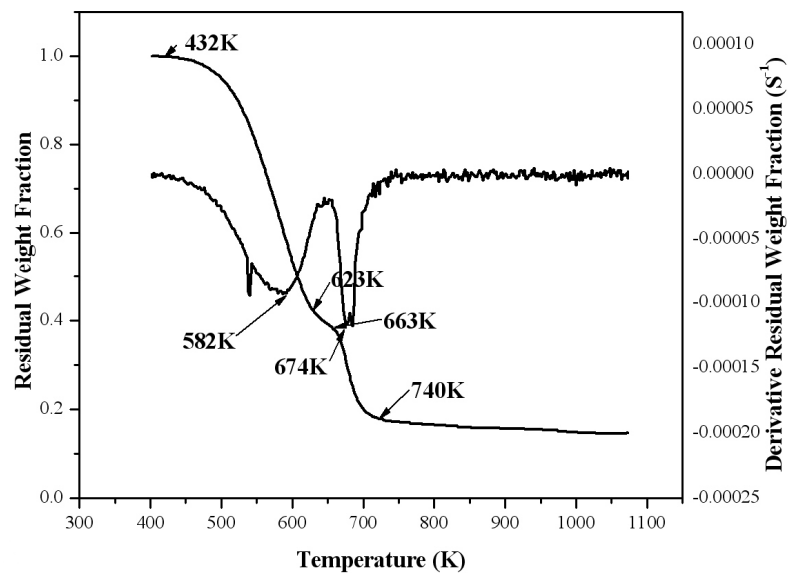
Figure 3-11 Dynamic TG curves of oat xylan

77
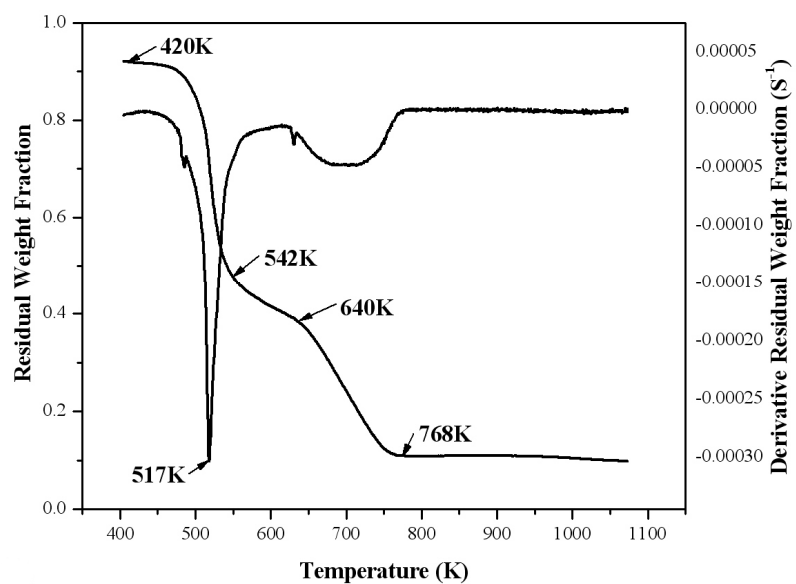
Figure 3-12 Dynamic TG curves of molecular weight 28000 lignin
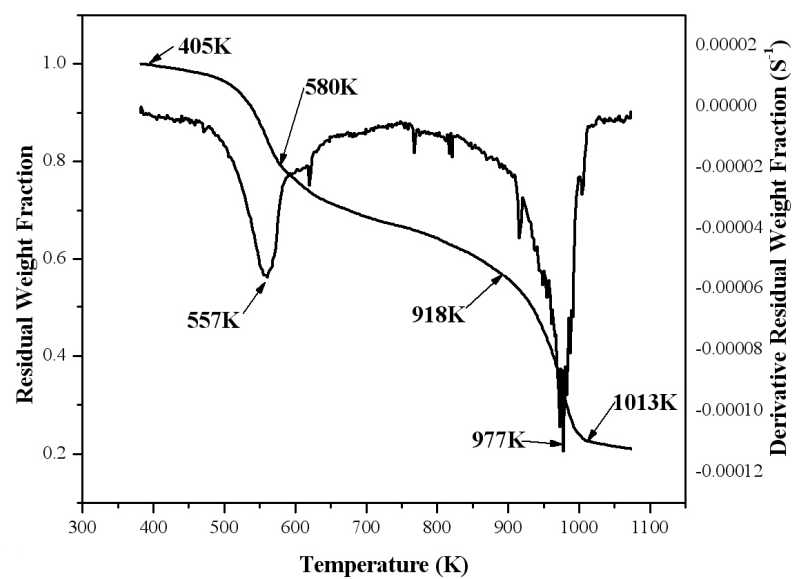
Figure 3-13 Dynamic TG curves of molecular weight 60000 lignin

Figures from 3-14 to 3-21 show the isothermal TG curves of BC softwoods and the major components in the typical torrefaction temperature range. From Figures 3-14 to 3-17, it can be seen that the significant weight loss of BC softwoods started from 533 K. From Figure 3-19, the weight loss of cellulose within 493- 543 K was very small, with a significant weight loss starting at 553 K. Figure 3-20 shows that the weight loss of xylan was very fast at temperatures higher than 523 K. Figure 3-21, on the other hand, shows that within the typical torrefaction temperature range the weight loss of lignin was limited. Increasing the reaction temperature also decreased the final residual weight fraction.
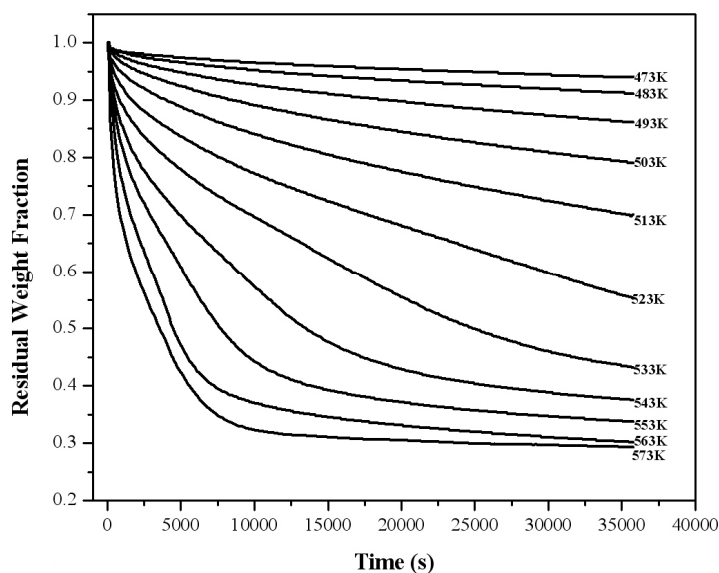
Figure 3-14 Isothermal TG curves of BC pine
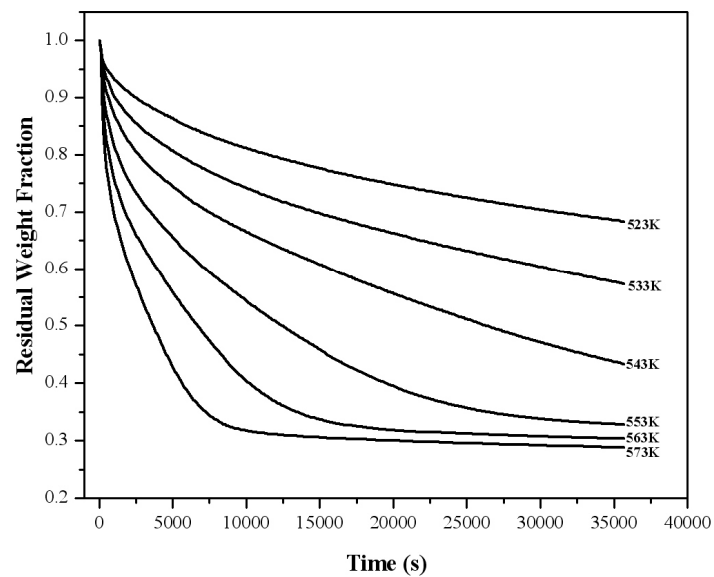
Figure 3-15 Isothermal TG curves of BC fir
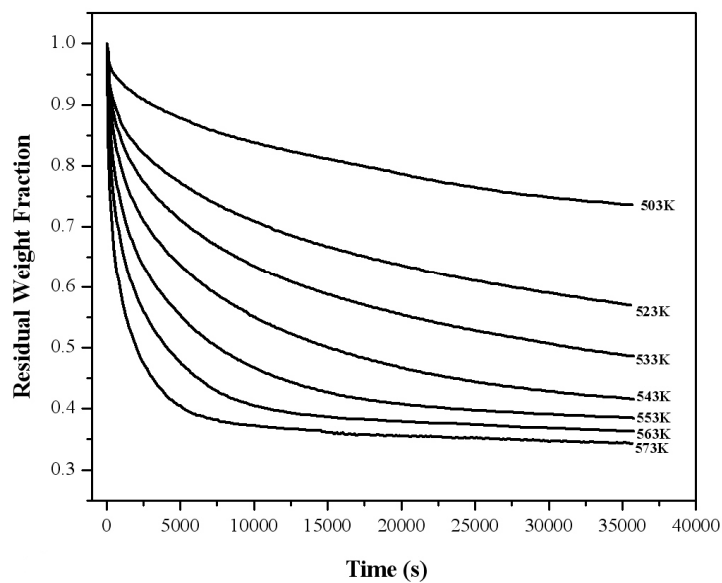
Figure 3-16 Isothermal TG curves of BC spruce
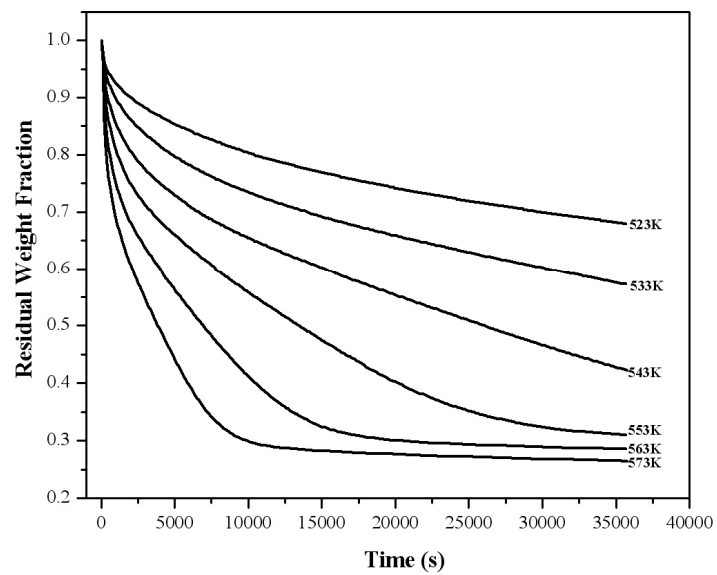
Figure 3-17 Isothermal TG curves of BC SPF
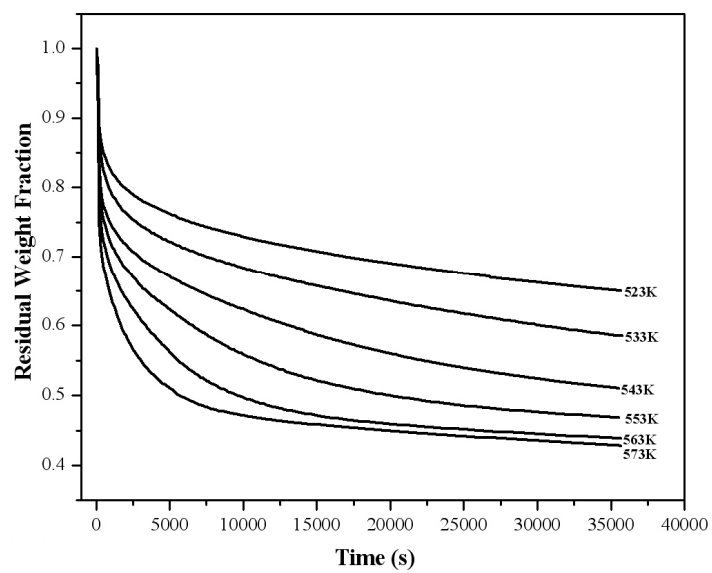
Figure 3-18 Isothermal TG curves of BC pine bark
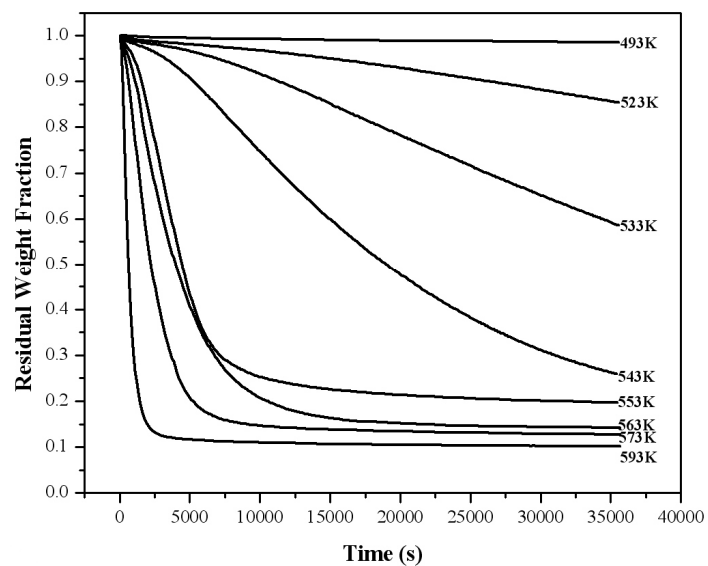
Figure 3-19 Isothermal TG curves of fibrous medium cellulose
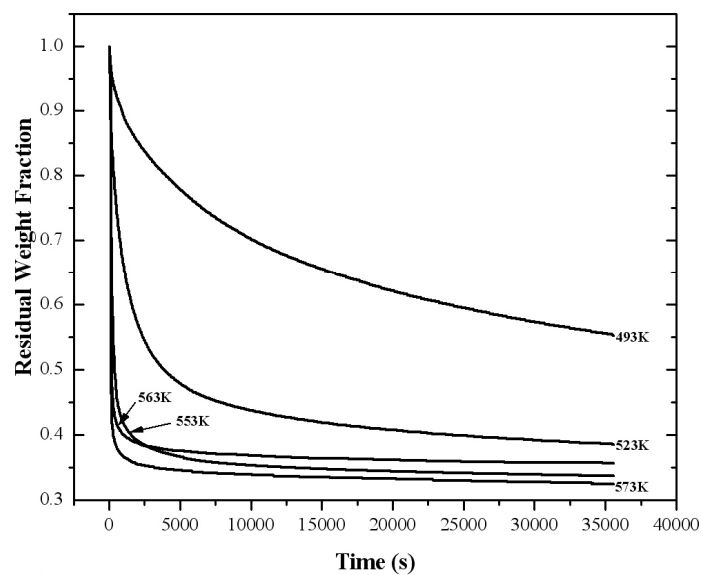
Figure 3-20 Isothermal TG curves of birchwood xylan
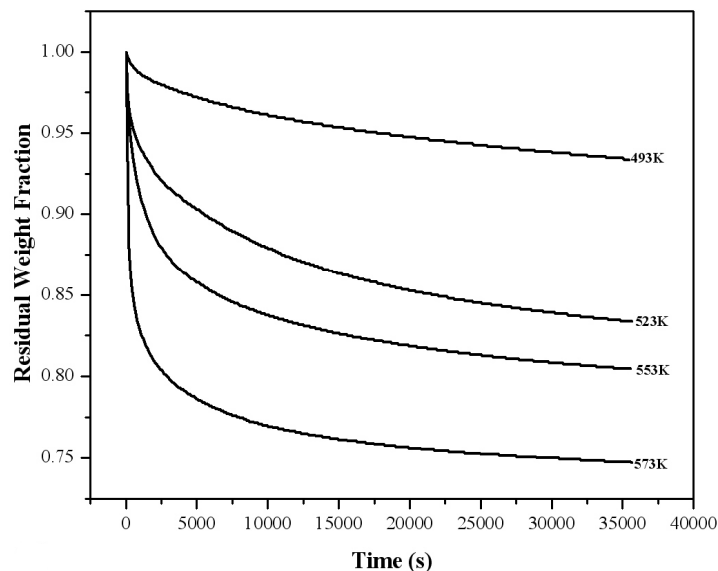
Figure 3-21 Isothermal TG curves of molecular weight 60000 lignin

3.3 Relationships between BC Pine and Three Major Components

Considering the weight loss of torrefaction was typically 20-40% (Bergman 2005), a ~30% weight loss was chosen as the base case for most calculations and analysis in this study. Figures 3-22 and 3-23 show the isothermal TG curves of BC pine, pine bark, and corresponding three major components at 553 K and 573 K. At 573K over a reaction time of 600 s, the weight losses of pine and pine bark were 28% and 33%, respectively. At the same temperature over the same reaction time, the weight loss of cellulose was 10%, the Birchwood xylan was 62%, the molecular weight 60000 lignin was 16%, and the molecular weight 28000 lignin was 18%, respectively. Similar trend was observed at 553 K. Therefore, the most weight loss of wood torrefaction was from the decomposition of hemicelluloses, followed by cellulose and lignin.
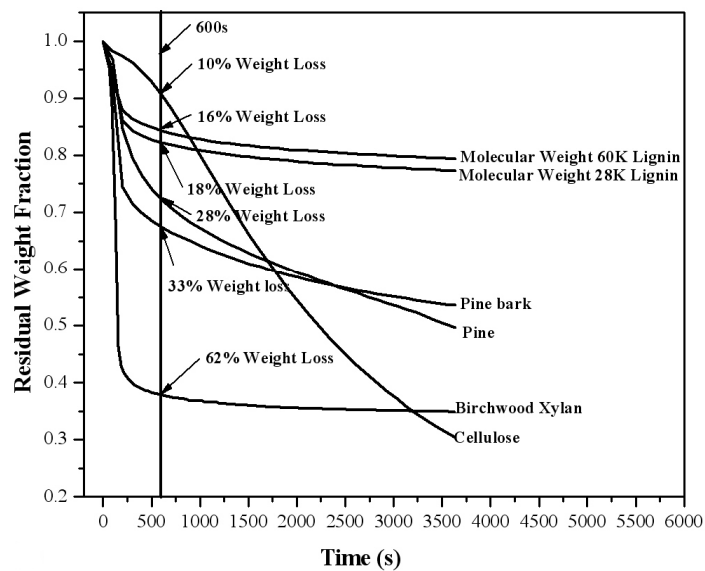
Figure 3-22 Isothermal TG curves of pine and pine bark and three major components at

573 K
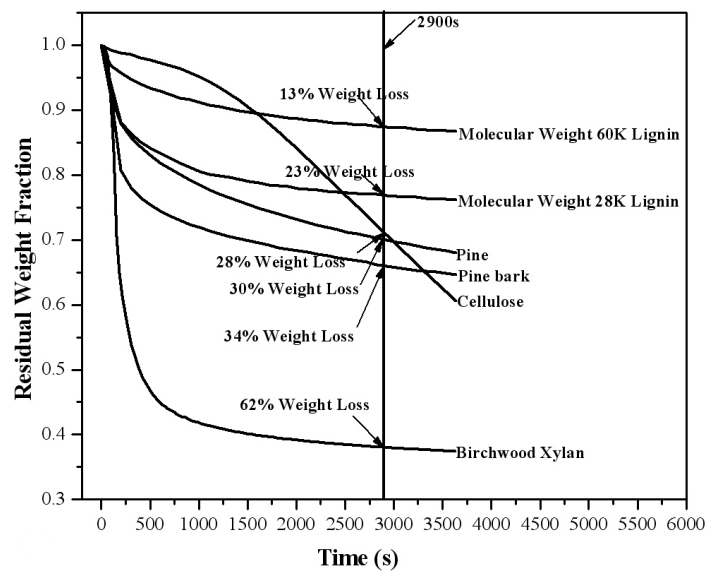
Figure 3-23 Isothermal TG curves of pine and pine bark and three major components at

553 K

Pine consists of 36.7% cellulose, 26.3% hemicelluloses, 33.6% lignin, 3.0% extractives, and 0.4% ash; pine bark contains 26.2% cellulose, 17.9% hemicelluloses, 41.01% lignin, 12.4% extractives, and 2.6% ash (see Table 2-1). If the pine and pine bark are assumed to be made up of cellulose, hemicelluloses and lignin, which decompose independently, the overall weight loss of pine and pine bark can be estimated based on the degradation of the three major chemical compositions when the interactions among the them are neglected.

Figures 3-24 and 3-25 compares measured pine and pine bark TG curves and the predictions based on the component contribution method using chemical compositions of pine and pine bark and the component torrefaction curves. It is seen from Figure 3-24 that at 573 K with the 30% weight loss for pine, the required residence time is 761 s based on TG data. At the same residence time of 761 s, the weight loss predicted from the summation of the individual weight losses of cellulose (36.7%), hemicelluloses (26.3%) and lignin (33.6%) (see Figure 3-24, multiplied by the weight fraction of each component (36.74% cellulose, 26.30% hemicelluloses and 33.61% lignin, see Table 2-1) is 27%. At 553 K, 32% weight loss of pine was predicted for the same given residence time to achieve 30% weight loss based on measured TG data. The relative difference between predicted and experimental data in general is within 10%. Therefore, the weight loss for the torrefaction of BC pine can be approximately estimated using the component contribution method based on torrefaction weight loss data for pure cellulose, xylan, and lignin samples.

For pine bark samples, the estimated weight loss is 21% at 573 K and 20% at 553 K at a corresponding measured weight loss of 30%, giving rise to a relative error of more than 25%. This suggests that the pine bark torrefaction kinetics is more complicated than wood, and cannot be approximated by the summation of the torrefaction kinetics of three

major organic components. The pine bark has 12% extractives and 3% ash whose thermal properties are quite different. Thus, the thermal decomposition behavior of pine bark cannot be described by the simple summation of the thermal degradation behavior of cellulose, hemicelluloses and lignin.
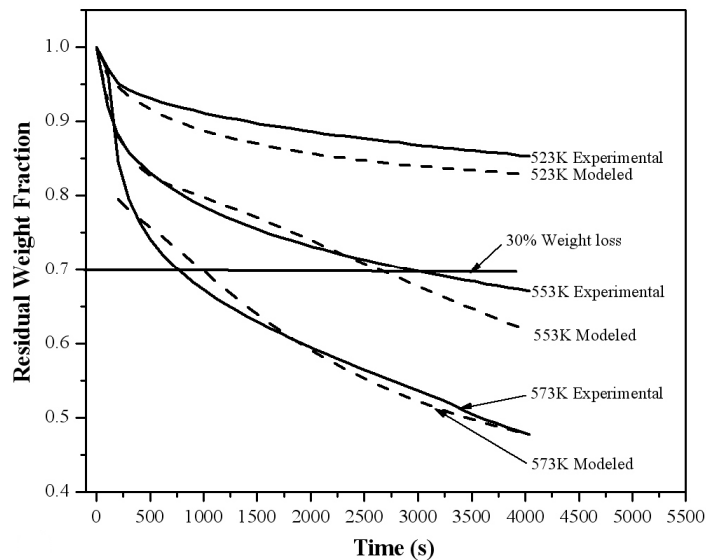
Figure 3-24 Comparison of measured pine TG curves versus predicted based on major components at pine
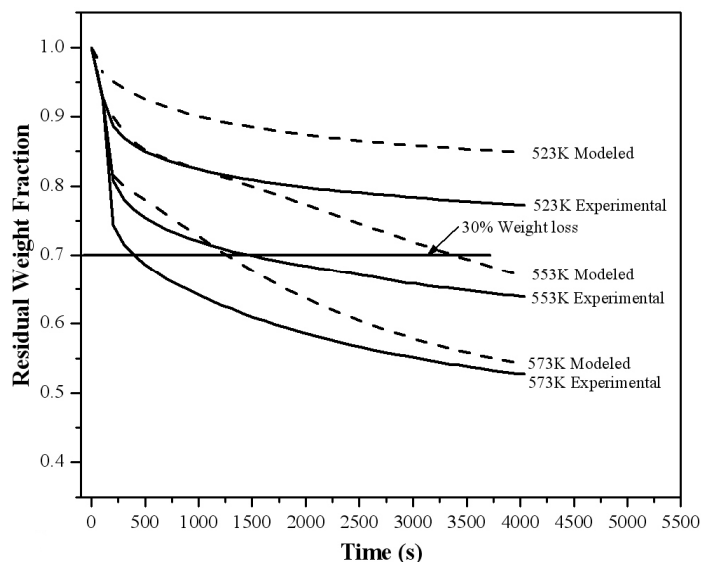
Figure 3-25 Comparison of measured pine bark TG curves versus predicted based on

major components at pine bark

3.4 A Kinetic Model for BC Softwood Torrefaction over Long Residence Time

Due to the complex compositions and structures of wood, and their associated transport properties, it is difficult to derive a widely acceptable thermal chemical conversion kinetic model for wood, even for compositions of wood, over a wide pyrolysis temperature range. Another difficulty is the mathematical method, including mathematical models and initial conditions, which also play an important role in the kinetic study. For torrefaction in a narrow and mild temperature range of 473-573K with low particle heating rate and long residence time, most residual weight fraction loss curves in Figures from 3-14 to 3-21 seem to follow an exponential decay model, with

different final residual weight fractions. Therefore, a simple one-step kinetic model may approximately describe the torrefaction of BC softwood.

The overall reaction equations for the one-step kinetic model with n^{th} order torrefaction reaction can be written as:

$$\frac{d\alpha}{dt} = k(1-\alpha)^n \tag{3-1}$$

$$k = A\exp(-\frac{E}{RT}) \tag{3-2}$$

$$\alpha = \frac{W_{TGA} - W_{final}}{1 - W_{final}} \tag{3-3}$$

If the overall torrefaction reaction is assumed to be first order, the residual weight fraction (W_{TGA}) can be expressed as:

$$W_{TGA} = W_{final} + (1 - W_{final}) \times \exp[-A\exp(-\frac{E}{RT})t] \tag{3-4}$$

The final residual weight fraction (W_{final}) can be obtained from the TG data if the residence time is long enough. At 573 K, 563 K and 553 K over 10 hours, the residual weight fraction of pine, fir, spruce and SPF may approximately represent the final residual weight fraction. But at the low temperatures, a residence time of a few days may be required to reach the final residual weight fraction [Rousset et al. 2006]. Therefore, the final residual weight fraction may be better obtained by directly fitting the TG experimental curve with the exponential decay model. In the current study, measured final residual weight was obtained for those temperatures when the final weight already

leveled off in the measured TG curves. For low temperatures, the final residual weight values were obtained by directly fitting the kinetic model equation to the TG curves. A comparison between the values obtained from the two methods for those runs at high temperature showed very little difference, confirming the consistency of the data obtained from the two different methods. Figure 3-26 shows the $\ln(\dfrac{1}{W_{final}}-1)$ of BC softwoods as a function $\dfrac{1}{T}$ for torrefaction. It is evident from Figure 3-27 that the final residual weight fraction had a very strong relationship with the torrefaction temperature. And the final residual weight fraction may be correlated to temperature by:

$$\ln(\frac{1}{W_{final}}-1) \approx a_0 + a_1 \times \frac{1}{T} + a_2 \times (\frac{1}{T})^2 \qquad (3\text{-}5)$$
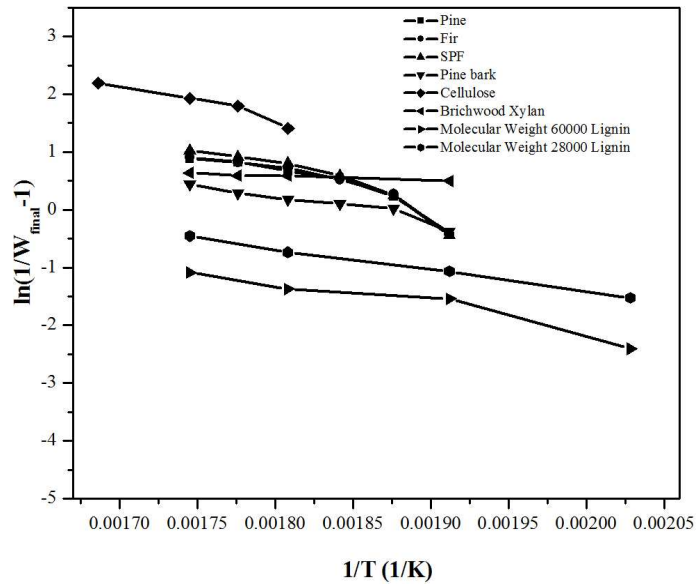
Figure 3-26 $\ln(\dfrac{1}{W_{final}}-1)$ versus $\dfrac{1}{T}$ for BC softwood and chemical compositions

torrefaction

89

Table 3-1 summarizes one-step model reaction kinetic constants and the final residual weight fraction constants of BC softwoods and chemical compositions. From Table 3-1, the final residual weight fraction constants for pine, fir spruce and SPF were very close, but substantially higher than pine bark. The apparent activation energies of BC softwoods varied widely from 95 to 130 $kJ\ mol^{-1}$, with the value for pine bark (69 $kJ\ mol^{-1}$) substantially lower. Reina (1998) reported an apparent activation energy of 125 $kJ\ mol^{-1}$ from the isothermal TG curves of forest waste (<1000 μm) in the range of 498-598 K. Akita and Kase (1967) reported that the reaction rate of the cellulose was $k = 6.6\times10^{16}\exp(-224000/RT)$ s^{-1}. Ramiah (1970) reported the reaction rate of hemicelluloses was $k = 7.8\times10^{12}\exp(-125000/RT)\,s^{-1}$ from the Isothermal TG curves in the range 488-523 K. Tang (1967) reported the activation energy of lignin was 87.8 $kJ\ mol^{-1}$ based on TG results under vacuum conditions in the range of 553-617 K.

Table 3-1 Summary of the one-step model reaction kinetic constants and the final residual weight fraction constants for BC softwoods and chemical compositions torrefaction

Items	Kinetic	Constants	Final	Weight	Constants
	E, $kJ\ mol^{-1}$	ln(A), s^{-1}	a_0	a_1	a_2
Pine	130.69	19.49	0.90	6.78E3	−3.84E6
Fir	127.92	18.86	0.90	6.96E3	−3.94E6
Spruce	94.92	12.48	0.82	4.72E3	−2.72E6
SPF	122.24	17.58	1.05	7.71E3	−4.37E6
Pine bark	69.41	6.37	0.35	4.01E3	−2.26E6
Cellulose	213.54	37.35	2.25	5.61E3	−3.34E6
Hemicelluloses	145.50	25.66	0.65	7.12E2	−4.14E5
Molecular Weight 60000 Lignin	76.05	8.52	−1.10	3.88E3	−2.21E6

The experimental and model fitted curves of BC softwoods and chemical compositions are shown in Figures from 3-27 to 3-34. It can be seen that at both 553 and 573 K the one-step model fitted well the data of pine, fir, spruce, SPF, and cellulose. The

agreement was poor at 533 K. For the pine bark, the agreement was generally very poor for all three tested temperatures. The one-step model for the Birchwood Xylan at the begin time was not good. For the lignin the model may be good for the very long residence time. The pine bark includes the more lignin, so the TG curves mostly like the lignin curves. Therefore, the one-component model can predict the reaction time reasonably well in the long residence time for BC softwoods.
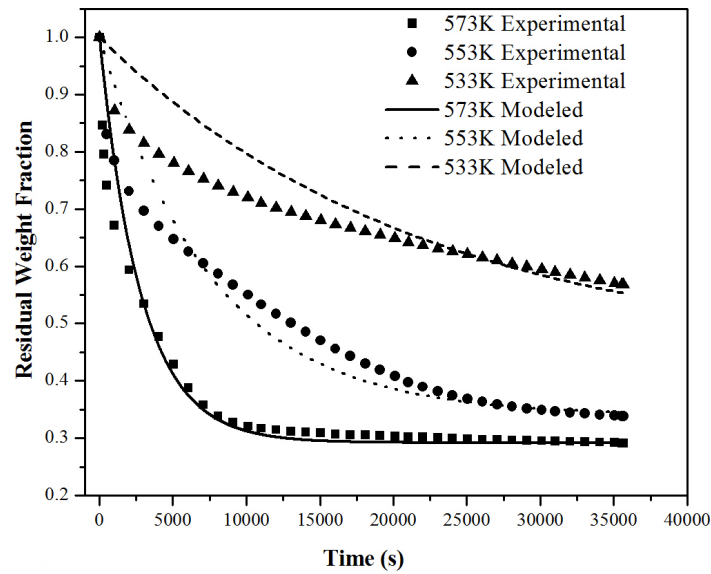
Figure 3-27 Experimental and one-step model fitted curves of BC pine
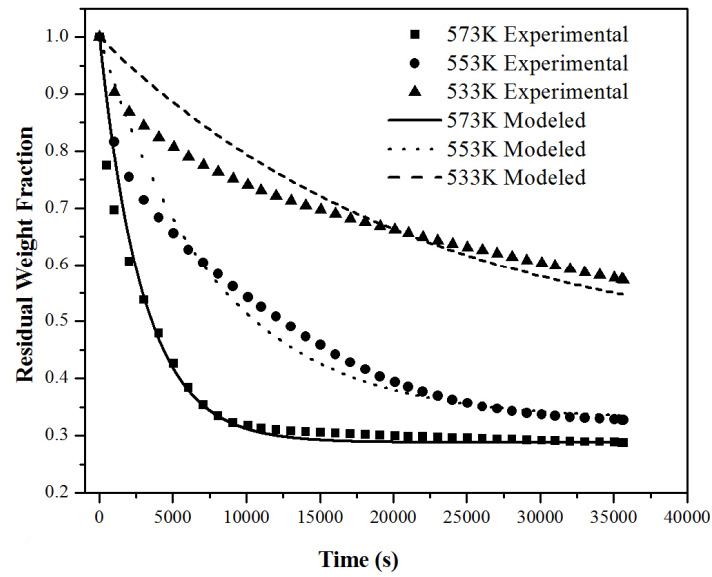
Figure 3-28 Experimental and one-step model fitted curves of BC fir
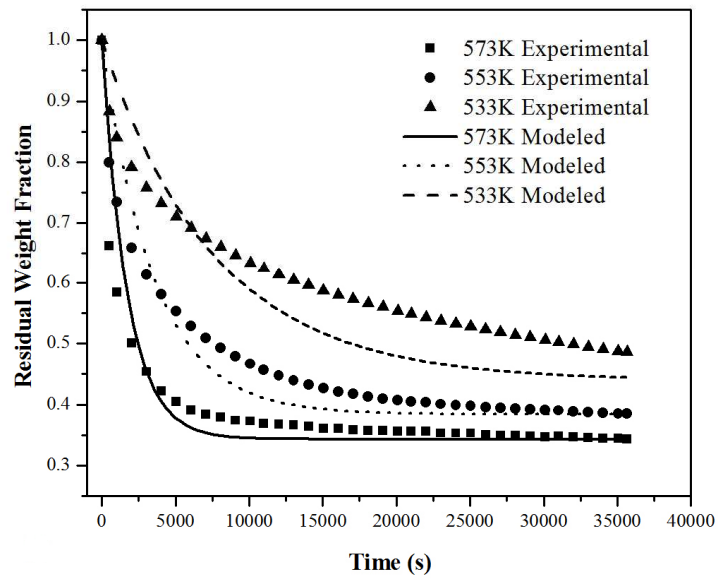
Figure 3-29 Experimental and one-step model fitted curves of BC spruce
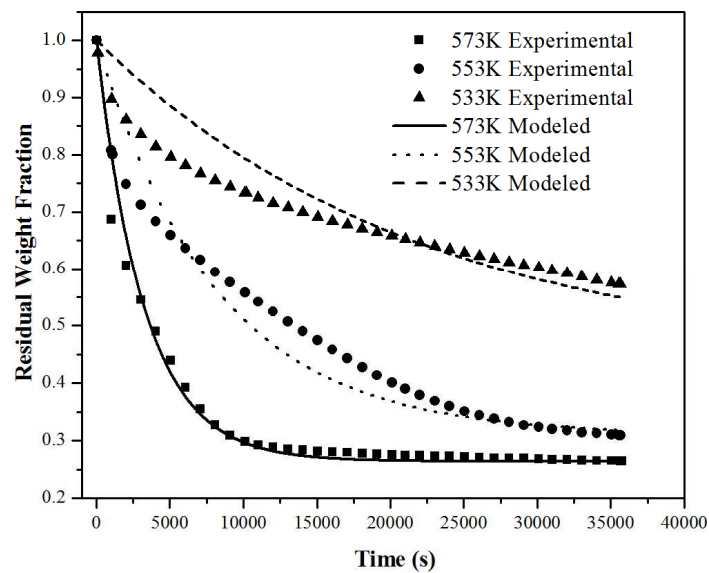
Figure 3-30 Experimental and one-step model fitted curves of BC SPF
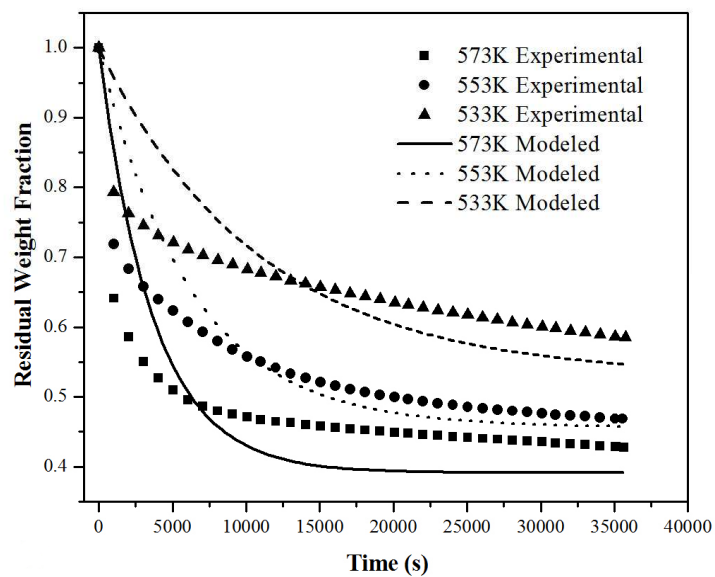
Figure 3-31 Experimental and one-step model fitted curves of BC pine bark
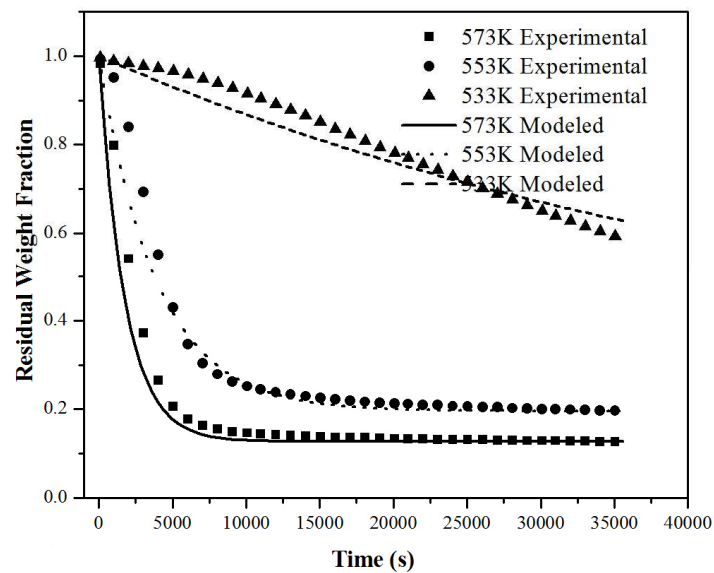
Figure 3-32 Experimental and one-step model fitted curves of fibrous medium cellulose
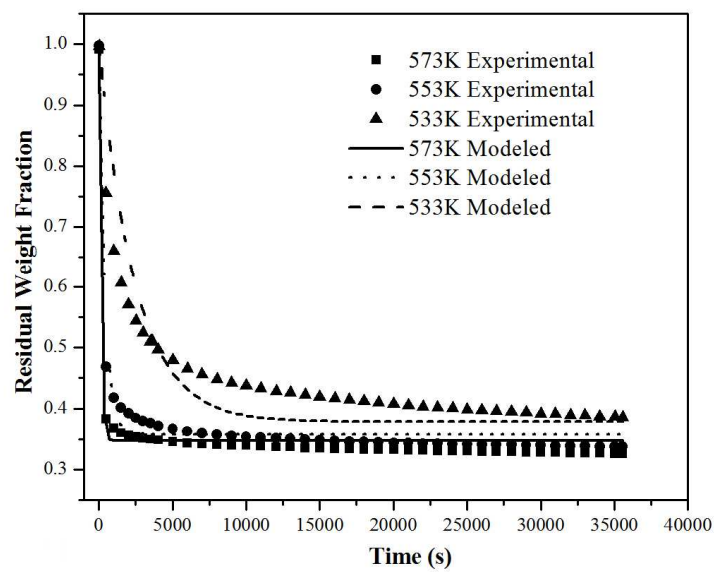
Figure 3-33 Experimental and one-step model fitted curves of birchwood xylan
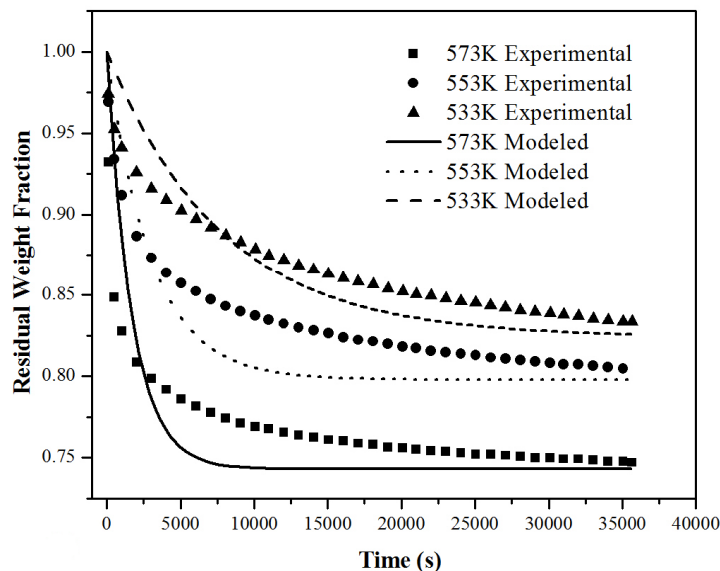
Figure 3-34 Experimental and one-step model fitted curves of molecular weight 60000 lignin

3.5 A Kinetic Model for BC Softwood Torrefaction over Short Residence Time

As shown in Figures from 3-27 to 3-34, the one-step torrefaction kinetic model gave a reasonable fit to the kinetics data over long residence times, but a poor agreement with the measured pyrolysis kinetic data at short residence time with low weight losses of relevance to torrefaction. As shown in the TG curves in Figures from 3-27 to 3-34, within the short residence time (<30 min) with less than 35% weight loss, most hemicelluloses will decompose within the first 30 min. The weight loss rate of lignin, on the other hand, was faster than the cellulose initially; but the weight loss of cellulose became faster than lignin after 30 min or so. To capture the torrefaction behaviour of BC softwoods, a two-component torrefaction reaction kinetic model was thus proposed and evaluated for

torrefaction within short residence time of commercial interest (i.e. a weight loss lower than 35% with a residence time shorter than 1 hour).

$$Wood \xrightarrow[\text{Fast· Reaction· Group}]{k_1} Volatiles + Chars$$

$$Wood \xrightarrow[\text{Medium· Reaction· Group}]{k_2} Volatiles + Chars$$
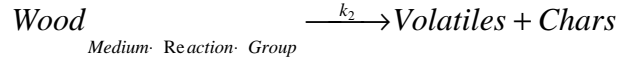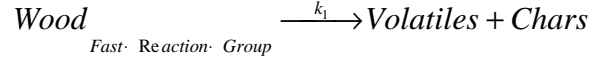
For two reaction groups, the conversion (reacted fraction) α_1, α_2 and the reaction rate, $\frac{\partial \alpha_1}{\partial t}$ and $\frac{\partial \alpha_2}{\partial t}$, are defined. The overall reaction rates are a linear combination of these partial reactions:

$$\frac{\partial w^{calc}}{\partial t} = -(C_1 \frac{\partial \alpha_1}{\partial t} + C_2 \frac{\partial \alpha_2}{\partial t}) \tag{3-6}$$

$$\frac{\partial \alpha_1}{\partial t} = A_1 e^{-\frac{E_1}{RT}} (1-\alpha_1)^{n_1} \tag{3-7}$$

$$\frac{\partial \alpha_2}{\partial t} = A_2 e^{-\frac{E_2}{RT}} (1-\alpha_2)^{n_2} \tag{3-8}$$

If the two overall reactions are assumed to be first order reactions, the residual weight fraction (W_{TGA}) of softwood samples is given by:

$$W_{TGA} = (1-C_1-C_2) + C_1 \times \exp(-A_1 e^{-\frac{E_1}{RT}} t) + C_2 \times \exp(-A_2 e^{-\frac{E_2}{RT}} t) \tag{3-9}$$

C_1 may be set as the hemicelluloses fractional content of BC softwood, and C_2 represents

96

the combined cellulose and lignin fractional content, with the values for BC softwood given in Table 2-1. The two-component torrefaction model reaction constants of BC softwood samples were estimated by the regression of the isothermal TG data at a time less than 7000 second, with the results shown in Table 3-2. E_1 and A_1 were the fast reaction group reaction kinetic constants, representing the thermal decomposition of the hemicelluloses of BC softwoods. E_2 and A_2 represented the thermal degradation rate of cellulose and lignin. From Table 3-2, the rate constants for pine, fir, spruce and SPF particles were seen to be very close, but different from pine bark.

Table 3-2 Two-component torrefaction model reaction constants of BC softwoods

Items			Reaction		Constants	
	C_1	C_2	E_1, *kJ mol^{-1}*	$\ln(A_1)$, *s^{-1}*	E_2, *kJ mol^{-1}*	$\ln(A_2)$, *s^{-1}*
Pine	0.263	0.704	115.57	18.56	225.38	38.34
Fir	0.250	0.722	110.75	17.18	240.94	41.69
Spruce	0.200	0.775	140.53	24.12	187.27	30.46
Pine bark	0.179	0.672	65.73	9.58	97.51	11.62

The experimental and model fitted curves of BC softwoods were compared in Figures from 3-35 to 3-38. It can be seen that in the 533-573 K range the current two-component torrefaction model gave a good fit to the isothermal TG experimental data over the short residence time, except for pine bark.

The thermal properties of pine bark are quite different from pine because of the 12% extractives and 3% ash contents. Thus, the pine bark torrefaction model with fixed C_1 and C_2 values based on hemicelluloses, cellulose and lignin many not be able to capture its complicated torrefaction behaviour.
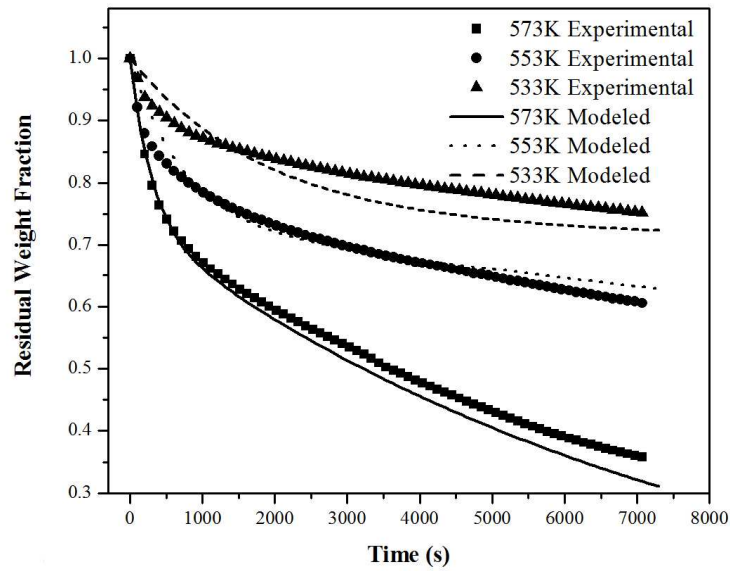
Figure 3-35 Experimental and two-component torrefaction model fitted curves of BC pine
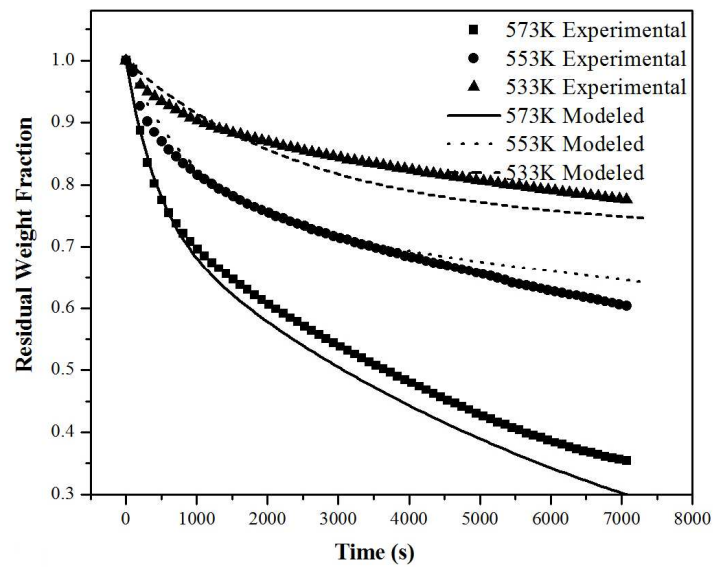
Figure 3-36 Experimental and two-component torrefaction model fitted curves of BC fir

98
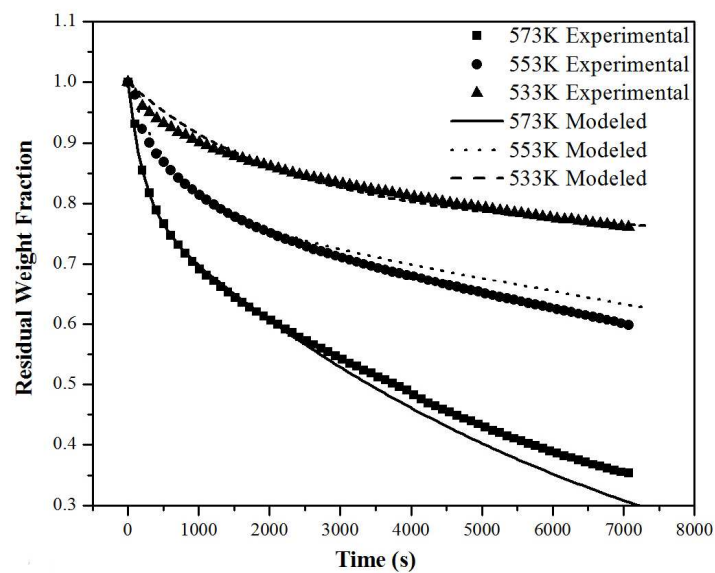
Figure 3-37 Experimental and two-component torrefaction model fitted curves of BC spruce
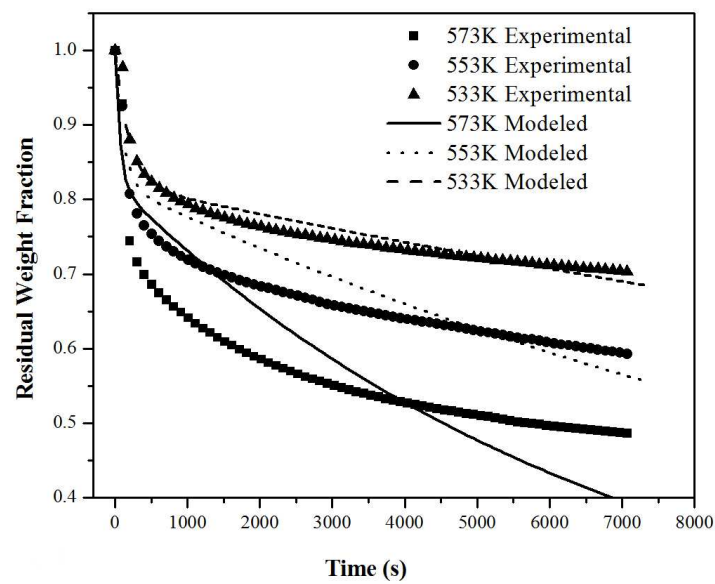
Figure 3-38 Experimental and two-component torrefaction model fitted curves of BC pine bark

99

3.6 An Empirical Kinetics Equation for BC Pine Bark over Short Residence Time

The thermal properties of pine bark are quite different than pine because of 12% extractives and 3% ash content. Thus, the pine bark torrefaction model may be more complicated than pine, and cannot be described by the normal reaction theories. To guide the design and optimization of torrefaction reactors, the hemi-experimental equation may be introduced. To fit the isothermal TG experimental data of the pine bark, the residual weight fraction (W_{TGA}) for the two-component model may be given by:

$$W_{TGA} = (1 - G_1 - G_2) + G_1 \times \exp(-k_1 t) + G_2 \times \exp(-k_2 t) \tag{3-10}$$

G_1 is the fractional content of the fast reaction group mostly as hemicelluloses. G_2 is the fractional content of the medium reaction group as cellulose and lignin. Table 3-3 shows the two-component model reaction kinetic constants and reaction group fraction constants of pine bark samples. k_1 is the fast reaction group reaction rate which may represent the thermal decomposition of the hemicelluloses content of pine bark. k_2 represented the thermal degradation rate of cellulose and lignin. From table 3-3, the fast reaction rate constant (k_1) of pine bark is about 10 times higher than the 2nd reaction (k_2). Decreasing the temperature decreased both fractions of the reaction groups (G_1 and G_2), which cannot be explained based on the content of hemicelluloses, cellulose, and lignin.

The experimental and model fitted curves of pine bark were compared in Figure 3-39. It can be seen that in the 533-573 K range the current two-component kinetic model gave a very good fit to the isothermal TG experimental data over the short residence time range of practical interest for pine bark torrefaction.

Table 3-3 Two-component model reaction rates and group fractions of pine bark

Temperature, K	G_1	G_2	k_1, s^{-1}	k_2, s^{-1}
573	0.303	0.234	5.92E-03	3.40E-04
563	0.283	0.271	5.45E-03	1.77E-04
553	0.251	0.209	5.46E-03	1.94E-04
543	0.232	0.155	5.37E-03	2.11E-04
533	0.192	0.136	4.19E-03	2.37E-04
523	0.143	0.123	5.91E-03	2.95E-04
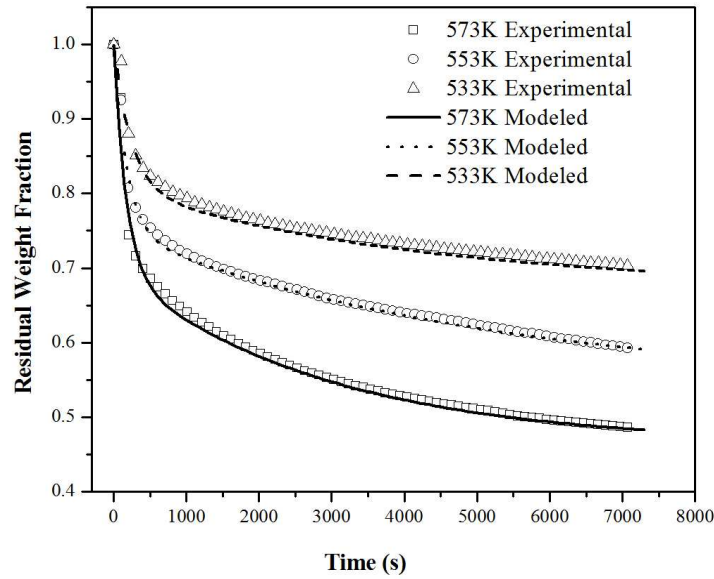
Figure 3-39 Experimental and hemi-experimental model fitted curves of pine bark

Figure 3-40 plots $\ln(\dfrac{1}{1-G_{1,or2}}-1)$ as a function of $\dfrac{1}{T}$ (T: reaction temperature) for pine bark. The reaction group fractions had a very strong correlation with the torrefaction temperature. From Figure 3-40, the following correlations between $\ln(\dfrac{1}{1-G_{1,or2}}-1)$ and $\dfrac{1}{T}$ were obtained by regression:
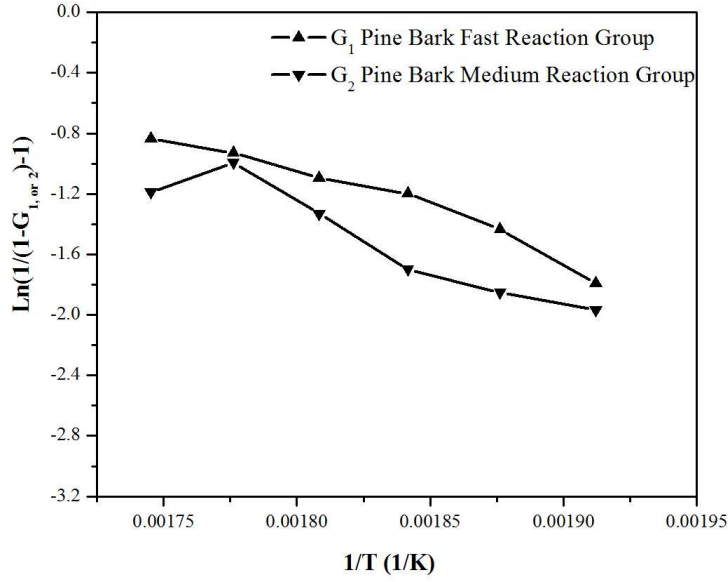
Figure 3-40 $\ln(\dfrac{1}{1-G_{1,or2}}-1)$ versus $\dfrac{1}{T}$ for pine bark

$$\ln(\frac{1}{1-G_1}-1)_{Pine\ Bark}=-0.80+5.09E3\times(\frac{1}{T})-2.91E6\times(\frac{1}{T})^2 \qquad (3\text{-}11)$$

$$\ln(\frac{1}{1-G_2}-1)_{Pine\ Bark}=-1.00+5.33E4\times(\frac{1}{T})-3.06E6\times(\frac{1}{T})^2 \qquad (3\text{-}12)$$

3.7 Summary

For the pine sample, the weight loss within the typical operating range of torrefaction can be reasonably predicted by the component contribution method based on the cellulose, hemicelluloses, and lignin fractions and their corresponding torrefaction kinetics, with less than 10% errors. However, such a component contribution method substantially underestimated the weight loss for the torrefaction of pine bark samples. The simple one-step kinetic model with the first order reaction can predict reasonably well the

reaction kinetic data obtained over the long residence time, and the final wood residual weight had a very strong relationship with the torrefaction temperature. Within the typical reaction temperature range and relatively short residence times of practical torrefaction reactions, the intrinsic torrefaction of BC softwoods can be well described by a two-component 1st order one-step decomposition kinetic model.

CHAPTER 4 TORREFACTION AND DENSIFICATION OF BC SOFTWOODS

In this chapter, the bench-scale tubular reactor unit has been used for the study of torrefaction of BC softwood residues. The MTI 50K press machine was used to make and evaluate torrefied pellets from torrefied softwood. The main objective of this study is to identify optimal torrefaction and densification conditions for the production of high quality torrefied wood pellets.

4.1 Experimental

4.1.1 Samples

Pine and spruce chips from FPInnovations, fir and SPF (a mixture of spruce, pine and fir) chips from Fiberco, pine bark and SPF shavings from Wood Pellet Association of Canada, have been tested in this study. The properties of BC softwood residues used in this study are given in Table 4-1. Figure 4-1 shows the particle size distribution of different samples. From Figure 4-1 (a), it is seen that the particle size distributions of spruce, pine, fir and SPF were very close, but different from pine bark. The true material density of BC softwoods was around 1400 $kg\ m^{-3}$. The pine bark had the high heating value.

Table 4-1 Properties of BC softwood particle samples

	0.79mm Screen Size					SPF shavings
	Spruce	Pine	Fir	SPF	Pine Bark	SPF
Moisture content, %wt	9.54	7.44	3.19	3.46	7.20	9.94
Bulk density, $kg\ m^{-3}$	199	225	232	176	310	156
True density, $kg\ m^{-3}$	1413	1412	1441	1430	1380	1346
High heating value, $MJ\ kg^{-1}$	18.33	18.60	18.38	18.56	19.52	18.13
Particle mean size (Sauter), mm	0.21	0.23	0.20	0.21	0.09	1.10
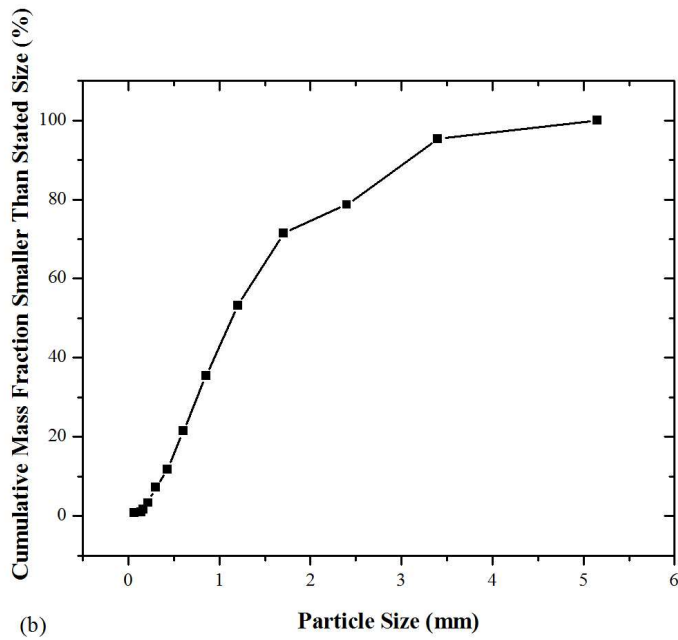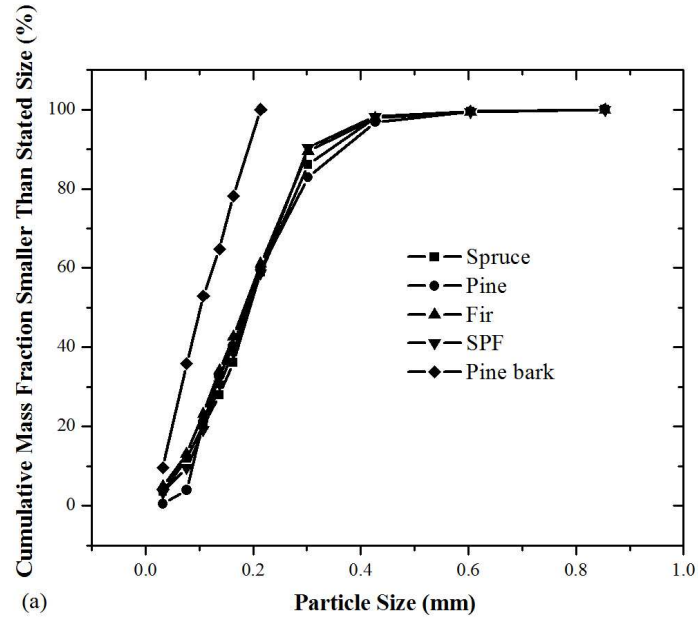
Figure 4-1 Cumulative particle size distributions

(a) Different BC softwood samples prepared using a grinder screen opening of 0.79 mm;

(b) 4.00 mm screen opening SPF shavings.

4.1.2 Experimental Design

The bench-scale fixed bed unit as described in Chapter 3 was used for torrefaction tests. Two sets of tests were conducted. In the first set, SPF shavings were torrefied at different temperatures and different residence times to investigate the effect of torrefaction temperature and residence time on the properties of torrefied sawdust and pellets. In the second set of tests, different species of softwood of similar particle size were torrefied at the same residence time and torrefaction temperature, followed by densification, to examine the performance of different wood species. For each sample, at least two replicates were tested for each reaction condition.

The MTI 50K press machine was used for compressing torrefied sawdust into pellets. In this study, the top hole of the cylinder was filled with approximately 0.5 gram samples to make a single pellet of 6.5 mm in diameter and 12 mm in length. The sample was pressed by applying a pressure of 125 or 156 MPa and holding for a few minutes. Then the machine was continued to press the sample until a maximum pressure of 156 or 187 MPa was reached. Normally, for making control pellets, the die temperature was maintained at 70 ^{o}C with the 125 MPa compression pressure and 1 minute holding time.

Both increasing the die temperature and preconditioning the sample to higher moisture content have been examined in this study to compress torrefied sawdust into pellets, with the die temperature ranging from 70 to 280 ^{o}C and the different pressure from 125 to 280 MPa. Preconditioning of torrefied sawdust added 0, 5, 10 and 15% water and waiting for 24-72 hours before compression was also explored.

The pellet density was obtained from measured mass and volume of individual pellets. Energy consumption was calculated from measured forces and displacement recorded

during compression. The moisture uptake of pellets was measured by placing the pellets into the humidity chamber set at 30 ^{o}C and 90% relative humidity. The Meyer hardness is determined by measured diametrical forces to break a pellet, as described in Chapter 3.

4.2 Temperature Gradient in the Tubular Reactor

Woody biomass has a very low thermal conductivity and heat capacity. Since wood torrefaction is an endothermic reaction, these properties may create some temperature gradients in the torrefaction reactor, which may affect the torrefaction performance.

To estimate the radial temperature gradient in the tubular fixed bed reactor, the torrefaction reaction was assumed to be a simple one-step reaction with zero order and the reaction volume remains constant. The equation of energy balance for torrefaction can then be simplified to:

$$\frac{\partial T}{\partial t} = \frac{k_s}{\rho_s C_p} [\frac{1}{r} \frac{\partial}{\partial r} (r \frac{\partial T}{\partial r})] - \frac{H_A k_0}{C_P} e^{-\frac{E}{RT}} \qquad (4\text{-}1)$$

where, T is the temperature, K; t is the time, s; k_s is the thermal diffusivity of bulk pine sawdust (roughly estimated from $\frac{1}{k_s} = \frac{\varepsilon}{k_a} + \frac{1-\varepsilon}{k_w}$ [Tsotsas and Martin 1987], k_w is the heat conductivity of pine, 0.109 $W\ m^{-1}\ K^{-1}$ [Bird 2002]; k_a is the heat conductivity of air, 0.025 $W\ m^{-1}\ K^{-1}$ [Bird 2002], ε is the void fraction of the packed bed of sawdust, 0.45); ρ_s is the density of pine sawdust, 200 $kg\ m^{-3}$ [Hu et al. 2005]; C_p is the heat capacity of pine, 1640 $J\ kg^{-1}\ K^{-1}$ [Hu et al. 2005]; H_A is the heat of decomposition, 792.15 $J\ g^{-1}$

[Ning et al. 2006]; k_0 is the pre-exponential factor, $1.40 \times 10^{10} s^{-1}$ [Wagenaar et al. 1994];

E is the apparent activation energy, 150 kJ mol^{-1} [Wagenaar et al. 1994]; R is the gas law constant, 8.3144 $J\ mol^{-1}\ K^{-1}$.

The above equation was solved numerically by using the MATLAB software with proper initial and boundary conditions. The initial condition was set as: that the temperature of sawdust was equal to 473 K at t=0. The boundary conditions were set to: that the wall surface temperature was constant at 573 K and $\frac{dT}{dr}\big|_{r=0} = 0$ at the centre. The simulated results in Figure 4-2 show that there exists a large radial temperature gradient in the unit, with the temperature difference between the wall and the center being more than 30 K after 500 second and remaining unchanged. It means that in the tubular fixed bed reactor the temperature gradient can lead to the non-uniform torrefaction conversion of sawdust along the radial direction.

The vertical temperature gradient was measured with a 10-point multi-thermocouple. The multi-thermocouple with a 48 mm interval was located in the center of the reactor tube to monitor the temperature profile (see Figure 4-3). Figure 4-4 shows the vertical temperature profiles in the reactor loaded with 0.2-0.3 mm diameter glass beads as a function of time. The furnace temperature was initially set to 340 ^{o}C. Figure 4-4 (a) shows that there exist significant vertical temperature gradients, with a relatively uniform temperature zone located in the middle section of the reactor. To reduce the vertical temperature gradients in the reactor, a hot N_2 flow was introduced. Figure 4-4 (b) shows the vertical temperature gradient profile in the reactor with 0.5 SCFM hot N_2 flow was reduced. As expected, the introduction of hot N_2 flow reduced the axial temperature gradient. Although not measured, the hot N_2 flow is also expected to reduce the radial temperature gradient significantly.
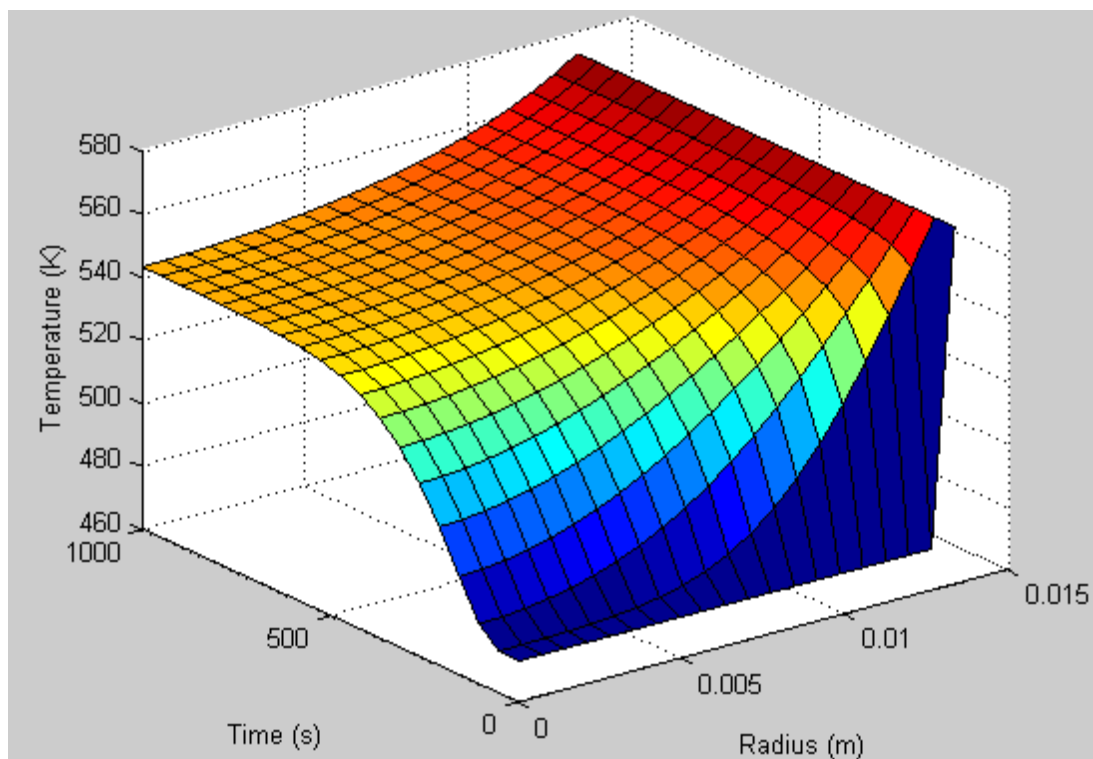
Figure 4-2 Radial temperature gradient profiles of pine sawdust in the packed bed unit
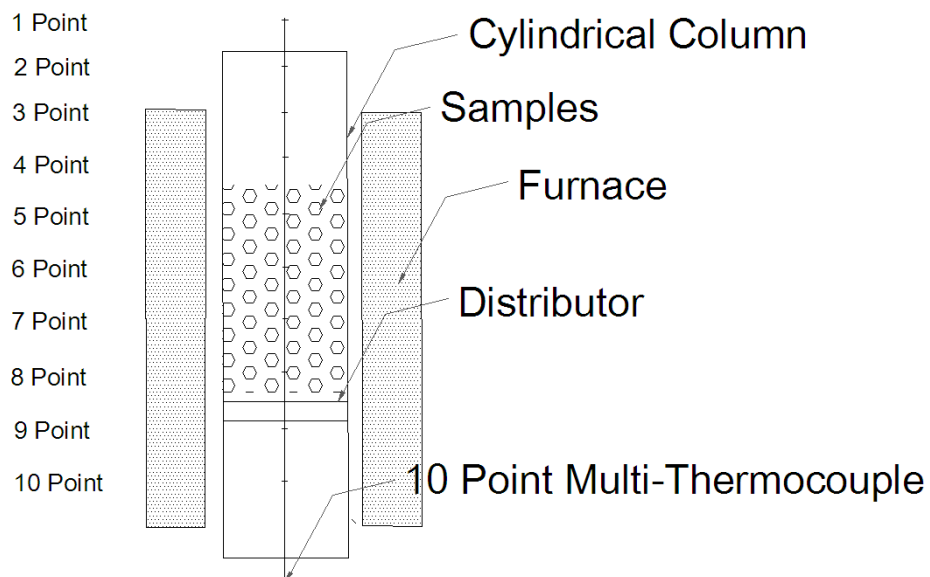
Figure 4-3 10-Point multi-thermocouple located in the reactor

To achieve uniform torrefaction of biomass samples, both the radial and vertical temperature gradients should be minimized. In the tubular fixed bed unit, a small reactor diameter should be used. In order to have enough samples prepared in each run for pelletization tests, a 27 mm diameter reactor tube was used in this study with a hot N_2 purge. From Figure 4-4 (b), the same temperature reaction zone of ~102 mm long located between point 6 and point 8 was chosen as the torrefaction reaction zone, loaded with sawdust particles.

Four thermocouples (CH0, CH1, CH2, and CH3) were used for monitoring the reactor temperatures (see Figure 2-17). CH0 was located in the centre of the tube 15 mm from the top of the reactor for measuring N2 gas temperature. CH1 was located in the centre of the tube 232 mm from the bottom of the reactor for measuring the biomass sample temperature. CH2 was attached onto the centre wall of the gas heater outside the reactor tube for monitoring the heater surface temperature. CH3 was also located outside the reactor tube wall at around 340 mm from the bottom of the reactor for measuring the furnace temperature.

Figure 4-5 shows the reactor temperature variation over time for a typical torrefaction reactor loaded with pine samples. The pre-heating time from the room temperature to 200 ^{o}C took about 25 minutes. It took about 10 min to further raise the temperature from 200 to 250 ^{o}C, and 20 min to 300 ^{o}C. The sample cooling from the torrefaction temperature to below 200 ^{o}C took less than 10 min to stop the torrefaction reaction. Figure 4-5 also shows that at the beginning of torrefaction, to maintain the same torrefaction temperature of the sample, the furnace temperature needs to be 30-40 ^{o}C higher than the sample temperature to maintain the target torrefaction temperature of sample because of the high torrefaction reaction rate. At the late stage with a low torrefaction rate, the temperature difference between the sample and the furnace was very small.
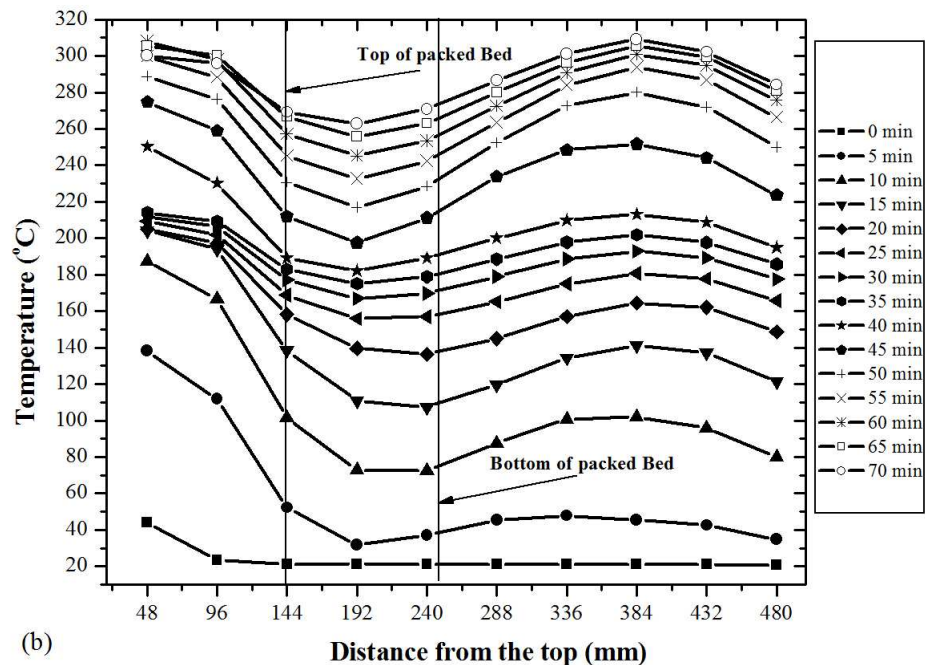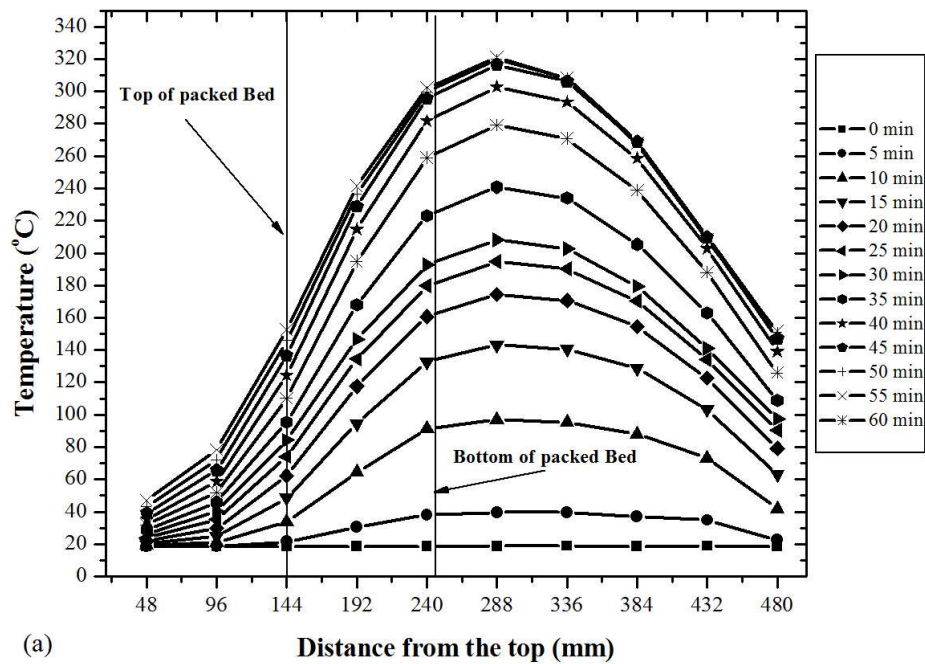
Figure 4-4 Measured vertical temperature gradient profile in the 27 mm reactor filled
with 0.2-0.3 mm glass beads
(a) Without nitrogen flow; (b) with 0.5 SCFM hot N_2 flow

(a)

(b)
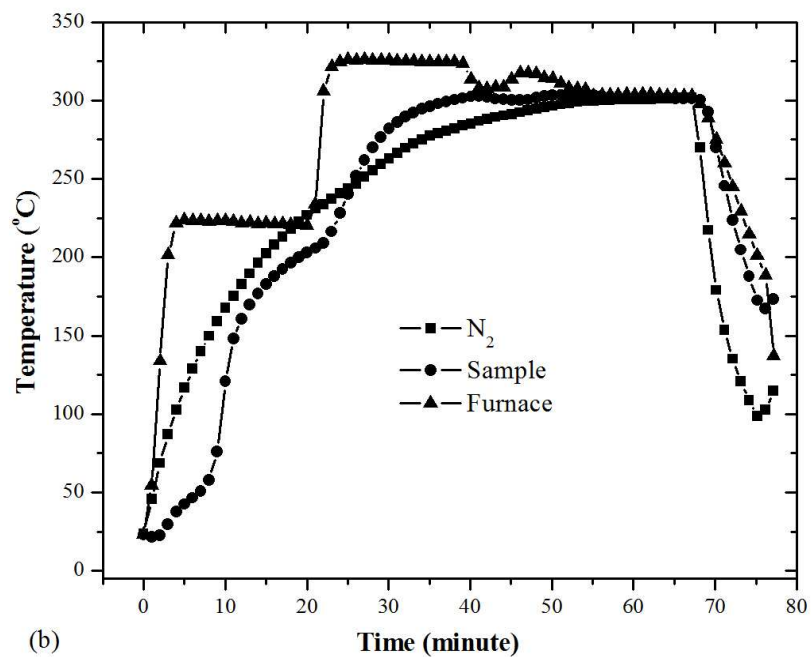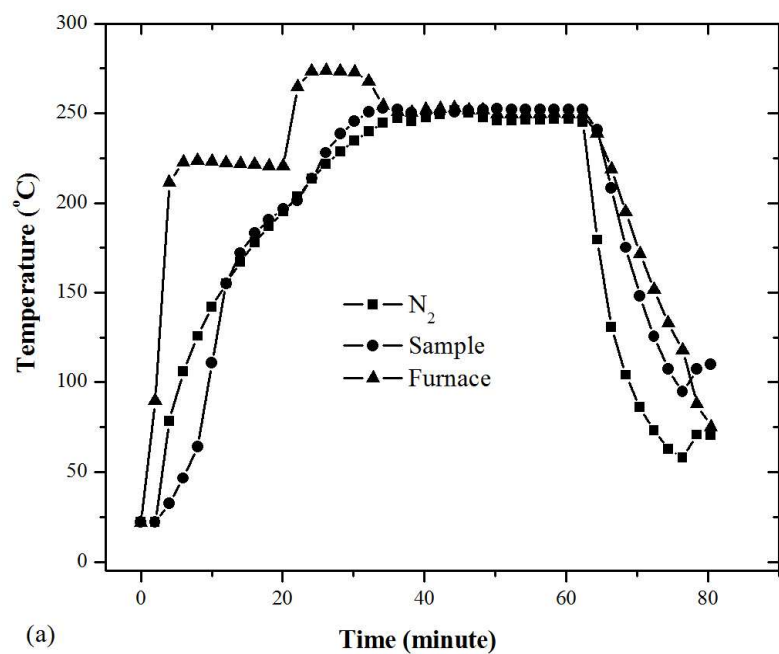
Figure 4-5 Typical reactor temperatures as a function of time for the torrefaction reactor with pine samples
(a) 250 ^{o}C 30 min, (b) 300 ^{o}C 30 min

112

4.3 Torrefaction Performance

Table 4-2 shows torrefaction results at temperatures of 240, 270, 300 and 340 $^{\circ}$C with a residence time of 60 minutes for SPF shavings, using the tubular fixed bed torrefaction unit with continuous nitrogen purging. Table 4-3 shows torrefaction results of different BC softwood species, including spruce, fir, pine, SPF and pine bark. As the temperature increased, the weight loss, high heating value, and the carbon content all increased, but the bulk density, the retaining energy, and oxygen content decreased. The higher true material density of torrefied sawdust than the control sawdust could be caused by the shrinkage of particles during torrefaction [Mani et al. 2004]. Because of the removal of water and oxygen-containing volatiles during torrefaction, the carbon content of the torrefied sawdust increased, giving rise to a higher HHV of torrefied sawdust. At the same time, the removal of volatiles decreased the energy yield.

Table 4-2 Torrefaction results at different temperatures for SPF shavings

Torrefaction Temperature, $^{\circ}$C	240	270	300	340
Residence time, min	60	60	60	60
Bulk density, kg m^{-3}	150	133	120	107
True material density, kg m^{-3}	1365	1355	1447	1447
High heating value, MJ kg^{-1}	20.89	23.11	25.32	29.49
Weight loss, %wt	13.3	33.8	50.7	60.6
Ash content, %wt	0.19	0.28	0.38	0.48
Energy yield, %	90.89	76.81	62.72	58.33
Elemental Analysis, %wt				
C	52.36	58.14	63.51	71.91
H	6.03	5.68	5.38	4.77
O	41.46	36.02	30.93	23.15
N	0.16	0.17	0.19	0.18

Figure 4-6 plots the HHV against the weight loss for all torrefied samples, which

revealed a strong correlation between them. The higher heating value increased steadily with increasing the severity of torrefaction, reaching 23 *MJ kg⁻¹* at a weight loss of 40%. For a 30% weight loss by torrefaction, the energy content increased by about 20%. From a linear regression between the higher heating value and the weight loss at weight losses less than 40%, the following relationship was obtained (excluding those data for the pine bark):

$$HHV_{TorrefiedSample} = (19.85 \pm 0.12) + (9.34 \pm 0.47) \times MassLoss \quad MJ \ kg^{-1} \quad (R^2 = 0.8862, \ N = 51)$$

(4-3)

Where 19.85 MJ/kg on the right hand side of the above equation most likely corresponds to the average heating value of the dry raw material. For a first approximation, the higher heating value of torrefied biomass particles with a given mass loss could be estimated by Equation (4-3).
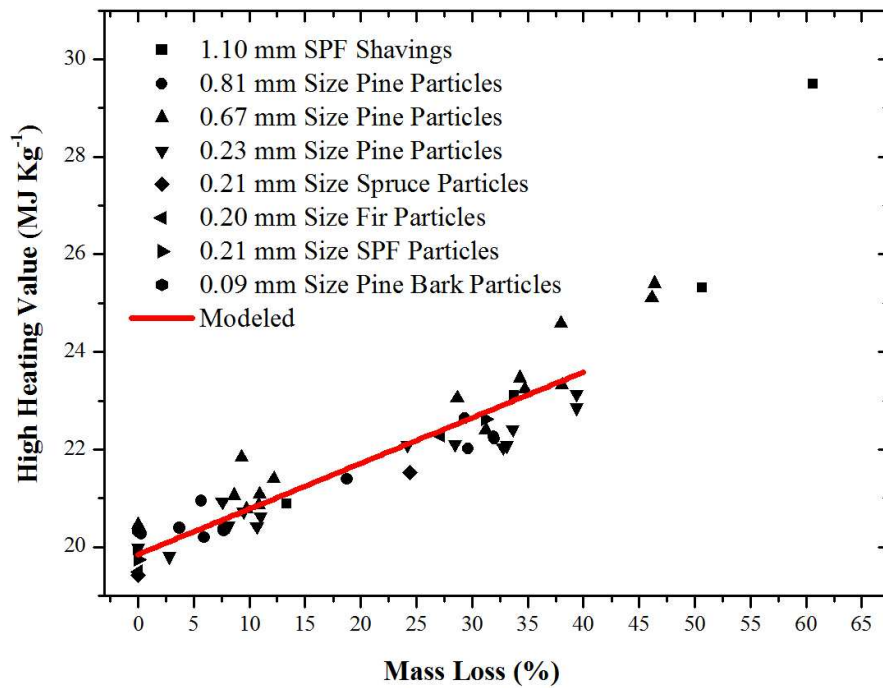
Figure 4-6 High heating value of BC softwood samples as a function of weight loss

114

Table 4-3 Torrefaction results of different BC softwood sawdust

Items	Spruce	Pine	Fir	SPF	Pine bark
Particle mean size, mm	0.21	0.23	0.20	0.21	0.09
Torrefaction temperature, $^{\circ}$C	280	280	280	280	280
Residence time, min	52	52	52	52	23
Bulk density, kg m^{-3}					
Raw materials	199	225	232	176	310
Dry raw materials	187	191	216	156	247
Torrefied materials	156	175	186	143	229
True material density, kg m^{-3}					
Raw materials	1413	1412	1441	1430	1380
Dry raw materials	1452	1444	1464	1471	1410
Torrefied materials	1513	1528	1586	1600	1719
High heating value, MJ kg^{-1}					
Raw materials	18.33	18.68	18.38	18.56	19.52
Dry raw materials	19.42	20.43	19.49	19.75	21.35
Torrefied materials	21.54	22.11	22.28	22.63	24.61
Weight loss, %wt	24.4	28.5	27.1	31.2	30.3
Energy yield, %	83.78	77.34	83.31	78.85	80.39
Elemental Analysis, %wt					
C	54.16	55.58	55.55	56.07	59.59
H	5.86	5.85	5.81	5.66	5.54
O	39.94	38.46	38.51	38.17	34.23
N	0.05	0.12	0.14	0.11	0.65

Figure 4-7 shows the van Krevlen diagram for untreated and torrefied BC softwood sawdust, including all tested data for dry raw materials and different torrefied materials. It is seen that both oxygen and hydrogen were removed selectively during torrefaction, and they were closely correlated as observed in pyrolysis. This could be explained by the selective removal of OH groups from the easy to decompose hemicelluloses during torrefaction. Similar results were reported by Madic et al. (2012) and Phanphanich et al. (2011). A linear correlation between the H/C and O/C ratios for BC softwoods was obtained by regression:

$$H/C = (0.434 \pm 0.017) + (1.565 \pm 0.030) \times O/C \quad (R^2=0.9932, N=21) \qquad (4\text{-}4)$$
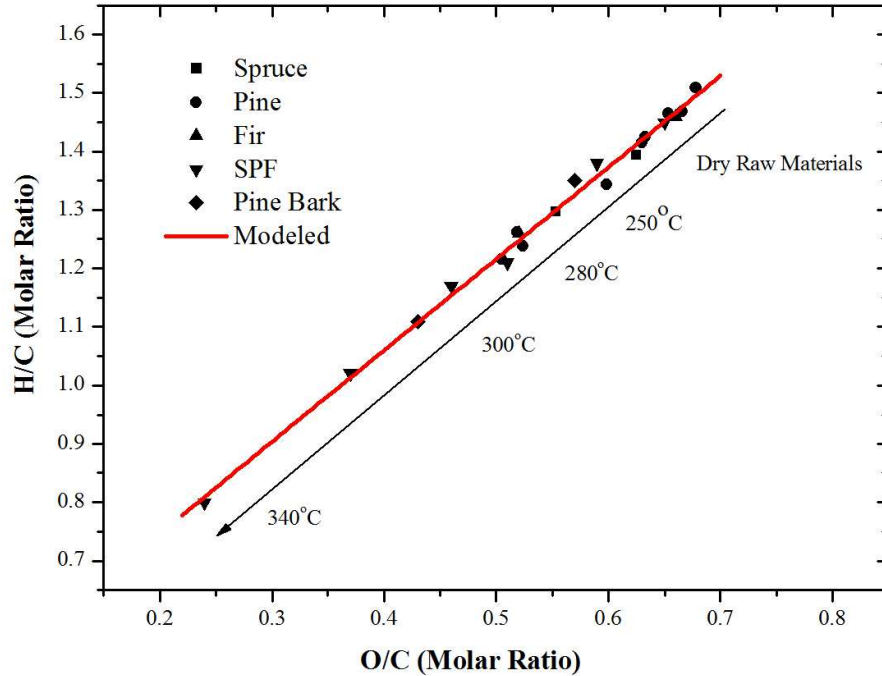
Figure 4-7 van Krevlen diagram of untreated and torrefied BC softwood sawdust

4.4 Comparison of Fixed Bed Data with TG Kinetic Data

Same BC softwood samples prepared in the same batch for the TG tests were torrefied in the fixed bed reactor. The weight loss results from the fixed bed reactor are given in Table 4-4, together with the results from TG tests. It is seen that the weight loss between TG analyzer and fixed bed tests are generally agree within 90%, except for the spruce sample which shows 20% lower weight loss from the fixed bed reactor than from the TG tests. These encouraging results give us the confidence in applying those kinetic equations for the modeling and designing of torrefaction reactors in the future.

Table 4-4 Comparison of weight loss results from TG analyzer and a fixed bed reactor

	Spruce	Pine	Fir	Pine bark
Temperature, K	553	553	553	553
Residence time, min	52	52	52	23
Weight loss from fixed bed, %wt	24.4	28.6	27.2	30.3
Weight loss from TGA, %wt	29.2	30.6	28.8	29.7
Weight loss from two-component kinetic model, %wt	27.9	30.8	28.7	30.0[*]

*: Empirical kinetics equation

4.5 Densification of BC Torrefied Softwood Samples

Table 4-5 summarizes experimental conditions attempted to densify torrefied BC softwood sawdust into pellets. Torrefied sawdust samples were found to be more difficult to be compressed into strong pellets under the same operating conditions as used for making the control pellets from untreated sawdust, even at a die temperature of 150 ^{o}C. The mold temperature had to be increased to over 170 ^{o}C, or the samples had to be preconditioned to the moisture content up to 10% in order to make strong torrefied pellets.

Table 4-5 Summary of tested densification conditions

Samples	Moisture Content, %	Die Temperature, ^{o}C	Pressure, MPa	Numbers of Pellets
Raw sawdust (0.23 mm pine)	7.44	70, 110, 170	31, 62, 125, 156	>50
Raw sawdust (spruce, pine, fir, SPF, pine bark)	3.19-9.94	70	125	>100
0.67 mm Torrefied pine sawdust (300°C for 15min)	0, 5, 10, 15 (Added)	70, 90, 100, 110,120,130,140,150	156, 187, 218	>50
Torrefied pine sawdust	10 (added)	110	156	>200
0.23 mm Torrefied pine sawdust (at 280 ^{o}C for 52 min)	<0.5	170, 200, 230, 260, 280	125, 156, 187, 218, 249, 280	>50
Torrefied sawdust (spruce, pine, fir, SPF, bark)	<1	170, 230	156	>100
Torrefied SPF shavings	<1	170, 230	156	>20

The density of wood pellets, which is the most important indicator of pellet quality, depends on the fiber source, moisture content, particle size, compression pressure, die temperature, die speed, and die configurations [Bissen 2009]. In this chapter, the effect of the sample moisture content, compression pressure, and die temperature on pellets quality have been examined.

Figure 4-8 shows the density of single torefied pellets as a function of the moisture content and the die temperature for the 0.67 mm torrefied pine sawdust. The torrefaction condition was at 300 ^{o}C for 15 min.   The compression pressure was set at 125 MPa with 1 min holding time. From 4-8, it can be seen that the highest single pellet density was obtained at 10% moisture content with a die temperature of 100 ^{o}C, and the density of torrefied pellets was lower than the control pellets.
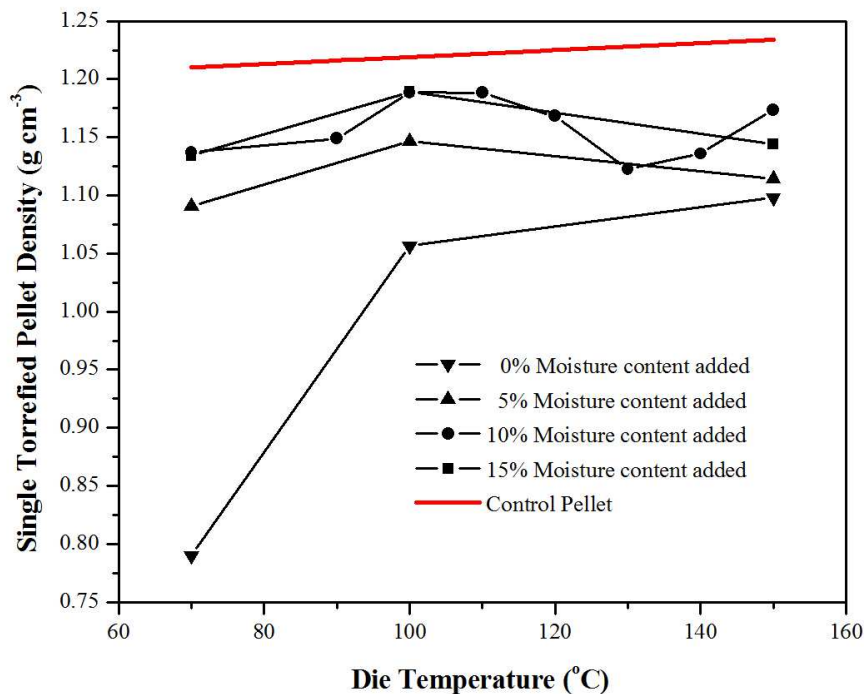
Figure 4-8 Single torrefied pellet density as a function of moisture content and die temperature
(0.67 mm torrefied pine sawdust at 300 ^{o}C for 15 min)

Figure 4-9 shows the density of single torrefied pellets as a function of compression pressure and die temperature. The test sample was 0.23 mm torrefied pine sawdust without any moisture added. The torrefaction condition was at 280 ^{o}C for 52 min.   The holding time for making pellets was 1 min. As expected, the pellet density increased with increasing the compression pressure and die temperature, and was more sensitive to the die temperature. At a die temperature of 230 ^{o}C or above, the torrefied pellet density became close to the control pellet density made at 70 ^{o}C, indicating that a higher temperature, or pressure, is required to make torrefied pellets of a density similar to control pellets.
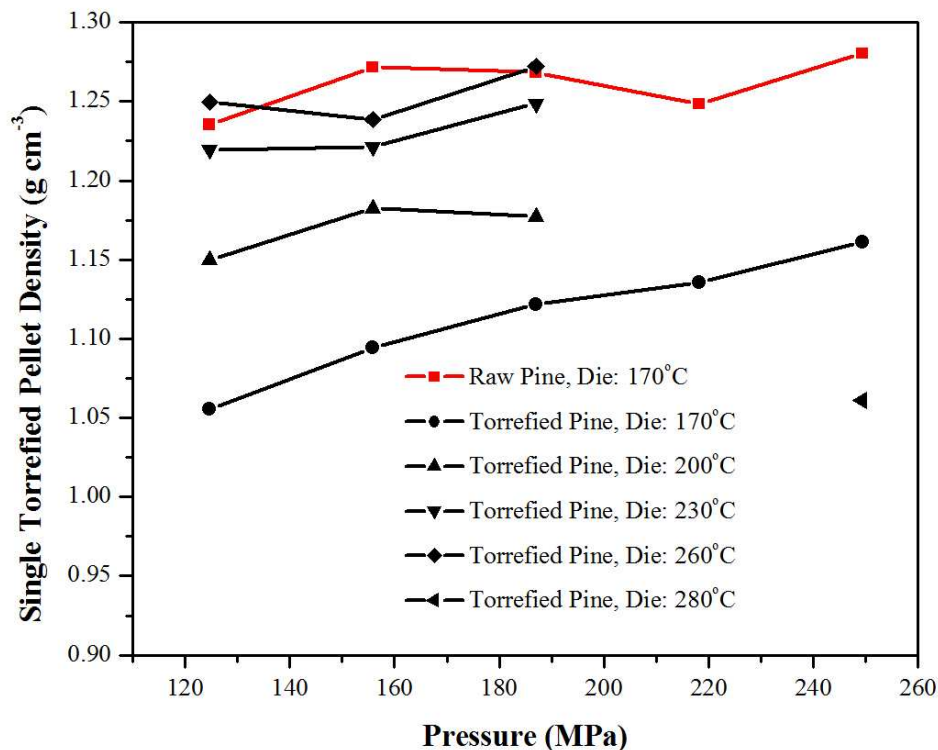
Figure 4-9 Density of single pellets as a function of compression pressure and die temperature
(0.23 mm torrefied pine sawdust at 280 ^{o}C for 52 min)

Figure 4-10 shows the energy consumption for making torrefied pellets as a function of compression pressure and die temperature. The test sample was 0.23 mm torrefied pine sawdust without any moisture added. The torrefaction condition was at 280 $^{\circ}$C for 52 min, and the holding time for compression was 1 min. The energy consumption of torrefied pellets is seen to be higher than the control pellets. The high die temperature can decrease the energy consumption, while high compression pressure increases the energy consumption.   At the temperature range of 170-230 $^{\circ}$C, the energy consumption was not sensitive to the temperature.
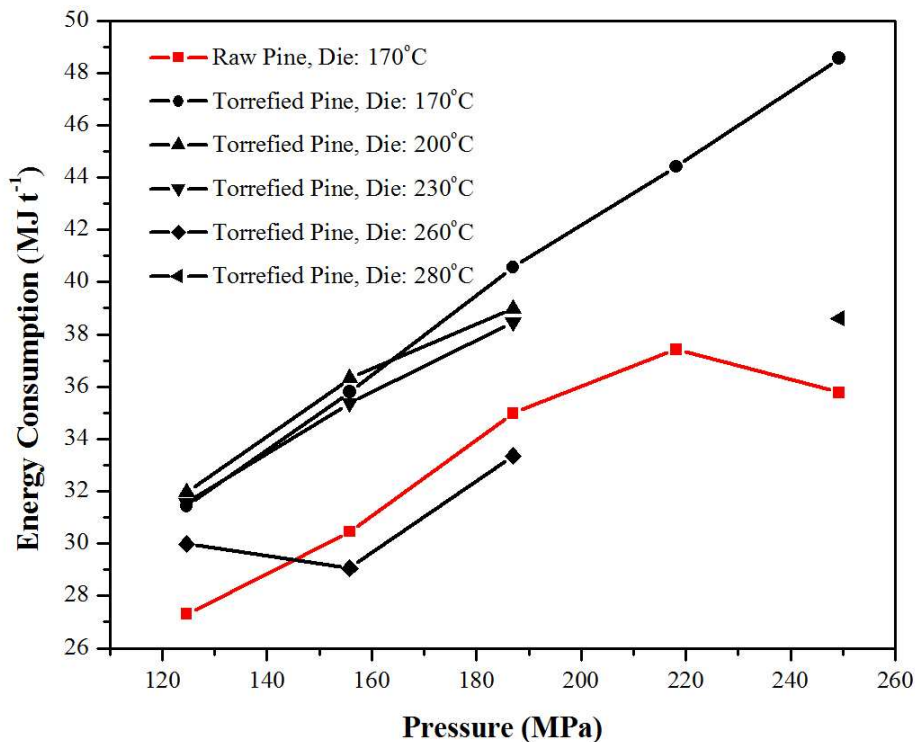
Figure 4-10 Energy consumption for making pellets as a function of compression
pressure and die temperature
(0.23 mm torrefied pine sawdust at 280 $^{\circ}$C for 52 min)

From Figures 4-8 to 4-10, it appears that the optimal densification conditions for making torrefied pellets is to precondition the sample to 10% moisture content and/or use a die temperature of ≥170 °C at a higher compression pressure.

Figure 4-11 shows the appearances of control and torrefied pellets made from different BC softwood species, including SPF shavings (at a die temperature of 170 °C), spruce, fir, pine, SPF and pine bark. Tables 4-6 and 4-7 show the properties of torrefied and control pellets made from different softwood residues. The moisture content of torrefied pellets was consistently lower than the control pellets because of the easy removal of unbonded free water from the torrefied sawdust during compression. The density of torrefied pellets was consistently lower than the control pellets when made under the same operating conditions. Increasing the die temperature can improve the density of torrefied pellets significantly. At a die temperature of 230 °C, the density of torrefied wood pellets made from the 30% mass loss torrefied sawdust became similar to the density of control pellets. Increasing the die temperature can improve the density of torrefied pellets significantly. As the torrefaction temperature increased, the density of torrefied pellets decreased. For sawdust torrefied at a temperature over 300 °C, both the hardness and the density of torrefied pellets became much lower. A large force had to be applied for making pellets from torrefied SPF residues prepared at a torrefaction temperature of 340 °C. The energy consumption for making pellets also increased as the torrefaction temperature increased. The energy consumption for making torrefied pellets from samples prepared at a torrefaction temperature of 300 °C was more than 50% higher than the control pellets. The Meyer hardness of torrefied pellets was comparable with the control pellets, although it was noticed that the torrefied wood pellets were more brittle than the control pellets. Based on the compression tests and pellet quality data (excluding pine bark), it appears to us that the optimal mass loss for making good torrefied softwood pellets should be around 30% at a torrefaction temperature of 270 to 280 °C for about 55

121

min.
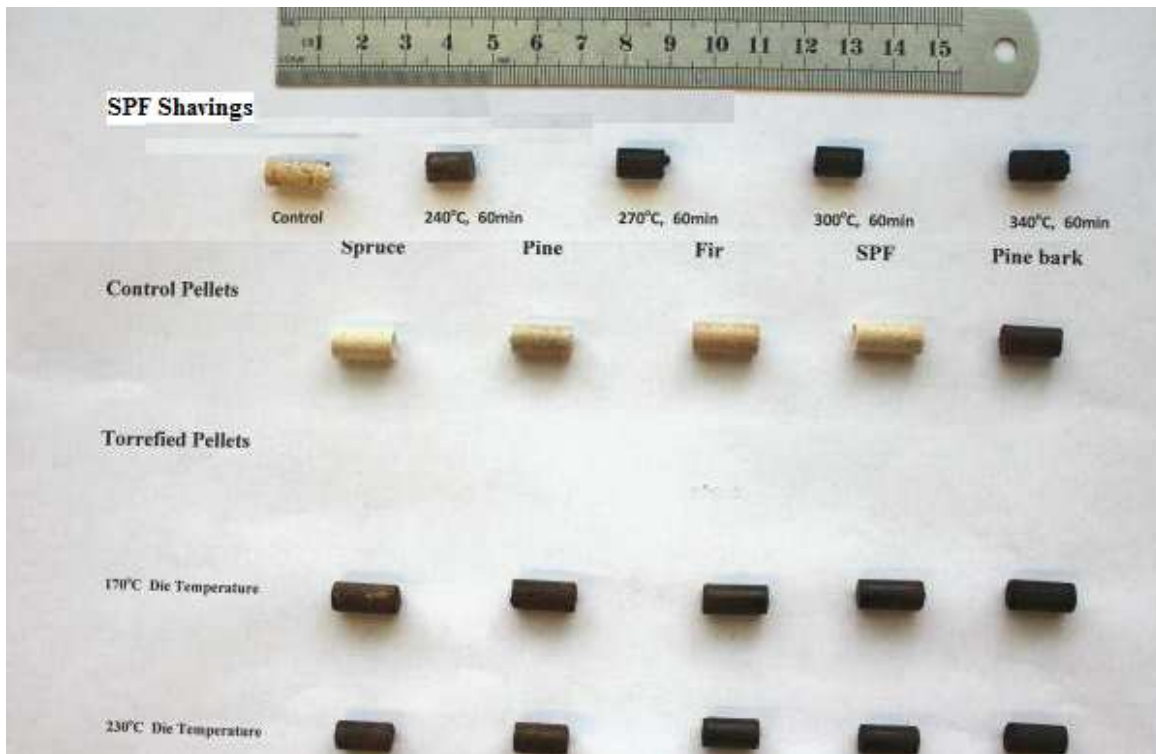
Figure 4-11 Control and torrefied pellets made from different BC softwood species

Table 4-6 Properties of torrefied and control pellets made from BC SPF shavings

SPF Shavings	Control	240°C 60min	270°C 60min	300°C 60min	340°C 60min
Die Temperature, 170°C					
Moisture content, %wt	7.00	0.42	0.35	0.04	0.17
Pellet density, kg m^{-3}	1210	1100	1000	910	700
Energy consumption, MJ t^{-1}	25.57	25.62	28.30	30.83	50.93
Meyer hardness, N mm^{-2}	6.39	8.88	5.62	4.68	<1
Die Temperature, 230°C					
Pellet density, kg m^{-3}	1210	1260	1200	1130	810
Energy consumption, MJ t^{-1}	25.57	34.79	43.29	49.91	55.35
Meyer hardness, N mm^{-2}	6.39	8.98	8.33	8.85	3.08

Table 4-7 Properties of torrefied and control pellets made from BC softwood residues

Different Wood Species	Spruce	Pine	Fir	SPF	Pine bark
Torrefaction Temperature, ^{o}C	280	280	280	280	280
Residence time, min	52	52	52	52	23
Control Pellets					
Moisture content, %wt	6.24	6.52	4.61	4.78	7.54
Pellet density, kg m^{-3}	1170	1210	1140	1150	1290
Energy consumption, MJ t^{-1}	29.06	27.49	31.41	31.23	18.72
Meyer hardness, N mm^{-2}	7.38	7.48	3.34	3.95	13.50
Torrefied Pellets					
Die Temperature, 170°C					
Moisture content, %wt	0.22	0.46	0.29	0.32	0.82
Pellet density, kg m^{-3}	1060	1080	1030	1010	980
Energy consumption, MJ t^{-1}	31.21	30.61	33.27	35.24	28.12
Meyer hardness, N mm^{-2}	5.53	5.62	5.28	5.20	3.37
Die Temperature, 230°C					
Moisture content, %	0.22	0.56	0.04	0.26	0.00
Pellet density, kg m^{-3}	1180	1220	1130	1150	1140
Energy consumption, MJ t^{-1}	30.74	31.56	34.05	35.64	28.26
Meyer hardness, N mm^{-2}	4.96	5.86	5.47	6.94	5.99

4.5 Moisture Uptake of BC Torrefied Pellets

The hydrophobicity of torrefied wood pellets was examined by measuring the saturated water uptake rate in a humidity chamber with 90% relative humidity air at 30 $_{o}$C over 48 hours. Figures from 4-12 to 4-17 plot the measured moisture uptake rate of control and torrefied pellets made from BC softwood residues. It is seen from Figures from 4-12 to 4-17 that it took less than 10 hours for most tested pellets to reach the saturated moisture content. The saturated moisture content of control pellets was 19±1% (wt), and the saturated moisture content of all torrefied pellets was less than 10% (wt), indicating substantial improvements in the hydrophobicity of torrefed wood pellets. The saturated moisture content of torrefied wood pellets also consistently decreased with increasing the degree of torrefaction in Figure 4-12 because of the increased removal of hydroxyl (-OH)

groups from the biomass [Phanphanich and Mani 2011, Pimchuai et al. 2010]. Increasing the die temperature for pelletization, Figure 10(b), also slightly lowered the saturated moisture content of torrefied wood pellets.

The moisture uptake kinetics data can be fitted to the following formula as recommended by ASABE Standard S448.1 (2006):

$$\frac{M_m - M_s}{M_i - M_s} = \exp(-k_m t) \tag{4-5}$$

where M_m is the instantaneous moisture uptake, M_s is the saturated moisture uptake, M_i is the initial moisture uptake, k_m is the adsorption rate constant in min^{-1}, and t is the exposure time in min.
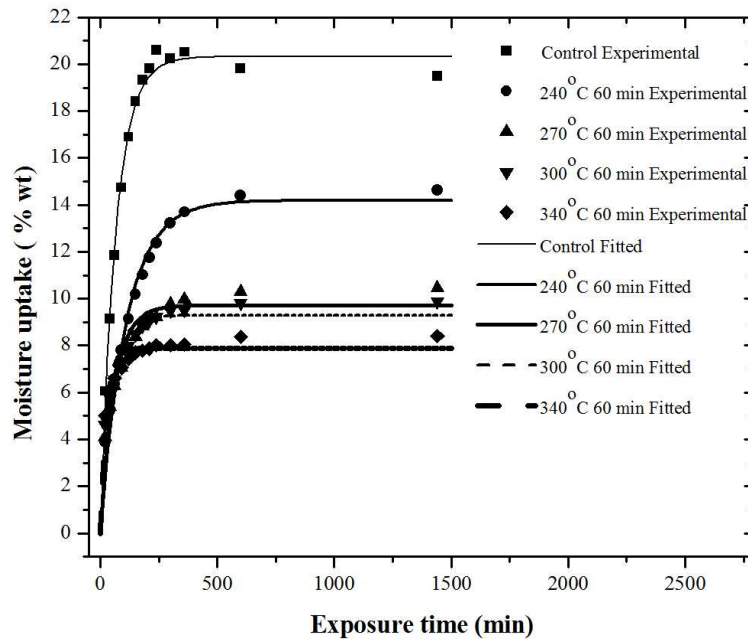
Figure 4-12 Moisture uptake rate of control and torrefied pellets made from BC 1.10 mm SPF shavings
(Pellets in a humidity chamber with 90% relative humidity air at 30 ^{o}C)
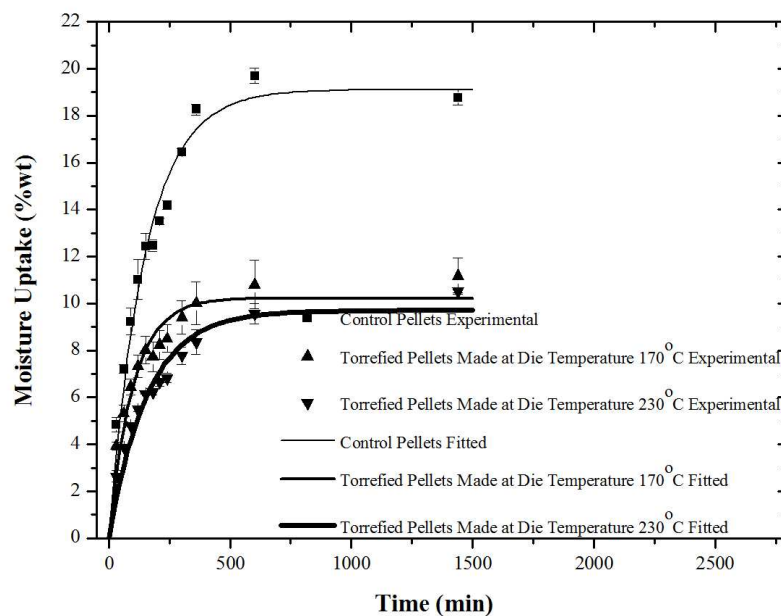
Figure 4-13 Moisture uptake rate of control and torrefied pellets made from BC 0.21 mm spruce particles at 280 $^{\circ}$C for 52 min
(Pellets in a humidity chamber with 90% relative humidity air at 30 $^{\circ}$C)
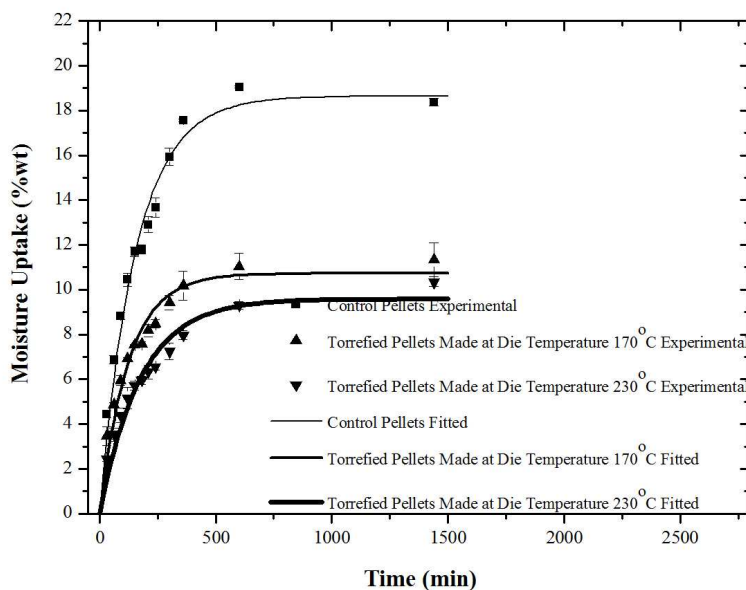
Figure 4-14 Moisture uptake rate of control and torrefied pellets made from BC 0.23 mm pine particles at 280 $^{\circ}$C for 52 min
(Pellets in a humidity chamber with 90% relative humidity air at 30 $^{\circ}$C)
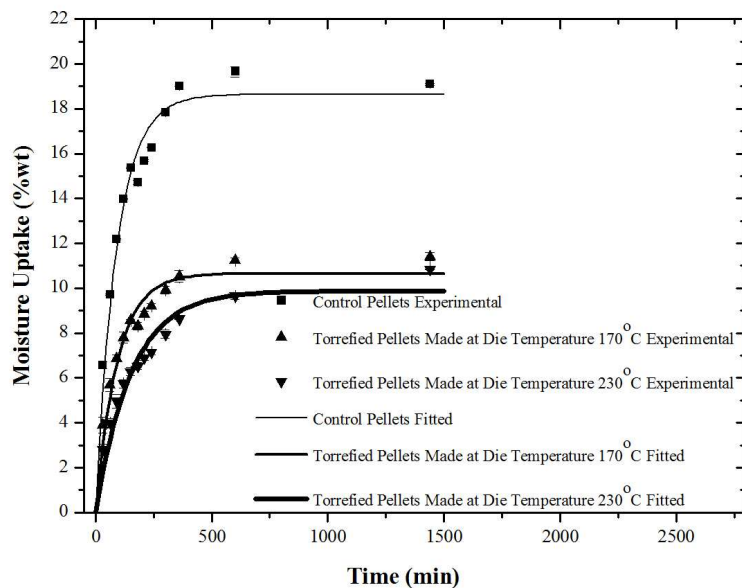
Figure 4-15 Moisture uptake rate of control and torrefied pellets made from BC 0.20 mm
fir particles at 280 $^{\circ}$C for 52 min
(Pellets in a humidity chamber with 90% relative humidity air at 30 $^{\circ}$C)
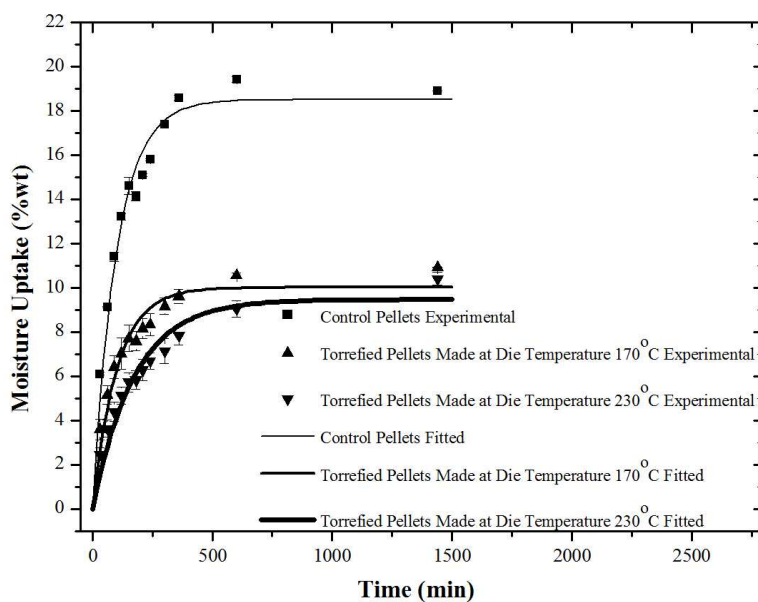
Figure 4-16 Moisture uptake rate of control and torrefied pellets made from BC 0.21 mm
SPF particles at 280 $^{\circ}$C for 52 min
(Pellets in a humidity chamber with 90% relative humidity air at 30 $^{\circ}$C)
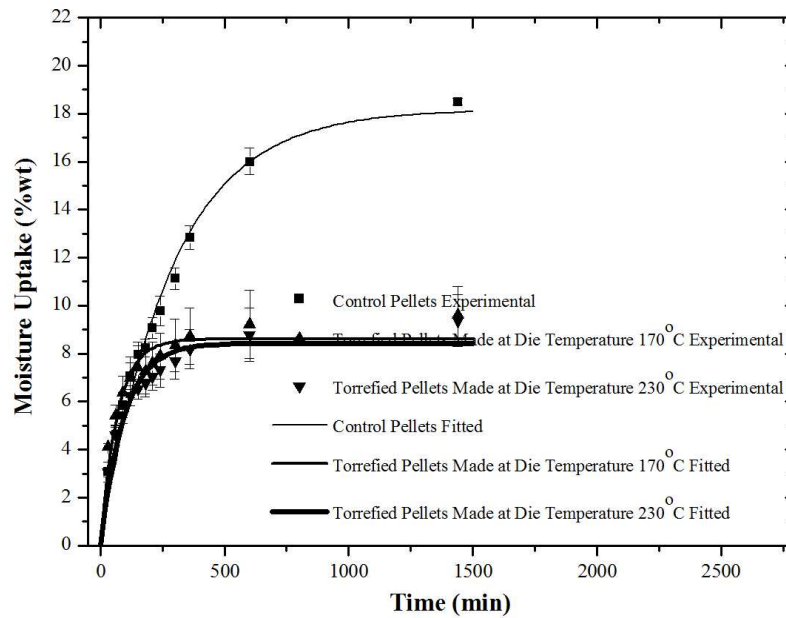
Figure 4-17 Moisture uptake rate of control and torrefied pellets made from BC 0.09 mm pine bark particles at 280 ^{o}C for 23 min
(Pellets in a humidity chamber with 90% relative humidity air at 30 ^{o}C)

Table 4-8 shows the saturated moisture uptake (M_s) and the adsorption rate constant (k_m) estimated from fitting experimental data for control and torrefied pellets made at different torrefaction temperatures and densified at different die temperatures. The M_s of torrefied pellets with ~30% mass loss ranged from 8 to 11%, about 50% lower than the control pellets (18-20%). The adsorption rate constant k_m of torrefied pellets was in the same order as the control pellets, which may be explained by the increased specific surface area of torrefied pellets because of the lower pellet density and the creation of new pores inside the torrefied particles. However, increasing the die temperature from 170 to 230 ^{o}C for pelletization significantly reduced the moisture adsorption rate constant, which may result from the increased pellet density and thermal modification of surface properties.

Table 4-8 Saturated moisture uptake and moisture uptake rate constant
(Pellets in a humidity chamber with 90% relative humidity air at 30 ^{o}C over 48 hours)

	Weight loss, %	Saturated moisture uptake, M_s, %	Adsorption rate constant, k_m, min^{-1}
1.10 mm SPF Shavings			
Control	0.0	20.32	0.01526
240 ^{o}C 60 min	13.3	14.18	0.00912
270 ^{o}C 60 min	33.8	9.72	0.01694
300 ^{o}C 60 min	50.7	9.28	0.02181
340 ^{o}C 60 min	60.6	7.88	0.03938
Different Wood Species			
0.21 mm Spruce			
Control	0.0	19.11	0.00676
280 ^{o}C 52 min Die 170	24.4	10.23	0.01015
280 ^{o}C 52 min Die 230	24.4	9.70	0.00630
0.23 mm Pine			
Control	0.0	18.64	0.00645
280 ^{o}C 52 min Die 170	28.5	10.72	0.00813
280 ^{o}C 52 min Die 230	28.5	9.59	0.00570
0.20 mm Fir			
Control	0.0	18.64	0.01117
280 ^{o}C 52 min Die 170	27.1	10.65	0.01084
280 ^{o}C 52 min Die 230	27.1	9.88	0.00654
0.21 mm SPF			
Control	0.0	18.51	0.01001
280 ^{o}C 52 min Die 170	31.2	10.01	0.00999
280 ^{o}C 52 min Die 230	31.2	9.47	0.00580
0.09 mm Pine Bark			
Control	0.0	18.17	0.00354
280 ^{o}C 23 min Die 170	30.3	8.60	0.01507
280 ^{o}C 23 min Die 230	30.3	8.43	0.01080

Figure 4-18 shows the relationship between the saturated moisture uptake and the mass loss, or severity of torrefaction, for torrefied pellets. It is seen that the saturated moisture uptake of torrefied wood pellets decreased steadily with the increase in the mass loss or the degree of torrefaction. The decrease in saturated moisture uptake appears to be more significant at the weight loss of 0 to 15%, and stays steady afterward. A correlation between the saturated moisture uptake (M_s) and the mass loss for control and torrefied pellets was obtained by regression:

$$\frac{M_s - (9.63 \pm 0.62)}{(18.64 \pm 0.26) - (9.63 \pm 0.62)} = \exp[(-0.0521 \pm 0.0090) \times \%\,MassLoss)]$$

$$(R^2 = 0.9417,\ N = 35)\ (4\text{-}6)$$

where the value of 18.64% most likely represents the average saturated moisture content of the raw material, while the value of 9.63% corresponds to the average saturated moisture content of charcoal.
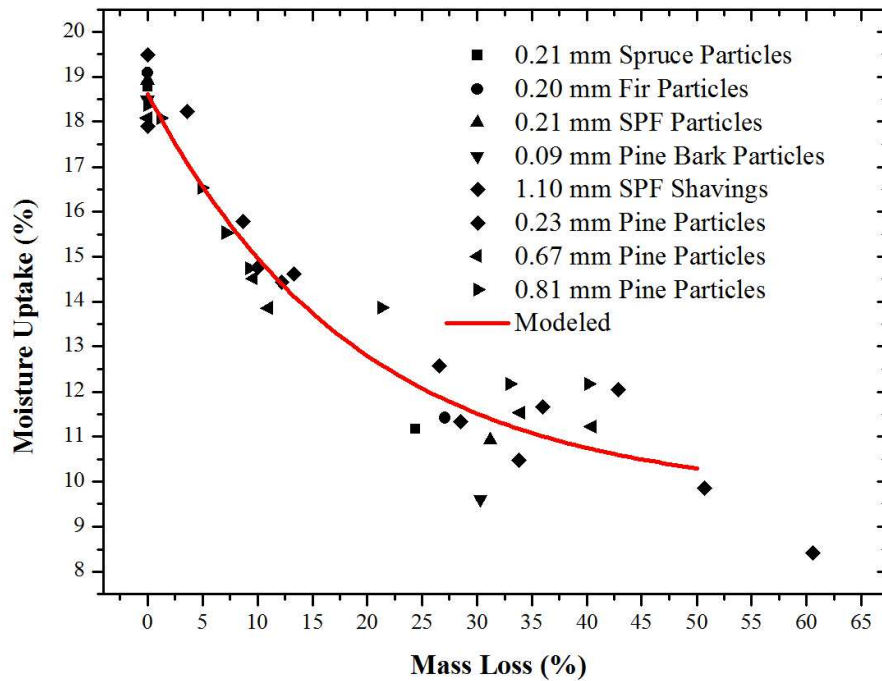
Figure 4-18 saturated moisture uptake as a function of torrefaction weight loss for all tested samples
(Pellets in a humidity chamber with 90% relative humidity air at 30 ^{o}C over 48 hours)

Table 4-9 shows the diametric, longitudinal and volumetric expansions of control and torrefied pellets made from BC softwood residues after moisture uptake. It is seen from Table 4-9 that at the optimal mass loss of around 30%, the volumetric expansion of

129

torrefied wood pellets made at a die temperature of 170 ^{o}C was around 30%. If the die temperature increased to 230 ^{o}C, the volumetric expansion of torrefied wood pellets with the same weight loss would decrease to around 10%. Comparing pellets made from two SPF samples of different particle sizes, the volumetric expansion of torrefied wood pellets made from small size particles was much lower than that made from large size particles. Deep torrefaction is seen to reduce the pellet expansion, and increased the quality of torrefied pellets.   Increasing the die temperature also can improve the quality of torrefied pellets.

Table 4-9 Expansion of control and torrefied pellets made from BC softwoods after moisture uptake

Items	Longitudinal expansion, %	Diametric expansion, %	Volumetric expansion, %
1.10 mm SPF Shavings			
Control	237	22	401
240°C 60min	67	14	118
270°C 60min	25	7	42
300°C 60min	14	9	35
340°C 60min	14	5	25
Different Wood Species			
0.21 mm Spruce			
Control	114	9	117
280°C 52min Die	30	5	34
280°C 52min Die	15	5	19
0.23 mm Pine			
Control	112	6	105
280°C 52min Die	26	3	21
280°C 52min Die	15	1	11
0.20 mm Fir			
Control	88	6	88
280°C 52min Die	26	4	25
280°C 52min Die	27	2	26
0.21 mm SPF			
Control	93	7	94
280°C 52min Die	21	2	20
280°C 52min Die	13	2	12
0.09 mm Pine Bark			
Control	41	4	41
280°C 23min Die	12	2	12
280°C 23min Die	12	3	13

Figure 4-19 shows the shape of the pellets before and after moisture uptake for control

pellets and torrefied pellets, both made from SPF shavings. On each picture, the pellet shown on the left was the one after moisture uptake, and the pellet on the right side was before the moisture uptake test. As shown in Figure 4-19(a), after the moisture uptake, the control pellet almost disintegrated. After the moisture uptake, pellets made from torrefied sawdust prepared at 240 ^{o}C for 60 minutes showed a large expansion (see Figure 4-19(b)). For those pellets made from torrefied samples with a weight loss of 33.8% (270 ^{o}C, 60 minutes), 50.7% (300 ^{o}C, 60 minutes) and 60.6% (340 ^{o}C, 60 minutes), respectively, there was little change in the pellet shape and the pellets remained in good conditions after the moisture uptake. Figure 4-20 shows the shape of the pellets before and after the moisture uptake for control pellets and torrefied pellets made from different BC softwood species. All torrefied pellets are seen to remain in their original shape after water uptake. Results shown in Figures 4-19 and 4-20 seem that the optimal weight loss for the production of high quality torrefied pellets was around 30 %.
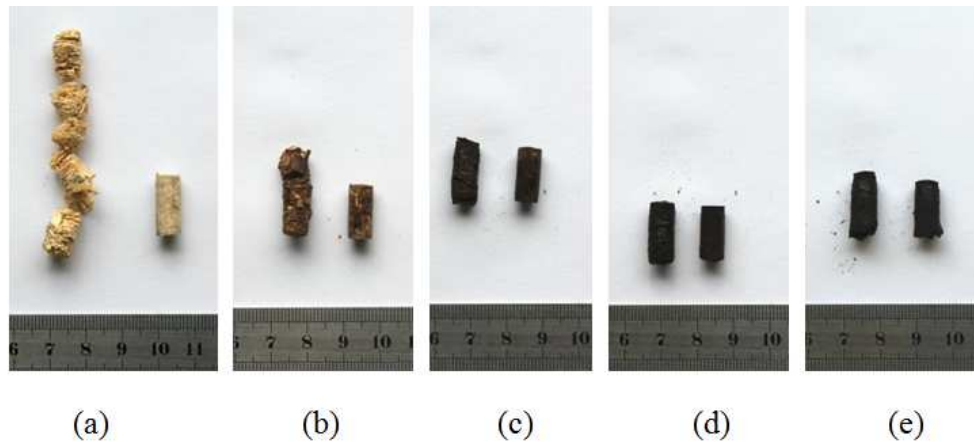
Figure 4-19 Shape changes of control and torrefied pellets made from SPF shavings
before and after moisture uptake
(a) Control pellets, (b) 13.3% weight loss (240 ^{o}C, 60 minutes), (c) 33.8% weight loss
(270 ^{o}C, 60 minutes), (d) 50.7% weight loss (300 ^{o}C, 60 minutes), (e) 60.6% weight loss
(340 ^{o}C, 60 minutes)
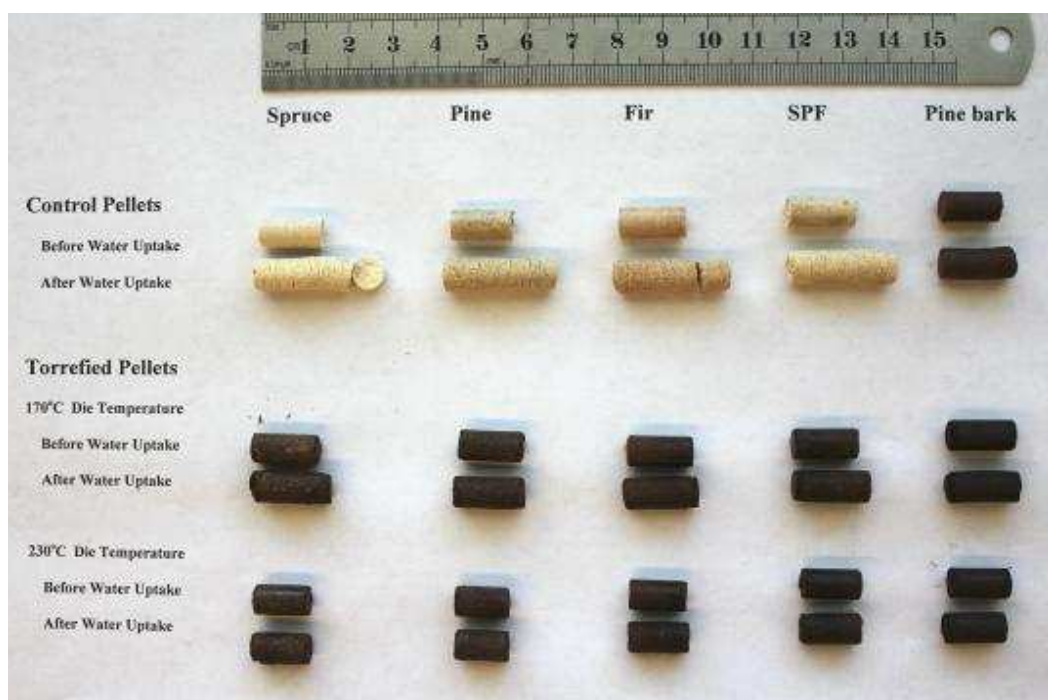
Figure 4-20 Shape changes of control and torrefied pellets made from different softwood species after moisture uptake

4.6 Summary

The mass loss of British Columbia softwood species during torrefaction mainly depended on the reaction temperature and the treatment time. The higher heating value of torrefied softwood had a close correlation with the mass loss, and deep torrefaction increased the higher heating value of torrefied sawdust.

Torrefied softwood was more difficult to be compressed into strong pellets using the same conditions for making the control pellets. Increasing the die temperature and adding moisture into torrefied sawdust can improve the quality of torrefied pellets. More energy was needed for compacting torrefied sawdust into pellets. The moisture content and density of torrefied pellets was lower than control pellets. Deep torrefaction increased the heating value and the hydrophobicity of torrefied pellets, but decreased the

energy yield and the hardness of torrefied pellets. Torrefied pellets have a similar moisture adsorption rate as the control pellets, but their saturated moisture contents are at least 50% lower than the control pellets at a given moist environment.

Considering the quality of torrefied pellets, the optimal torrefaction conditions appeared to correspond to a mass loss of around 30%, which gave a 20% increase in pellet higher heating value. The suitable densification conditions for torrefied softwood based on the current study corresponded to a die temperature of 170 to 230 ^{o}C and lower die temperatures could be used when the torrefied sawdust was preconditioned to a moisture content of around 10%.

CHAPTER 5 PARTICLE SIZE EFFECT ON TORREFACTION AND DENSIFICATION

Although the reaction temperature, reaction residence time, and wood species were considered to be the most influential parameters, particle size is also an important design parameter for torrefaction and densification. Prins et al. (2006) postulated that for pyrolysis of wood below 573 K, the reactions were the rate-limiting step for particles smaller than 2 mm where the impact of intra-particle heat and mass transfer becomes insignificant. In this chapter, both a TG and a fixed bed reactor were used to study the particle size effect on torrefaction. A press machine, MTI 50K, was used to make torrefied pellets for the evaluation on the quality of the torrefied pellet based on density, durability and equilibrium water uptake rate.

5.1 Experimental

5.1.1 Samples

Pine chips from Fiberco and FPInnovations have been used as the test material in this study. Figure 5-1 shows the three pine sawdust samples prepared from Fiberco pine chips. Figure 5-2 shows the three samples of pine sawdust particles made from FPInnovations pine.

Figure 5-1 Three pine sawdust samples made from Fiberco pine chips
(a) <250 μm, (b) 250-500 μm, (c) 500-1000 μm
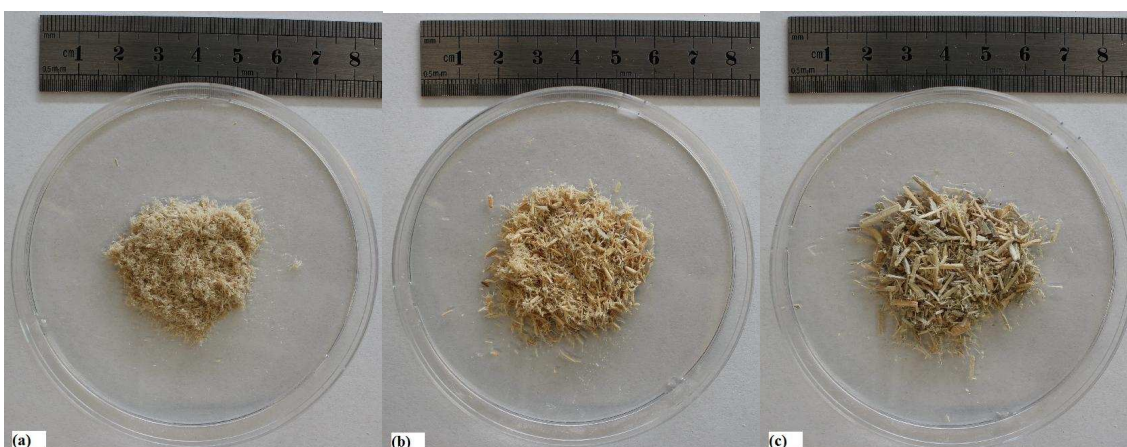
Figure 5-2 Three pine sawdust samples made from FPInnovations pine chips
(a) 0.79 mm screen size, (b) 3.18 mm screen size, (c) 6.35 mm screen size

The three pine sawdust samples (particle size: 0.23 mm, 0.67 mm, 0.81 mm) made from FPInnovations chips were used for the study of the particle size effects in the fixed bed reactor. Three samples made from Fibreco pine chips plus the 0.23 mm particle size sample from FPInnovation wood chips were used for the TGA study.

135

5.1.2 Equipment and Procedures

A bench-scale fixed bed unit as described in Chapter 3was used for torrefaction tests. For the fixed bed tests, two operating parameters were investigated for each particle sample. The temperature was chosen to be 523 K and 573 K, and the residence time was selected as 15 min and 30 min, which fell into the typical ranges of torrefaction conditions of commercially relevant. For each sample, at least two replicates were tested for each reaction condition.

Pelletization was carried out in the MTI 50K press machine as described in Chapter 3. In each test, approximately 0.5 g samples were used to make a single pellet of 6.5 mm in diameter and ~12 mm in length. A pressure of 156 MPa was applied with a few minutes of holding time. To make control pellets, the die temperature was maintained at 343 K with the 125 MPa pressure and 1 minute holding time. The torrefied samples were preconditioned over 24-72 hours to adjust their moisture content to 10% in order to compress torrefied sawdust into pellets.

5.2 Torrefaction Performance

Figure 5-3 shows the TG weight loss curves of three pine sawdust samples made from Fiberco chips at the torrefaction temperatures of 573K and 553K. It can be seen that the particle size affected the weight loss during torrefaction. As the particle size increased, the weight loss rate decreased. As the temperature increased, the difference in weight loss for different particle sizes widened, indicating a more significant effect at higher temperatures.

Table 5-1 summarizes the fixed bed reactor torrefaction results of pine samples with

different particle sizes, operated at two temperatures and two residence times. As the temperature increased, the weight loss, high heating value, and the carbon content all increased, but the bulk density, the retaining energy, and oxygen content decreased. The effects of temperature, residence time and wood species on torrefaction were already reported in Peng et al. (2011), so the discussion in the current study only focused on particle size effect. As can be seen, smaller particles lost their weight faster than larger particles, and the difference was more significant at higher torrefaction temperatures. At 523 K, the weight loss differences were around 4%. At 573 K, the differences increased to 7%. This implies that the inter-particle heat and mass transfer could influence the torrefaction rate of large particles.

(a)

(b)
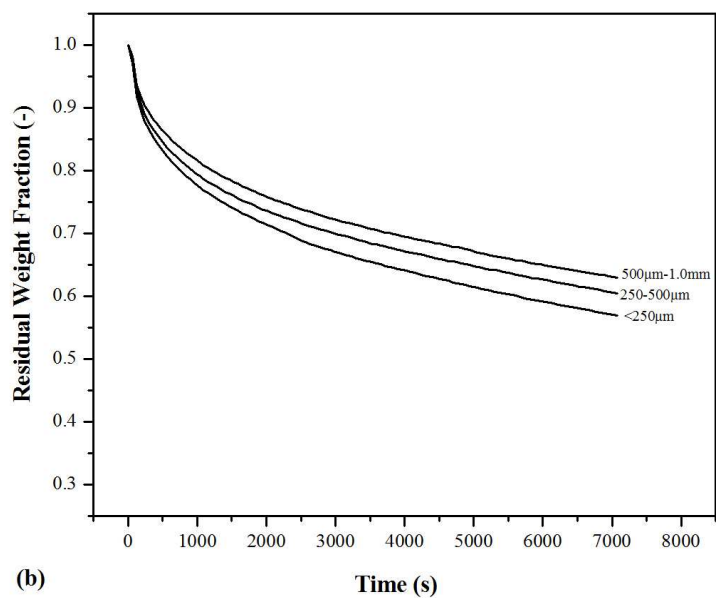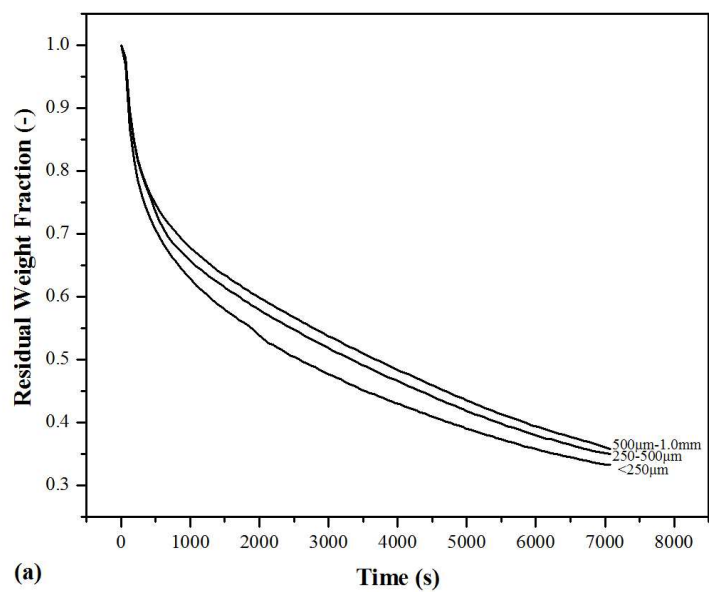
Figure 5-3 Weight loss curves of three pine sawdust samples made from Fiberco chips in the TGA
(a) 573K, (b) 553K.

Table 5-1 Fixed bed torrefaction results of three pine samples of different sizes

Torrefaction Temperature, K	523	523	573	573
Residence time, min	**15**	**30**	**15**	**30**
0.23 mm size particles				
Bulk density, kg m^{-3}	157	159	137	136
True density, kg m^{-3}	1419	1421	1397	1393
High heating value, MJ kg^{-1}	20.58	20.51	22.06	23.02
Weight loss, %wt	10.03	12.22	35.97	42.86
Weight loss from TGA, %wt	8.46	10.87	31.73	39.23
Energy yield, %	92.67	90.08	70.69	65.82
Element Analysis, %wt				
C	49.59	50.55	55.03	55.34
H	6.09	6.05	5.74	5.76
O	44.33	43.33	39.17	38.85
N	0.00	0.08	0.07	0.06
0.67 mm size particles				
Bulk density, kg m^{-3}	197	201	174	170
True density, kg m^{-3}	1431	1421	1526	1516
High heating value, MJ kg^{-1}	21.25	21.09	23.27	24.38
Weight loss, %wt	9.60	10.97	33.94	40.45
Energy yield, %	93.89	91.77	75.13	70.96
Element Analysis, %wt				
C	51.36	51.53	56.09	58.62
H	6.09	6.06	5.73	5.61
O	42.46	42.31	38.07	35.71
N	0.09	0.10	0.11	0.06
0.81 mm size particles				
Bulk density, kg m^{-3}	165	168	133	135
True density, kg m^{-3}	1381	1373	1366	1353
High heating value, MJ kg^{-3}	20.57	20.35	22.33	22.24
Weight loss, %wt	7.14	9.22	33.00	35.64
Energy yield, %	94.04	90.95	73.65	70.46
Element Analysis, %wt				
C	49.51	50.64	55.35	55.19
H	6.19	6.03	5.71	5.75
O	44.20	43.27	38.95	39.07
N	0.11	0.07	0.00	0.00

5.3 Modeling of Particle Size Effect

Peng et al. (2012) developed a two-component reaction kinetic model for torrefaction within short residence time with the weight loss less than 40% as below:

$$Wood_{\textit{Fast}\cdot \textit{Reaction}\cdot \textit{Group}} \xrightarrow{k_1} Volatiles + Chars$$

$$Wood_{\textit{Medium}\cdot \textit{Reaction}\cdot \textit{Group}} \xrightarrow{k_2} Volatiles + Chars$$

where k_1 and k_2 are the global reaction rates of the fast reaction group and the medium reaction group, respectively.

The fast reaction group may represent the decomposition of hemicelluloses. The medium reaction group is the decomposition of cellulose and lignin. If the two overall reactions are assumed to be first order reactions, the residual weight fraction (W_{TGA}) of wood samples is given by:

$$W_{TGA} = (1 - C_1 - C_2) + C_1 \times \exp(-k_1 t) + C_2 \times \exp(-k_2 t) \tag{5-1}$$

where C_1 may be set as the hemicelluloses content of pine, C_2 represents the combined cellulose and lignin contents of pine.

The observed global reaction rates of the fast reaction group, $r_1(obs)$, and the medium reaction group, $r_2(obs)$, from equation (5-1) are:

$$r_1(obs) = -C_1 \times k_1 \times \exp(-k_1 t) \tag{5-2}$$

$$r_2(obs) = -C_2 \times k_2 \times \exp(-k_2 t) \tag{5-3}$$

Based on TGA data for biomass particles prepared from Fibreco pine chips, using equations (5-2) and (5-3) with $C_1=0.263$ and $C_2=0.704$ [Peng et al. 2012], the observed global reaction rate constants were obtained and tabulated in Table 5-2. As one expected, the observed global reaction rate constant decreased with increasing the mean particle size.

Table 5-2 Observed global reaction rates (k_1 and k_2) with different size pine particles

Particle	Observed	global	reaction	rates
Size, µm	k_1, s^{-1}		k_2, s^{-1}	
573K				
125	5.19E-03		1.40E-04	
375	3.86E-03		1.20E-04	
750	3.43E-03		1.10E-04	
553K				
125	1.48E-03		4.00E-05	
375	1.25E-03		3.00E-05	
750	9.70E-04		2.00E-05	

5.3.1 Temperature Gradient within the Particles

Wood torrefaction is an endothermic reaction. The heat is transferred from the hot gas across the boundary layer to the particle surface then to the particle inside by thermal conduction. A temperature gradient will be created across the surface boundary as well within the particle, which may affect the torrefaction reaction rate. The Biot number and the Pyrolysis number are first estimated to examine whether there is a substantial temperature gradient within the particles.

The Biot number (Bi) represents the ratio between the heat convection from the surrounding fluid to the particle surface and the heat conduction within the particle, which thus determines the relative importance of the heat conduction within the particle

and the heat convection from fluid to particles [Bird et al. 2012].

$$Bi = \frac{\alpha L_C}{\lambda} = \frac{Particle \quad Outside \quad Convection \quad Heat \quad Transfer \quad Rate}{Particle \quad Inside \quad Conductivity \quad Heat \quad Transfer \quad Rate} \qquad (5\text{-}4)$$

where α is the convection heat transfer coefficient in $W\ m^{-2}\ K^{-1}$, L_C is the ratio of the particle volume to surface area in m, λ is the thermal conductivity of particles in $W\ m^{-1}\ K^{-1}$.

If Bi $<<0.1$, the resistance to conduction within the particle is much less than the resistance to convection across the fluid boundary layer. Hence the temperature within the particle can be reasonably assumed to be uniform.

The convection heat transfer coefficient between particles and fluid in the TGA and the fixed bed reactor are estimated from the literature. Since the velocity of the nitrogen flow in the TGA is very low (0.0065 m s^{-1} at 573K), the heat transfer between the particles and the flowing nitrogen in the TGA can be treated as free convection. The velocity of nitrogen flow in the fixed bed reactor is 0.87 m s^{-1} at 573K, so the heat transfer between the particles and the nitrogen in the fixed bed can be treated as forced convection. The heat transfer coefficient between particles and gases in the packed bed ranges 3-20 W m^{-2} K^{-1} for free convection and 10-100 W m^{-2} K^{-1} for forced convection [Bird et al. 2002].

The convection heat transfer coefficient can be also estimated by semi-experimental equations. For small Reynolds numbers (Re), the convective heat transfer coefficient can be estimated by the following Chilton-Colburn factor (j_H) [Bird et al. 2002]:

$$j_H = (\frac{\alpha}{C_{PC}G})(\frac{C_{PC}\mu}{\lambda_C})^{2/3} = 2.19\,\mathrm{Re}^{-2/3}$$ (5-5)

$$\mathrm{Re} = \frac{d_P G}{6(1-\varepsilon)\beta\mu}$$ (5-6)

where d_p is the particle diameter in *m*, C_{PC} is the heat capacity of the nitrogen gas in *kJ kg^{-1} K^{-1}*, ε is the fraction of free space, μ is the viscosity of nitrogen gas in *kg m^{-1} s^{-1}*, G is the superficial mass flux ($u \times \varepsilon \times \rho_C$, nitrogen gas velocity in *m s^{-1}* $\times$ fraction of space $\times$ nitrogen gas density in *kg m^{-3}*), λ_C is the heat conductivity of the nitrogen gas in *w m^{-1} K^{-1}*, β is the particle-shape factor, 1 for spherical particle. In the current study the shape factor equals is 1.

Using equations (5-5) and (5-6) with a pine thermal conductivity $\lambda=0.109$ *W m^{-1} K^{-1}* [Hu et al. 2005] and particle size, the convection heat transfer coefficient has been estimated. Using equation (5-5) and $L_C=d_P/6$ (d_p, particle diameter in *m*), the Bi has been calculated and shown in Table 5-3. From Table 5-3, the Bi is seen to be much less than 0.1. Therefore the temperature gradient inside particles is expected to be very small, and the particles can be treated as having a uniform temperature in this study.

Table 5-3 Estimated Biot numbers of different size pine particles

Particle Size, μm	u m s⁻¹	ε [a]	ρ_C [b] kg m⁻³	μ [b] kg m⁻¹ s⁻¹	C_PC [b] J kg⁻¹ K⁻¹	λ_C [b] W m⁻¹ K⁻¹	α, TGA	W m⁻² K⁻¹ Fixed bed	Biot TGA	Number Fixed bed
573K										
125	6.5E-03	0.49	0.60	2.8E-05	1.04	4.3E-02	20.00		0.004	
375	6.5E-03	0.49	0.60	2.8E-05	1.04	4.3E-02	9.62		0.006	
750	6.5E-03	0.49	0.60	2.8E-05	1.04	4.3E-02	6.06		0.007	
553K										
125	6.2E-03	0.49	0.62	2.8E-05	1.04	4.2E-02	20.32		0.004	
375	6.2E-03	0.49	0.62	2.8E-05	1.04	4.2E-02	9.77		0.006	
750	6.2E-03	0.49	0.62	2.8E-05	1.04	4.2E-02	6.16		0.007	
573K										
230	8.7E-01	0.49	0.60	2.8E-05	1.04	4.3E-02		68.14		0.024
670	8.7E-01	0.49	0.60	2.8E-05	1.04	4.3E-02		33.41		0.034
810	8.7E-01	0.49	0.60	2.8E-05	1.04	4.3E-02		29.44		0.036
523K										
230	7.9E-01	0.49	0.65	2.7E-05	1.04	4.0E-02		69.31		0.024
670	7.9E-01	0.49	0.65	2.7E-05	1.04	4.0E-02		33.98		0.035
810	7.9E-01	0.49	0.65	2.7E-05	1.04	4.0E-02		29.94		0.037

[a]ε from measurement of pine particle; [b]ρ_C, μ, C_PC, and λ_C from Perry (1997).

The pyrolysis number (P'_y) was defined as the ratio of heat convection rate and chemical reaction rate [Pyle and Zaror 1984].

$$P'_y = \frac{\alpha}{k_i \rho C_P L_C} = \frac{Particles\ \ Outside\ \ Convection\ \ Heat\ \ Transfer\ \ Rate}{Particles\ \ Inside\ \ Reaction\ \ Rate} \qquad (5\text{-}7)$$

where ρ is the particle density in $kg\ m^{-3}$, C_P is the heat capacity of particles in $J\ kg^{-1}\ K^{-1}$, k_i is the global reaction rate in s^{-1}, i is the ith reaction group.

Using the observed global reaction rates in Table 5-2 and the convection heat transfer coefficients in Table 5-3, the Pyrolysis number has been estimated and shown in Table 5-4. The P'_y is generally very larger than 1, which indicates that the external heat transfer

rate is much faster than the reaction rate inside the particle. As a result, the external heat transfer will be able to provide sufficient heat energy to sustain the torrefaction reaction or, in other words, the endothermic reaction of torrefaction will not cause the particle surface temperature to decrease.

Table 5-4 Estimated Pryolysis number of different size pine particles

Particle Size, μm	Reaction k_1	rate k_2	α W m^{-2} K^{-1}	ρ [a] kg m^{-3}	C_P [a] J kg^{-1} K^{-1}	Pyrolysis For k_1	Number For k_2
573K							
125	5.19E-03	1.40E-04	20.00	440	1640	256.37	9503.92
375	3.86E-03	1.20E-04	9.62	440	1640	55.24	1776.84
750	3.43E-03	1.10E-04	6.06	440	1640	19.58	610.55
553K							
125	1.48E-03	4.00E-05	20.32	440	1640	913.51	33799.82
375	1.25E-03	3.00E-05	9.77	440	1640	173.33	7221.89
750	9.70E-04	2.00E-05	6.16	440	1640	70.35	3412.13
[a] ρ and C_P from Hu et al. (2005) .							

Both the Biot number and Pyrolysis number show that the temperature gradient within the particle is very small during torrefaction and can thus be neglected in modeling the particle size effect in the current study.

5.3.2 Development of a Hard Core Particle Model

During torrefaction, volatiles (gases and liquid products) can simply be represented by one single species [Prins et al 2006c]. For a single spherical particle with a single gas species as shown in Figure 5-4, the heat and mass balance equations can be derived as [Bird et al. 2002]:

$$\frac{\partial}{\partial t}(\rho C_P T) = \lambda[\frac{1}{r^2}\frac{\partial}{\partial r}(r^2\frac{\partial T}{\partial r})] + \Delta H \cdot r_{\text{Reaction}} \tag{5-8}$$

$$\frac{\partial C}{\partial t} = D_m [\frac{1}{r^2} \frac{\partial}{\partial r}(r^2 \frac{\partial C}{\partial r})] + r_{\text{Reaction}} \tag{5-9}$$

where ρ is the density of biomass in $kg\ m^{-3}$, t is the time in s, C_p is the heat capacity of biomass in $J\ kg^{-1}\ K^{-1}$, T is the temperature in K, λ is the thermal conductivity of biomass in $W\ m^{-1}\ K^{-1}$, ΔH is the decomposition heat of biomass in $J\ m^{-3}$, r_{Reaction} is the real global reaction rate, r is the radii of sphere in m, D_m is the diffusivity of volatiles in $m^2\ s^{-1}$.
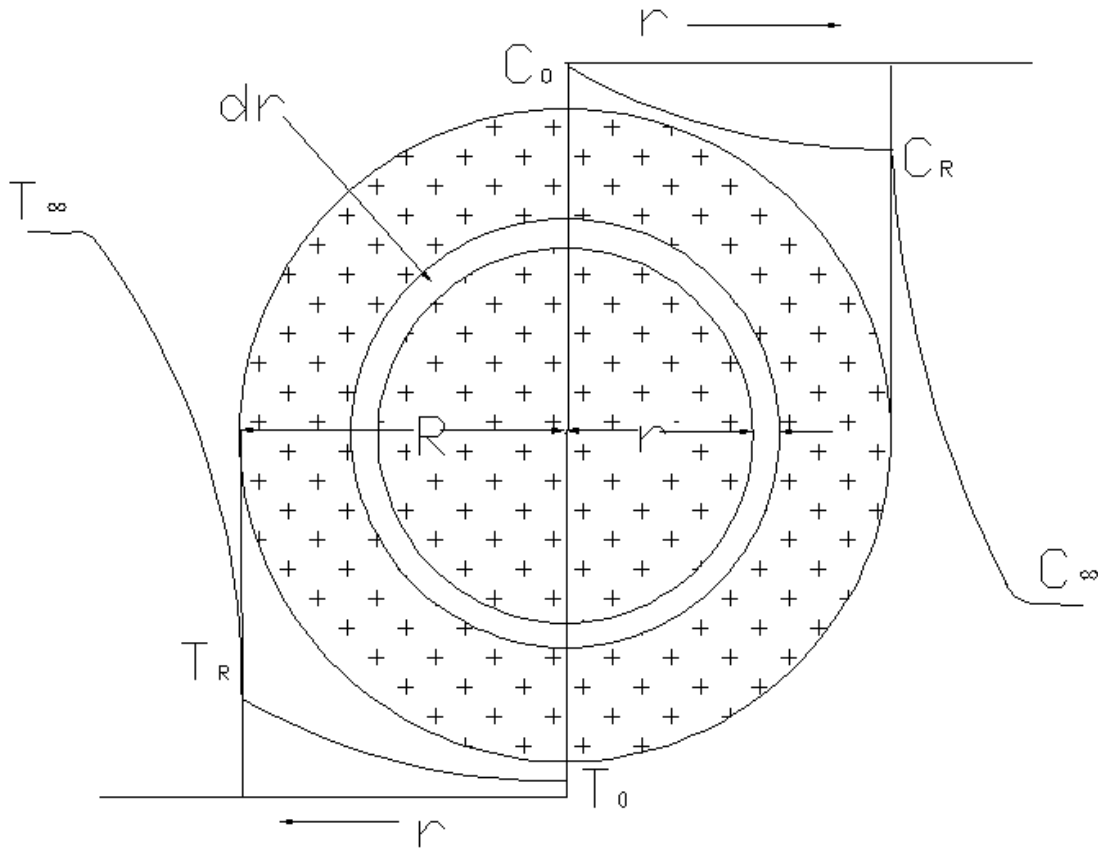
Figure 5-4 Shell heat and mass balances on spherical coordinate system

(Temperature inside particles $T = T(r, t, R, T_{initial})$ and Concentration of volatiles inside

particles $C = C(r, t, R, T_{initial})$)

From 250 to 300 $^{\circ}$C, the decomposition of wood is mainly associated with the hemicelluloses across the whole particle, while there is little change in lignin and celluloses. Therefore, little shrinking in the biomass particle is expected during torrefaction, as reported by Bergman and Prins (2005). For biomass torrefaction with a weight loss of less than 40% in this study, we can reasonably assume that the diameter of particles does not change (non-shrinkage core) during the torrefaction. Also, the previous analysis showed that there is expected to be negligible temperature gradient within particles, so that the particle is treated as having a uniform temperature. By further assuming that the global reactions are first order reactions, and the reaction is under a pseudo steady state with little change of vapour phase concentration inside particles with time, Equations (5-8) and (5-9) can be reduced to:

$$D_m[\frac{1}{r^2}\frac{d}{dr}(r^2\frac{dC}{dr})]+k_rC=0 \tag{5-10}$$

where k_r is the real intrinsic reaction constant in s^{-1}.

With the following boundary conditions:

$$\left.\frac{dC}{dr}\right|_{r=0}=0 \tag{5-11}$$

$$C\big|_{r=R}=C_R \tag{5-12}$$

Equation (5-10) is solved to give the concentration inside the particle:

$$\frac{C}{C_R}=\frac{\sinh(\Phi\frac{r}{R})}{\frac{r}{R}\sinh(\Phi)} \tag{5-13}$$

where Φ is the Thiele module, defined as:

$$\Phi = R\sqrt{\frac{k_r}{D_m}}$$

(5-14)

with D_m as a constant.

Define the effectiveness factor (η) as:

$$\eta = \frac{r(obs)}{r_{\text{Reaction}}} = \frac{Observed \quad global \quad reaction \quad rate}{Real \quad global \quad reaction \quad rate}$$

(5-15)

If there is no concentration gradient inside the particle, the real global reaction rate will be:

$$r_{\text{Reaction}} = \frac{4}{3}\pi R^3 k_r C_R$$

(5-16)

The observed global reaction rate (r(obs)) is thus related to the Thiele module by:

$$r(obs) = 4\pi RD_m \Phi C_R (\frac{1}{\tanh \Phi} - \frac{1}{\Phi})$$

(5-17)

The following relationship can be derived for first order reaction and spherical particles [Fogler 2006]:

$$\eta = \frac{r(obs)}{r_{\text{Reaction}}} = \frac{3}{\Phi}(\frac{1}{\tanh \Phi} - \frac{1}{\Phi})$$

(5-18)

A Weisz-Prater number can be used to estimate the impact of internal diffusion on the reaction [Weisz and Prater 1954]:

$$C_{WP} = \frac{Observed\quad global\quad reaction\quad rate}{A\quad diffusion\quad rate} = \eta \times \Phi^2 = \frac{-r(obs)\rho d_P^{\;2}}{D_m C_R} = 3(\frac{\Phi}{\tanh\Phi} - 1)$$

(5-19)

If C_{WP} is much less than 1, there are no diffusion limitations and no concentration gradient is expected within the particles.

5.3.3 Estimation of Thiele Module and Effectiveness Factor

Theoretically, the Thiele module ($\Phi = R\sqrt{\dfrac{k_r}{D_m}}$) can be calculated for the given particle diameter, reaction rate constant and the effective diffusivity of gases. In the current study, k_r can be estimated by eliminating internal diffusion using very fine sawdust particles. For a given particle pore size, the diffusivity of volatiles, D_m, can be first approximated by the Knudsen diffusion coefficient, D_k, which can be estimated by [Chen 1990]:

$$D_K = 9700 \times a \times (\frac{T}{M_T})^{0.5}, \quad cm^2\;s^{-1}$$

(5-20)

where a is the pore size in *cm*, T is the temperature in K and M_T is the molecular weight. For solid wood, the particle pore size ranges from 2-10 nm (for microfibril) to 1-5 µm (for wall cell layers) [Harrington 2002].

The average molecular weight of the torrefation volatiles can be estimated from the typical volatile composition reported in the literature, as shown in Table 5-5. The Knudsen diffusion coefficients at different temperatures estimated from Equation (5-20) are given in Table 5-6.

Table 5-5 Estimated average molecular weight of torrefaction volatiles [a]

	CH_3COOH	H_2O	HCOOH	CH_3OH	CO_2	CO	Total	M
Molecular Weight	60	18	46	32	44	28		
573K	5.00%	13.00%	2.00%	4.00%	4.00%	1.00%	29.00%	33
553K	3.00%	8.00%	1.00%	1.75%	4.20%	0.75%	18.70%	34
523K	1.75%	7.00%	0.25%	0.25%	3.00%	0.25%	12.50%	31

[a] Vapour composition data from Prins et al. 2006c

Table 5-6 Estimated Knudsen diffusion coefficients for volatiles in solids wood

Pore size, cm	D_k, m^2/s		
	573K	553K	523K
Microfibril			
2.00E-07	8.08E-07	7.82E-07	7.97E-07
1.00E-06	4.04E-07	3.91E-07	3.98E-07
Wall cell layer			
1.00E-04	4.04E-04	3.91E-04	3.98E-04
5.00E-04	2.02E-03	1.96E-03	1.99E-03

Using the Knudsen diffusion coefficients values in Table 5-6, the Thiele module can be estimated by Equation (5-14), and the effective factor by Equation (5-18). The results show a η value very close to 1 for all particles tested in this work, which does not agree with the experimental data as shown in see Figure 5-3 and Table 5-1 where the observed reaction rate constants decreased significantly with increasing the particle size. This may be related to the uncertainty in the estimation of the effective diffusion coefficient, D_m. Torrefaction volatiles (gases) are generated from wood decomposition. Once generated, the volatiles then penetrate through the pores with some of whom just created from the cracked solid wood. As well, those newly created pores from decomposed wood change with time as the reaction proceeds. Typical D_m values of gases through solid ranges

from 10^{-9}-10^{-14} m^2 s^{-1} [Bird et al. 2002], which is much lower than the estimated Knudsen diffusion coefficient in Table 5-6. In the following section, attempt has been made to back out D_m values for biomass torrefaction volatiles through the wood based on fitting the non-shrinkage reaction model to the experimental TGA data.

Based on equation (5-2) for the fast reaction, r_1, we can obtain the following two ratios for the three different particle sizes (denoted 1, 2 and 3):

$$\frac{r_{12}(obs)}{r_{11}(obs)} = \frac{-C_1 \times k_{12} \times \exp(-k_{12}t)}{-C_1 \times k_{11} \times \exp(-k_{11}t)} = \frac{k_{12}}{k_{11}} \times \exp[-(k_{12} - k_{11}) \times t]$$ (5-21)

$$\frac{r_{13}(obs)}{r_{12}(obs)} = \frac{-C_1 \times k_{13} \times \exp(-k_{13}t)}{-C_1 \times k_{12} \times \exp(-k_{12}t)} = \frac{k_{13}}{k_{12}} \times \exp[-(k_{13} - k_{12}) \times t]$$ (5-22)

where, $r_{11}(obs)$ $r_{12}(obs)$ and $r_{13}(obs)$ are the reaction rates of the fast reaction group with different particle sizes, k_{11} k_{12} and k_{13} are the apparent reaction rate constants of the fast reaction with different particle sizes.

At the start of the reaction, t=0, which corresponds to the observed initial reaction rate, Equations (5-21) and (5-22) become:

$$\frac{r_{12}(obs)}{r_{11}(obs)} = \frac{k_{12}}{k_{11}}$$ (5-23)

$$\frac{r_{13}(obs)}{r_{12}(obs)} = \frac{k_{13}}{k_{12}}$$ (5-24)

Similarly one can obtain following two equations for the 2nd reaction, r$_2$:

$$\frac{r_{22}(obs)}{r_{21}(obs)} = \frac{k_{22}}{k_{21}}$$

(5-25)

$$\frac{r_{23}(obs)}{r_{22}(obs)} = \frac{k_{23}}{k_{22}}$$

(5-26)

By assuming that ρ, D_m and C_R (Pyrolysis number >>1) are the same for different particle sizes during torrefaction with a low weight loss, and combining equations (5-14), (5-19), (5-23) and (5-24), one can derive following equations:

$$\frac{k_{12}d_{P2}^{\,2}}{k_{11}d_{P1}^{\,2}} = \frac{(\dfrac{\Phi_{12}}{\tanh \Phi_{12}} - 1)}{(\dfrac{\Phi_{11}}{\tanh \Phi_{11}} - 1)}$$

(5-27)

$$\frac{\Phi_{12}}{\Phi_{11}} = \frac{d_{P2}}{d_{P1}}$$

(5-28)

$$\frac{k_{13}d_{P3}^{\,2}}{k_{12}d_{P2}^{\,2}} = \frac{(\dfrac{\Phi_{13}}{\tanh \Phi_{13}} - 1)}{(\dfrac{\Phi_{12}}{\tanh \Phi_{12}} - 1)}$$

(5-29)

$$\frac{\Phi_{13}}{\Phi_{12}} = \frac{d_{P3}}{d_{P1}}$$

(5-30)

where, Φ_{11} Φ_{12} and Φ_{13} are the Thiele modules of the fast reaction group with different particle sizes, and d_{P1}, d_{P2} and d_{P3} are the mean diameter of different particle sizes.

Using the kinetics rate constants in Table 5-2, following equations can be obtained from Equations (5-27) and (5-28):

$$\frac{(3.86\times10^{-3})\times(3.75\times10^{-4})^2}{(5.19\times10^{-3})\times(1.25\times10^{-4})^2} = \frac{(\dfrac{\Phi_{12}}{\tanh\Phi_{12}}-1)}{(\dfrac{\Phi_{11}}{\tanh\Phi_{11}}-1)} \tag{5-31}$$

$$\frac{\Phi_{12}}{\Phi_{11}} = \frac{d_{P2}}{d_{P1}} = \frac{3.75\times10^{-4}}{1.25\times10^{-4}} = 3 \tag{5-32}$$

Substituting Equation (5-32) to (5-31), we obtain:

$$6.69 = \frac{(\dfrac{3\Phi_{11}}{\tanh(3\Phi_{11})}-1)}{(\dfrac{\Phi_{11}}{\tanh\Phi_{11}}-1)} \tag{5-33}$$

Solving Equation (5-33) we obtain:

$\Phi_{11} = 0.91$ for d_{P1}=1.25E-4 m

   and

$\Phi_{12} = 3\Phi_{11} = 3\times0.95 = 2.73$ for d_{P1}=3.75E-4 m

$\Phi_{13} = 6\Phi_{11} = 6\times0.95 = 5.46$ for d_{P1}=7.50E-4 m

Following the same procedure by substituting kinetics data for different particle size particles in Table 5-3 into Equations (5-29) and (5-30), we can obtain series of values for Φ_{11}, Φ_{12}, and Φ_{13}. Similar procedures were followed to derive equations for the medium reaction group for the calculation of Φ_{21}, Φ_{22}, and Φ_{23}. The estimated Thiele module values are summarized in Table 5-7. It is seen that the Thiele module generally increased with increasing the particle size.

Table 5-7 Thiele module values obtained from fitting the non-shrinkage particle to the experimental data and from calculated from Knudsen diffusion coefficient

Particle size, μm	Φ_1 from data fitting	Φ_1 from Knudsen diffusion	Φ_2 from data fitting	Φ_2 from Knudsen diffusion
573K				
125	0.60	0.014	0.35	0.002
375	1.79	0.042	1.06	0.007
750	3.58	0.085	2.11	0.014
553K				
125	0.56	0.008	0.85	0.001
375	1.69	0.023	2.54	0.004
750	3.38	0.046	5.08	0.008

The particle effectiveness factor and Weisz-Prater number for different size particles were further calculated based on the Thiele modules in Table 5-8. As shown in Table 5-8, for the small size particle (<0.125 mm), effectiveness factor is close to 1 and Weisz-Prater number is less than 1, suggesting that the observed global reaction rate may present the real reaction rate for the small size particles during torrefaction. For medium size particles (0.375 mm) the internal diffusion can affect the torrefaction reaction. For large size particles (0.750 mm), the internal diffusion will greatly limit the reaction.

Table 5-8 Particle effectiveness factor and Weisz-Prater number for different size particles

Particle Size, μm	Observed global reaction rate, s^{-1}		Effectiveness factor, η		Weisz-Prater number, C_{WP}	
	k_1	k_2	For k_1	For k_2	For k_1	For k_2
573K						
125	5.19E-03	1.40E-04	0.98	0.99	0.35	0.12
375	3.86E-03	1.20E-04	0.84	0.93	2.68	1.04
750	3.43E-03	1.10E-04	0.61	0.79	7.76	3.53
553K						
125	1.48E-03	4.00E-05	0.98	0.96	0.31	0.68
375	1.25E-03	3.00E-05	0.85	0.73	2.42	4.71
750	9.70E-04	2.00E-05	0.63	0.47	7.16	12.23

From results in Tables 5-7 and 5-8, the real/intrinsic reaction rate constant (k_r) and the effective volatiles diffusivity (D_m) of pine particles during torrefaction can be further estimated with the results shown in Table 5-9. It is seen that the D_m values fitted from experimental data are orders smaller than the Knudsen diffusion coefficients D_k shown in Table 5-6, confirming the speculation that the diffusion of volatiles through the newly created micropores are the dominating mass transfer step in biomass torrefaction process, at least at the early stage of torrefaction. Simpson and Liu (1991) reported the diffusivity of water vapor through wood in the order of 4E-11 to 8E-11 m^2 s^{-1}. In view that water vapor is one of the major components in the volatiles generated during torrefaction (see Table 5-5), D_m values from this study seem to be consistent with the literature data.

Table 5-9 Real reaction rate constant (k_r) and volatiles effective diffusivity (D_m) of pine particles

	Real reaction constant (k_r), s^{-1}	Volatiles diffusivity (D_m), m^2 s^{-1}
Fast Reaction Group (k_1)		
573K	5.41E-03	1.68E-10
553K	1.52E-03	6.73E-11
Medium Reaction Group (k_2)		
573K	1.43E-04	9.79E-12
553K	4.20E-05	8.63E-13

It has been shown that if the internal diffusion is the dominant limiting step, the global reaction rate will be inversely proportional to the particle size to a power of 1 [Fogler 2006]. For external diffusion controlled process, the global reaction rate is expected to be inversely proportional to the particle size to a power of 2/3. If the global reaction rate is independent of the particle size, then the process is controlled by the intrinsic reaction kinetics. Based on the current TGA test data for three different particle sizes, it was found that the global reaction rate is inversely proportional to the particle size to a power of 0.24. This again can be related to the unique pore generation and enlarging process associated the torrefaction of biomass.

5.3.4 Prediction of Fixed Bed Reactor Data

In this section the kinetic model of the particle size effect developed from fitting TGA data of three different sizes, the reaction kinetics equations are in conjunction with the effective factors for the fixed bed unit. As shown in Table 5-1, the 0.23 mm pine particle sample prepared from the FPInnovation pine chips were tested in both the TGA and the fixed bed reactor. Although the weight loss from the fixed bed unit was very close to that obtained from the TGA tests, the weight loss from the fixed bed reactor was generally found to be consistently higher than the TGA unit because of a higher purging gas velocity. To enable us to directly compare the fixed bed and the TGA data, we first introduce a unit scale factor (Γ):

$$\Gamma = \frac{Global\ reaction\ rate\ that\ would\ result\ in\ the\ fixed\ bed\ unit}{Global\ reaction\ rate\ that\ would\ result\ in\ the\ TGA} \qquad (5\text{-}34)$$

The average unit scale factor was then calculated using the weight loss data of the 0.23 mm size particles from both TGA and fixed reactor (see Table 5-1). The average unit scale factor is found to be 1.29 (see Table 5-10), which indicates that the torrefaction reaction rate is fast in the fixed bed reactor than in the TGA. This can be likely explained by the improved heat and mass transfer rate in the fixed bed reactor where there is a higher nitrogen gas velocity through the packed particle bed than in the TGA.   It should be noted that the unit scale factor might be different for the fast reaction and the medium reaction, although the same value of 1.29 was applied in the following calculations.

Table 5-10 Unit scale factors between the fixed bed reactor and the TGA

Torrefaction Conditions	Γ	Mass	loss, %
		From Fixed Bed	From TGA
573K 15min	1.35	35.97	31.73
573K 30min	1.17	42.86	39.23
523K 15min	1.59	10.03	8.46
523K 30min	1.03	12.22	10.87
Average	1.29		

Incorporating the effectiveness factor (η) and the unit scale factor (Γ) into Equation (5-1), the residual weight fraction of softwood samples can be expressed as:

$$W_{TGA} = (1 - C_1 - C_2) + C_1 \times \exp(-\eta_1 \Gamma k_1 t) + C_2 \times \exp(-\eta_2 \Gamma k_2 t) \tag{5-35}$$

Figure 5-5 shows the experimental fixed bed reactor data and model predictions for the three size pine sawdust particles. It can be seen that at both 523 and 573K Equation (5-35) captured the right trends of both temperature and particle size effects and also gave a reasonably good agreement with the experimental data.
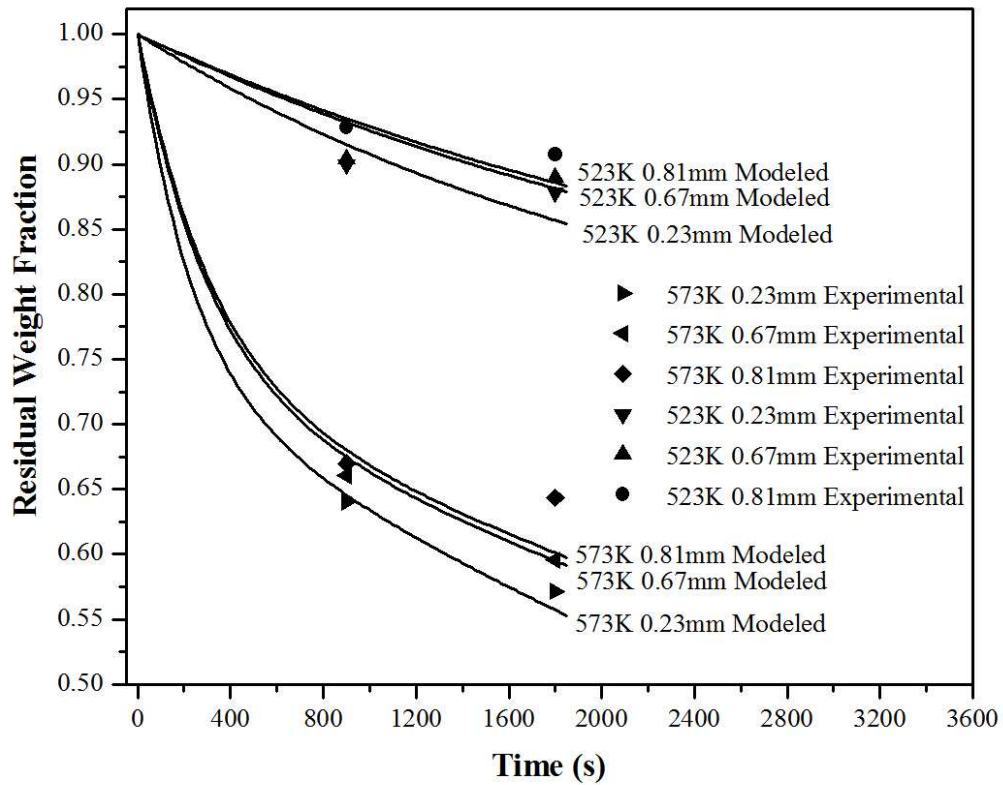
Figure 5-5 Experimental fixed bed torrefaction data and model predictions for three different size pine particles at 573K and 523K

5.4 Densification Performance

Figure 5-6 shows the control and torrefied pellets made from three sizes of torrefied pine particles preconditioned to 10% moisture content at a die temperature of 373 K. Visually they appear to be very similar.

Figure 5-6 Control and torrefied pellets made from different size pine sawdust samples

The measured properties of torrefied and control pellets made from different size pine sawdust samples are given in Table 5-11. It can be seen that the moisture content of pellets generally decreased while the pellet density and Meyer hardness slightly decreased with increasing the degree of torrefaction treatment. The energy consumption for making pellets increased significantly with the increase in the degree of torrefaction treatment. All these findings are consistent with those reported previously in the literature [Peng et al. 2011; Li et al. 2012]. As the particle size increased, the moisture content of the pellets slightly increased while the pellet density remained approximately the same. The energy consumption for making pellets was almost the same for pellets made from 0.23 mm and 0.67 mm sawdust samples, but was quite higher for 0.81 mm sawdust sample. On the opposite, the Meyer hardness was almost the same for pellets made from 0.23 mm and 0.67 mm sawdust samples, but was higher for that made from 0.81 mm sawdust sample, indicating a strong correlation between the energy consumption and the hardness of the pellets. The finding also indicates the existence of a suitable range of

particle size for making torrefied pellets without too high an energy consumption.

Table 5-11 Properties of torrefied and control pellets made from different size pine samples

Items	Control	523K 15min	523K 30min	573K 15min	573K 30min
0.23mm size particles					
Moisture content, %wt	6.52	3.06	4.00	2.94	1.96
Pellet density, kg m^{-3}	1210	1200	1180	1120	1120
Specific energy, MJ t^{-1}	27.5	37.9	40.8	51.2	55.9
Meyer hardness, N mm^{-2}	7.48	4.57	5.13	4.17	5.76
0.67mm size particles					
Moisture content, %wt	6.80	3.58	3.56	2.91	2.71
Pellet density, kg m^{-3}	1230	1250	1240	1170	1160
Specific energy, MJ t^{-1}	26.7	35.4	35.3	41.2	42.9
Meyer hardness, N mm^{-2}	3.44	2.93	2.89	4.04	3.83
0.81mm size particles					
Moisture content, %wt	6.81	4.27	4.55	4.56	3.92
Pellet density, kg m^{-3}	1230	1200	1170	1140	1120
Specific energy, MJ t^{-1}	28.2	53.0	62.6	75.6	78.1
Meyer hardness, N mm^{-2}	6.49	5.09	5.80	7.10	6.95

Figure 5-7 shows the moisture uptake rate of control and torrefied pellets made from different size pine samples as a function of exposure time in the humidity chamber. As can be seen, both the moisture uptake rate and the saturated moisture uptake decreased with increasing the degree of torrefaction. The 473 K torrefied sample gave only slightly lower water uptake rate, while the sample treated at 573 K reduced the saturated water uptake from ~18% to ~12%, representing a 1/3 reduction.
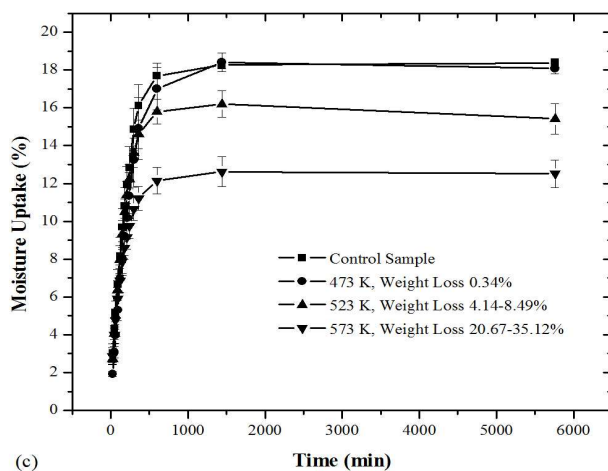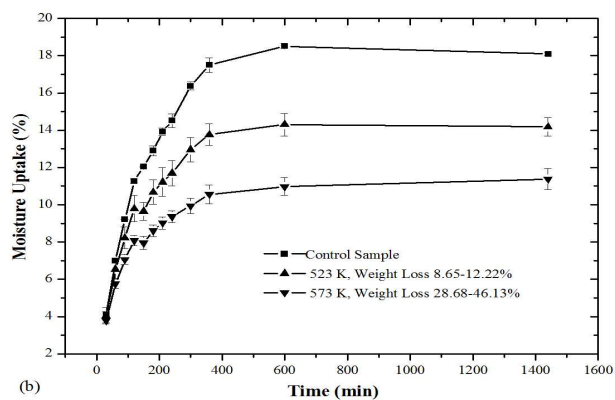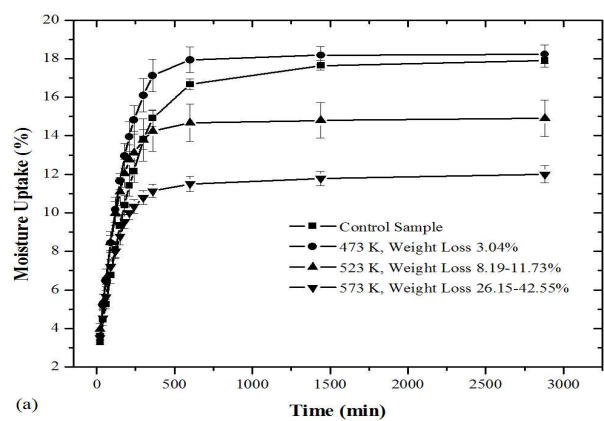
Figure 5-7 Moisture uptake rate of control and torrefied pellets made from different size

pine samples (a) 0.23 mm, (b) 0.67 mm, (C) 0.81 mm

Figure 5-8 shows the shapes of torrefied pellets after the moisture uptake for control pellets and pellets made from three sizes of torrefied pine particles. After moisture uptake, the control pellets and the pellets made from the 523 K torrefied sawdust of 0.67 mm and 0.81 mm broke down, but those made from torrefied sawdust with about 30% weight loss still remained in shape. The diametric, longitudinal and volumetric expansions of control and torrefied pellets made from different size pine sawdust samples after moisture uptake were also measured for those unbroken pellets and given in Table 5-12. It is observed that deep torrefaction reduced the pellet expansion, and the quality of pellets made from the torrefied small particles seems to be generally better than that made from large particles.

Figure 5-8 Shapes of control and torrefied pellets made from three sizes of pine particles after moisture uptake

Table 5-12 Expansion of control and torrefied pellets made from different size pine
samples after moisture uptake

	Longitudinal expansion, %	Diametric expansion, %	Volumetric expansion, %
0.23mm size particles			
Control	112	6	105
523K 15min	63	8	91
523K 30min	65	8	95
573K 15min	36	6	55
573K 30min	27	6	43
0.67 mm size particles			
Control	Broken	broken	broken
523K 15min	Broken	broken	broken
523K 30min	Broken	broken	broken
573K 15min	43	6	48
573K 30min	45	7	49
0.81mm size particles			
Control	Broken	broken	broken
523K 15min	Broken	broken	broken
523K 30min	Broken	broken	broken
573K 15min	39	10	68
573K 30min	29	9	54

5.5 Summary

Both the TGA and fixed bed reactor torrefaction test results showed that the torrefaction rate was affected by the particle size, especially at high temperatures. Although the temperature gradient inside particles of smaller than 1 mm during torrefaction is very small, the internal diffusion of generated vapours inside particles imposes an impact on the global torrefaction reaction rate. The hard core particle model with a first order torrefaction reaction could be applied to give a reasonable prediction of the reaction rate data, accounting for the particle size effect. By fitting the reaction model to the TGA weight loss data, the effective diffusivity of torrefaction volatiles was extracted, which was orders of magnitude lower than the Knudsen diffusion coefficient estimated based on

the microfibril pores of the solids wood. Furthermore, the densification tests showed that the energy consumption for making torrefied pellets increased with increasing the particle size and the degree of torrefaction, and the quality torrefied pellets (hydrophobicity and hardness) could be improved with decreasing the particle size and increasing the severity of torrefaction treatment.

CHAPTER 6 OXYGEN CONCENTRATION EFFECT ON TORREFACTION AND DENSIFICATION

Wood torrefaction is an endothermic reaction, which needs energy input to the reactor. On the other hand, the gas phase (volatiles) of torrefaction products contains high energy, which can be burned to provide needed energy for torrefaction. Compared to indirect heat transfer, it will be much more efficient if the combustion flue gases can be directly contacted with the sawdust for torrefaction and drying. A few papers have reported wood torrefaction in the oxygen-present environment using combustion flue gases [Bilbao et al. 1997; Senneca et al. 2002; Senneca et al. 2004; Garcı́a-Ibañez et al. 2005; Senneca 2007; Uemura et al. 2011], but no one has studied the properties of torrefied pellets that made from an oxidative torrefaction condition. In this chapter, the oxidative torrefaction kinetics was first investigated in a TG analyzer (TGA) using 0.23 mm pine particles at 0%, 3%, 6%, 10%, and 21% flue gas oxygen concentrations. A fluidized bed reactor with the 0%, 3%, and 6% oxygen was then used to produce torrefied samples, which were compressed into torrefied pellets using a press machine. The main objective of this chapter is to identify the oxygen concentration effect on the torrefaction and densification of biomass sawdust.

6.1 Experimental

6.1.1 Materials

0.23 mm pine particles were prepared using pine chips from FPInnovations in a hammer mill installed with 0.79 mm screen, and were used for the TGA test. The sawdust sample (a mixture of spruce and fir with spruce as the main component) from RONA furniture

store in Vancouver was separated into six size fractions, with the 250-355 μm particles being used in the fluidized bed reactor test.

6.1.2 Equipment and Procedures

A sample of several (5-20) milligrams of 0.23 mm Pine particles for each TG experiment was put into a platinum sample cell, which was then located on a sample pan hanging inside a furnace tube with a mixture (0%, 3%, 6%, 10% and 21% of the oxygen concentration) of nitrogen and air as the carrying gas, at a flow rate of 50 *ml (STP) min^{-1}*. The TG test was conducted as following: (1) heating from the room temperature to 110 ^{o}C at a rate of 50 *K min^{-1}*, (2) holding at 110 ^{o}C for 10 min to have the sample dried, (3) heating up to the torrefaction temperature at a rate of 50 *K min^{-1}*, (4) holding at the torrefaciton temperature for 10 hours for torrefaction, (5) heating up to 800 ^{o}C at a rate of 50 *K min^{-1}* to complete the TGA test. Several torrefaction temperatures were chosen for the isothermal experiments.

The batch fluidized bed reactor as described in Chapter 2 was used in this study. The fluidized bed reactor was heated up to the target torrefaction temperature slowly and kept stable for at least 10 min. The raw sample was then added into the reactor from the top feeding port. After torrefaction over the targeted residence time, the pre-heater and furnace heater were turned off to allow the unit to cool down, followed by the cut-off of sweeping gas when the sample temperature dropped to below 200 ºC. Finally, after the sample temperature decreased to the room temperature, the torrefied sample was discharged from the bottom of the reactor.

6.2 Torrefaction Performance in TGA

Figures from 6-1 to 6-3 show the TG curves of pine particles at different temperatures and different oxygen levels. It is seen that oxygen concentration significantly affects the weight loss during torrefaction, especially more significant when the oxygen changes from zero to 3%.
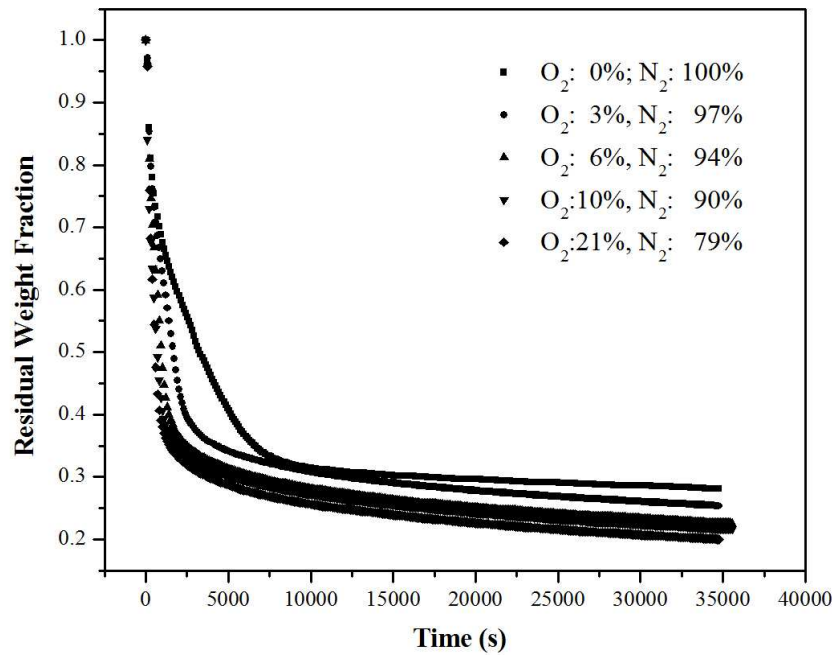
Figure 6-1 TG curves of 0.23 mm pine particles at 300℃ at different oxygen levels
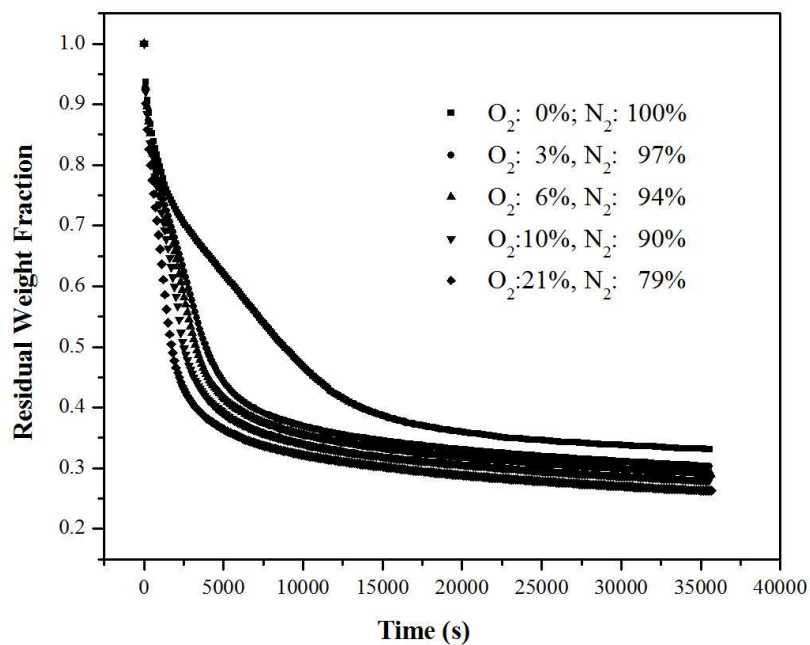
Figure 6-2 TG curves of 0.23 mm pine particles at 280℃ at different oxygen levels
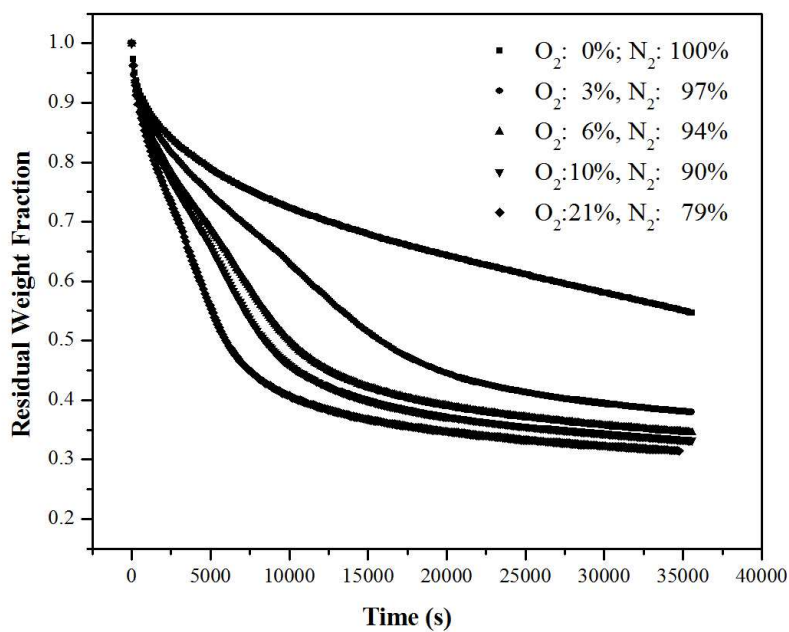
Figure 6-3 TG curves of 0.23 mm pine particles at 260℃ at different oxygen levels

Table 6-1 compares the weight loss for all runs in Figure 6-2 at 280℃ with different oxygen levels, corresponding to a 30% weight loss for 2640 s in the absence of oxygen in the flue gas. Table 6-1 shows that the residence time required for achieving 30% weight loss at 3% oxygen was 1690 s, much less than 2640 s required at 0% oxygen. The final residual weight fraction also decreased slightly with the increase of the oxygen concentration. This means that the low oxygen concentration in the flue gas (3 to 6% in typical combustion flue gases) will accelerate the degradation of wood during torrefaction. Therefore, one of the advantages of the use of combustion flue gases for direct contact heating for biomass torrefaction is the shortened residence time.

Table 6-1 Residence time for 30% weight loss and the final residual weight for torrefaction at 280 ^{o}C with different oxygen levels

	O_2 Concentration				
	0%	3%	6%	10%	21%
Time for 30% weight loss, s	2640	1690	1540	1260	840
Weight loss for 2644 s, %wt	30.0	38.6	43.2	51.4	57.6
Final residual weight fraction	0.3308	0.3026	0.2897	0.2806	0.2630

6.3 Mechanism of Oxygen Effect on Torrefaction

Based on the TG data shown in Figure 6-2, the differences in weight loss between the runs with oxygen presence and the base case with 0% oxygen were calculated and presented in Figure 6-3 to illustrate the oxygen effect. It is seen that within less than 3000 s (or 50 min), the weight loss caused by the oxygen presence increased significantly. This is likely related to the oxidation of unstable component of biomass, in parallel to the thermal cracking in the absence of oxygen. Beyond certain time >3000 s, the oxygen effect appears to be diminishing, likely due to the depletion of those active and unstable oxidative components in the biomass (mostly hemicelluloses) owing to thermal cracking and oxidation. As a result in Figure 6-4, the weight loss difference between the cases with and without oxygen presence decreases. Note that the small difference in weight loss over

long residence time can be attributed to the slow oxidation reaction of produced chars.
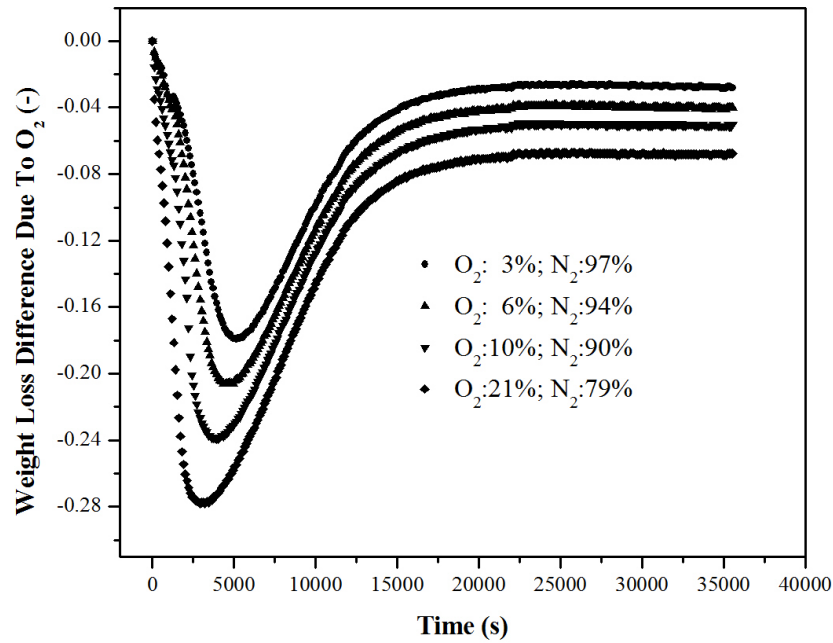
Figure 6-4 Weight loss difference curves of 0.23 mm pine particles due to the oxygen presence at different oxygen levels at 280℃ during oxidative torrefaction

Senneca et al. (2002) suggested that the low-temperature oxidation of solid fuel consists of two parallel pathways. One is the thermal cracking or torrefaction and the other one is the oxidation.

$$Fuel \xrightarrow{Pyrolyssi} Volatiles + Chars$$

$$Fuel \xrightarrow{Oxidation} H_2O + CO_2 + CO$$

$$Volatiles + Chars \xrightarrow{Oxidation} H_2O + CO_2 + CO$$
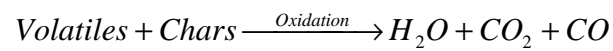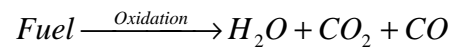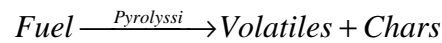
Following the above mechanism, Uemura et al. (2010) developed a parallel reaction

170

kinetics model for the oxidative torrefaction of oil palm empty fruit bunches (EFB) with oxygen concentrations of 0-15%. The overall conversion of biomass consists of the decomposition of hemicelluloses component, which is identical to the torrefaction reaction in the absence of oxygen, and the oxidation reaction of the whole biomass.

6.4 Development of a Kinetic Model for Oxygen Effect on Torrefaction

Peng et al. (2012) developed a two-component reaction kinetic model for torrefaction within short residence time with the weight loss less than 40% as below:

$$Wood_{Fast\cdot Reaction\cdot Group} \xrightarrow{k_1} Volatiles + Chars$$

$$Wood_{Medium\cdot Reaction\cdot Group} \xrightarrow{k_2} Volatiles + Chars$$

where k_1 and k_2 are the global reaction rates of the fast reaction group and the medium reaction group, respectively.

The fast reaction group may represent the decomposition of hemicelluloses. The medium reaction group is the decomposition of cellulose and lignin. If the two overall reactions are assumed to be first order reactions, the residual weight fraction (W_{TGA}) of wood samples is given by:

$$W_{TGA} = (1 - C_1 - C_2) + C_1 \times \exp(-k_1 t) + C_2 \times \exp(-k_2 t) \tag{6-1}$$

where C_1 may be set as the fractional hemicelluloses content of pine, C_2 represents the combined fractional cellulose and lignin contents of pine.

Senneca et al. (2004) proposed a power law kinetic model for the oxidation of biomass during oxidative pyrolysis of solid fuels:

$$\frac{dx}{dt} = -k_{O_2} x P_{O_2}^n \qquad (6\text{-}2)$$

where x is the solid conversion (dry basis), t is the reaction time, k_{O_2} is the oxidation reaction rate, P_{O_2} is the partial pressure of oxygen level in the atmosphere, n is the oxygen reaction order.

By dividing the biomass into two reactive components (Peng et al., 2012) and assuming that the oxidative torrefaction consists of two parallel reactions (Uemura et al., 2010; Senneca et al., 2004), with one representing torrefaction and the other for oxidation, the following kinetic equations can be derived:

$$-r_{overall} = (-r_{torrefaction}) + (-r_{oxidation}) \qquad (6\text{-}3)$$

$$-r_{torrefaction} = (-r_{fast\ group\ torrefaction}) + (-r_{medium\ group\ torrefaction}) \qquad (6\text{-}4)$$

$$-r_{oxidation} = (-r_{fast\ group\ oxidation}) + (-r_{medium\ group\ oxidation}) \qquad (6\text{-}5)$$

$$r_{fast\ group\ torrefaction} = \frac{dr_{fast\ group\ torrefaction}}{dt} = -k_1 \times C_{fast\ group} \qquad (6\text{-}6)$$

$$r_{medium\ group\ torrefaction} = \frac{dr_{medium\ group\ torrefaction}}{dt} = -k_2 \times C_{medium\ group} \qquad (6\text{-}7)$$

172

$$r_{fast\ group\ oxidation} = \frac{dr_{fast\ group\ oxidation}}{dt} = -k_{O1}' \times C_{fast\ group}^{m1} \times C_{O_2}^{n1} = -k_{O1} \times C_{fast\ group}^{m1} \times y_{O_2}^{n1} \qquad (6\text{-}8)$$

$$r_{medium\ group\ oxidation} = \frac{dr_{medium\ group\ oxidation}}{dt} = -k_{O2}' \times C_{medium\ group}^{m2} \times C_{O_2}^{n2} = -k_{O2} \times C_{medium\ group}^{m2} \times y_{O_2}^{n2} \quad (6\text{-}9)$$

where $-r_{overall}$ is the overall reaction rate of pine, $-r_{torrefaction}$ is the torrefaction reaction rate of pine, $-r_{oxidation}$ is the oxidation reaction rate of pine, $-r_{fast\ group\ torrefaction}$ is the torrefaction reaction rate of the fast reaction group, $-r_{medium\ group\ torrefaction}$ is the torrefaction reaction rate of the medium reaction group, $-r_{fast\ group\ oxidation}$ is the oxidation reaction rate of fast reaction group, $-r_{medium\ group\ oxidation}$ is the oxidation reaction rate of the medium reaction group, $C_{fast\ group}$ is the fast reaction group weight fraction, $C_{medium\ group}$ is the medium reaction group weight fraction, y_{O2} is the oxygen mole fraction, k_{O1} $(= k_{O1}' C_o^{n1})$ is the lumped oxidation reaction rate constant of the fast reaction group, k_{O2} $(= k_{O2}' C_o^{n2})$ is the lumped oxidation reaction rate constant of the medium reaction group, m1 and m2 are the oxidation reaction order for the fast reaction group and the medium reaction group, and n1 and n2 are the oxygen reaction order for the fast reaction group and the medium reaction group, respectively. Reactions (6-6) and (6-7) are assumed to be first order reactions, as used in Chapter 3.

If the two oxidation reactions are assumed to be first order reactions with respect to the biomass concentration and the oxygen is in excess amount in the TG test, the residual weight fraction (W_{TGA}) of softwood samples is given by:

$$W_{TGA} = (1 - C_1 - C_2) + C_1 \times \exp[-(k_1 + k_{O1} \times y_{O_2}^{n1})t] + C_2 \times \exp[-(k_2 + k_{O2} \times y_{O_2}^{n2})t] \qquad (6\text{-}10)$$

By regression of the experimental data in Figures from 6-1 to 6-3 over the range of

173

approximately 0 to 40% weight loss before the first inflection point like in Figure 6-4, against equation (6-10) using the least square fitting method, the reaction rates were estimated and shown in Table 6-2.

Table 6-2 Reaction rates from fitting Eq.(6-10) to Figures from 6-1 to 6-3 data

Items	O_2 Concentration				
	0%	3%	6%	10%	21%
Reaction temperature, 300°C					
Observed torrefaction reaction rate, s^{-1}					
$k_1 + k_{O1} \times y_{O2}^{n1}$	2.9E-03	3.1E-03	3.4E-03	3.8E-03	4.0E-03
$k_2 + k_{O2} \times y_{O2}^{n2}$	1.1E-04	1.8E-04	3.6E-04	5.9E-04	6.3E-04
Oxidation reaction rate, s^{-1}					
$k_{O1} \times y_{O2}^{n1}$	0.0E+00	2.1E-04	4.9E-04	9.1E-04	1.1E-03
$k_{O2} \times y_{O2}^{n2}$	0.0E+00	7.0E-05	2.5E-04	4.8E-04	5.2E-04
Reaction temperature, 280°C					
Observed torrefaction reaction rate, s^{-1}					
$k_1 + k_{O1} \times y_{O2}^{n1}$	8.0E-04	8.6E-04	9.0E-04	9.8E-04	1.7E-03
$k_2 + k_{O2} \times y_{O2}^{n2}$	2.3E-05	1.1E-04	1.3E-04	1.7E-04	2.3E-04
Observed oxidation reaction rate, s^{-1}					
$k_{O1} \times y_{O2}^{n1}$	0.0E+00	6.0E-05	1.0E-04	1.8E-04	9.0E-04
$k_{O2} \times y_{O2}^{n2}$	0.0E+00	8.7E-05	1.1E-04	1.5E-04	2.1E-04
Reaction temperature, 260°C					
Observed torrefaction reaction rate, s^{-1}					
$k_1 + k_{O1} \times y_{O2}^{n1}$	2.7E-04	3.6E-04	4.6E-04	5.7E-04	7.0E-04
$k_2 + k_{O2} \times y_{O2}^{n2}$	7.1E-06	2.0E-05	3.0E-05	3.0E-05	5.0E-05
Oxidation reaction rate, s^{-1}					
$k_{O1} \times y_{O2}^{n1}$	0.0E+00	9.0E-05	1.0E-04	1.1E-04	4.3E-04
$k_{O2} \times y_{O2}^{n2}$	0.0E+00	1.3E-05	2.3E-05	2.3E-05	4.3E-05

The reaction rates for the equation 6-10 can be defined:

$$k_1 = A_1 e^{-\frac{E_1}{RT}} \tag{6-11}$$

$$k_2 = A_2 e^{-\frac{E_2}{RT}} \tag{6-12}$$

$$k_{O1} = A_{O1} e^{-\frac{E_{O1}}{RT}} \tag{6-13}$$

$$k_{O2} = A_{O2}e^{-\frac{E_{O2}}{RT}} \tag{6-14}$$

where E_1 and A_1 are the torrefaction reaction kinetic constants of the fast reaction group without oxygen. E_2 and A_2 represent the torrefaction reaction kinetic constants of the medium reaction group without oxygen. E_{O1} and A_{O1} are the oxidation reaction kinetic constants the fast reaction group. E_{O2} and A_{O2} represent the kinetic constants of the medium reaction group.

Equations 6-11 to 6-14 are rearranged to give:

$$\ln(k_1) = \ln(A_1) + (-\frac{E_1}{RT}) \tag{6-15}$$

$$\ln(k_2) = \ln(A_2) + (-\frac{E_2}{RT}) \tag{6-16}$$

$$\ln(k_{O1} \times y_{O2}{}^{n1}) = \ln(A_{O1}) + (-\frac{E_{O1}}{RT}) + (n1) \times \ln(y_{O2}) \tag{6-17}$$

$$\ln(k_{O2} \times y_{O2}{}^{n2}) = \ln(A_{O2}) + (-\frac{E_{O2}}{RT}) + (n2) \times \ln(y_{O2}) \tag{6-18}$$

The values of E_1, E_2, A_1, and A_2 were estimated by linear regression of experimental rate constant data presented in Table 6-2 against equations 6-15 and 6-16. The values of E_{O1}, E_{O2}, A_{O1}, A_{O2}, nl, and n2 were estimated by linear regressions of data in Table 6-2 using equations 6-17 and 6-18. The obtained reaction kinetic constants of the two-component torrefaction and oxidation model are summarized in Table 6-3.

From Table 6-2, at 280 $^{\circ}$C with 3% carrier gas oxygen, the oxidation reaction rate of the

fast reaction group and the medium reaction group were 6.0E-5 s^{-1} and 8.7E-5 s^{-1}, respectively. Compared with the torrefaction rate of fast reaction group (k_1) value of 8.0E-4 s^{-1} at 280 ^oC, the oxidation rate of fast reaction group was much slower than the torrefaction rate of fast reaction group. But the oxidation rate of medium reaction group was much higher than the torrefactation rate of medium reaction group (k_2=2.3E-5 s^{-1}). Table 6-2 also shows that the observed torrefaction reaction rate of fast reaction group ($k_1+k_{O1}\times C_{O2}^{n1}$) at the low oxygen concentration (from 0% to 6%) remains almost the same. Since the fast reaction group mainly represents the hemicelluloses while the medium reaction group mainly represents the cellulose and lignin of pine, these results suggest that the presence of oxygen during oxidative torrefaction substantially increased the conversion of cellulose and the lignin, but not hemicelluloses. However, the higher reaction order of the fast reaction group on oxygen (n1) indicates that the oxidation of hemicelluloses is more sensitive the oxygen concentration (see Table 6-3).

Table 6-3 Two-component torrefaction and oxidation model reaction constants

Items	Unit	Amount
Fast reaction group		
Torrefaction kinetic constants		
E_1	kJ mol^{-1}	145.9
$\ln(A_1)$	s^{-1}	24.71
Oxidation kinetic constants		
E_{O1}	kJ mol^{-1}	86.62
$\ln(A_{O1})$	s^{-1}	13.11
n1		1.0
Medium reaction group		
Torrefaction kinetic constants		
E_2	kJ mol^{-1}	168.6
$\ln(A_2)$	s^{-1}	26.17
Oxidation kinetic constants		
E_{O2}	kJ mol^{-1}	153.4
$\ln(A_{O2})$	s^{-1}	25.86
n2		0.69

The experimental and fitted curves of 0.23 mm BC pine samples with different oxygen

concentrations at different temperatures were compared in Figures 6-5, 6, and 7. It can be seen that the current two-component torrefaction and oxidation model gave a good fit to the isothermal TG experimental data over the short residence time range at a weight loss of 0-40%, typical for torrefaction operation.
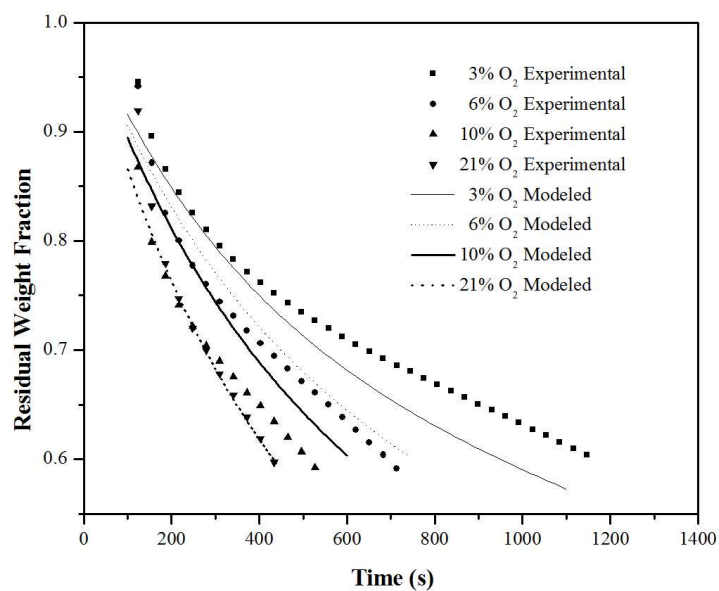
Figure 6-5 Comparison of experimental and fitted TG curves for 0.23 mm pine particle sample at 300 $^\circ$C.
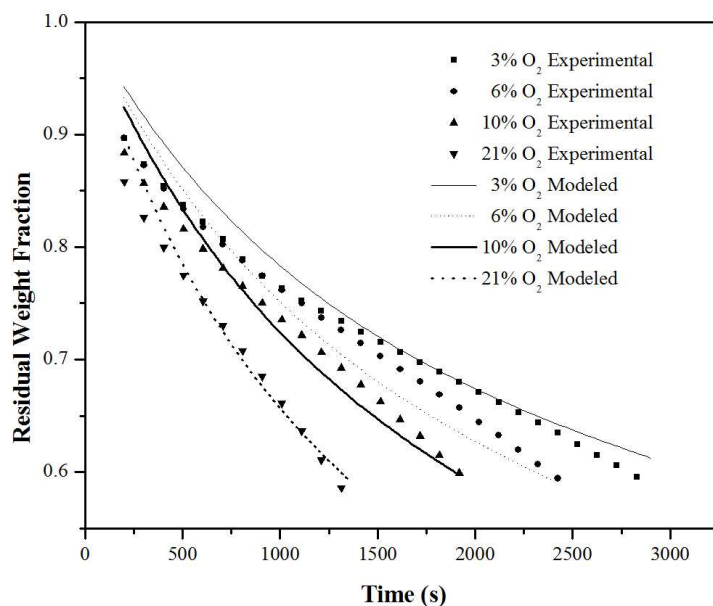
Figure 6-6 Comparison of experimental and fitted TG curves for 0.23 mm pine particle

sample at 280 ^{o}C.
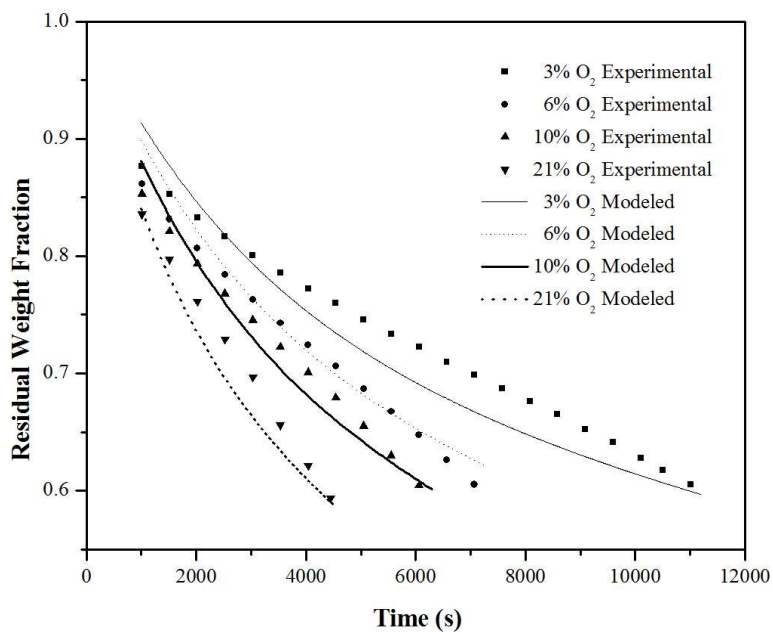
Figure 6-7 Comparison of experimental and fitted TG curves for 0.23 mm pine particle

sample at 260 ^{o}C

178

6.5 Torrefaction in the Fluidized Bed Reactor

Our previous research [Li et al. 2012; Peng et al. 2012] showed that pellets produced from the torrefied sawdust with around 30%(wt) weight loss had a higher hardness than those with less or higher than 30 wt.% weight loss. As a result, we targeted 30 wt% weight loss for torrefaction to evaluate the effect of oxygen content in the carrier gas on the qualities of torrefied sawdust and pellets. Based on the TG test results, it is seen that the sawdust lost its weight fast in the presence of oxygen in the carrier gas due to the contribution of gas phase oxygen to the oxidation of biomass. The torrefaction temperature and residence time for each run was selected based on the TG test results. The specific test conditions and the weight losses from all selected tests are given in Table 6-4.

Table 6-4 Summary of selected test conditions and measured weight losses of 250-355 μm particles from fluidized bed tests

#	Torrefaction Temperature, ℃	Residence time, min	O_2, %	Weight loss, %
1	250	42	3	30
2	270	25	3	31.5
3	270	24	3	29.8
4	290	4	3	30
5	290	7	3	36
6	270	12	6	31
7	270	30	0	36

Table 6-5 presents the results from the ultimate analysis of torrefied and untreated feedstock. When the conventional torrefied biomass (sample 7) is compared with the dry raw material, the elemental carbon content of torrefied biomass increased, but hydrogen and oxygen contents of torrefied biomass decreased, resulting in decreased H/C and O/C ratios. This may be due to the release of volatiles rich in hydrogen and oxygen, such as water and carbon dioxide. Lower hydrogen and oxygen contents of torrefied biomass are

also associated with reduction in hydroxyl (− OH) groups during torrefaction. Similar observations were also reported by Madic et al. (2012) and Phanphanich et al. (2011). Similar trends were found for oxidative torrefied biomass in comparison to the untreated raw biomass. When the oxidative torrefied biomass (samples 1-6) is compared with the regular torrefied biomass (sample 7), there is very little difference in their elemental contents. This may be due to the fact that oxidative torrefaction is a complex combined process of devolatilization, carbonization and oxidation, in which torrefaction and oxidation undergo in parallel and do not interact with each other [Bergman et al. 2005; Uemura et al. 2011]. At the same weight loss, the increase of oxygen concentration in the carrier gases imposed little effect on the HHV of torrefied sawdust, consistent with the results reported by Uemura et al. (2011). In addition, to investigate the effect of oxidative torrefaction treatment on the component of product, Table 6-4 compares the dichloromethane (DCM) extractives and lignin content of dry raw material and three torrefied samples under 0%，3% and 6% O_2 at the same temperature. It can be found that torrefaction decreased the extractives, but increased the relative lignin content compared with untreated biomass. Besides, oxidative torrefied samples had a slightly higher lignin content than regularly torrefied samples. The DCM-extractable content of biomass is a measure of substances such as waxes, fats, resins, photosterols and non-volatile hydrocarbons. It is likely that most of the extractives are removed during the torrefaction process. The relative increase in the lignin content by torrefaction is likely due to thermal degradation of lignin, which is relatively inactive during torrefaction compared with cellulose and hemi-cellulose [Chen et al. 2011b]; whilst other studies attribute this trend to the volatilization of some of the carbohydrate fractions and the formation of acid-insoluble degradation products during torrefaction [Stelte et al. 2011a; Yan et al. 2009]. The significance of both extractives and lignin contents for the pelletization of sawdust will be discussed in section 6.6.

Table 6-5 Chemical composition analysis of torrefied and untreated 250-355 μm particles

#	Torrefaction Conditions	N , %	C. %	H. %	O, %	DCM Extractives, %	Lignin Content, %
0	Dry raw material	1.79±0.13	46.52±0.11	6.22±0.01	45.48±0.04		
1	250℃,42min, 3%O_2; 30 %wt	0.33±0.03	50.45±0.07	5.26±0.04	43.96±0.06		
2	270℃,25min, 3%O_2; 31.5 %wt	0.39±0.01	51.75±0.49	5.51±0.03	42.36±0.01	0.063	53.3
3	270℃,24min, 3%O_2; 29.8 %wt	0.335±0.11	51.32±0.22	5.56±0.13	42.80±0.19		
4	290℃, 4min, 3% O_2; 30 %wt	0.37±0.04	51.59±0.34	5.5±0.01	42.54±0.37		
5	290℃,7min, 3% O_2; 36 %wt	0.46±0.09	53.51±0.04	5.41±0.11	40.63±0.16		
6	270℃,12min, 6% O_2; 31 %wt	0.28±0.01	52.22±0.12	5.54±0.04	41.98±0.09	0.11	47.5
7	270℃,30min, 0% O_2; 36 %wt	0.39±0.02	52.14±0.11	5.87±0.02	41.61±0.11	0.22	42.8

Measured particle density of raw sawdust and selected torrefied sawdust samples are shown in Table 6-6. The torrefied sawdust tends to have higher particle density than raw sawdust, which may be due to the shrinkage of particles during torrefaction and/or the reduction in internal particle pores [Mani et al. 2004]. On the other hand, oxidative torrefaction in the presence of flue gas O_2 increased the particle density compared with torrefied sawdust without the presence of any oxygen, likely due to the oxidation of more light hydrocarbons in the biomass.

Table 6-6 Particle density HHV and energy yields over torrefaction of raw and torrefied 250-355 μm particles

#	Torrefaction Conditions	Particle density, $kg\ m^{-3}$	HHV, $MJ\ kg^{-1}$	Energy yield, %
0	Untreated dry sawdust	1441±25	18.93	
1	250℃, 42 min, 3% O_2; 30 %wt	1525±18	20.98±0.03	77.56±0.11
2	270℃, 25 min, 3% O_2; 31.5 %wt	1521±33	20.80±0.66	75.26±2.37
3	270℃, 24 min, 3% O_2; 29.8 %wt	1522±22	21.34±0.52	79.15±1.96
4	290℃, 4 min, 3% O_2; 30 %wt	1541±31	21.21±0.11	78.42±0.41
5	290℃, 7 min, 3% O_2; 36 %wt	1562±50	21.82±0.09	73.76±0.32
6	270℃, 12 min, 6% O_2; 31 %wt	1637±31	21.04±0.14	76.69±0.51
7	270℃, 30 min, 0% O_2; 36 %wt	1449	21.31±0.39	72.03±1.34

The HHV and energy yields over torrefaction of raw and torrefied sawdust are also

summarized in Table 6-6. As expected, torrefaction increased the sawdust HHV markedly because of the removal of low carbon content hemicelluloses. At the same weight loss, the increase of oxygen concentration in the carrier gases during torrefaction imposed little effect on the HHV of torrefied sawdust, consistent with the results reported by Uemura et al. (2011) who postulated that torrefaction and oxidation occurred in parallel during oxidative torrefaction, with the two reactions not interacting with each other. The energy yields of test runs with 30% weight loss were in the range of 75.2-79.2%, for that of 36% weight loss were in the range of 72.0-73.8%, with no clear correlation with the level of O_2 in the carrier gas. It seems that the amount of oxygen added to the torrefaction reactor did not have an obvious effect on the energy yield of torrefied biomass. Therefore, the energy yield is essentially determined by the mass yield no matter whether or not O_2 is present in the carrier gas. Table 6-5 also shows that the energy yield decreased with increasing the severity of torrefaction or the weight loss. Similar observation was also reported in the study of Bridgeman, et al. (2008) and Mani et al. (2011).

6.6 Pelletization and Properties of Torrefied Pellets

There are two energy consumption processes associated with pellet making. One is the compression of sawdust for pelletization, which accounts for the major energy consumption, and the other is from the extrusion of the pellets out of the die, with a much less energy being consumed.

The results in Table 6-7 demonstrate that more energy was consumed to make pellets from torrefied sawdust than the raw untreated sawdust at the same die temperature (170 $^{\circ}$C) and compression force (4000 N, 125 MPa). For torrefied sawdust prepared at different carrier gas oxygen contents, the energy consumption for compression and extrusion were very similar to those prepared without the presence of oxygen in the

carrier gas. This may be due to the lack of water and low hemicelluloses content in the torrefied sawdust. Water acts as a plasticizer, lowering the softening temperature of the wood polymers; whilst hemicelluloses bind lignin and cellulose fibrils and provide flexibility in the plant cell wall [Stelte et al. 2011a]. Their degradation embrittles wood, making it easier to be comminuted into small particles [Chen et al. 2011b; Stelte et al. 2011a; Yildiz et al. 2006]. As a result, pelletization parameters such as the friction coefficient and Poisson ratio are likely to be affected, leading to increased energy consumption [Chen et al. 2011b; Stelte et al. 2011a]. Besides, extractives have been shown to play an important role during the densification process and are likely to act as the lubricant to lower the friction between the pellet and the metal wall [Stelte et al. 2011a; Stelte et al. 2011c]. As the extractives in torrefied sawdust are decreased, higher energy consumption is expected during densification. The oxidative torrefaction at O_2 less than 6% did not change the properties of torrefied sawdust compared to regular torrefaction in the absence of O_2, leading to similar energy consumption associated with pelletization. The energy consumed for compressing torrefied sawdust at a die temperature of 170 ^{o}C, however, is lower than that of the raw untreated sawdust at a die temperature of 70 ^{o}C. This is most likely due to that lignin acts as a binding agent, which softens at elevated temperatures and helps the binding process [Kaliyan and Morey 2009], consequently leading to less energy consumption.

The Meyer hardness of prepared pellets was obtained from the stress-strain curve from the crushing tests, following the procedures as mentioned in the literature [Lam et al. 2011; Doyle et al. 1985; Tabil et al. 2002]. As shown in Table 6-7, the Meyer Hardness of torrefied pellets is generally lower than the control pellets made from raw sawdust under the same die temperature of 170 ^{o}C and a compression force of 4000 N, which is consistent with the results reported by Stelte et al. (2011a). This may be due to that during torrefaction the amount of available hydrogen bonding sites is reduced, so that the

strength of torrefied pellets is lowered compared to pellets made from untreated sawdust [Stelte et al. 2011b]. Besides, the moisture content of the torrefied sawdust is lower, which results in an increase in the glass transition temperatures of the remaining hemicelluloses and lignin [Stelte et al. 2011b]. Stelte et al. (2011a) thus postulated that torrefaction might reduce the inter-diffusion of the wood polymers between adjacent particles in a pellet and thus the formation of solid bridges between them. The resulting pellets are more brittle than pellets made from untreated sawdust. However, the Meyer hardness of all torrefied pellets is higher than the control pellets prepared with a die temperature of 70℃ (1.44 N mm^{-2}), which is the temperature commonly used in making regular untreated wood pellets, confirming that torrefied pellets as strong as regular pellets can be produced at the expenses of a higher die temperature and higher compression energy consumption. Table 6-9 further shows that with the increase of oxygen content in the carrier gas for torrefaction, the Meyer hardness became slightly lower, which may be due to the oxidative removal of lignin, an important binding agent, from the biomass.

Table 6-7 Energy consumptions associated with compression and extrusion of pellets Meyer hardness Saturated moisture adsorption of pellet s the pellet density before and after moisture uptake of 250-355 μm particles

#	Torrefaction Conditions	Compression Energy, $kJ\ kg^{-1}$	Extrusion Energy, $kJ\ kg^{-1}$	Hardness , $N\ mm^{-2}$	Moisture adsorption, %	Pellet density [a] $kg\ m^{-3}$	Pellet density [b] $kg\ m^{-3}$
0	Dry raw material (170℃)	17.69±2.39	0.195±0.09	5.04±1.79	13.78±3.55	1098±53	578±48
0	Dry raw material (70℃)	36.40	0.125	1.44	20.47	1050	0.501
1	250℃,42min,3%O$_2$; 30%wt	26.28	0.490	2.81±0.84	11.06±1.63	953±33.4	723±7.7
2	270℃,25min,3%O$_2$; 31.5%wt	27.06±1.00	0.443±0.034	2.39±0.61	13.10±2.73	971±16.5	693±10
3	270℃,24min,3% O$_2$;	25.68±0.74	0.308±0.170	2.10±0.59	13.26±3.31	990±10.7	694±29
4	290℃, 4min, 3% O$_2$; 30%wt	26.57±1.19	0.325±0.070	2.38±0.17	14.21±6.86	965±17.2	680±16
5	290℃,7min, 3% O$_2$; 36%wt	29.50±1.96	0.354±0.160	2.64±0.52	12.85±5.16	951±47.8	651±69
6	270℃,12min, 6% O$_2$; 31%wt	28.46±1.28	0.209±0.144	2.10±0.58	15.65±3.56	958±26.6	681±30
7	270℃,30min, 0% O$_2$; 36%wt	27.15±0.13	0.272±0.031	2.97±0.55	9.03±1.96	992±29.9	757±3.7

a. The Pellet Density before moisture uptake; b. The Pellet Density after moisture uptake.

The hydrophobilicity of prepared pellets was examined in a humidity chamber. The

saturated moisture content was obtained after exposing the pellets to the moist air at 30 ^{o}C and 90% relative humidity for 48 hours inside the humidity chamber. As shown in Table 4, all torrefied pellets have a higher hydrophobicity than untreated control pellets, which may be due to the loss of hydroxyl ($-$OH) groups from biomass during torrefaction [Phanphanich et al. 2011; Pimchuai et al. 2010]. For control pellets, extrusion at a die temperature of 170 ℃ also improved the hydrophobicity largely likely because of the thermal modification of pellet surface during higher temperature compaction and extrusion. For those pellets produced from torrefaction using the carrier gas containing oxygen, their hydrophobicity was reduced. The density of prepared regular and torrefied pellets before and after water uptake was measured by a multipycnometer, and shown in Table 6-9. Comparing samples 0 to 7 prepared in this study at the same die temperature of 170 ^{o}C, it is seen that before moisture absorption, the density of torrefied pellets is about 10% lower than the control pellet made from raw sawdust (run 0). This is mainly due to the formation of more inter-particle gaps and voids by torrefaction, which leads to a lower pellet density. However, all torrefied biomass pellets have a similar density, insensitive to the oxygen content used in the preparation of torrefied sawdust. While after moisture absorption, the pellet density decreased from about 1 to 0.7 for torrefied pellets. But for control pellet, its density decreased from 1 to 0.58 or 0.501 for the condition of die temperatures of 170 ℃ and 70 ℃, respectively, indicating that a more significant expansion in the volume after water uptake than torrefied pellets. As a result, the hydrophobilicity of torrefied pellets will have an advantage over the control pellet from the pellet handling logistics point of view.

6.7 Summary

Oxidative torrefaction of sawdust with a carrier gas containing 3% to 6% O_2 was investigated in a TG and a fluidized bed reactor, with the properties of the torrefied

sawdust and pellets compared with regular torrefaction without any O_2, as well as the dry raw material. It is found that the oxidative torrefaction kinetics can be well modeled by two parallel reactions, one for thermal degradation and the other one for biomass oxidation. The oxidative torrefaction process produced torrefied sawdust and pellets of similar properties as to normally torrefied sawdust and corresponding pellets, especially on the density, energy consumption for pelletization, higher heating value and energy yield. For moisture adsorption and hardness of the torrefied pellets, the oxidative torrefaction process showed slightly poor but negligible performance, which may likely be related to the structure change caused by the oxidation. Therefore, from the process integration and cost point of view, it is feasible to use oxygen laden combustion flue gases as the carrier gas for torrefaction of biomass.

Compared to the control pellets, torrefied pellets made at the same die temperature have a lower density and hardness although more energy is required to compress torrefied sawdust into pellets. However, torrefied sawdust can be made into dense and strong pellets of high hydrophobicity at a higher die temperature than normally used in the production of regular control pellets.

CHAPTER 7 ECONOMICAL EVALUATION OF TORREFIED WOOD PELLETS

Torrefaction can increase the energy density of wood on the mass basis, and solve the problems of the durability and biological degradation associated with conventional pellets. Pelletization, on the other hand, can increase the volumetric energy density. In this chapter, the torrefaction and densification results of previous chapters are used to conduct an economical evaluation of Canadian torrefied wood pellets in comparison to regular wood pellets.

7.1 Summary of Torrefaction and Densification

Based on this work and previous studies (e.g. Bergman, 2005), the optimal torrefaction conditions were found to correspond to a weight loss of around 30% at a reactor temperature from 250 to 350 ^{o}C, giving a 20% increase of the heating value. The increase of the heating value is proportional to the weight loss of torrefaction. The optimal densification conditions for making durable torrefied pellets are at a die temperature $\geq$110 ^{o}C using a higher compression pressure with the torrefied sawdust preconditioned to 10% moisture content.

Table 7-1 summarizes the torrefaction and densification results of different BC softwoods with around 30% weight loss. The torrefied pellet density is slightly lower than the control pellet density. At a die temperature of 230 ^{o}C, the torrefied pellet density is close to the control pellet density and the energy density of torrefied pellets is about 22% higher than the energy density of control pellets. The results in Table 7-1 are used as the base case for the economical analysis of torrefied pellets for BC softwoods.

Table 7-1 Torrefaction and densification results of BC softwoods with 30% weight loss

Items	BC Softwood		Pine	Values for case studies	
	low	high	bark	BC Softwood	Pine bark
Control pellets (70 ^{o}C die Temperature)					
HHV, *MJ kg^{-1}*	18.13	18.79	19.52	18.55	19.50
Bulk density, *kg m^{-3}*	665	718	753	700	750
Single pellet density, *kg m^{-3}*	1140	1230	1290	1200	1290
Energy density, *GJ m^{-3}*	12.22	13.48	14.69	12.99	14.63
Moisture content, %(wt)	4.61	7.00	7.54	7.00	7.50
Torrefied pellets (230 ^{o}C die Temperature)					
Weight loss, %wt	24.40	35.97	30.30	30.00	30.00
HHV, *MJ kg^{-1}*	21.54	23.27	24.61	22.65	24.50
Energy yield, %	70.69	83.78	80.39	80.12	80.39
Bulk density, *kg m^{-3}*	659	712	665	700	670
Single pellet density, *kg m^{-3}*	1130	1220	1140	1200	1150
Energy density, *GJ m^{-3}*	14.69	15.73	16.37	15.86	16.42
Torrefied/Control				1.22	1.12
Moisture content, %(wt)	0.04	0.56	0.00	0.25	0.50

7.2 Canadian Wood Pellet Sources

In order for an alternative energy source to be competitive in the market, it has to be abundantly available and affordable with a low production and transportation cost.   In Canada, there are abundant forests and a large lumber and paper industry, which generate wood residues. The available Canadian wood pellet sources and CO_2 emission reduction potentials are shown in Table 7-2. Bradley (2008) reported that the unused available annual forest biomass in Canada was 16.8 million bone-dry metric tones (BDt) (including 1.9 million BDt of mill residues, 2.1 million BDt of wood bark piles, and 12.8 million BDt of wood harvest residue), which can be converted to 14 Mt wood pellets for at least 10 years. Another source is the MPB infested trees.   Kumar and Sokhansanj (2005) estimated that there were 200 to 700 million cubic meters of MPB infested wood in BC, which can be used to produce 5-16 Mt wood pellets for at least 20 years. Adding to the current production, Canada can provide 20 ~ 30 Mt wood pellets per year for at least 10 years, which will reduce the CO_2 emission by 20 ~ 70 Mt per year.   This supply of wood

pellets from Canada, if fully utilized, should meet the current demand of wood pellets in the world for a long time. We thus believe that the Canadian wood pellet industry will have a great potential to grow at a rapid pace to fill in the growing gaps between the world pellet demand and supply, supported by available wood residues and MPB-infested trees.

Table 7-2 Canadian available wood pellet residues and reduced CO_2 emission

	Items	Sources per year	Wood Pellets per year, Mt	CO_2 reduction potential, Mt
1	Mill wood residues	1.9 million BDt[a]	1.6	1.6-3.7
2	Wood bark piles	2.1 million BDt[a]	1.8	1.7-4.1
3	Wood harvest residues	12.8 million BDt[a]	10.7	10.4-25.0
4	MPB infested trees	200-700 million m^3 [b]	5-16	4.9-37.6
5	Current wood pellet production		1.5	1.5-3.5
	Total		20-30	20-70

Source: a. Bradley (2008), b. Kumar and Sokhansanj (2005)

7.3 Production Costs of Canadian Conventional Wood Pellets

Although there is an abundant supply of raw materials for the production of wood pellets in Canada, whether the Canadian wood pellets can further penetrate the world market still largely depends on their costs, including both the production and transportation costs. In this section, the standard cost analysis and engineering economics analysis methods are followed to estimate the production cost of wood pellets, including the capital cost, variable cost, fixed cost, depreciation cost and return on total capital investment (ROI). The capital cost of plants normally depends on the plant scale and types of raw materials to be processed.

In Canada, the capacity of wood pellet plants ranges from 24,000 to 180,000 t annum^{-1}. Table 7-3 shows the capital costs for several wood pellet plants of various capacities as reported in the literature. The results showed that the specific capital investment for a

wood pellet plant of 80,000 t annum^{-1} in capacity was around \$110 per t annum^{-1}, and the specific capital investment for an 180,000 t annum^{-1} capacity was about \$100 per t/a. The capital cost for Pacific BioEnergy Corp was low because of the use of some used equipments. On the other hand, the capital cost for Premium Pellet Ltd. was high because of the construction of a supply pipeline for raw materials.

Table 7-3 Typical Wood Pellet Plant Capital Cost

Items	Capacity t annum^{-1}	Total Plant Capital \$	Specific Capital Investment \$ t^{-1} annum
a 3 t/h plant in Canada [a]	24,000	3,196,000	133.2
a 10 t/h plant in Canada [a]	80,000	9,075,000	113.4
a 22.5 t/h plant in Canada [b]	180,000	18,149,324	100.8
Premium Pellet Ltd. in Vanderhoof [c]	180,000	20,000,000	133.3
Pacific BioEnergy Corp. in Prince George [d]	180,000	15,000,000	83.3

Source: a. Zakrisson (2002) and exchange rate 1€=15090\$; b. Witte (2008); c. Urbanowski (2005); d. Witte (2008);

Table 7-4 shows costs of the current and future forest biomass in Canada. These costs are the gate cost for Canadian wood pellet plants. In Canada, wood pellets are currently only produced from the mill wood residues. Most bark is used for landscaping because of its high ash content. The harvest residues are still hardly used because of the high collection and transportation costs. The high cost associated with the production of wood chips from MPB infested trees still limits their direct use as the feedstock for pellets, but should be explored in the future.

Table 7-4 Estimated current and future costs of forest biomass in Canada \$/t

Items	Current	Future
Mill Wood Residues	13	20
Wood Bark Piles	0-2	5
Wood Harvest Residues (50-100 km transport distance)	25-46	20-37
MPB infested Wood Chips	65	65

Source: Peng et al. (2010)

A production plant can be divided into two types of facilities. The first type includes all production equipment to convert raw materials into products. The capital costs for those facilities are normally referred to as the inside battery limits (ISBL). The second type of facilities includes general utilities (such as instrument, utility air and nitrogen, water, etc.), administrative buildings, steam generation facilities, cooling systems, electrical distribution systems, etc. The capital costs for the second type facilities are called the outside battery limits (OSBL).

The operating cost is represented by the total cash cost of production which is the out-of-pocket expense incurred to the owner before working capital, capital investment depreciation, and return on total capital investment are included. The total cash cost can be broken down into variable costs and fixed costs. Fixed costs are business expenses that are not dependent on the production rate [Jake and Price 2003], while variable costs are the sum of marginal costs that change with an increase or decrease in the production rate [Garrison et al. 2009]. Normally, fixed costs include labors, maintenance, direct overhead costs of a plant at its full capacity (management cost), general plant overhead (administration, logistics, advertisement costs etc), insurance, and property tax. Variable costs include raw materials and utilities. Return on total capital investment (ROI) is defined as the profit of investment in the project, which is equivalent to the interest of investment. The cash cost plus ROI gives the total production cost.

For a wood pellet plant of 80, 000 t annum^{-1} in capacity, the total plant capital cost is around $9.08 million, including $5.51 million ISBL cost and $ 3.57 million OSBL cost [Peng et al. 2006]. The detailed wood pellet costs for current operations are summarized in Table 7-5. The following assumptions were used:

- All facilities are constructed in the designated year.
- The operating time is 8,000 hours per year.

- 0.23 BDt wood residues (at a price of $ 13 per ton) are required as the fuel for the drying operation for producing one ton pellets [BW McCloy & Associates Inc. 2005].

- Variable costs: 1.1 BDt wood residues (price is at $ 13 per ton) are required as the feedstock for each tonne of pellets produced. 300 kWh of electricity (price is at $40/MWh) is required and an additional cost of $5 is allocated for the consumption of other utilities such as diesel fuel and lubricants etc. for producing one ton pellets. For the case analyzed, the cost is $33.33 per ton.

- Fixed costs: Fourteen full time workers at a salary and benefit of $40,000 year^{-1} person^{-1}, two foremen at a cost of $45,000 year^{-1} person^{-1}, and one supervisor at $55,000 year^{-1} are required. Maintenance is 5% of the inside battery limits capital cost. Direct overhead is 40% of labor costs. General plant overhead is 50% of labor and maintenance costs. Insurance is at 0.5% of total plant capital cost. Property tax is at 1.0% of total plant capital cost. For this case, the fixed cost is $22.83 per ton.

- Total cash cost: The cash cost, which equals fixed cost plus variable cost, is $56.16 per ton.

- Depreciation costs of capital investment are normally considered as 10% inside battery limits cost plus 5% outside battery limits cost. For this case, the cost is $9.11 per ton.

- Cost of production equals the total cash cost plus depreciation cost. For this case, the cost is $65.28 per ton.

- ROI: Normally the return on total capital investment is 10%. For this case, the cost is $11.34 per ton.

- Cost of production plus ROI: For this case, the cost is $76.62 per ton.

Table 7-5 Cost break-down for Canadian wood pellets

	Items	Units	
1	**Plant start-up**		1Q 2012
2	**Analysis Date**		1Q 2012
3	**Location**		Prince George
4	**Feedstock (Moisture content 40%wt)**	kt annum^{-1}	149
4.1	Raw material (Moisture content 40%wt)	kt annum^{-1}	123
4.2	Fuel (Moisture content 40%wt)	kt annum^{-1}	26
5	**Production Capacity**	kt annum^{-1}	80
6	**Capital Cost**		
6.1	**Inside Battery Limits**	M$	5.51
	Dryer	M$	3.67
	Hammer Mill	M$	0.55
	Pellet Machine	M$	0.92
	Cooler	M$	0.37
6.2	**Outside Battery Limits**	M$	3.56
	Storage, Conveyors, Separators	M$	1.33
	Peripheral Equipment	M$	0.66
	Buildings	M$	1.57
	Total Plant Capital	M$	9.07
7	**Production Cost**		
7.1	**Variable Costs**	$ t^{-1}	33.33
	Raw Materials	$ t^{-1}	14.30
	Utilities	$ t^{-1}	19.03
7.2	**Fixed Costs**	$ t^{-1}	22.83
	Worker	$ t^{-1}	7.00
	Foremen	$ t^{-1}	1.13
	Supervisor	$ t^{-1}	0.69
	Maintenance	$ t^{-1}	3.44
	Direct Overhead	$ t^{-1}	3.66
	General Plant Overhead	$ t^{-1}	5.22
	Insurance, Property Tax	$ t^{-1}	1.70
	Total Cash Cost	$ t^{-1}	56.16
7.3	**Depreciation,10%ISBL+5%OSBL**	$ t^{-1}	9.11
	Cost of Production	$ t^{-1}	65.28
7.4	**Return on total capital investment (10%)**	$ t^{-1}	11.34
	Cost of Production + ROI	$ t^{-1}	76.62

Source: capital costs from Zakrisson (2002) at an exchange rate of 1€=1.5090$

For plants of different sizes using various types of raw materials in Canada, wood pellets costs are estimated and summarized in Table 7-6. The cost of Canadian wood pellet with

an assumed 10% return on total capital investment ranges from $65 t^{-1} ($3.5 GJ^{-1}) to $115 t^{-1} ($6.2 GJ^{-1}), depending on the mill wood residues cost and the plant size. Costs for producing wood pellets using wood bark, wood harvest residues and MPB infested wood are also estimated with the results shown in Table 7-5. Although the wood bark piles and wood harvest residues are currently not used in BC wood pellet plants, the lower cost bark piles and the abundant harvest residues may be used as the market expands in the future. When the MPB infested trees are used as raw materials, the pellet production cost for a large pellet plant is about $132 t^{-1} ($7.1$ GJ^{-1}), which is more expensive than pellets from other wood residues.

Table 7-6 Estimated costs of Canadian wood pellet at 10% ROI ($ t^{-1}) for different capacities

Raw material costs	24,000 t annum^{-1}		80,000 t annum^{-1}		180,000 t annum^{-1}	
	CAD$/t	CAD$/GJ	CAD$/t	CAD$/GJ	CAD$/t	CAD$/GJ
Mill Residues, $ BDt^{-1}						
13	114.6	6.2	76.6	4.1	64.7	3.5
20	123.9	6.7	85.9	4.6	74.0	4.0
Bark Piles, $ BDt^{-1}						
0-2	97.3-100.0	5.0-5.1	59.3-62.0	3.0-3.2	47.4-50.1	2.4-2.6
5	104.0	5.3	66.0	3.4	54.1	2.8
Harvest Residues (50-100 km transport distance), $ BDt^{-1}						
25-46	130.6-158.5	7.0-8.5	92.6-120.5	5.0-6.5	80.7-108.6	4.4-5.9
20-37	123.9-146.5	6.7-7.9	85.9-108.5	4.6-5.9	74.0-96.6	4.0-5.2
MPB infested woods, $/BDt						
65					132.2	7.1

Since Canadian wood pellets are mainly manufactured in the Prince George region, with majority of pellets exported to Netherlands and Sweden. Table 7-7 shows the estimated transportation cost of wood pellets from Prince George to Europe, as reported by Hoque (2006). For Canadian wood pellets to reach Europe, pellets need to be transported by train from Prince George to Vancouver port, and then loaded to ocean vessels and transported to Netherlands or Sweden. The total transportation cost of wood pellets from Prince George

to Netherlands is about \$95 t^{-1} (\$5.1 GJ^{-1}), and the total transportation cost of bark pellets from Prince George to Netherlands is about \$89 t^{-1} (\$4.5 GJ^{-1}), which slightly lower than white pellets because of their higher energy content.

Table 7-7 Typical bulk wood pellet delivery costs from Prince George to Europe

Items	Unit	Softwood pellets		Bark pellets	
		Netherlands	Sweden	Netherlands	Sweden
From Prince George to Vancouver Port	\$ t^{-1}	22.9	22.9	21.4	21.4
Transfer, intermediate storage, and loading	\$ t^{-1}	11.2	11.2	10.4	10.4
From Vancouver Port to import Port by Sea	\$ t^{-1}	48.0	55.4	44.8	51.7
Transfer, handling and transportation to customers	\$ t^{-1}	12.9	12.9	12.1	12.1
Total	\$ t^{-1}	95.0	102.5	88.7	95.6
	\$ GJ^{-1}	5.1	5.5	4.5	4.9

Source: Hoque (2006) at an exchange rate 1US\$=1.0660CND\$.

7.4 Production Costs of Canadian Torrefied Wood Pellets

The capital cost of a torrefied wood pellet plant depends on the torrefaction process to be used. Table 7-8 compares the total capital investment of a 180 kt annum^{-1} conventional pellet plant and a 138 kt annum^{-1} torrefied pellet plant using three different types of torrefaction reactors in Canada, including dryer, hammer mill, torrefaction reactors, pellet machine, cooler, storage, conveyors, separators, peripheral equipment, and buildings. It is assumed that the same dryer, hammer mill will be used to process the same amount of raw biomass feedstock, with 30% weight loss during torrefaction, a conventional plant producing 180 kt pellets per year will be now comparable to a torrefied pellet plant producing 138 kt (70% of 180 kt) torrefied pellets per year. One can also compare the conventional plant and the torrefied pellet plant at the same production capacity where the grinders and dryers will be larger in the torrefied pellet plant. The total capital investment data for a 180 kt annum^{-1} conventional pellet plant were obtained from Witte (2008), and the capital cost for each item was estimated based on a 80 kt annum^{-1} wood pellet plant [Urbanowski 2005] using the 0.8th power scaling relationship. The capital

investment costs for three torrefaction reactors of 138 kt annum^{-1} in capacity were estimated based on a 227 kt annum^{-1} torrefied wood plant data [Bergman, Zwart, and Kiel 2005] applying a 0.8th power scaling relationship between the capital cost and the capacity (Ulrich 1984). The outside battery limits cost of a 138 kt a annum^{-1} torrefied pellet plant was obtained based on the data from Bergman Zwart and Kiel (2005) and Bergman (2005) by applying a 0.8th power scaling relationship, and the capital cost for each other item was estimated based on a 56 kt annum^{-1} torrefied wood pellet plant [Bergman 2005], again applying the 0.8th power scaling relationship. The results show that the specific capital investment for building a torrefied pellet plant of 138 kt annum^{-1} capacity in Canada ranges from \$156 to \$364 per t aannum^{-1} for three different types of torrefaction reactors.

Table 7-8 Capital investment of a 180 kt annum^{-1} conventional pellet and a 138 kt annum^{-1} torrefied pellet plant with three different torrefaction reactors in Canada

	Items	Capital Investment, M\$				Life in Years
		180 kt annum^{-1}	138 kt annum^{-1} torrefied pellets			
		Conventional pellets	Moving Bed	Rotating Drum	Screw Reactor	
1	**In Side Battery Limits**	**11.02**	**15.16**	**23.05**	**39.25**	
1.1	Dryer	7.34	7.34	7.34	7.34	10
1.2	Hammer Mill	1.10	1.10	1.10	1.10	10
1.3	Torrefaction Reactors	0.00	4.65	12.54	28.74	10
1.4	Pellet Machine	1.84	1.52	1.52	1.52	10
1.5	Cooler	0.74	0.56	0.56	0.56	10
2	**Out Side Battery Limits**	**7.13**	**6.39**	**9.11**	**11.00**	
2.1	Storage, Conveyors, Separators	2.67	2.39	3.41	4.11	20
2.2	Peripheral Equipment	1.32	1.19	1.69	2.04	20
2.3	Buildings	3.14	2.82	4.01	4.85	20
	Total	**18.15**	**21.55**	**32.16**	**50.25**	
	Specific Investment (\$ t^{-1} annum^{-1})	101	156	233	364	

Source: Witte (2008); Bergman (2005); Urbanowski (2005); Bergman, Zwart, and Kiel (2005); Conversion: 1€=1.5090\$.

It is seen that the moving bed torrefaction process has the lowest capital investment,

because of a small reactor volume and its simple design. Therefore, the moving bed torrefaction process is selected for the economical analysis of the Canadian torrefied wood pellet plant. For a torrefied pellet plant of 138 kt annum^{-1} in capacity using the moving bed torrefaction process, the total plant capital cost is around $21.55 M, including $15.16M inside battery limits cost and $6.39 M outside battery limits cost. The total production cost of Canadian torrefied pellets used in this study, including the variable costs, fixed costs, depreciation, and the return on total capital investment, are estimated based on following assumptions:

- All facilities are constructed in the designated year.

- The plant is operated 8,000 hours per year.

- The torrefied pellets process was thermally balanced by combusting torrefaction gas vapours to provide required heat for drying and torrefaction.

- Raw material: For each metric tonne pellet produced, 1.43 BDt of wood residues (40% moisture content) are required as the feedstock, which takes into consideration of 30% torrefaction weight loss and 10% general processing loss.

- Utilities: 100 kWh of electricity is required for producing one tonne pellets. Electricity price is at $40/MWh. An additional cost of $6 per ton pellets is allocated to the consumption of other utilities such as the diesel fuel and lubricants etc.

- Labours: Fourteen full time workers at a salary and benefit of $40,000 year^{-1} person^{-1}, two foremen at a cost of $45,000 year^{-1} person^{-1} and one supervisor at $55,000 year^{-1} are assumed to be needed to operate a 138 kt annum^{-1} plant.

- Maintenance: 5% of the inside battery limits capital cost.

- Direct overhead: 45% of labour costs, which are management costs.

- General plant overhead: 50% of labour and maintenance costs, which also include administration, logistics and advertisement costs, etc.

- Insurance and property tax: insurance is 0.5% of total plant capital cost and property tax is at 1.0% of total plant capital cost.

The detailed break-down wood pellet costs are estimated based on the above assumptions with the results   summarized in Table 7-9.

Table 7-9 Cost break-down of Canadian torrefied wood pellets

	Items	**Units**	
1	**Analysis Date**		1Q2012
2	**Location**		Prince George
3	**Feedstock (Moisture content 40%wt)**	kt annum^{-1}	277
4	**Production Capacity**	kt annum^{-1}	138
5	**Capital Investment**		
	ISBL	M$	15.16
	OSBL	M$	6.39
	Total Plant Capital	M$	21.55
6	**Production Cost**		
6.1	**Variable Costs**	$ t^{-1}	28.27
	Raw Materials	$ t^{-1}	18.59
	Utilities	$ t^{-1}	9.68
6.2	**Fixed costs**	$ t^{-1}	19.84
	Worker	$ t^{-1}	4.06
	Forman	$ t^{-1}	0.65
	Supervisor	$ t^{-1}	0.40
	Maintenance	$ t^{-1}	5.49
	Direct Overhead	$ t^{-1}	2.12
	General Plant Overhead	$ t^{-1}	4.78
	Insurance, Property Tax	$ t^{-1}	2.34
	Total Cash Cost	$ t^{-1}	48.11
6.3	**Depreciation, 10%ISBL+5%OSBL**	$ t^{-1}	13.30
	Cost of Production	$ t^{-1}	61.41
6.4	**Return on total capital investment (10%)**	$ t^{-1}	15.62
	Cost of Production + ROI	$ t^{-1}	77.03

Costs for torrefied pellets from a 138 kt annum^{-1} torrefied wood pellet plant using mill wood residues, wood bark piles, wood harvest residues, and MPB infested wood as the feedstock are estimated with the results shown in Table 7-10. The cost of Canadian torrefied pellets with a 10% ROI ranges from $77.03t^{-1} ($3.40 GJ^{-1}) to $87.04 t^{-1} ($3.84 GJ^{-1}) using mill wood residues, $58.44 t^{-1} ($2.39 GJ^{-1}) to $65.59 t^{-1} ($2.68 GJ^{-1}) using

wood bark, \$87.04 t^{-1} (\$3.84 GJ^{-1}) to \$124.22 t^{-1} (\$5.48 GJ^{-1}) using wood harvest residues, and \$151.39 t^{-1} (\$6.68 GJ^{-1}) using MPB infested trees as the feedstock.

Table 7-10 Total costs of Canadian torrefied wood pellets

	Feedstock and price	\$ t^{-1}	\$ GJ^{-1}
1	**Mill Wood Residues, \$ BDt^{-1}**		
	13	77.03	3.40
	20	87.04	3.84
2	**Wood Bark Piles, \$ BDt^{-1}**		
	0-2	58.44-61.30	2.39-2.50
	5	65.59	2.68
3	**Wood Harvest Residues (50-100 km transportation distance), \$ BDt^{-1}**		
	25-46	94.19-124.22	4.16-5.48
	20-37	87.04-111.35	3.84-4.92
4	**MPB infested woods, \$ BDt^{-1}**		
	65	151.39	6.68

Based on the bulk density of control wood pellets, torrefied wood pellets and torrefied bark pellets, the cost for transporting Canadian torrefied wood pellets from Prince George to Europe was estimated, with the results shown in Table 7-11.

Table 7-11 Torrefied wood pellet transportation and delivery costs from Prince George to Europe

		Softwood Pellets		Bark Pellets	
Items	**Unit**	**Netherlands**	**Sweden**	**Netherlands**	**Sweden**
From Prince George to Vancouver Port	\$ t^{-1}	22.92	22.92	23.95	23.95
Transfer, intermediate storage, and loading	\$ t^{-1}	11.19	11.19	11.69	11.69
From Vancouver Port to import Port by Sea	\$ t^{-1}	47.97	55.43	50.12	57.91
Transfer, handling and transportation to customers	\$ t^{-1}	12.92	12.92	13.50	13.50
Total	**\$ t^{-1}**	95.00	102.46	99.25	107.05
	\$ GJ^{-1}	4.19	4.52	4.05	4.37

Note: Exchange rate 1US\$=1.0660\$.

Based on a torrefied pellet plant of 138 kt annum^{-1} in capacity with a wood residues price of \$13 per ton (see Table 7-9), a sensitivity analysis of production cost plus ROI (10%) on the raw material price, the total capital investment and the production rate was conducted

with the results shown in Table 7-12.   It can be seen that the production rate and the total capital investment have the most significant influence on the cost plus ROI, while the raw material price had a limited impact on the cost plus ROI.

Table 7-12 Sensitivity analysis of production cost plus ROI (10%)

	Cost of Production Plus ROI (10%), $ per ton
Base case	**77.03**
Raw material price increase 30%	82.61
Raw material price increase 50%	86.33
Raw material price increase 100%	95.62
Raw material price decrease 30%	71.45
Raw material price decrease 50%	67.74
Total capital investment increase 30%	88.88
Total capital investment decrease 30%	65.18
Production rate increase 30%	65.78
Production rate decrease 30%	97.93

7.5 Comparisons between Conventional Wood Pellets and Torrefied Wood Pellets

Table 7-13 compares the properties and costs of conventional and torrefied wood pellets. Compared with conventional wood pellets, torrefied wood pellets can enhance almost 22% of the energy density, which can reduce the cost for long distance transportation. For Canadian torrefied wood pellets, the production cost per GJ will be 3% lower (for a mill wood residues price of $13 t^{-1}), the transportation cost from Prince George to Netherlands will be 18 % lower, leading to a total 12% saving in cost. Therefore, torrefied wood pellets are a better option than conventional wood pellets exported from Canada to Europe.

Table 7-13 Comparisons between conventional and torrefied wood pellets in Canada

	Items	Unit	Conventional Wood Pellets	Torrefied Wood Pellets
1	**Pellet Properties**			
1.1	**Bulk Density**	kg m^{-3}	700	700
1.2	**High Heating Value as received**	MJ kg^{-1}	18.55	22.65
1.3	**Energy Density**	GJ m^{-3}	12.99	15.86
1.4	**Moisture Content**	%wt	7	0.25
2	**Feedstock (moisture content 40%wt)**	kt annum^{-1}	335	277
2.1	**Raw material (moisture content 40%wt)**	kt annum^{-1}	277	277
2.2	**Fuel (moisture content 40%wt)**	kt annum^{-1}	58	0
3	**Capacity**	kt annum^{-1}	180	138
4	**Total Capital Investment**	M\$	18.1	22.1
	Specific Investment	\$ t^{-1}	101	175
5	**Total Production Costs**			
5.1	**Mill Wood Residues, \$13 t^{-1}**	\$ t^{-1}	64.72	77.03
		\$ GJ^{-1}	3.50	3.40
5.2	**MPB infested Trees, \$65 t^{-1}**	\$ t^{-1}	132.22	151.39
		\$ GJ^{-1}	7.10	6.68
6	**Total Transportation Costs to Netherlands**	\$ t^{-1}	95.00	95.00
		\$ GJ^{-1}	5.10	4.19
7	**Total Costs**			
7.1	**Mill Wood Residues, \$13 t^{-1}**	\$ t^{-1}	159.72	172.03
		\$ GJ^{-1}	8.60	7.59
7.2	**MPB infested Trees, \$65 t^{-1}**	\$ t^{-1}	227.22	246.39
		\$ GJ^{-1}	12.20	10.87

7.6 Summary

A simplified economical analysis showed that it costs more to product torrefied pellets in Canada, but torrefied wood pellets will cost less in transportation. Therefore the profitability can be improved for torrefied wood pellets produced in Canada and or exported to the European market, compared to the conventional wood pellets.

CHAPTER 8 CONCLUSIONS AND RECOMMENDATIONS FOR FUTURE WORK

8.1 Overall Conclusions

Wood pellets as a renewable energy from densified wood residues have very low greenhouse gas emissions compared to coal and other solids fossil fuels. The wood pellet market has grown rapidly in Europe since 1990s, contributed mainly by the worldwide rising fossil fuel prices and accompanying high fossil fuel taxes in Europe and incentives to renewable fuels. Wood pellets hold an extremely promising future, and the future market may shift to North America. In comparison with conventional pellets, torrefied pellets can be much higher in the energy density, which will lower transportation cost significantly for long distance transportation. Therefore, the torrefaction process may be suitable for Canadian wood pellets exported to international market.

Torrefaction is a thermal treatment without air or oxygen in the temperature range of 473-573 K. Based on a review on the pyrolysis kinetics of three chemical components (cellulose, hemicelluloses, and lignin) and wood at low temperatures of relevance to torrefaction conditions, a series of TG experiments have been carried out to study the intrinsic torrefaction kinetics of major chemical components and BC softwoods. The weight loss during BC softwood torrefaction was found to be mainly associated with the decomposition of hemicelluloses, although there was also certain degree of decomposition of cellulose and lignin. The weight loss of the BC softwoods during torrefaction could be approximately estimated from the chemical composition of wood species and the weight loss data for torrefaction of pure cellulose, hemicelluloses, and lignin, respectively. Based on the fitting of the TG curves of BC softwoods and three

chemical components, a two-component and one-step first order reaction kinetic model was developed, which gave a good agreement with data over short residence time, and can be used to guide the design and optimization of torrefaction reactors over the weight loss range of 0 to 40% at the temperature range of 533-573 K, which covers the typical range of industrially relevant operations.

Torrefaction of BC softwoods, including pine fir spruce SPF (a mixture of spruce, pine and fir) and pine bark, has been conducted in a bench-scale tubular fixed bed unit at the temperatures of 240-340 °C. A MTI press machine was used for the densification tests in order to identify the suitable conditions for making torrefied pellets. Results showed that the mass loss of BC softwoods mainly depended on the torrefaction temperature and the residence time. The heating value of torrefied softwood had a close relationship with the mass loss, increasing with increasing the severity of torrefaction. Torrefied softwoods were more difficult to be compressed into strong torrefied pellets using the same conditions as used for making the control (regular, untreated, non-torrefied, conventional) pellets. Increasing the die temperature and adding moisture into torrefied particles can improve the quality of torrefied pellets. The moisture content and density of torrefied pellets were lower than control pellets. More energy was needed for compacting torrefied softwood particles into torrefied pellets. Deep torrefaction increased the heating value and the hydrophobicity of torrefied pellets, but decreased the energy yield and the hardness of torrefied pellets. Considering the quality of torrefied pellets, the optimal torrefaction conditions were found to be around 30% mass loss, which gave a 20% increase in pellet heating value. The suitable densification conditions for torrefied softwoods corresponded to a die temperature of about 230 °C, or over 110 °C for torrefied softwood particles conditioned to 10% moisture content.

The particle size effect on torrefaction of pine particles and formation of torrefied pellets has been studied in both the TGA and the tubular fixed bed reactor. The fixed bed reactor was also used to produce torrefied samples for a single-die press unit for the densification test. Both the TGA and fixed bed reactor torrefaction test results showed that the torrefaction rate was affected by the particle size, especially at high temperatures. Although the temperature gradient inside particles of smaller than 1 mm is very small during torrefaction, the internal diffusion of generated vapours inside particles imposes an impact on the global torrefaction reaction rate. The hard core particle model with a first order torrefaction reaction can predict the reaction data reasonably well, with the data-fitted effective vapour diffusivity coefficient as the input parameter. The densification tests showed that more energy was required to make pellets from larger torrefied particles, while the water uptake and Meyer hardness tests of pellets revealed that good quality torrefied pellets could be obtained from fine torrefied sawdust particles.

Oxidative torrefaction of sawdust with a carrier gas containing 3% to 6% O_2 was investigated in a TG and a fluidized bed reactor, with the properties of the torrefied sawdust and pellets compared with those prepared from regular torrefaction without any O_2. It is found that the oxidative torrefaction kinetics can be well modeled by two parallel reactions, one for thermal degradation and the other one for biomass oxidation. The oxidative torrefaction process produced torrefied sawdust and pellets of similar properties as to normally torrefied sawdust and corresponding pellets, especially on the density, energy consumption for pelletization, higher heating value and energy yield. For moisture adsorption and hardness of the torrefied pellets, the oxidative torrefaction process showed slightly poor but negligible performance, which may likely be related to the structural change caused by the oxidation. Therefore, from the process integration and cost point of view, it is feasible to use oxygen laden combustion flue gases as the carrier gas for torrefaction of biomass. Compared to the control pellets, torrefied pellets made at the

same die temperature have a lower density and hardness although more energy is required to compress torrefied sawdust into pellets. However, torrefied sawdust can be made into dense and strong pellets of high hydrophobicity at a higher die temperature than normally used in the production of regular control pellets.

Compared with conventional wood pellets, torrefied wood pellets can enhance almost 22% of the energy density, which can reduce the cost for long distance transportation. For Canadian torrefied wood pellets, the production cost per GJ will be 4% higher (for a mill wood residues price of \$13/t), but the transportation cost from Prince George to Netherlands will be 18 % lower, leading to a total 10% saving in the total cost. Therefore, torrefied wood pellets are a better option than conventional wood pellets exported from Canada to Europe. Torrefied wood pellets can reduce the transportation cost of wood pellets, especially suitable for pellets produced in Canada and exported to Europe with a long transportation distance. The Canadian torrefied wood pellets can improve the profitability of Canadian wood pellets exported to the European market, compared to the conventional wood pellets.

8.2 Recommendations for Future Work

The current study investigated the torrefaction of BC softwoods in order to develop a torrefaction and densification process for the production of high quality torrefied wood pellets. Much work still needs to be done in this topic. The following research subjects are recommended for future works based on this study.

- To identify the suitable operating conditions of the torrefaction of sawdust particles of wide size distributions in fluidized bed reactors.

- To optimize the conditions for the densification of torrefied sawdust to torrefied pellets, including die temperature, pressure or compression force, particle size, and the moisture

content in a continuous densification machine.

- To simulate the combined torrefaction and pelletization process by using the torrefaction kinetics of BC softwoods, reactor configurations and the suitable densification conditions.

- To improve the cost analysis using more up-to-date values for the capital and operating cost to the torrefaction process and the cost of the raw materials.

REFERENCES

Adapa, P. K., Schoenau, G. J., Tabil, L. G., Arinze, E. A., Singh, A., Dalai, A. K., 2007. Customized and value-added high quality alfalfa products – a new concept. Agricultural Engineering International: the CIGR Ejournal, IX(June), 1-28.

Akita, K., Kase, M., 1967. Determination of kinetics parameters for pyrolysis of cellulose and cellulose treated with ammonium phosphate by differential thermal analysis and thermal gravimetric analysis. Journal of Applied Polymer Science, 5(part A-1), 833-848.

Avat, F., 1993. Contribution a letude des traitements thermiques du bois (200-300ºC): transformations chimiques et caracterisations physico-chimiques. Saint-Etienne, Ecole nationale Superieure des Mines de Saint-Etienne, 237.

Bergman, P. C. A., 2005. Combined torrefaction and pelletisation the TOP process. Energy Research Centre of the Netherlands report, ECN-C--05-073.

Bergman, P. C. A., Boersma, A. R., Zeart, R. W. R., Kiel, J. H. A., 2005. Torrefaction for biomass co-firing in existing coal-fired power stations. Energy Research Centre of the Netherlands report, ECN-C--05-013. Netherlands.

Bergman, P. C. A., Kiel, J. H. A., 2005. Torrefaction for biomass upgrading. Energy Research Centre of the Netherlands report, ECN-RX--05-180.

Bergman, P. C. A., Prins, M. J., 2005. Torrefaction for entrained-flow gasification of biomass. Energy Research Centre of the Netherlands report, ECN-C--05-013.

Bilbao, R., Mastral, J. F., Aldea, M. E., Ceamanos, J., 1997. The influence of the percentage of oxygen in the atmosphere on the thermal decomposition of lignoceellulosic materials. Journal of Analytical and Applied Pyrolysis, 42, 189-202.

Bilbao, R., Millera, A., Arauzo, J., 1989. Kinetics of weight loss by thermal decomposition of xylan and lignin. Influence of experimental conditions.

Thermochimica Acta, 143, 137-148.

Bioenergy, 2000. A new process for torrefied wood manufacturing. General bioenergy, Vol. 2, No. 4.

Biologie et Multimédia -Université Pierre et Marie-Curie, 2002.

Bird, R.B., Stewart, W. E., Lightfoot, E.N., 2002. Transport Phenomena. John Wiley & Sons, Inc, New York.

Bissen, D., July 13, 2009. Biomass densification document of evaluation. Zachry Engineering Corporation, Minneapolis, MN, USA.

Blasi, C. D., 2008. Modeling chemical and physical processes of wood and biomass pyrolysis. Energy and Combustion Science, 34, 47-90.

Blasi, C. D., Branca, C., 2001. Kinetics of primary product formation from wood pyrolysis. Ind Eng Chem Res, 40, 5547-5556.

Blasi, C. D., Signorelli, G., Russo, C. D., Rea, G., 1999. Product distribution from pyrolysis of wood and agricultural residues. Ind Eng Chem Res, 38, 2216-2224.

Blasi, C. D., Lanzetta, M., 1997. Intrinsic kinetics of isothermal xylan degradation in inert atmosphere. J. Anal. Appl. Pyrolysis, 40-41, 287-303.

Boyd, T., de Vries, D., Kempthorne, H., Wearing, J., Wolff, I., 2011. Mass & Energy Balance for Torrefied Pellet Production. In: Biomass Pelletization Workshop, May 17-18. Canada: Vancouver.

Bradbury, A. G. W., Sakai, Y., Shafizadeh, F., 1979. A kinetic model for pyrolysis of cellulose. J. Appl. Poly. Sci, 23, 3271-3280.

Bradley, D. 2008. Future Trends in Biomass Supply, Policy, Markets. 2008 Bioenergy Conference &Exhibition, June 3-5, 2008. Canada: Prince George.

Branca, C., Blasi, C. D., 2003. Kinetics of the isothermal degradation of wood in the temperature range 528-708 K. J Anal Appl Pyrol, 67, 207-219.

Bridgeman, T.G., Jones, J.M., Shield, I., Williams, P.T., 2008. Torrefaction of reed canary grass, wheat straw and willow to enhance solid fuel qualities and combustion

properties. Fuel, 87, 844–856.

Broido, A., Kilzer, F. J., 1965. Speculations on the nature of cellulose pyrolysis. Pyrodynamics, 2, 151-163.

Broido, A., Winstein, M., 1971. Proceedings of the 3rd International Conference on Thermal Analysis. Ed. H. G. Wiedermann.

BW McCloy & Associates Inc., 2005. Estimated Production, Consumption and Surplus Mill Wood Residues in Canada-2004. A National Report.

Chan, W. R., Kelbon, M., Krieger, B. B., 1985. Modeling and experimental verification of physical and chemical processes during pyrolysis of large biomass particle. Fuel, 64, 1505-1513.

Chen, G. Y., Fang, M.X., Andries, J., Luo, Z. Y., Spliethoff, H., Cen, K. F., 2003. Kinetics study on biomass pyrolysis for fuel gas production. Journal of Zhejiang University Science, 4, 441-447.

Chen, G. T., 1990. Chemical Reaction Engineering. ISBN 7-5025-0785-X/G, Chemical Industry Press, Beijing, China. (Chinese)

Chen, W. H., Cheng, W. Y., Lu, K. M., Huang, Y. P., 2011. An evaluation on improvement of pulverized biomass property for solid fuel through torrefaction. Applied Energy, 88(11), 3636-3644.

Chen, W. H., Hsu, H. C., Lu, K. M., Lee, W. J., Lin, T. C., 2011. Thermal pretreatment of wood (Lauan) block by torrefaction and its influence on the properties of the biomass. Energy, 36(5), 3012-3021.

Chen, W. H., Kuo, P. C., 2011a. Torrefaction and co-torrefaction characterization of hemicellulose, cellulose and lignin as well as torrefaction of some basic constituents in biomass. Energy, 36, 803-811.

Chen, W. H., Kuo, P. C., 2011b. Isothermal torrefaction kinetics of hemicellulose, cellulose, lignin and xylan using thermogravimetric analysis. Energy, 36, 6451-6460.

Chew, J. J., Doshi, V., 2011. Recent advances in biomass pretreatment – Torrefaction fundamentals and technology. Renewable and Sustainable Energy Reviews, 15, 4212-4222.

Couhert, C., Salvador, S., Commandre, J-M., 2009. Impact of torrefaction on syngas production from wood. Fuel, 88, 2286-2290.

Deng, J., Wang, G. J., Kuang, J. H., Zhang, Y. L., Luo, Y. H., 2009. Pretreatment of agricultural residues for co-gasificaion via torrefaction. Journal of Analytical and Applied Pyrolysis, 86, 331-337.

Delta Research Corportation, 2006. Study of torrefaction as pretreatment method for biomass.

Doyle, J., Walker, J.C.F., 1985. Indentation hardness of wood. Wood and Fiber Science, 17(3), 369-376.

Energy Information Administration Official Energy Statistics from the U.S. Government, 2009. Short-Term Energy Outlook. http://www.eia.doe.gov, Accessed Feb 12, 2009.

European Biomass Industry Association, 2012. Pyrolysis. http://www.eubia.org/211.0.html, Accessed April 15, 2012.

Fairbridge, Ross, R. A., Sood, S. P., 1978. A kinetic and surface study of the thermal decomposition of cellulose powder in inert and oxidation atmospheres. Journal of Applied Polymer Science, 22, 497-510.

Felfli, F.F., Luengo, C.A., Suárez, J.A., Beatón, P.A., 2005. Wood briquette torrefaction. Energy for Sustainable Development, 9, 19–22.

Fogler, H. S., 2006. Elements of Chemical Reaction Engineering. ISBN 7-5025-9256-2, Pearson Education Asia Ltd and Chemical Industry Press.

Font, R., Marcilla, A., Verdu, E., Devesa, J., 1990. Kinetics of the pyrolysis of almond shells and almond shells impregnated with CoCl2 in a fluidized bed reactor and in a pyroprobe 100. Ind Eng Chem Res, 29, 1846-1855.

Garcı´a-Iban˜ez, P., Sa´nchez, M., Cabanillas, A., 2006. Thermogravimetric analysis of olive-oil residue in air atmosphere. Fuel Processing Technology, 87, 103-107.

Garrison, R. H., Noreen, E. W., Brewer, P. C. 2009. Managerial Accounting (13e ed.). McGraw-Hill Irwin, ISBN 978-0-07-337961-6.

Gaur, S., Thomas, B., 1998. Thermal data for natural and synthetic fuels. Marcel Dekker, Inc., New York.

Gil, M.V., Oulego, P., Casal, M.D., Pevida, C., Pis, J.J., Rubiera, F., 2010. Mechanical durability and combustion characteristics of pellets from biomass blends. Bioresource Technology, 101(22), 8859-8867.

Gilbert, P., Ryu, C., Sharifi, V., Swithenbank, J., 2009. Effect of process parameters on pelletization of herbaceous crops. Fuel, 88(8),1491-1497.

Golova, O., 1975. Chemical effects of heat on cellulose. Russian Chemical Reviews, 44, 687-697.

Gorton, W. C., Knight, J.A., 1984. Oil from biomass entrained-flow pyrolysis. Biotechnol. Bioeng. Symp., 14, 15-20.

Gronli, M.G., . A Theorical and Experimental Study of the Thermal Degradation of Biomass Pyrolysis, Wood, Tar, Char. Ph.D. Thesis, Trondheim University, Trondheim, 1996.

Gronli, M. G., Blasi, C. D., 2002. Thermogravimetric analysis and devolatilization kinetics of wood. Ind Eng Chem Res, 41, 4201-4208.

Gronli, L.H.S.E.A., 1992. Thermogravimetric analysis of four scandinavian wood species under non isothermal conditions. Nordic Seminar on biomass combustion, Trondheim.

Hakkila, P., 1978. Harvesting small-sized wood for fuel. Folia Forestalia 342, The Finnish Forest Research Institute, Helsinki.

Halpern, Y., Patal, S., 1969. Pyrolytic reactions of carbohydrates, Part VII, Simultaneous DTA-TGA study of the thermal decomposition of cellulose in vacuo. Israel J.

Chem., 7, 685-691.

Hamburg, Topell on torrefaction, Workshop IEA Bioenergy Task 32 – New Biomass Co-firing Concepts, 2009.

Harrington, J.J., 2002. Hierarchical modelling of softwood hygro-elastic properties. Ph.D. thesis, University of Cantenbury, Christchurch, New Zealand.

Haryanto, A., Hong, K. S., 2011. Modeling and simulation of an oxy-fuel combustion boiler system with flue gas recirculation. Computers & Chemical Engineering, 35(1), 25-40.

Hirata, T., 1974. Bull. Gov. For. Exp. Sta. Japan, 263, 1-11.

Holley, C. A., 1983. The densification of biomass by roll briquetting. Proceedings of the Institute for Briquetting and Agglomeration(IBA), 18, 95-102.

Honjo, T., Fuchihata, M., Ida, T., Sano, H., 2002. Prospect on new fuel BCDF (Bio-Carbonized-Densified-Fuel): The effect of semi-carbonization. In: Proceedings of the first world conference on Pellets. Sweden: Stockholm.

Hoque, M., Sokhansanj, S., Bi, H.T., Mani, S., Jafari, L., Lim, C.J., Zaini, P., Melin, S., Sowlati, T., and Afzal, M., 2006. Economics of pellet production for export market. Presented in the CSBE/SCGAB 2006 Annual Conference, July 16 - 19, 2006, Canada: Edmonton.

Hu, Y.C., Fan, L.W., Huang, J.L., Hong, R.H., Yu, Z.T., 2005. Theoretical and experimental study on transient measurement of wood thermal properties. Journal of Zhejiang University, 39(11), 1793-1796.

Jake, M., Price, A., 2003. Economics: Principles in Action. Upper Saddle River, New Jersey 07458. ISBN 0-13-063085-3.

James, J., 2009. Using Torrefied Wood as a Coal Replacement for Pellet and Cellulosic Ethanol Production, Agri-Tech Producers, LLC.

Kaliyan, N., Morey, R. V., 2009. Factors affecting strength and durability of densified biomass products. Biomass Bioenergy, 33, 337-359.

Kleinschmidt, C. P., 2011. Overview of international developments in torrefaction. 6800 ET Arnhem, Netherlans.

Koukios, E. G., 1994. Progress in thermochemical, solid-state refining of biofuels-From research to commercialization. In: Advances in Thermochemical Biomass Conversion, Proceedings of the International Conference, 11-15 May 1992. Interlaken, Switzerland. Edited by AV Bridgwater, Blackie Academic & Professional, London, 2: 1678-1693.

Koufopanos, C. A., Maschio, G., Lucchesi, A., 1989. Kinetic Modeling of the Pyrolysis of Biomass and Biomass Components. Can. J. Chem. Eng., 67, 75-84.

Kumar, P. C. F., Sokhansanj, S., 2005. Feedstock Availability and Power Costs Associated with Using BC's Beetle-Infested Pine (final report). Canada: BIOCAP report.

Kutney, Biocarbon: The BC Pellet, BioEnergy Conference & Exhibition, Prince George, June 3 –5, 2008.

Lam, P. S., 2011. Steam explosion of biomass to produce durable wood pellets. PhD thesis, the University of British Columbia, Vancouver, Canada.

Lam, P. S., Sokhansanj, S., Bi, X. T., Lim, C. J., Melin, S., 2011. Energy Input and Quality of Pellets Made from Steam-Exploded Douglas Fir (Pseudotsuga menziesii). Energy & Fuels, 25, 1521–1528.

Lehtikangas, P., 1999. Lagringshandbok för trädbränslen. SLU, ISBN 91-576-5564-2.

Li, H., Liu, X.H., Legros, R., Bi, X. T., Lim, C. J., Sokhansanj, S., 2012. Torrefaction of sawdust in a fluidized bed reactor. Bioresource Thechnology, 103 (1), 453-458.

Li, H., Liu, X. H., Legros, R., Bi, X. T., Lim, C. J., Sokhansanj, C., 2012a. Pelletization of torrefied sawdust and properties of torrefied pellets. Applied Energy, In Press, Corrected Proof, Available online 29 January 2012.

Li, Y., Liu, H., 2000. High Pressure densification of wood residues to form an upgrade fuel. Biomass and Bioenergy. 19(3), 177-186.

Liu, H., Li, Y., 2000. Compacting biomass and municipal solid wastes to form an

upgraded fuel, Final Technical Report, OSTI ID: 837464.

Maa, P. S., Bailie, R. C., 1973. Influence of particle size and environmental conditions on high temperature pyrolysis of cellulosic material –I. Theoretical. Combusion Science and Technology, 7,257-269.

Mani, S., Tabil, L. G, Sokhansanj, S., 2003. An overview of compaction of biomass grinds. Powder Handling & Process, 15(3), 160-168.

Mani, S., Tabil, L.G., Sokhansanj, S., 2004. Grinding performance and physical properties of wheat and barley straws, corn stover and switchgrass. Biomass and Bioenergy, 27 (4), 339–352.

McMullen, J., Fasina, O. O., Wood, C. W., Feng, Y., 2005. Storage and handling characteristics of pellets from poultry litter. Applied Engineering in Agriculture, 21(4), 645-651.

Medic, D., Darr, M., Shah, A., Potter, B., Zimmerman, J., 2012. Effects of torrefaction process parameters on biomass feedstock upgrading. Fuel, 91(1), 147-154.

Melin, S., 2006. Wood Pellets-Material Safety Data Sheet (MSDS). Canada: Delta Research Corporation Report.

Melin, S., March 9, 2011. Torrefied Wood: A New Emerging Energy Carrier. Presentation to Canadian Clean Power Coalition.

Melin, S., Swaan, J., 2008. Wood Pellet Export Histrory - Opportunity's – Challenges. Canada: Wood Pellet Association of Canada press.

Miller, R. S., Bellan, J., 1996. A generalized biomass pyrolysis model based on superimposed cellulose, hemicellulose and lignin kinetics. *Combust Sci Technol,* 126, 97-137.

Min, K., 1977. Vapor-phase thermal analysis of pyrolysis products from cellulosic materials. Combust. Flame, 30, 285-294.

Mohan, D. J., Steele, P. H., 2006. Pyrolysis of wood/biomass for bio-oil: a critical review. Energy & Fuels, 20, 848-889.

NewEarth, http://www.newearth1.net/newearth-eco-technology.html, Accessed Aug 6, 2009.

Nielsen, N. P. K., Gardner, D. J., Poulsen, T., Felby, C., 2009. Importance of temperature, moisture content, and species for the conversion process of wood into fuel pellets. Wood Fiber Sci., 41(4), 414-425.

Ning, P., Yang, Y. H., Peng, J.H., Zhang, S.M., 2006. Study on Pyrolysis and Charring of Coconut Shell by Thermal Analysis. Chemistry and Industry of Forest Products, 26(1): 49-52.

Obernberger, I., Thek, G., 2004. Physical characterization and chemical composition of densified biomass fuels with regard to their combustion behavior. Biomass and Bioenergy, 27, 653-669.

OECD SIDS, 2005. SIDS initial assessment report for linear alkylbenzene sulfonate (LAS). Paris, France.

Orfao, J. J. M., Antunes, F. J. A., Figuereido, J. L., 1999. Pyrolysis kinetics of lignocellulosic materials-three independent reactions model. Fuel, 78, 349-358.

Orfao, J. J. M., Figueiredo, J. L., 2001. A simplified method for determination of lignocellulosic materials pyrolysis kinetics from isothermal thermogravimetric experiments. Thermochimica Acta, 380(1), 67-78.

Pa, A., Bi, X. T., Sokhansanj, S., 2011. A life cycle evaluation of wood pellet gasification for district heating in British Columbia. Bioresource Technology, 102(10), 6167-6177.

Pach, M., Zanzi, R., Bjornbom, E., 2002. Torrefied biomass a substitute for wood and charcoal. In: 6th Asia-pacific international symposium on combustion and energy utilization, Kuala Lumpur, Malaysia, May 20-22.

Parks, W. G., M.H.G.R.G. Petrarca, A., 1955. Abst. of Papers, 127th ACS Meeting, Cincinnati, OH.

Peng, J. H., Bi, H. T., Sokhansanj, S., Melin, S., & Hoque, M. 2006. A Business Analysis

of BC's Wood Pellet Opportunities. Presented in the 57th Canadian Chemical Engineering Conference, Canada: Edmonton.

Peng, J. H., Bi, H. T., Sokhansanj, S., Lim, J. C., Melin, S., 2010. An Economical and Market Analysis of Canadian Wood Pellets. Int. J. Green Energy, 7, 128-142.

Peng, J. H., Bi, H. T., Sokhansanj, S., Lim, J. C., 2010. Development of Torrefaction Kinetics for BC Softwood. In: ISGA2010, December 5-8, Fukuoka, Japan.

Peng, J. H., Bi, X.T., Sokhansanj, S., Lim, C. J., September 2011. Torrefaction and Densification of Different Species of Softwood Residues. Submitted to Fuel.

Peng, J. H., Bi, X.T., Lim, C. J., Sokhansanj, S., 2012. Development of Torrefaction Kinetics for British Columbia Softwoods. *International Journal of Chemical Reactor Engineering,* published March 2012.

Perry, R. H., 1997. PERRY'S CHEMICAL ENGINEERS' HANDBOOK. ISBN 0-07-049841-5, A Division of The McGraw-Hill Companies.

Phanphanich, M., Mani, S., 2011. Impact of torrefaction on the grindability and fuel characteristics of forest biomass. Bioresource Technology, 102, 1246–1253.

Pimchuai, A., Dutta, A., Basu, P., 2010. Torrefaction of Agriculture Residue to Enhance Combustible Properties. Energy & Fuels, 24, 4638–4645.

Prins, M. J., Ptasinski, K. J., Janssen, F. J. J. G., 2006a. More efficient biomass gasification via torrefaction. Energy, 31, 3458-3470.

Prins, M. J., Ptasinski, K. J., Janssen, F. J. J. G., 2006b. Torrefaction of wood Part 1. Weight loss kinetics. J.Anal. Appl. Pyrolysis, 77, 28-34.

Prins, M. J., Ptasinski, K. J., Janssen, F. J. J. G. J., 2006c. Torrefaction of wood Part 2. Analysis of products. Anal. Appl. Pyrolysis, 77, 35-40.

Pyle, D.L., Zaror, C.A., 1984. Heat transfer and kinetics in the low temperature pyrolysis of solids. Chem. Eng. Sci., 39, 147–158.

Rakos, C., 2008. Production and market trends-an EU perspective. 2008 Bioenergy Conference &Exhibition, Canada: Prince George.

Ramiah, M. V., 1970. Thermogravimetric and Differential Thermal Analysis of Cellulose, Hemicellulose and lignin. J. Appl. Polym. Sci., 14, 1323-1337.

Reed, T., Bryant, B., 1978. Densified biomass: a new form of solid fuel. Solar energy research institute. United States: Colorado.

Reina J, P. L., 1998. Kinetic study of the pyrolysis of waste wood. , Ind Eng Chem Res, 37, 4290-4295.

Roberts, A. F., 1971. The heat of reaction during the pyrolysis of wood. Comb. Flame, 17, 79-86.

Rogers, F. E., Ohlemiller T. J., 1980. Cellulosic insulation materiel-1. Overall degradation kinetics and reaction heats. Combustion Science and Technology, 24, 129-137.

Rousset, P., 2004. Choix et Validation Expérimentale d'un Modèle de Pyrolyse Pour le Bois Traité par Haute Température: de la Micro-particule au Bois Massif. Ph.D. Thesis, ENGREF, Nancy.

Rousset, P., Turner, I., Donnot, A., Perré, P., 2006. The choice of a low-temperature pyrolysis model at the microscopic level for use in a macroscopic formulation. Ann. For. Sci. 63, 213-229.

Roy, C., Lemieux, R., Caumia, B. D., Blanchette, D., April 5-10, 1987. Processing of wood chips in a semicontinuous multiple-hearth vacuum-pyrolysis reactor. Pyrolysis Oil from Biomass, 16-30.

Rumpf, H., 1962. The strength of granules and agglomerates, in Agglomeration, pp. 379-419. W. A. Knepper, New York, NY: John Wiley and Sons.

Salisbury, F. B., Ross, C. W., 1992. Plant Physiology. Wadsworth Publishing Co., Belmont, CA.

Senneca, O., 2007. Kinetics of pyrolysis, combustion and gasification of three biomass fuels. Fuel Processing Technology, 88, 87-97.

Senneca,O., Chirone, R., Salatino, P., 2002. A Thermogravimetric Study of Nonfossil Solid Fuels. 2. Oxidative Pyrolysis and Char Combustion. *Energy & Fuels*, *16,*

661-668.

Senneca,O., Chirone, R., Salatino, P., 2004. Oxidative pyrolysis of solid fuels. J. Anal. Appl. Pyrolysis, 71, 959–970.

Shafizadeh, F. J., 1982. Introduction to pyrolysis of biomass. Anal. Appl. Pyrolysis, 3, 283-305.

Shafizadeh, F., 1985. Pyrolytic reactions and products of biomass, in: R.P. Overend, T.A. Miline, L.K. Mudge (Eds.). Fundamentals of Biomass Thermochemical Conversion, Elsevier, London, 183-217.

Shafizadeh, F., Chin, P., 1977. Thermal deterioration of wood. ACS Symp Ser, 43, 57-81.

Shafizadeh, F., McGinnis, G. D., 1971. Chemical composition and thermal analysis of cottonwood. Carbohydrate Research, 16(2), 273-277.

Shimizu, K., Teramni, F., 1969. *J. Jpn. Wood Res. Soc.* 16, 114.

Simpson, W. T., Liu, J. Y., 1991. Dependence of the water vapor diffusion coefficient of aspen (Populus spec.) on moisture content. Wood Sci. Technol., 26, 9-21.

Sims, H. C., Hassler, C. C., Bean, T. L., September, 1988. Wood Densification. Extension Service, West Virginia University, Publication No. 838.

Sjostrom, E., 1993. Wood Chemistry: Fundamentals and Applications. San Diego, Academic Press, Inc.

Stamm, J., 1956. Thermal degradation of wood and cellulose. Ind. Eng. Chem., 48, 413-417.

Stelte, W., Clemons, C., Holm, J. K., Sanadi, A. R., Ahrenfeldt, J., Shang, L., Henriksen, U. B., et al., 2011a. Pelletizing properties of torrefied spruce, Biomass and Bioenergy (2011), doi:10.1016/j.biombioe.2011.09.025.

Stelte, W., Clemons, C., Holm, J. K., Ahrenfeldt, J., Henriksen, U. B., Sanadi, A. R., 2011b. Thermal transitions of the amorphous polymers in wheat straw, Industrial Crops & Products, 34, 1053-1056.

Stelte, W., Holm, J. K., Sanadi, A. R., Barsberg, S., Ahrenfeldt, J., Henriksen, U. B.,

2011c. A study of bonding and failure mechanisms in fuel pellets from different biomass resources. Biomass and Bioenergy, 35(2), 910-918.

Stelte, W., Holm, J. K., Sanadi, A. R., Barsberg, S., Ahrenfeldt, J., Henriksen, U. B., 2011d. Fuel pellets from biomass: The importance of the pelletizing pressure and its dependency on the processing conditions. Fuel, 90(11), 3285-3290.

Stelte, W., Clemons, C., Holm, J. K., Ahrenfeldt, J., Henriksen, U. B., Sanadi, A. R., 2011e. Thermal transitions of the amorphous polymers in wheat straw. Industrial Crops & Products, 34, 1053-1056.

Tabil, L.G., Sokhansanj, S., Crerar, W.J., Patil, R.T., Khoshtaghaza, M.H., Opoku, A., 2002. Physical characterization of alfalfa cubes: I. Hardness. Canadian Biosystems Engineering, 44, 355-363.

Tan, Y., Croiset, E., Douglas, M. A., Thambimuthu, K. V., 2006. Combustion characteristics of coal in a mixture of oxygen and recycled flue gas. Fuel, 85(4), 507-512.

Tang, M. M., Bacon, R., 1964. Carbonization of cellulose fibers-I. Low temperature pyrolysis. Carbon, 2, 211-214.

Tang, W. K., 1967. Effect of inorganic salts on pyrolysis of wood, alpha-cellulose and lignin. , Forest Prod. Lab, Madison, Wis., Paper 71.

Thomas, R. J., 1977. Wood structure and chemical composition. ACS Symposium Series, 43, 1-23.

Thurner, I., Roussent, P., Remond, R., Perre, P., 2010. An experimental and theoretical **...** thermal treatment of wood (Fagus sylvatica L.) in the range 200-260 $^{\circ}$C. International Journal of Heat and Mass Transfer, 4, 715-725.

Thurner, F., Mann, U., 1981. Kinetic investigation of wood pyrolysis. Ind Eng Chem Proc Des Dev, 20, 482-488.

Tsotsa, E., Martin, H., 1987. Thermal Conductivity of Packed Beds: A Review. Chem. Eng. Process, 22, 19-37.

Uemura, Y., Omar, W., Othman, N. A., Yusup, S., Tsutsui, T., 2011. Torrefaction of oil palm EFB in the presence of oxygen. Fuel, In Press, Corrected Proof, Available online 19 November 2011.

Ulrich, G. D. 1984. A Guide to Chemical Engineering Process Design and Economics. New York, NY, John Wiley & Sons.

Urbanowski, E. 2005. Strategic Analysis of A Pellet Fuel Opportunity in Northwest British Columbia. Canada: Simon Fraser University Master Thesis.

US Department of Agriculture 2009. Notice of Funds Availability (NOFA) for the Collection, Harvest, Storage, and Transportation of Eligible Material. Federal Register 27767, Vol. 74, No. 111, Thursday, June 11, 2009.

Uslu, A., Faaij, A. P.C., Bergman，P.C.A., 2008. Pre-treatment technologies, and their effect on international bioenergy supply chain logistics. Techno-economic evaluation of torrefaction, fast pyrolysis and pelletisation，Energy, 33(8), 1206-1223.

Van der Stelt, M. J. C., Gerhauser, H., Kiel, J. H. A., Ptasinski, K. J., 2011. Biomass upgrading by torrefaction for the production of biofuels: A review. Biomass and Bioenergy, 35, 3748-3762.

Varhegyi, G., Jakab, E., Antal, M. J., 1994. Is the Broido-Shafizadeh Model for Cellulose Pyrolysis True?. Energy Fuels, 8(6), 1345-1352.

Wagenaar, B. M., Prins, W., Swaaij van. W. P. M., 1993. Flash pyrolysis kinetics of pine wood. Fuel Proc Technol, 36, 291-302.

Wannapeera, J., Fungtammasan, B., Worasuwannarak, N., 2011. Effects of temperature and holding time during torrefaction on the pyrolysis behaviors of woody biomass. Journal of Analytical and Applied Pyrolysis, 92, 99–105.

Ward, S. M., Braslaw, J., 1985. Experimental weight loss kinetics of wood pyrolysis under vacuum. Combust Flame, 61, 261-269.

Weisz, P. B., Prater, C. D., 1954. Interpretation of Measurements in Experimental

Catalysis. ISBN 9780120078066, Advances in Catalysis, 6, 143.

Williams, P. T., Besler, S., 1993. The Pyrolysis of Rice Husks in a Thermogravimetric Analyzer and Static Batch Reactor. , Fuel, 72, 151-159.

Williams, P. T., Besler, S., 1994. Thermogravimetric analysis of the component of biomass. Advances in thermochimical biomass conversion. A. V. Bridgewater. London, Blackie Academic & Professional.

Winkler, W., 2011. Briquetting features and advantages. in: Biomass Pelletization Workshop, Vancouver, Canada, May 17-18.

Witte, M. 2008. A Discussion of Pacific BioEnergy Corp. 2008 Bioenergy Conference &Exhibition, June 3-5, 2008, Canada: Prince George.

Yan, W., Acharjee, T. C., Coronella, C. J., Vasquez, V. R., 2009. Thermal Pretreatment of Lignocellulosic Biomass. Environmental Progress & Sustainable Energy, 28, 435-440.

Yildiz, S., Gezer, E. D., Yildiz, U. C., 2006. Mechanical and chemical behavior of spruce wood modified by heat. Building and Environment, 41, 1762-1766.

Zakrisson, M. 2002. A Comparison of international Pellet Production Costs. Sweden: Swedish University of Agricultural Sciences and Department of Forest Management and Products Report.